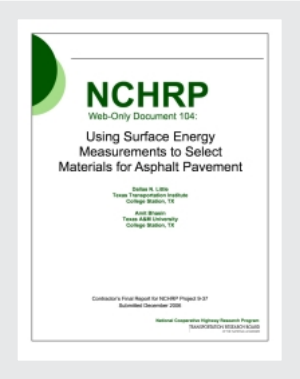

Final Report for NCHRP RRD 316: Using Surface Energy Measurements to Select Materials for Asphalt Pavement

DETAILS

0 pages | | PAPERBACK
ISBN 978-0-309-43174-3 | DOI 10.17226/22001

AUTHORS

ACKNOWLEDGMENT

This work was sponsored by the American Association of State Highway and Transportation Officials (AASHTO), in cooperation with the Federal Highway Administration, and was conducted in the National Cooperative Highway Research Program (NCHRP), which is administered by the Transportation Research Board (TRB) of the National Academies.

THE NATIONAL ACADEMIES

Advisers to the Nation on Science, Engineering, and Medicine

The **National Academy of Sciences** is a private, nonprofit, self-perpetuating society of distinguished scholars engaged in scientific and engineering research, dedicated to the furtherance of science and technology and to their use for the general welfare. On the authority of the charter granted to it by the Congress in 1863, the Academy has a mandate that requires it to advise the federal government on scientific and technical matters. Dr. Ralph J. Cicerone is president of the National Academy of Sciences.

The **National Academy of Engineering** was established in 1964, under the charter of the National Academy of Sciences, as a parallel organization of outstanding engineers. It is autonomous in its administration and in the selection of its members, sharing with the National Academy of Sciences the responsibility for advising the federal government. The National Academy of Engineering also sponsors engineering programs aimed at meeting national needs, encourages education and research, and recognizes the superior achievements of engineers. Dr. William A. Wulf is president of the National Academy of Engineering.

The **Institute of Medicine** was established in 1970 by the National Academy of Sciences to secure the services of eminent members of appropriate professions in the examination of policy matters pertaining to the health of the public. The Institute acts under the responsibility given to the National Academy of Sciences by its congressional charter to be an adviser to the federal government and, on its own initiative, to identify issues of medical care, research, and education. Dr. Harvey V. Fineberg is president of the Institute of Medicine.

The **National Research Council** was organized by the National Academy of Sciences in 1916 to associate the broad community of science and technology with the Academy's purposes of furthering knowledge and advising the federal government. Functioning in accordance with general policies determined by the Academy, the Council has become the principal operating agency of both the National Academy of Sciences and the National Academy of Engineering in providing services to the government, the public, and the scientific and engineering communities. The Council is administered jointly by both the Academies and the Institute of Medicine. Dr. Ralph J. Cicerone and Dr. William A. Wulf are chair and vice chair, respectively, of the National Research Council.

The **Transportation Research Board** is a division of the National Research Council, which serves the National Academy of Sciences and the National Academy of Engineering. The Board's mission is to promote innovation and progress in transportation through research. In an objective and interdisciplinary setting, the Board facilitates the sharing of information on transportation practice and policy by researchers and practitioners; stimulates research and offers research management services that promote technical excellence; provides expert advice on transportation policy and programs; and disseminates research results broadly and encourages their implementation. The Board's varied activities annually engage more than 5,000 engineers, scientists, and other transportation researchers and practitioners from the public and private sectors and academia, all of whom contribute their expertise in the public interest. The program is supported by state transportation departments, federal agencies including the component administrations of the U.S. Department of Transportation, and other organizations and individuals interested in the development of transportation.
www.TRB.org

www.national-academies.org

TABLE OF CONTENTS

TABLE OF CONTENTS

LIST OF FIGURES

FIGURE Page

LIST OF TABLES

TABLE Page

ACKNOWLEDGMENTS

The research reported herein was performed under NCHRP Project 9-37 by the Texas Transportation Institute, Texas A&M University; Western Research Institute, Laramie; and University of Rhode Island. The Texas Transportation Institute was the contractor for this study. The work undertaken at Western Research Institute and University of Rhode Island was performed under a sub-contract with the Texas Transportation Institute.

Dallas N. Little, E.B. Snead Chair Professor, Texas A&M University, was the principal investigator The author of this report is Amit Bhasin, Associate Research Scientist, Texas Transportation Institute.

The work was done under the general supervision of Dr. Dallas Little. The work at Western Research Institute was done under the supervision of Dr. Troy Pauli. The work at the University of Rhode Island was done under the supervision of Dr. Arijit Bose.

SUMMARY

Surface free energy, or simply surface energy, of asphalt binders and aggregates is an important material property that influences the performance of asphalt mixes. Principles of thermodynamics can be used to quantify the propensity of asphalt binders to debond from aggregate surfaces in the presence of water based on their surface energy components. This probably is directly related to the moisture sensitivity of asphalt mixes. Principles of fracture mechanics can be combined with the work of cohesion and adhesion derived from surface energy components of the asphalt binder and aggregates and other material properties of asphalt mastics to model crack growth behavior. These models can be used to predict the fatigue and healing characteristics of asphalt mixes.

In order to use surface energy measurements to select materials for better performing asphalt pavements, it is imperative that simple, accurate, and reliable test methods be used to measure the surface energy components of asphalt binders and aggregates, and the link between surface energy and performance of mixes must be established and validated. In this study various candidate test methods to measure the surface energy components of these materials were selected based on an exhaustive literature review. These methods were evaluated based on technical criteria such as precision, accuracy, ability to provide all three surface energy components, and ability to evaluate samples representative of the material being investigated. Practical considerations such as capital outlay for the equipment required for each test method and expertise required to perform tests were also evaluated. Based on this research it is recommended that the Wilhelmy plate method be used to measure the surface energy components of asphalt binders and the universal sorption device (USD) be used to measure the surface energy components of aggregates, respectively. Alternatively, the sessile drop method can also be used to measure the surface energy components of asphalt binders and the micro calorimeter can be used to measure the surface energy components of aggregates, with some refinements. Protocols to measure the surface energy components of asphalt binders and aggregates were developed by customizing each test method for use with these materials. Inverse gas chromatography (IGC) and atomic force microscopy (AFM) were identified as advanced tools to characterize surfaces of aggregates and asphalt binders including surface energy components. This report documents the test and analysis protocols for each test method.

Four energy parameters were proposed as independent measures of the moisture sensitivity of any combination of asphalt binder and aggregate. These energy parameters can be derived from the surface energy components of the asphalt binders and the aggregates. The effectiveness of these parameters in distinguishing the moisture sensitivity of various asphalt mixes was evaluated by comparing field and laboratory performance of various asphalt mixes. The moisture sensitivity of laboratory mixes demonstrated a fair degree of correlation with the energy parameters. Comparison of the energy parameters with the field performance of mixes suggests that a threshold value of the former can be used to distinguish between mixes that are moisture sensitive and those that are not. It is envisaged that in the future an extensive database of field performance and energy parameters can be developed to determine these threshold values. The threshold values can then be used as a materials selection tool by which to eliminate combinations of asphalt binders and aggregates that are potentially moisture sensitive.

An advantage of this methodology is that by independently measuring the surface energy components of various asphalt binders and aggregates, the energy parameters and, hence the

moisture sensitivity of all possible combinations of these materials can be analytically derived. This analysis demonstrated that if an asphalt mixture is moisture sensitive, it does not necessarily imply that either the aggregate or the asphalt binder will perform poorly when combined with other asphalt binders or aggregates, respectively.

Surface energies of asphalt binders and aggregates were also used in conjunction with other material properties derived using simple tests with the dynamic mechanical analyzer (DMA) to model crack growth behavior in asphalt mastics. A limited comparison of field results was made to demonstrate the combined use of surface energy and other material properties to predict fatigue life of asphalt mixtures.

CHAPTER 1
INTRODUCTION AND RESEARCH APPROACH

This chapter presents an overview of the project background, the objectives and scope of this project, and research methodology used to achieve the project objectives.

1.1 BACKGROUND

Hot mix asphalt (HMA) is a composite material primarily composed of mineral aggregates bound together using asphalt binder. Various forms of distress in HMA pavements, such as moisture damage and fatigue cracking, are closely related to the quality of adhesion between these materials in dry and wet conditions. Adhesion between the asphalt binder and aggregate can be quantified if the surface free energies of both these materials are known. Surface free energy is also combined with other intrinsic material properties using fundamental principles of fracture mechanics to model and predict growth of fatigue cracks.

The inability to accurately and efficiently measure the surface free energy components of asphalt binders and aggregates has been a major hurdle in consideration of this property when selecting materials that promote better performing asphalt mixtures. This gap generated the need for research in two areas related to this subject. The first was to determine and/or develop efficient test methods that can be used on a routine basis to measure surface free energy components of these materials. A detailed background on the measurement of surface energy is provided in Appendix A. The second was to quantitatively determine the relationship of surface free energy of asphalt binders and aggregates to the performance of asphalt mixtures.

1.1.1 Surface Free Energy and Moisture Damage

Moisture induced damage is a primary form of distress in HMA pavements. The economic impact of moisture damage due to premature pavement failure and excessive maintenance costs has prompted research in this area for over a century. Identification of asphalt mixtures that are prone to moisture damage is an important part of the material selection and mixture design process. Several highway agencies rely on mechanical tests conducted on asphalt mixtures in dry and moisture conditioned states to evaluate the moisture sensitivity of these mixes. Results from this methodology are easy to interpret and provide a gross estimate of the cumulative effects of material and mixture properties on moisture sensitivity of asphalt mixtures. However, despite these advantages and the popularity and simplicity of this approach, this methodology suffers from drawbacks such as,

- poor correlation with field performance,
- extended testing time,
- inability to associate material properties with the mechanisms that cause moisture damage in asphalt mixtures, and
- inability to identify corrective measures to address specific mechanisms of failure.

Incorporation of tests that measure fundamental material properties related to adhesion and moisture damage can help overcome some if not most of these shortcomings.

An important material property that is related to the moisture sensitivity of asphalt mixtures is the surface free energy of the asphalt binder and the aggregate. Surface free energies of these materials can be used to quantitatively determine the interfacial adhesive bond strength between these two materials and the tendency of water to displace this bond based on fundamental principles of thermodynamics. The importance of surface free energies of asphalt

binder and aggregate in determining the moisture sensitivity of asphalt mixtures is well established in the literature. However, until recently not much has been done to develop methods to measure the surface free energy of these materials. Efficient and accurate methods to measure surface free energies of asphalt binders and aggregates combined with principles of adhesion and debonding based on thermodynamics can be used to select materials that produce asphalt mixtures that are more resistant to moisture damage.

1.1.2 Surface Free Energy and Fatigue Cracking

Principles of fracture mechanics were used to model the crack growth behavior and healing characteristics of asphalt mixtures. The advantage of this approach over using conventional methods to measure fatigue cracking characteristics of asphalt mixtures is that the former can be used to analytically predict the fatigue cracking life of mixes based on simple laboratory tests that measure fundamental material properties. Surface energy of asphalt binders and aggregates are important material property inputs in this methodology.

In summary, efficient and accurate methods to measure the surface energies of asphalt binders and aggregates on a routine basis can assist in selection of materials with which to design asphalt mixtures that are more resistant to moisture damage. Surface energies of these materials can also be combined with other material properties and used with the principles of fracture mechanics to determine the fatigue cracking and healing characteristics of asphalt mixtures.

1.2 OBJECTIVES AND SCOPE OF STUDY

The objective of this research is to identify and develop the most suitable methodology to measure surface energy of asphalt binders and aggregates and to conduct a limited study validating the ability of surface energy to predict the performance of asphalt mixtures. The efforts in this research are guided by the expectation that this methodology will ultimately be used for routine screening and selection of materials for optimum performance of asphalt pavements. The efforts of this research are also guided by the realization that material selection is only a part of the strategic objective of producing reliably performing pavements.

1.3 RESEARCH METHODOLOGY

The specific research tasks defined to achieve the research objectives were as follows:

- **Task 1. Evaluation of current methods by which to measure surface energy:** The objective of this task was to conduct a detailed review of all the direct and indirect methods available to measure the surface energy of asphalt binders and aggregates and their interfacial adhesive bond strengths. Results from this review were used to select candidate test methods for evaluation in other tasks. Mathematical models based on fracture mechanics that relate material properties (including surface energy) to the performance of asphalt mixtures were also reviewed in this task.
- **Task 2. Experiment design:** The objective of this task was to develop an experiment design for Tasks 4 and 5. Literature review from Task 1 was the key input to accomplishing this task.
- **Task 3. Interim report:** The objective of this task was to prepare an interim report describing the work done in Tasks 1 and 2. This report documented the work plan for phase 2 and served as a platform to incorporate panel review comments and suggestions for accomplishing the project objectives.

- **Task 4. Material characterization:** This task was designed to address two aspects related to the measurement of surface energy of asphalt binders and aggregates. The first objective was to compare various test methods that measure surface energy based on their precision, accuracy, and potential for use routine use. The second objective was to measure the surface energy characteristics of several different asphalt binders and aggregates with different chemical and mineralogical composition, respectively, and assess the typical range of values of the surface energies of these materials. This task also included customization of the selected test methods and development of protocols to measure the surface energy of asphalt binders and aggregates.
- **Task 5. Performance evaluation:** The motivation to develop simple and accurate test methods to measure surface energy of asphalt binders and aggregates is to be able to use this property to select materials that produce better performing asphalt mixtures. Performance of asphalt mixtures is assessed based on resistance to moisture induced damage, fatigue cracking, and permanent deformation. The most direct application of surface energy is to quantify the adhesion between various combinations of asphalt binders and aggregates and their tendency to debond in the presence of water. In this task, emphasis was placed on a limited validation of the relationship between surface energy (and concomitant bond energy calculations) to moisture sensitivity of asphalt mixtures determined from field and laboratory performance of several different asphalt mixtures. The application of surface energy (in conjunction with other material properties measured by conducting simple tests on asphalt mastics using a DMA) to the fatigue cracking characteristics of different asphalt mixtures was also demonstrated in this task.
- **Task 6. Development of methods and manual:** The objective of this task was to document the test protocol for the recommended test methods in American Association of State Highway and Transportation Officials (AASHTO) standard format based on the work done in Task 4. Mathematical procedures to compute various thermodynamic parameters using surface energy of these materials and their relationship to the performance of asphalt mixtures were also documented in the form of a users guide in this task.
- **Task 7. Work plan for future validation:** This research was able to evaluate a limited but carefully selected and representative set of mixtures. It is important to extend the database to a broader range of combinations of aggregates and asphalt binders and to consider the impact of aging, processing, and modification on these components. This research identifies the methods best suited for selection of mixtures based on surface energy properties that will produce better performing asphalt mixtures. However, additional testing, verification, and refinement are required in order to produce the final and definitive procedures for using surface energy measurements to select asphalt mixture components, design the mixtures, apply this approach in monitoring the quality of the mix during construction, and monitor long-term performance under specific traffic and environmental conditions. The purpose of this task is to prepare a work plan for further validation of the use of surface energy measurement methodology for selection and specification of materials for asphalt pavements through additional laboratory and field experiments.
- **Task 8. Final report:** This task documents the results pertaining to the various tasks executed in this research. Results from Tasks 4 and 5 are included in Chapters 2 and 3 of

this report. Task 7, which is the work plan for future validation, is documented in Chapter 4 of this report. Documents pertaining to Task 6 are included in the appendices of this report.

CHAPTER 2
FINDINGS

This chapter presents a summary of the important findings from the various tasks accomplished in this research. Figure 1 illustrates the order of the information presented in this chapter and broadly describes the flow of this research.

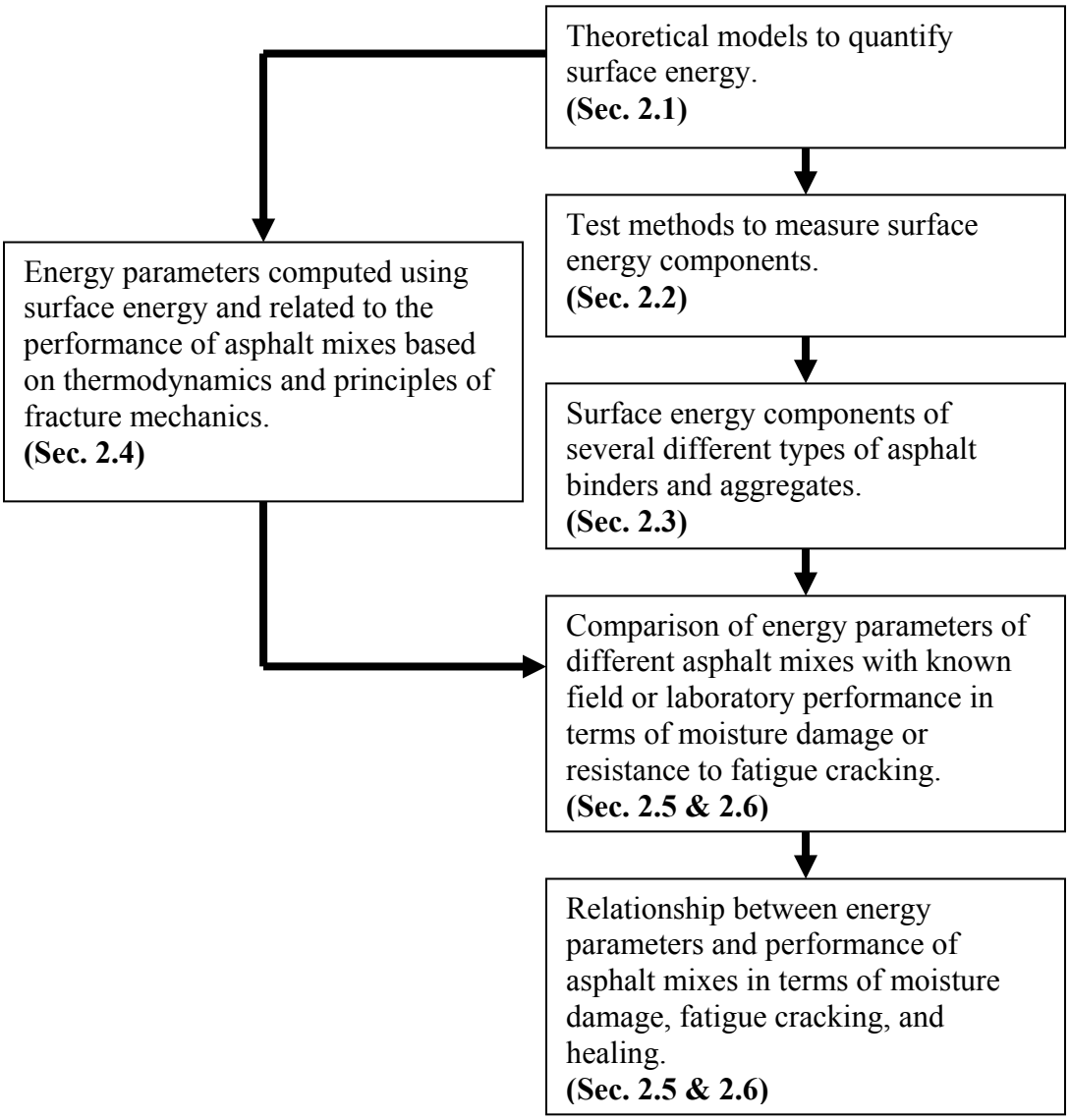

Figure 1. Research Flow and Areas Related to Summary of Findings.

2.1 RELEVANT PRINCIPLES RELATED TO SURFACE ENERGY

This section summarizes some of the important theories, definitions, and terms related to surface energy of materials. These definitions and concepts will be used throughout this report in the presentation of findings, the presentation of details pertaining to the measurement of surface energy, and the description of the application of these principles to evaluate the

performance of asphalt mixtures. Therefore, it is important to consider this information first and foremost in this section.

2.1.1 Surface Energy of Materials

Molecules in the bulk of a material are surrounded on all sides by other molecules, and as a result these molecules have a higher level of bond energy compared to the molecules on the surface (Figure 2). Therefore, work must be done in order to extract the molecules from the bulk and create a new area of surface molecules. This work is equal to the surface free energy of the material. A formal definition of surface free energy is the magnitude of work required to create a unit area of a new surface of the material in a vacuum and is commonly denoted by the Greek letter γ *(1)*.

The term "free energy" is used in this context since the definition is based on work done, which is different from the total excess energy. The most common units of surface free energy are ergs/cm^2 or mJ/m^2. The terms surface tension, surface energy, and surface free energy are often used interchangeably, although surface free energy is technically the correct term when used in the context of the principles of thermodynamics.

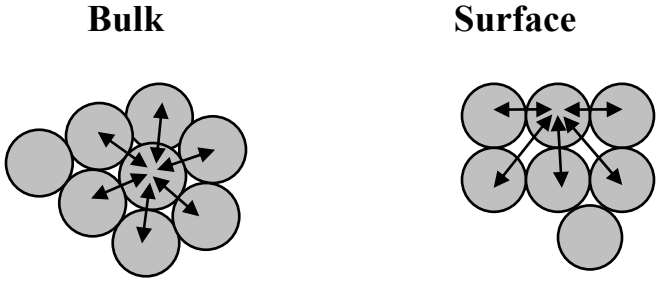

Figure 2. Differences in Intermolecular Forces at the Surface and in the Bulk.

Several theories explain the molecular origin of surface free energy of solids. The two most popular theories are the two-component theory and the acid-base theory. Fowkes *(2)* introduced the idea that the total surface free energy of a material is actually made up of two components. He attributed these components to dispersion forces (nonpolar intermolecular interactions such as Lifshitz-van der Waals (LW) forces) and forces related to specific interactions such as hydrogen bonding. He also proposed that the total surface free energy or surface tension is a linear combination of these interactions expressed as follows:

$$\gamma^{Total} = \gamma^{Dispersive} + \gamma^{Specific} \quad \textbf{[1]}$$

This model which separates the surface free energy of materials into its components is also referred to as the two -component theory. The other theory that is widely applied to explain the surface energy components of various materials is the Good-van Oss-Chaudhury (GVOC) or acid-base theory *(3)*. According to this theory, the total surface free energy of any material is divided into three components based on the type of molecular forces on the surface. These components are: 1) the nonpolar component, also referred to as the LW or the dispersive component, 2) the Lewis acid component, and 3) the Lewis base component. The total surface free energy is obtained by combining these components as follows:

$$\gamma = \gamma^{LW} + \gamma^{+-} = \gamma^{LW} + 2\sqrt{\gamma^{+}\gamma^{-}} \quad \textbf{[2]}$$

where, γ is the total surface free energy of the material, γ^{LW} is the Lifshitz-van der Waals (LW) or dispersive component, γ^{+-} is the acid-base component, γ^{+} is the Lewis acid component, and γ^{-} is the Lewis base component. In this research, the acid-base theory was preferred over the two component theory, since the specific or polar interactions between any two materials can be more rationally explained and quantified using the acid-base theory.

2.1.2 Work of Adhesion between Two Materials

According to the acid-base theory, the work of adhesion, W_{AB}, between two materials 'A' and 'B' can be expressed as a function of their respective surface free energy components as follows:

$$W_{AB} = 2\sqrt{\gamma_A^{LW}\gamma_B^{LW}} + 2\sqrt{\gamma_A^{+}\gamma_B^{-}} + 2\sqrt{\gamma_A^{-}\gamma_B^{+}} \quad \textbf{[3]}$$

The phenomenological explanation for the work of adhesion is the amount of external work that is required to separate two materials at their interface in a vacuum (Figure 3). For an asphalt binder-aggregate system, equation [3] is used to compute this work of adhesion when the surface free energy components of both these materials are known.

2.1.3 Work of Cohesion

Harkins and Cheng *(4)* defined the work of cohesion of a liquid as the work required to separate a column of the liquid with unit cross sectional area in two. This definition can extend to solids. From the definition of surface free energy, it is easy to derive the total work of cohesion, W_{AA}, of a material 'A' as:

$$W_{AA} = 2\gamma_A \quad \textbf{[4]}$$

where, γ_A is the surface energy of the material. Work of cohesion of asphalt binders is an important parameter that is used in some of the basic equations of fracture mechanics to determine the energy required for growth of microcracks within the asphalt binder phase or mastic phase of the asphalt mixture.

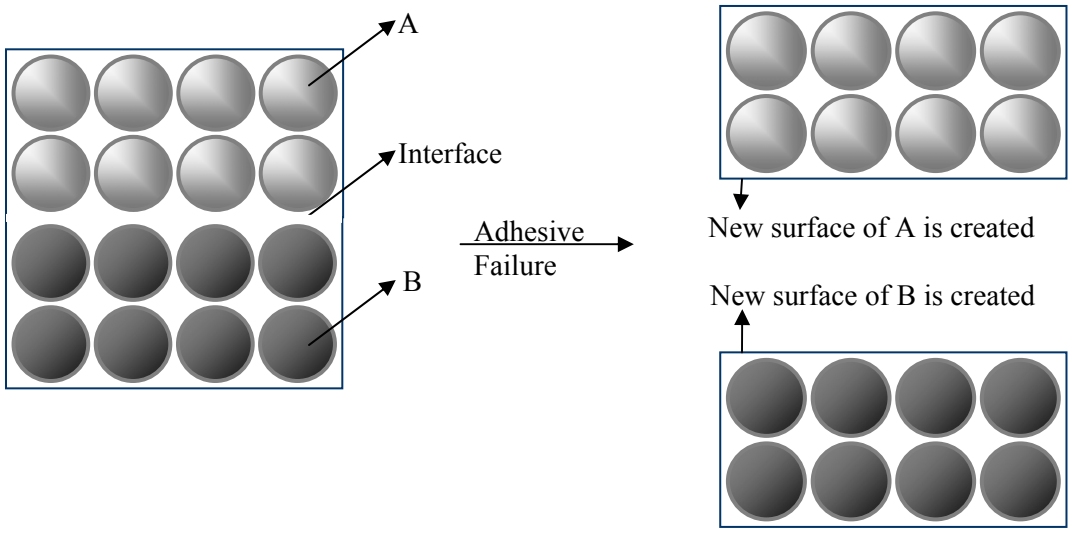

Figure 3. Adhesive Failure between Two Materials 'A' and 'B'.

2.1.4 Propensity of One Material to Displace Another from an Interface

In order to quantify the propensity of one material to displace another, the interfacial energies of these materials must be known. An interface may be defined as a special type of surface that forms a common boundary between two different materials. Figure 3 shows the idealized representation of an interface between two materials 'A' and 'B.' The molecules of both these materials at the interface are subjected to unequal forces compared to their respective bulk molecules. This creates a misbalance of forces at the interface and results in interfacial energy between the two materials, represented as γ_{AB}. Analogous to the surface free energy in a vacuum, the interfacial energy between two materials is defined as the work required to create a unit area of the interface by separating the two materials in a vacuum. Also, the relationship between the work of adhesion between two materials, the total surface energy of the two materials, and their interfacial energy is given by:

$$W_{AB} = \gamma_A + \gamma_B - \gamma_{AB} \quad \textbf{[5]}$$

Equations [3] and [4] are used together to determine the interfacial energy between any two materials when their individual surface energy components are known.

Consider a three-phase system comprising asphalt binder, aggregate, and water (Figure 4) where these components are represented by 'B,' 'A,' and 'W,' respectively. The following processes occur when water displaces the asphalt binder from the binder-aggregate interface. First, a part of the interface of the aggregate with the binder is eliminated (AB). Based on the definition of interfacial energy, the external work required for this is $-\gamma_{AB}$. Similarly, two new interfaces, between water and binder (BW), and between water and aggregate (AW), are created. The work done for the formation of these two new interfaces is $\gamma_{WB} + \gamma_{WA}$. Therefore, the total work done for water to displace binder from the surface of the aggregate is $\gamma_{WB} + \gamma_{WA} - \gamma_{AB}$. If the displacement process is thermodynamically favorable then it must be associated with an overall reduction in free energy of the system. In other words, the total work done on the system during the displacement process must be less than zero. Results from this research indicate this is true for almost all asphalt binder-aggregate systems, suggesting that displacement of asphalt binder by water is a thermodynamically favored phenomenon. In this context, the energy associated with the displacement of binder by water from the bitumen-aggregate interface, or debonding, is referred to as the work of debonding and is expressed as:

$$W_{ABW}^{wet} = \gamma_{AW} + \gamma_{BW} - \gamma_{AB} \quad \textbf{[6]}$$

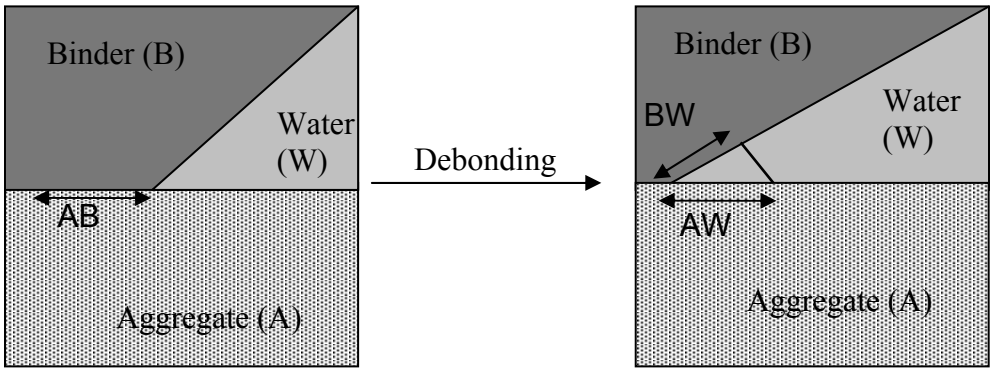

Figure 4. Displacement of Binder from Binder-Aggregate Interface by Water.

The magnitude of work of debonding is a function of the surface energy components of the asphalt binder and aggregate. Accordingly, the potential for water to displace binder depends on the surface energy components of the binder and the aggregate.

2.2 SELECTION OF TEST METHODS TO MEASURE SURFACE ENERGY

The previous section describes the relationship between the surface energy components of materials and the work of adhesion, work of cohesion, and work of debonding. These parameters may be used to select materials for asphalt mixtures that are more resistant to moisture damage. They can also be used together with the principles of fracture mechanics to determine the fatigue cracking and healing characteristics of asphalt mixtures. Effective use of this methodology depends largely on the ability to measure the surface energy components of asphalt binders and aggregates with adequate precision, and accuracy using reasonable resources.

In Task 1 of this research, a literature review, was conducted to identify candidate test methods to measure the surface energy components of asphalt binders and aggregates. Some degree of customization of each test method was necessary to enable their use for measuring surface energy components of these materials. The considerations that were used to select and compare the candidate test methods included:

Information related considerations

- compatibility with surface energy theory, i.e., ability to provide three surface energy components,
- ability to characterize the natural surface, and
- ability to provide a representative measure of the bulk property of the material.

Operation related considerations

- complexity of sample preparation and testing,
- availability of equipment and required modification,
- robustness and maintainability of equipment, and
- sample preparation and testing time.

2.2.1 General Methodology to Measure Surface Energy Components

Direct measurement of surface energy components of solids is rarely feasible. However, it is possible to measure various forms of physical interactions between solids and liquids or gases that are due to the surface energies of these materials. Examples of such interactions are formation of finite contact angles of liquids on solid surfaces, vapor adsorption of gases on clean solid surfaces, and evolution of heat when solids are immersed in a liquid. Accordingly, various indirect methods such as the contact angle approach, gas adsorption, inverse gas chromatography, and micro calorimetry *(5)* have been developed to measure surface energies of solids. Each method requires an appropriate theory is selected to relate the physically measured interaction with the work of adhesion between the two materials. For example, the Young-Dupre equation is used to relate the contact angle of a liquid on a solid surface to their work of adhesion.

The basic algorithm to determine the three surface energy components of any solid is similar for most test methods. The work of adhesion between an unknown solid and a known probe liquid is determined experimentally. The work of adhesion is expressed as a function of the three surface energy components of the solid and probe liquid or vapor using equation [3]:

$$W_{XP} = 2\sqrt{\gamma_X^{LW}\gamma_P^{LW}} + 2\sqrt{\gamma_X^{+}\gamma_P^{-}} + 2\sqrt{\gamma_X^{-}\gamma_P^{+}} \quad \textbf{[7]}$$

where, W_{XP} is the work of adhesion between the probe liquid or vapor denoted by the suffix P and the solid denoted by the suffix X. The three unknowns in equation [7] are the square roots of the surface energy components of the solids. Therefore, experimentally measuring the work of adhesion of the solid with at least three different probe liquids or vapors generates a set of three linear equations that can be solved to determine the three unknown surface energy components of the solid.

Asphalt binders have low energy surfaces, i.e., the surface energy of asphalt binders are typically less than the surface energy of the probe liquids that are used to measure the work of adhesion. On the other hand, aggregates have high energy surfaces, i.e. the surface energy of aggregates are typically greater than the surface energy of the probe liquids that are used to measure the work of adhesion. Therefore, the test methods suitable to measure the surface energy components of asphalt binder may not be suitable to measure the surface free energy components of aggregates.

2.2.2 Test Methods to Measure Surface Energy Components

Based on the literature review conducted in Task 1, the four candidate test methods selected to determine the surface energy components of asphalt binders were:

- Wilhelmy plate method (WP),
- sessile drop method,
- atomic force microscopy (AFM), and
- inverse gas chromatography (IGC).

The four test methods selected to measure the surface energy components of aggregates were:

- universal sorption device (USD),
- inverse gas chromatography,
- sessile drop method, and
- micro calorimeter.

Table 1 presents a comparison of the selected test methods based on the criteria and considerations described earlier. Chapter 3 presents a more detailed description of the specific advantages and limitations of each test method. Appendices B through D present the protocols for the recommended test methods in AASHTO format and appendices E through G present the protocols for the remaining test methods.

2.3 TYPICAL VALUES OF SURFACE ENERGY COMPONENTS

2.3.1 Materials and Tests

An important objective of Task 4 was to characterize the surface energy components for a suite of asphalt binders and aggregates using "gold standard" tests. The gold standard tests for measuring surface energy components of asphalt binder and aggregates are the Wilhelmy plate method and the USD, respectively. These tests were selected as gold standards based on the following criteria:

- The tests were already used in previous studies to measure the surface energy components of these materials.

Table 1(a). Test Methods to Measure Surface Free Energy of Asphalt Binders.

		Wilhelmy plate	**Sessile drop**	**Atomic force microscopy**	**Inverse gas chroma-tography**
Measured parameter related to work of adhesion		Dynamic contact angle of probe liquids on sample surface	Static contact angle of probe liquids on sample surface	Force – distance curves using different cantilever tips	Retention time of probe vapors when passed through sample column
Output		All three surface energy components	All three surface energy components	Surface energy (Measurement of individual components requires further research)	All three surface energy components
Asphalt binder sample description		Glass slide with thin coating of asphalt binder	Flat surface with thin flat coating of asphalt binder	Glass slide with solvent cast film of asphalt binder	Capillary column with wall coated with asphalt binder
Time requirement for one binder	Test time in days*	3	3	3	3
	Operator man hours	15	15	15	12
Operator training and expertise**		Average	Average	High	Average to High
Capital cost estimate (US$)		30,000	20,000	40,000	150,000[+]
Recommendations		Recommended for routine testing	Recommended for routine testing with some method developments	Recommended for use as an advanced materials characterization tool with emphasis on polar species and different phases within the asphalt binders	
Procedure descriptions		Section 3.2.2 Appendix B	Section 3.2.4 Appendix D	Section 3.2.6 Appendix G	Section 3.2.5 Appendix F
Additional computational descriptions		Appendix E	Appendix E	Appendix G	Appendix F

***** Indicates number of working days required for one operator to prepare sample, run all replicate tests with all probe liquids, and report results. Also see description of 'operator man hours.' The entire time of the operator is not dedicated to this test alone since some tests run with only minimal operator assistance.

****** Average – indicates requirement of a an operator with one to two days of training, High – indicates requirement of a highly skilled operator preferably with a technical background with a training time of about one week.

[+] Indicates cost of a commercially available device. Regular gas chromatographs may be retrofit to function as IGC with lower costs.

Table 1(b). Test Methods to Measure Surface Free Energy of Aggregates.

		Universal Sorption Device	**Inverse gas chroma-tography**	**Sessile drop**	**Micro calorimeter**
Measured parameter related to work of adhesion		Adsorption isotherm	Retention time of probe vapors when passed through sample column	Static contact angle of probe liquids on sample surface	Enthalpy of immersion of aggregates in probe liquids
Output		All three surface energy components	All three surface energy components	All three surface energy components	All three surface energy components
Aggregate sample description		Size fraction passing #4 sieve and retained on #8 sieve	Particles about 1mm in size	Aggregate surface polished to about 1 mm fineness	Size fraction passing #100 sieve and retained #200 sieve
Time requirement for one aggregate	Test time in days*	11	3	4	3
	Operator man hours	20	10	18	10
Operator training and expertise**		High	Average to High	Average	Average
Capital cost estimate (US$)		70,000***	150,000[+]	20,000	40,000
Recommendations		Recommended for testing of aggregates with emphasis on developing a general catalog of aggregate surface energies.	Recommended for use as an advanced materials characterization tool with emphasis on high energy polar functional groups on aggregate surfaces and pure minerals.	Conventional test protocol cannot be accurately used to measure surface energy components. Further research on measuring interfacial contact angles using two liquids simultaneously is recommended.	Recommended for use when rough estimates of surface energy components are required. Further research to quantify entropy can significantly improve the applicability of this method.
Procedure descriptions		Section 3.2.3 Appendix C	Section 3.2.5 Appendix F	Section 3.2.4 Appendix D	Section 3.2.7 Appendix H
Additional computational descriptions		Appendix E	Appendix F	Appendix D	Appendix H

* Indicates number of working days required for one operator to prepare sample, run all replicate tests with all probe liquids, and report results. Also see description of 'operator man hours.' The entire time of the operator is not dedicated to this test alone. Some tests are run with only minimal operator assistance.

** Average – indicates requirement of a an operator with one to two days of training, High – indicates requirement of a highly skilled operator preferably with a technical background with a training time of about one week.

*** Does not include cost of automated manifold developed in this project.

[+] Indicates cost of a commercially available device. Regular gas chromatographs may be retrofit to function as IGC with lower costs.

- The relation between the physical properties measured by these tests, work of adhesion, and the surface energy components is relatively well established in the literature.
- Results from these tests have been correlated to some extent with the performance of the asphalt mixtures.

The surface energy components of nine different types of asphalt binders and five different types of aggregates were measured using the Wilhelmy plate method and the USD, respectively. All materials were obtained from the Strategic Highway Research Program (SHRP) Materials Reference Library (MRL), Reno, Nevada. In addition to these materials, the surface energy components of 12 modified binders and four minerals were also determined using the Wilhelmy plate method and the USD, respectively. Binder modifications included aging, addition of liquid antistrip agents, and addition of fine filler material. A subset of these materials was also tested using the candidate test methods other than the gold standard tests. Section 3.2.1 provides more details of the materials selected for testing and test methods.

2.3.2 Surface Energy Components of Asphalt Binders and Aggregates

Table 2 presents a summary of observations based on surface energy measurements of several different types of asphalt binders and aggregates with different test methods.

Table 2. Typical Range of Surface Energy Components of Asphalt Binders and Aggregates.

Parameter	Asphalt Binders	Aggregates
Total Surface Energy	The total surface energy is typically in the range of 15 to 45 ergs/cm^2.	The total surface energy is typically in the range of 50 to 400 ergs/cm^2, although the magnitude of the base component is significantly higher.
Lifshitz-van der Waals component	This component is the most significant contributor to the total surface energy. Based on results from the Wilhelmy plate test and sessile drop, this component varies significantly depending on the type of binder.	The magnitude of this component is smaller (30 to 60 ergs/cm^2)compared to the magnitude of the base component (200 to 1000 ergs/cm^2).
Acid–Base component	Most asphalt binders have very small magnitudes of the acid or base component, typically of the order of 0 to 3 ergs/cm^2. This is consistent with the fact that most asphalt binders are weak acids or bases. These small magnitudes can be scaled when multiplied with larger magnitudes of the acid–base components of the aggregate while computing the work of adhesion.	Most aggregates have a small magnitude of the acid component ranging from 0 to 100 ergs/cm^2. The base component of the aggregates is much higher ranging from 200 to 1000 ergs/cm^2.

2.4 PARAMETERS BASED ON SURFACE ENERGY AND THEIR RELATIONSHIP TO PERFORMANCE OF ASPHALT MIXTURES

The link between performance of asphalt mixtures and the surface energy components of their constituent materials is provided by the fundamental principles of thermodynamics and

fracture mechanics. This section provides a summary of the parameters (derived from the surface energy components of asphalt binders and aggregates) that can be used to select materials that are more resistant to moisture damage and can predict the fatigue cracking characteristics of asphalt mixtures.

2.4.1 Moisture Damage

The most evident form of moisture damage is stripping of asphalt binder from the aggregate surface due to exposure to moisture. The correlation between the surface properties of these materials and their tendency to strip in the presence of water is relatively well established in the literature. The three quantities based on the surface energies of asphalt binders and aggregate that are related to the moisture sensitivity of an asphalt mixture are:

- work of adhesion between the asphalt binder and aggregate (W_{AB}),
- work of debonding or reduction in free energy of the system when water displaces asphalt binder from a binder-aggregate interface (W_{ABW}^{wet}), and
- work of cohesion of the asphalt binder or mastic (W_{BB}).

The above three quantities are computed using equations [3], [4], and [6], respectively, and using the surface free energy components of the individual materials. For an asphalt mixture to be durable and have a relatively low sensitivity to moisture, it is desirable that the work of adhesion, W_{AB}, between the asphalt binder and the aggregate be as high as possible. Furthermore, the greater the magnitude of work of debonding when water displaces the asphalt binder from the binder-aggregate interface, W_{ABW}^{wet}, the greater the thermodynamic potential that drives moisture damage will be. Therefore, it is desirable that this quantity be as small as possible. In this research, the two energy terms W_{AB} and W_{ABW}^{wet} were combined into a single parameter that is directly proportional to the moisture resistance of the asphalt mixture as follows:

$$ER_1 = \left| \frac{W_{AB}}{W_{ABW}^{wet}} \right| \qquad \textbf{[8]}$$

The energy parameter, ER_1, was computed for various combinations of different asphalt binders and aggregates by measuring their surface energy components individually. Combinations of binders and aggregates with a higher value of ER_1, will be less sensitive to moisture damage.

Equation [8] defines ER_1 as a parameter that can be used to estimate the moisture sensitivity of asphalt mixtures based on the hypothesis that moisture sensitivity is directly proportional to the dry adhesive bond strength, and inversely proportional to the work of debonding or the reduction in free energy during debonding. The latter term is determined from equation [6], which is reiterated as follows:

$$W_{ABW}^{wet} = \gamma_{AW} + \gamma_{BW} - \gamma_{AB}$$

The term γ_{AB} in equation [6] refers to the interfacial bond energy between the bitumen and the aggregate. Therefore, it can be argued that W_{AB} in the bond energy parameter ER_1 is redundant because the contribution of interfacial energy is accounted for indirectly in the term W_{ABW}^{wet}. However, an important factor that is not accounted for in the energy parameter ER_1 is the wettability of aggregate by the asphalt binder.

Although wettability and adhesion are both related to the surface free energy of materials, they represent different attributes. Wettability refers to the ability of one material to wet the surface of another material. The phenomenological explanation for wetting is as follows. One material will wet the surface of another material if the cohesive bond energy of the former is less than the work of adhesion of the latter. On the other hand, work of adhesion is a measure of the work required to separate the two materials from their interface. For example, commercial epoxy glue might not wet a clean plastic surface, but it develops a very strong adhesive bond with the surface to which it is applied. Wettability also influences the ability of a material to penetrate and impregnate itself into the microtextural features of the solid surface. Therefore, for a given aggregate surface, a bitumen with greater wettability has a stronger affinity to coat the aggregate surface than a bitumen with lower wettability. Better coating of an aggregate surface results in fewer "weak points" or locations for the initiation of moisture damage and corresponds to lower moisture sensitivity of the mix.

Therefore, the wettability of the asphalt binder with the aggregate and reduction in free energy when water causes debonding were combined into another energy parameter ER_2 that is directly proportional to the moisture sensitivity of the asphalt mixture. Mathematically, this is expressed as follows:

$$ER_2 = \left| \frac{W_{AB} - W_{BB}}{W_{ABW}^{wet}} \right| \quad \textbf{[9]}$$

where, W_{BB} is the cohesive bond energy of the bitumen and other terms are as previously described.

The moisture sensitivity of asphalt mixtures is also (intuitively) inversely related to the overall microtexture of the aggregate surfaces, which is approximately proportional to its specific surface area (SSA). In order to accommodate the influence of surface roughness at a micro level, two additional parameters were considered:

$$ER_1 * SSA = \left| \frac{W_{AB}}{W_{ABW}^{wet}} \right| * SSA \quad \textbf{[10]}$$

and

$$ER_2 * SSA = \left| \frac{W_{AB} - W_{BB}}{W_{ABW}^{wet}} \right| * SSA \quad \textbf{[11]}$$

In summary, if the surface energy components for different asphalt binders and aggregates and the specific surface area of the aggregates are known, the four energy parameters described above can be easily calculated for all possible combinations of these materials. The combination of asphalt binder and aggregate with the highest magnitude of energy parameters will be relatively more resistant to moisture damage than other combinations. The energy parameters ER_1 and ER_2 are dimensionless quantities and were selected in Task 2 of this project for use with the dimensionless pi term approach to model performance of asphalt mixtures based on material properties. The SSA of aggregates was combined with these two terms in Section 2.6 and was compared with laboratory performance of certain mixes.

2.4.2 Fatigue Cracking and Healing

Fatigue cracking and healing of asphalt mixtures is a process that is concentrated mostly in the mastic phase (asphalt binder + material passing the # 16 sieve) of the mix *(6)*. Initiation and growth of cracks in the asphalt mastic is dependent on several material properties such as the

creep compliance characteristics of the undamaged part of the mix, the rate of energy dissipated due to crack growth, and work of adhesion between the binder and the aggregate, which is determined from the surface energies of the components. It is therefore necessary that any method that predicts fatigue cracking in asphalt mixtures must take into account the effect of all the important material properties in tandem and not just the effect of surface energy and concomitant work of adhesion or cohesion in isolation.

The material properties, other than surface energy, that are required to model and predict the growth of fatigue cracks can be obtained by conducting simple tests using the DMA on asphalt mastics. The use of a DMA in conjunction with surface energy measurements to predict fatigue cracking and healing characteristics of asphalt mixtures was envisioned and emphasized during the early stages of this project.

In 1984 Schapery *(7)* demonstrated that load induced energy that causes cracks to form in a viscoelastic medium is stored on the newly formed crack faces within the body. Researchers from the Texas Transportation Institute used Schapery's theory of damage in viscoelastic materials to develop equations to model the growth of fatigue cracks in asphalt mastic based on the properties of its constituent materials. The incremental growth in a crack described by the crack growth index, $R(N)$, at any given number of load cycles, N, is given by the following equation:

$$\Delta R(N) = R(N) - R(1) = \left[\frac{(2n+1)^{n+1}}{(4\pi)^n} \left(\frac{G_R}{E_1} \right)^n \left(\frac{b}{\Delta G_f} \right)^n N \right]^{\frac{1}{2n+1}} \quad \textbf{[12]}$$

where,

$$n = 1 + \frac{1}{m} \quad \textbf{[13]}$$

$R(1)$ is the crack radius index in the first cycle. This term is considered to be negligible in this analysis for a large value of N. $\Delta R(N)$ is the change in crack radius index for $N > 1$. Various terms related to material properties used in equations [12] and [13] are described as follows. Crack growth in asphalt mixtures can occur either within the binder or at the binder-aggregate interface. The former is referred to as cohesive cracking and the latter is referred to as adhesive cracking. Typically, adhesive failure will occur if asphalt binder film is very thin and cohesive failure will occur if it is very thick *(8)*. Researchers at the Texas Transportation Institute are currently developing models to identify if the crack propagation is predominantly cohesive or adhesive for any given type of mix. The term ΔG_f refers to the adhesive bond energy or cohesive bond energy depends on whether the crack propagation is predominantly adhesive or cohesive in nature, respectively. The adhesive bond energy that has the same magnitude as the work of adhesion is computed from the surface energy components of the asphalt binder and the aggregate using equation [3]. The cohesive bond energy that has the same magnitude as the work of cohesion is computed from the surface energy components of the asphalt binder using equation [4].

The terms m and E_1 are obtained by conducting a low magnitude constant strain relaxation test on the mastic sample and fitting the following form to the measured modulus, $E(t)$, with respect to time t:

$$E(t) = E_0 + E_1 t^m \quad \textbf{[14]}$$

In equation (13), G_R is the reference undamaged shear modulus of the mastic obtained from the first cycle of a low strain test in the DMA under the assumption that no damage occurs in the sample during that cycle. Appendix I presents a brief description of the methodology for testing mastic samples with the DMA.

Hysteresis in the stress-strain curve for a given load cycle is a measure of the dissipated energy due to damage for perfectly elastic materials. However, for viscoelastic materials, a significant part of the hysteresis is due to the viscoelastic nature of the material, which causes it to recover or relax over a period of time. For these materials, the dissipated energy due to damage may be quantified by eliminating the effect of time-dependent recovery or relaxation from the total hysteresis. One method for doing this is to measure the hysteresis from a stress-pseudo-strain curve in lieu of a stress-strain curve. The dissipated energy measured in this manner is referred to as the dissipated pseudo-strain energy (DPSE). In a cyclic load test, the pseudo-strain is obtained by correcting the strain amplitude for viscoelastic recovery as follows:

$$\varepsilon^R(t) = \frac{1}{G_R}\left(\varepsilon_0 \left|G^*(\omega)\right| \sin\left(\omega t + \phi\right)\right) \quad \textbf{[15]}$$

where, $\varepsilon^R(t)$ is the pseudo-strain, $\varepsilon_0(t)$ is the strain amplitude, $\left|G^*(\omega)\right|$ is the linear viscoelastic dynamic modulus in shear, G_R is the reference modulus as described previously, and ϕ is the linear viscoelastic phase angle. The last two terms are experimentally measured using the DMA at a low strain amplitude. In a cyclic load test the DPSE, denoted as W_R, is measured as the area in the stress-pseudo-strain hysteresis curve for any given cycle. The parameter *b* in equation [12] is obtained by determining the relationship between the DPSE and number of load cycles, *N* (N > 1), from experimental data using the following form:

$$W_R = a + b\ln(N) \quad \textbf{[16]}$$

For some asphalt mastics, the relationship between the DPSE and number of load cycles is better expressed using the following form instead of equation [16]:

$$W_R = a + cN^b \quad \textbf{[17]}$$

In such cases, a modified form of equation [12] must be used. Details pertaining to the relevant equation for this case and derivations for all the aforementioned equations can be found elsewhere *(9-11)*.

Kim et al. *(6)* evaluated two SHRP-classified binders, AAD-1 and AAM-1 by including these binders as part of a mastic and testing them in the DMA mode. The mechanical response during DMA testing was monitored using three indicators: change in dynamic modulus, change in pseudo-stiffness, and change in DPSE. Ten, 2-minute rest periods were introduced during the torsional, controlled-strain fatigue testing. The cumulative effect of the rest periods was to extend the life of the samples by approximately 30 percent for the mastic containing AAM-1 and approximately 12 percent for the mastic containing AAD-1. The incremental rest periods were introduced when the mastics incurred approximately equal levels of damage during the experiments. Introducing the rest periods when approximately the same level of damage has occurred in the samples is important, as the healing response is indeed sensitive to the level of damage incurred at the time of the rest period.

In summary, important material properties can be derived by measuring the surface energy components of asphalt binder and aggregates and by conducting simple mechanical tests using the DMA. These material properties are used to mathematically model the increment in crack growth index, $\Delta R(N)$, from its initial size at any given number of load cycles, *N*, using

principles of fracture mechanics. The parameter $\Delta R(N)$ is directly related to the fatigue cracking characteristics of the asphalt mixture. Also note that the terms $\left(\frac{G_R}{E_1}\right)$ and $\left(\frac{b}{\Delta G_f}\right)$ in equation (13) are dimensionless quantities based on the material properties. These terms were selected based on improvisations to the model used for experiment design in phase I of this project. In order to compare the fatigue characteristics of various mixes, a predetermined value of N was selected for all materials and the value of $\Delta R(N)$ was determined. A material with a smaller value of $\Delta R(N)$ for a given number of load cycles will demonstrate better resistance to fatigue cracking.

2.5 ENERGY PARAMETERS AND FIELD PERFORMANCE OF ASPHALT MIXTURES

In section 2.4.1, four energy parameters were proposed as indicators of the moisture sensitivity of asphalt mixtures. These parameters can easily be determined using the surface energy components of asphalt binders and aggregates. In section 2.4.2 a crack growth index was proposed as an indicator of the fatigue cracking characteristics of asphalt mixtures. This parameter can be determined using the surface energy components of the asphalt binder and the aggregate and by conducting simple tests on the asphalt mastic using the DMA. This section demonstrates the correlation between these parameters and field performance of selected asphalt mixtures.

2.5.1 Moisture Damage

The most direct approach to evaluate the relationship between energy parameters and resistance of asphalt mixtures to moisture damage is to compare these parameters for various mixes with their known field performance. Unlike laboratory tests, it is difficult to control and quantify the moisture sensitivity of field mixes on a uniform scale due to the differences in environmental and field conditions that influence these mixes. Nevertheless, it is still possible to qualitatively assess moisture sensitivity of the field mixes. This subsection presents the findings from an independent study that compared moisture sensitivity of field mixes with two of the four energy parameters proposed earlier in equations [8], [9], [10], and [11]. The last two energy parameters that include the effect of SSA were not included in the comparison since adequate replicate data to establish the SSA of aggregates were not available. The results presented in this section are based on the experimental and analytical techniques used to measure surface energies and calculate energy parameters that were developed in this research *(10)*.

A total of eight field mixes from Texas and Ohio were included in this study. The moisture sensitivity of these mixes was classified as "good" or "poor" based on the inspection of pavements, field cores, and laboratory tests *(10)*. The eight mix designs comprised six different types of asphalt binders and eight different types of aggregates. Some mixes had a combination of more than one type of aggregate. Surface energy components of each type of asphalt binder and aggregate were determined using the Wilhelmy plate method and the USD method, respectively. The test protocols developed in this research were used for these measurements. Since the final test protocol, Appendix B, was not available at the time these components were tested, ethylene glycol was not used as one of the five probe liquids to measure the surface energy components of the asphalt binder.

Surface energy values of the asphalt binder and aggregate were measured and used to compute the energy parameters ER_1 and ER_2. One advantage of this methodology is that because surface free energy components of various asphalt binders and aggregates are measured individually, it is possible to compute the energy parameters for all possible combinations of binder and aggregate and not just the combinations for the selected eight mixes. The energy parameters were calculated for each binder-aggregate pair for mixes that contained more than one type of aggregate. It is reasonable to consider that the binder-aggregate combination that provides the poorest or most critical values of these parameters will govern the performance of the mix. Figures 5 and 6 illustrate the comparison of field performance with the two energy parameters.

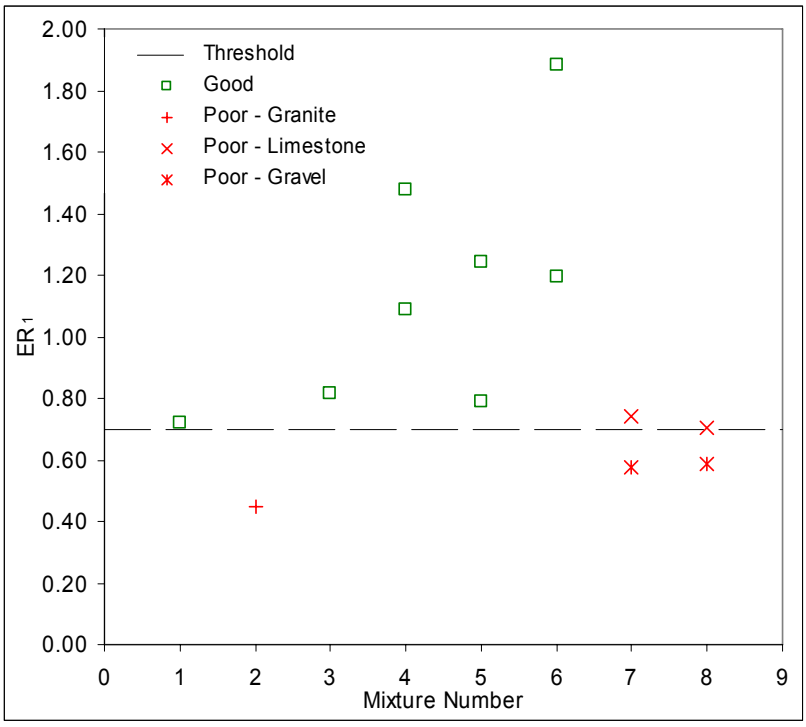

Figure 5. Field Performance of Mixes vs. ER_1.

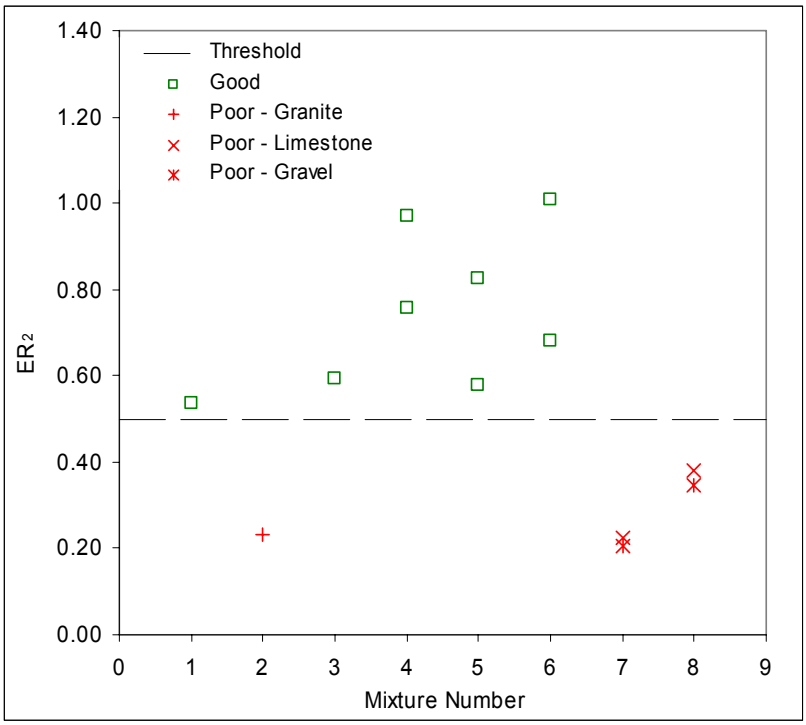

Figure 6. Field Performance of Mixes vs. ER_2.

Important Observations

Mixes 7 and 8 contain more than one aggregate (limestone and gravel), and both mixes were reported to be moisture sensitive based on field performance. Since both aggregates were present in significant proportions in each mix, it is reasonable to consider that failure of any one type of aggregate can render the entire mix moisture sensitive. Based on the data, it appears that a threshold value of the energy parameter can be derived to differentiate between mixes that were reported to have good performance with at least one combination of binder and aggregate from the mixes that were reported to have poor moisture resistance. The aforementioned comparisons do not normalize the effect of differences due to traffic or environment, which certainly contribute to some variability in the results. Therefore, while a generalized conclusion can be made that energy parameters may be used to segregate mixes based on their moisture sensitivity, data from this limited comparison must not be considered as conclusive.

2.5.2 Fatigue Cracking

Section 2.4.2 presents a model that incorporates the effect of surface energy of asphalt binders and aggregates and material properties measured using the DMA to predict fatigue cracking characteristics of asphalt mixtures. In another independent study conducted in conjunction with this research, three asphalt mixtures with fair, intermediate, and good fatigue performance were selected based on qualitative field performance *(10, 11)*. The methodologies developed in this research were used to measure the surface energy components of the asphalt binder and aggregates used in these mixes with the Wilhelmy plate method and the USD, respectively. Samples prepared from mastics used to fabricate these mixes were tested using the DMA to obtain material properties as described in section 2.4.2. Equation (13) was used to

determine the change in crack growth index after 50,000 cycles. Table 3 summarizes the results from this study.

Table 3. Fatigue Cracking of Field Mixes and Crack Growth Modeled Using Surface Energy Measurements.

Mix	Fatigue cracking reported from qualitative field observations	ΔR @ 50,000 cycles			
		Case: ΔG_f is adhesive bond energy[1]		Case: ΔG_f is cohesive bond energy[2]	
		Avg.	St. Dev.	Avg.	St. Dev.
A	Good	6.5	0.54	5.9	0.57
B	Intermediate	10.4	2.24	7.6	1.17
C	Fair	15.1	1.34	11.1	1.13

1 Considered predominately adhesive failure in the mastic.
2 Considered predominately cohesive failure in the mastic.

The value of ΔR presented in Table 3 is the increase in crack growth from the initial state of the mix until after the application of the 50,000 load cycles. This value is determined by taking into account the effect of surface energies of the binder and aggregate and material properties determined by conducting a test on the mastic sample using the DMA. Although the mixes are limited in number, these data demonstrate the importance of including the work of adhesion or cohesion (as it is related to change in crack length in equation [12]) based on surface energy of the constituent asphalt binder and aggregates to estimate the crack growth characteristics of asphalt mixtures.

2.6 ENERGY PARAMETERS AND LABORATORY PERFORMANCE OF ASPHALT MIXTURES

The previous section presented results that compare the moisture sensitivity and fatigue cracking characteristics based on field performance of asphalt mixtures with parameters determined using the surface energies of their constituent materials. The field performance of these mixes was only qualitatively established and not normalized for the effect of possible differences in traffic and environment. Therefore, controlled laboratory characterization of moisture sensitivity, fatigue cracking, and healing characteristics of some asphalt mixtures was required to further demonstrate the relationship between energy parameters and performance of asphalt mixtures.

This section describes the relationship between the four energy parameters (equations [8], [9], [10], and [11]) and the moisture sensitivity of asphalt mixtures measured using mechanical tests in the laboratory. The application of work of adhesion (determined using surface energy measurements) and the material properties obtained using the DMA to predict the fatigue cracking and healing characteristics of asphalt mixtures using equation [12] are also demonstrated. A strong correlation between the work of adhesion and fatigue cracking of asphalt mixtures is not likely since the former is only one of a number of important material properties that are used as inputs in a fatigue cracking model to predict the latter. However,

Table 3 does demonstrate a good comparison of the field performance of asphalt mixtures with the performance predicted using equation [12].

2.6.1 Materials and Laboratory Tests

Twelve mixtures were selected for the mechanical tests using aggregates RA (granite), RK (basalt), and RL (limestone) and asphalt binders AAB, ABD, AAD, and AAE. Among the nine neat asphalt binders measured using the Wilhelmy plate method, asphalt AAB has the lowest cohesive bond energy of about 27 ergs/cm^2 and the asphalt ABD has the highest cohesive bond energy of about 65 ergs/cm^2. Among the 45 possible combinations of nine asphalt binders and five aggregates with known surface energies, the work of adhesion between AAB and RL was one of the highest and that between AAD and RA was one of the lowest. Similarly, the magnitude of work of debonding when water displaces asphalt from the asphalt-aggregate interface was one of the highest for the combination of AAD and RL and one of the lowest for the combination of AAB with RK. Another important factor that differentiated the three selected aggregates was their specific surface area. The specific surface areas of RA, RL, and RK were on the order of 0.1, 1, and 10 m^2/g, respectively. Therefore, selection of these three aggregates and binders provides a range of different values for binder and mastic cohesion, binder-aggregate adhesion, and binder-aggregate debonding. The selected asphalt mixtures were designed using the same aggregate gradation.

Two types of mechanical tests were conducted on the selected mixes. The first was mechanical tests on dry and moisture conditioned samples of whole mixes. Appendix I presents details of the mixtures, mechanical tests, and the moisture conditioning procedure. The ratio of a mechanical property of the mix in a wet condition to the property in a dry condition was used as a measure of the moisture sensitivity of the asphalt mixture. Results from other studies indicate that use of three linear variable displacement transducers (LVDTs) with two replicate samples for similar test setups in compression yield a standard error of about 9 to 13 percent *(12)*. This was used as a guideline in this study and tests were conducted with at least two replicate specimens for each mixture design and each condition (dry or moisture conditioned) and three LVDTs per specimen.

Table 4 presents a summary of tests and responses that were selected to quantify moisture sensitivity. In addition to the tests mentioned in Table 4, dynamic modulus in compression was also measured on the asphalt mixture samples. However, the ratio of compressive modulus of moisture conditioned samples to compressive modulus of dry samples for different mix designs did not vary significantly, and therefore these are not included here. Fatigue life in the direct tension mode of loading for the asphalt mixtures is defined as the number of load cycles until the sample accumulates 1 percent permanent deformation. This criterion was selected because accurate measurements of strain until failure could not be practically measured for all samples.

The second type of mechanical tests were conducted only on the mastic portion of the selected asphalt mixtures using the DMA. These tests were used to determine the material properties (other than work of adhesion) that are input to model the fatigue cracking and healing characteristics of asphalt mixtures. Appendix I presents further details of this test method.

Table 4. Summary of Mechanical Tests and Parameters to Quantify Moisture Sensitivity of Asphalt Mixtures.

Test Type	Test Parameters	Parameters to estimate moisture sensitivity	Sample Size
Dynamic Modulus (Tension)	Haversine loading in tension at 10 Hz and 25°C at low stress level for 200 cycles	Ratio of wet to dry tension modulus of mix	Diameter: 75 mm Height: 150 mm Obtained by sawing & coring a 100 mm diameter and 175 mm high sample compacted using the Superpave gyratory compactor
Dynamic Creep	Haversine loading in tension at 10 Hz and 25°C at high stress level until sample fails	Ratio of wet to dry number of load cycles required for 1% permanent deformation	

2.6.2 Moisture Damage

Two different parameters derived from laboratory tests were used to quantify the moisture sensitivity of asphalt mixtures (Table 4). Four energy parameters (equations [8], [9], [10], and [11]) were proposed in the earlier sections of this report as independent measures of the moisture sensitivity of the asphalt mixtures based on the surface energy components of asphalt binders and aggregates and the specific surface area of the latter. Detailed statistical analysis of laboratory test indicates there is a significant correlation between laboratory performance of the mixes and the energy parameters.

The statistical analysis was conducted on two data sets. In the first data set, moisture sensitivity of the asphalt mixtures measured in the laboratory was quantified as the ratio of the average wet tensile modulus or fatigue life to the average dry tensile modulus or fatigue life. This data set was comprised a total of twelve points, each corresponding to a mixture type. In the second data set, moisture sensitivity of the asphalt mixtures was quantified as the ratio of the wet tensile modulus or fatigue life to the dry tensile modulus or fatigue life for each pair of replicates. This data set comprised a total of 24 points with a set of two points corresponding to two replicates for each mixture type. Statistical analysis from both these data sets showed very similar results. Results based on the first data set only are presented here because this data set demonstrated better compliance to various assumptions required for the statistical analysis such as normality of errors and constant variance. Figures 7 through 14 illustrate the correlation of the four energy parameters (equations [8], [9], [10], and [11]) with the moisture sensitivity of asphalt mixtures measured in the laboratory, along with the 95 percent confidence limits (C.L.).

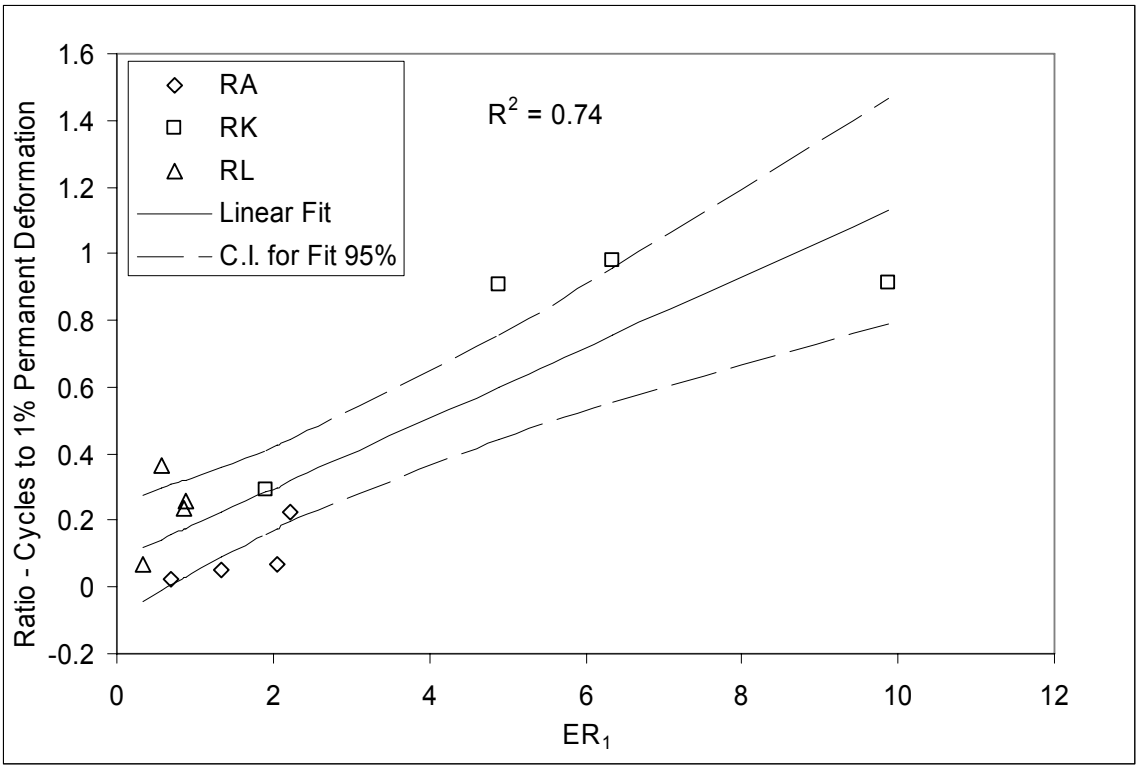

Figure 7. Laboratory Performance of Mixes Based on Fatigue vs. ER_1.

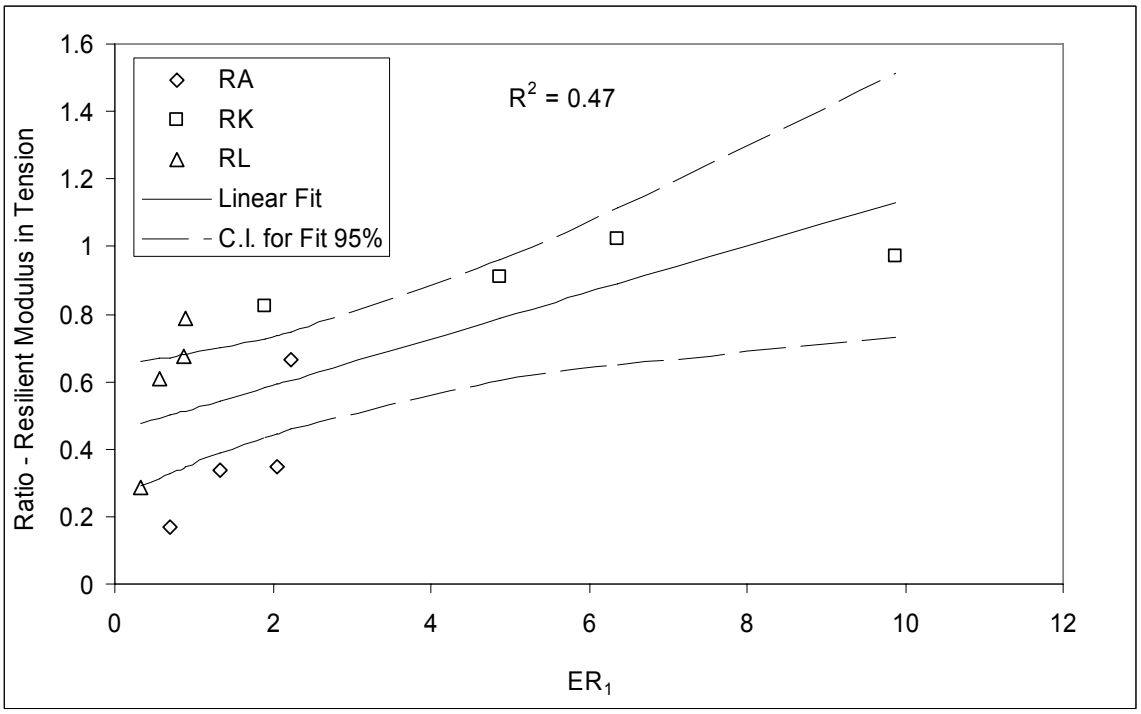

Figure 8. Laboratory Performance of Mixes Based on Resilient Tension Modulus vs. ER_1.

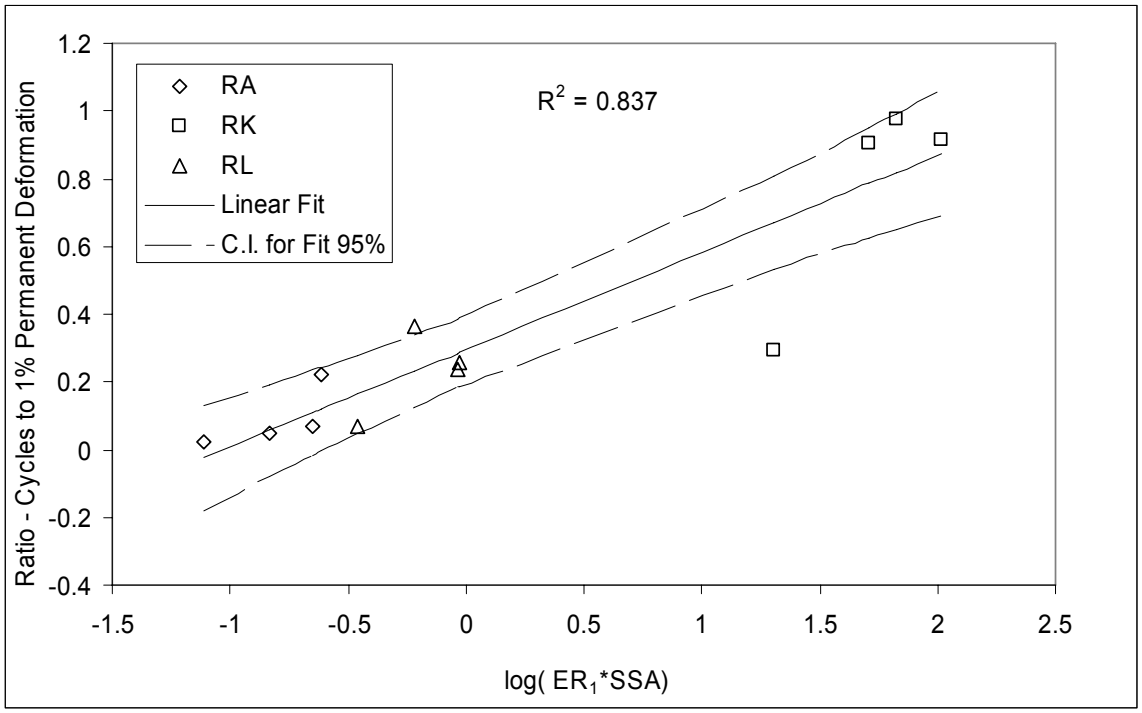

*Figure 9. Laboratory Performance of Mixes Based on Fatigue vs. ER_1*SSA.*

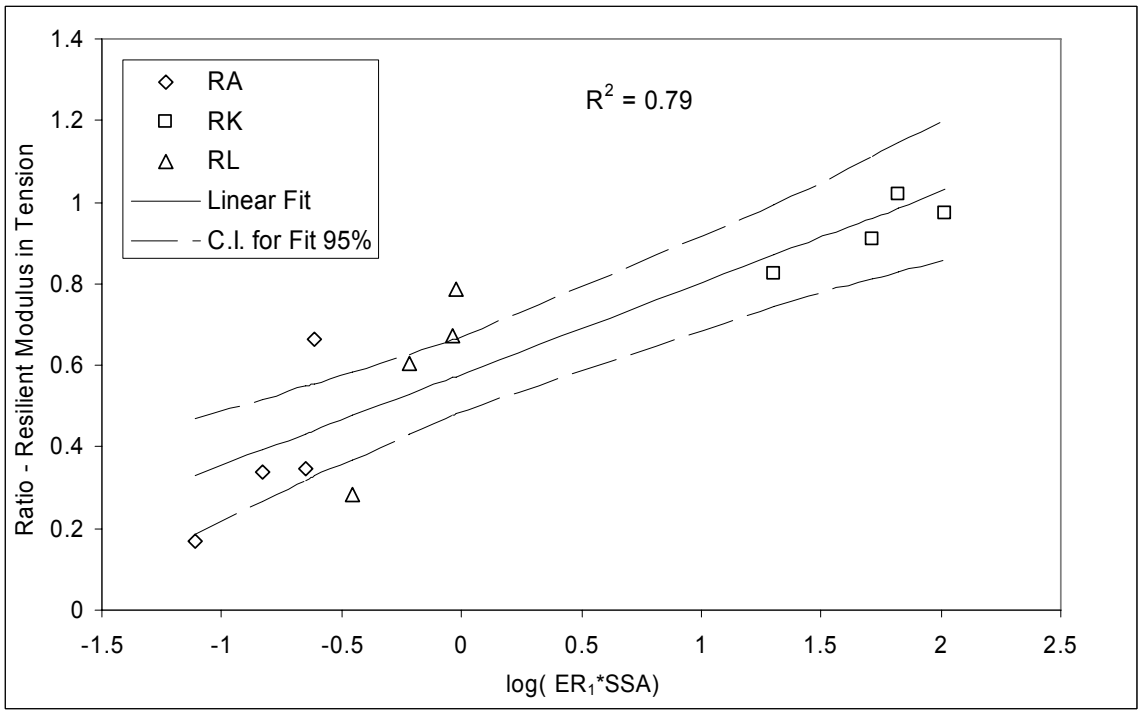

*Figure 10. Laboratory Performance of Mixes Based on Resilient Tension Modulus vs. ER_1*SSA.*

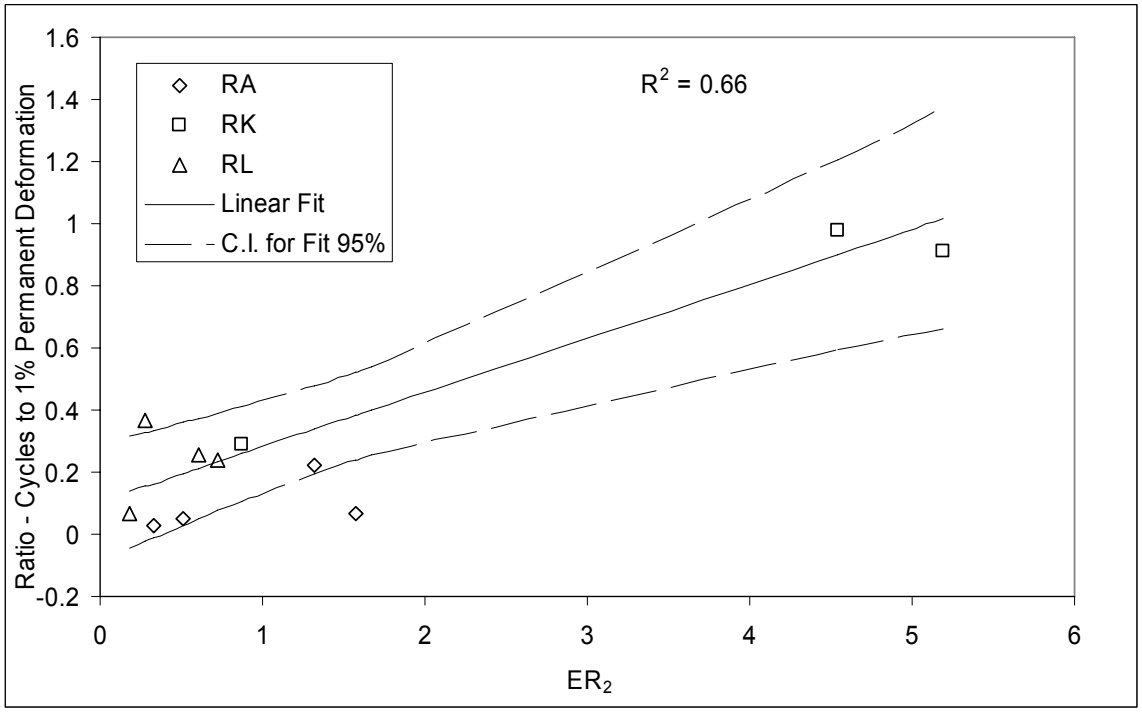

Figure 11. Laboratory Performance of Mixes Based on Fatigue vs. ER_2.

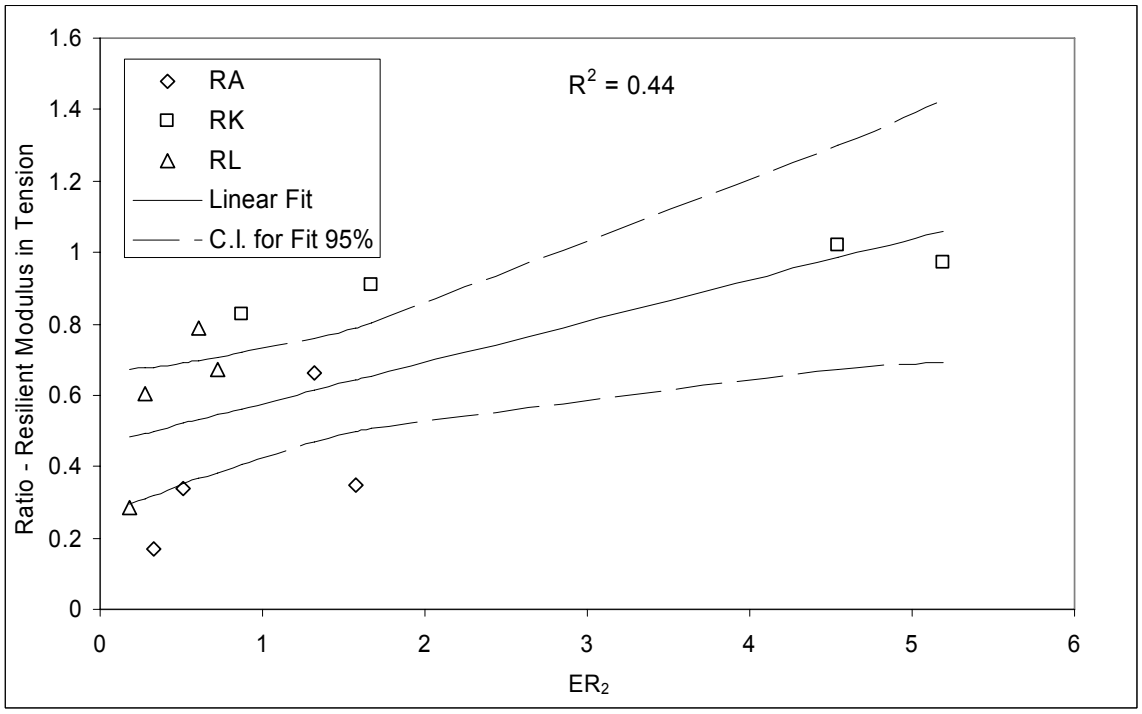

Figure 12. Laboratory Performance of Mixes Based on Resilient Tension Modulus vs. ER_2.

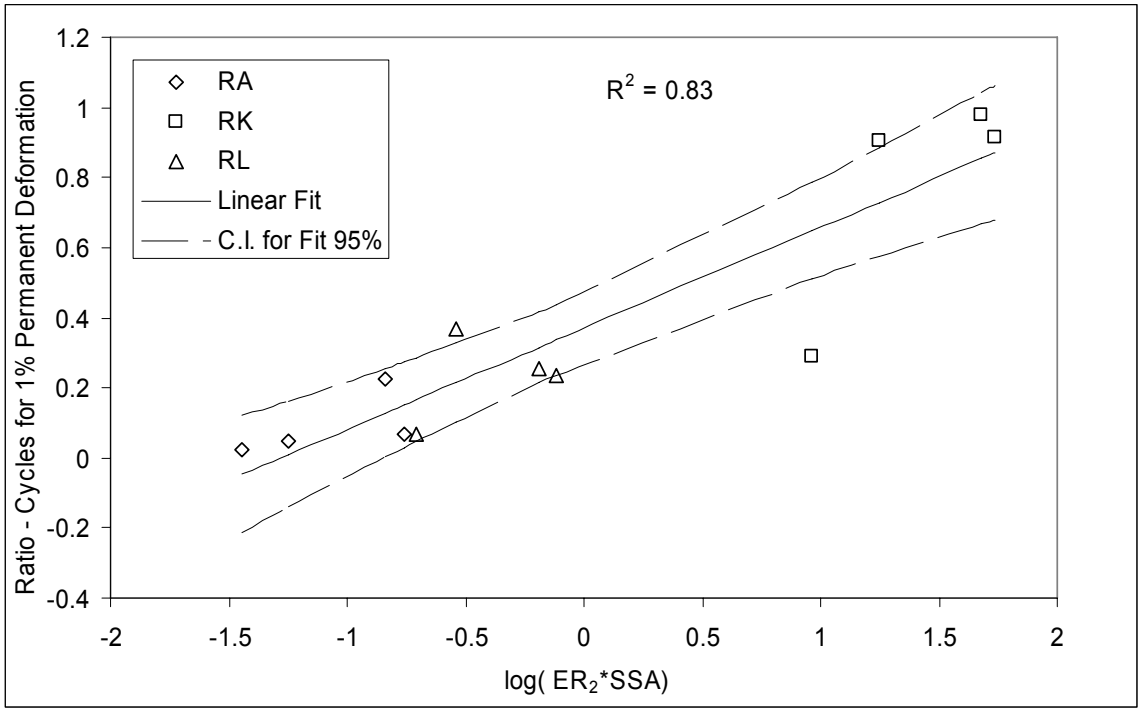

*Figure 13. Laboratory Performance of Mixes Based on Fatigue vs. ER_2*SSA.*

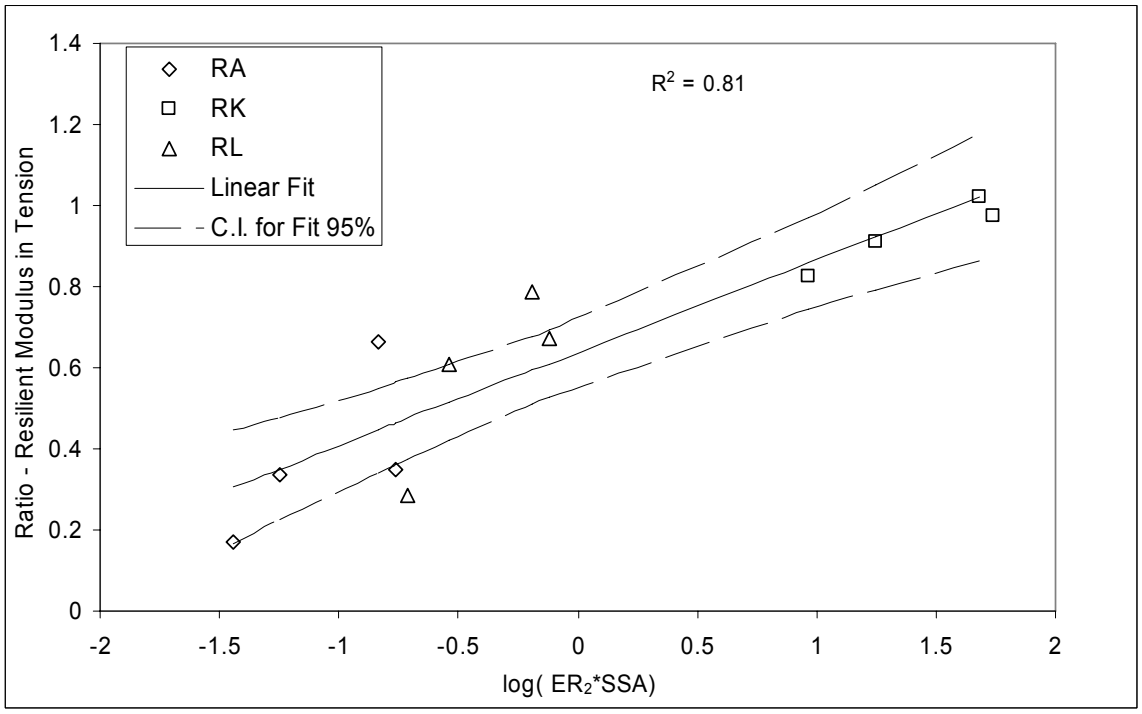

*Figure 14. Laboratory Performance of Mixes Based on Resilient Tension Modulus vs. ER_2*SSA.*

Important Observations

Important observations based on the results presented in Figures 7 through 14 are as follows:

- The correlation between the bond energy parameters multiplied by the specific surface area of the aggregates and the moisture sensitivity of the asphalt mixtures is presented on a log-normal scale. Because the specific surface areas of the three aggregates differed by an order of magnitude and using a log scale facilitated the comparison.
- Examination of Figures 7 and 8 shows that when the parameter ER_1 is used without taking into consideration the SSA of the aggregates, there is a fair correlation between the energy parameter and the performance for each aggregate type. However, the overall correlation of the laboratory performance of the mix with the energy parameter was not as good when all twelve mixes comprised the three different aggregate types were considered. This indicates that another material property related to aggregates, such as the SSA, must also be included with the energy parameters to predict performance.
- Detailed statistical analysis revealed that the residual errors for Figures 7 through 10 were not random, suggesting the need to include another term in the model. The observed trends in the residual errors were reduced significantly when SSA was also included with the energy parameter. Figure 15 illustrates a typical comparison of residual errors between ratio of load cycles for 1 percent permanent deformation versus ER_1 and log ratio of load cycles for 1 percent permanent deformation versus $\log(ER_1 * SSA)$.

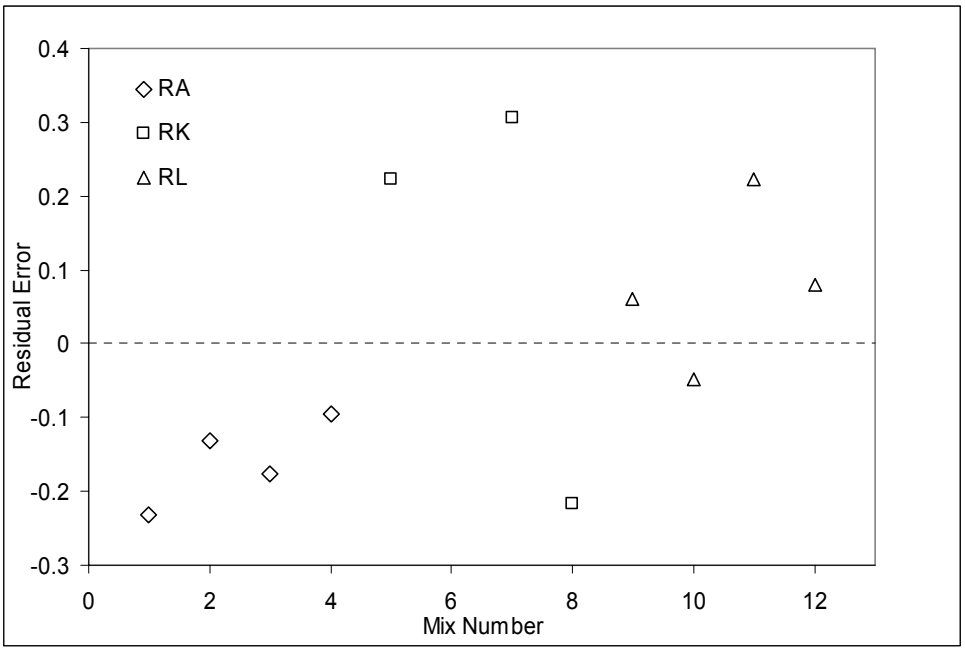

Figure 15(a). Residuals for Ratio of Cycles to 1 Percent Permanent Deformation vs. ER_1.

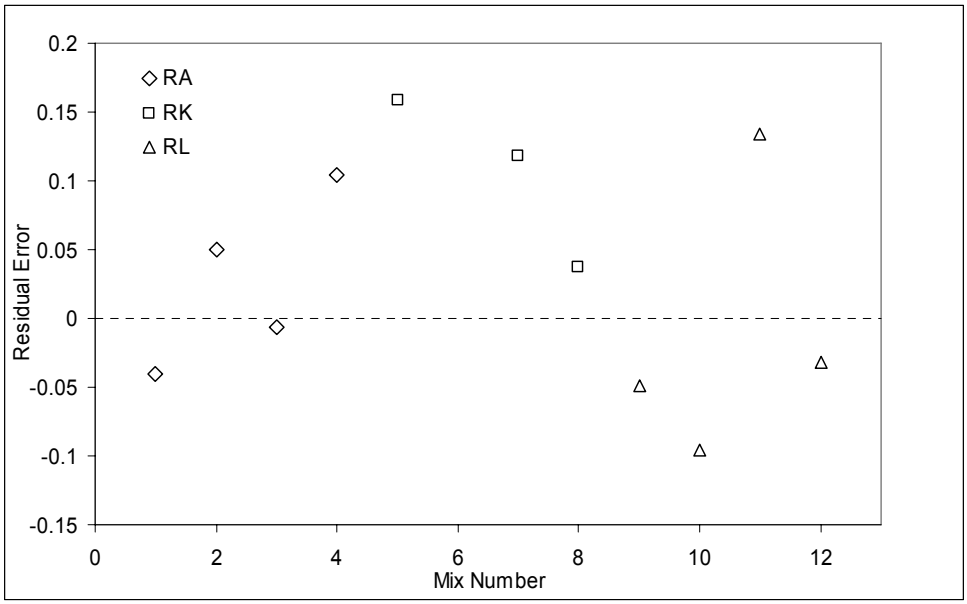

*Figure 15(b). Residuals for log (Ratio of Cycles to 1 Percent Permanent Deformation) vs. log (ER_1*SSA).*

- Although some of the energy parameters relate better to moisture sensitivity of mixes than others, it is recommended that all four parameters be considered in future research and evaluative studies. All of these parameters can be computed for any asphalt binder-aggregate pair by measuring their surface energy components and the SSA of the aggregates. The SSA of aggregates is measured using the USD as a part of the test that is used to measure the surface energy components.
- In general, the results indicate that the surface energy components and concomitant energy parameters can be effectively used as a materials selection tool to identify combinations of aggregates and asphalt binders that result in moisture sensitive asphalt mixtures. In this laboratory testing various mixture properties such as aggregate gradation and volumetrics were tightly controlled. Therefore, models such as those presented in section 2.4.2 must be employed to predict performance of mixes with the realization that bond energies and SSA offers a way to compare moisture resistance on a relative basis.

2.6.3 Fatigue Cracking and Healing

This section presents a summary of how the surface energy components and the concomitant work of adhesion between asphalt binder and aggregates can be combined with other material properties measured using the DMA into a single parameter that predicts the crack growth characteristics of different asphalt mixtures. Figure 16 illustrates a flow diagram of tests and properties that are required to predict the fatigue cracking characteristics of the asphalt mixture. Unlike moisture damage, a direct correlation between fatigue cracking life or healing from laboratory experiments and the work of adhesion cannot be drawn, since the latter is only one important material property used as an input to accurately estimate the fatigue cracking life of the mix. Figures 17(a) and 17(b) present a comparison of the fatigue life of full asphalt mixtures measured in the laboratory with the crack growth index $\Delta R(N)$ considering

predominantly cohesive and adhesive failures in the mastic, respectively. The crack growth index was determined using surface energy measurements and material properties by testing the mastic samples with the DMA. The fatigue life was determined from the direct tension test on the dry mixes used for the laboratory evaluation of moisture sensitivity. Appendix I presents details of the cyclic load tests on the asphalt mixtures in the direct tension mode and tests with the DMA on asphalt mastics that were used to estimate the fatigue life and derive material properties used to calculate the crack growth index.

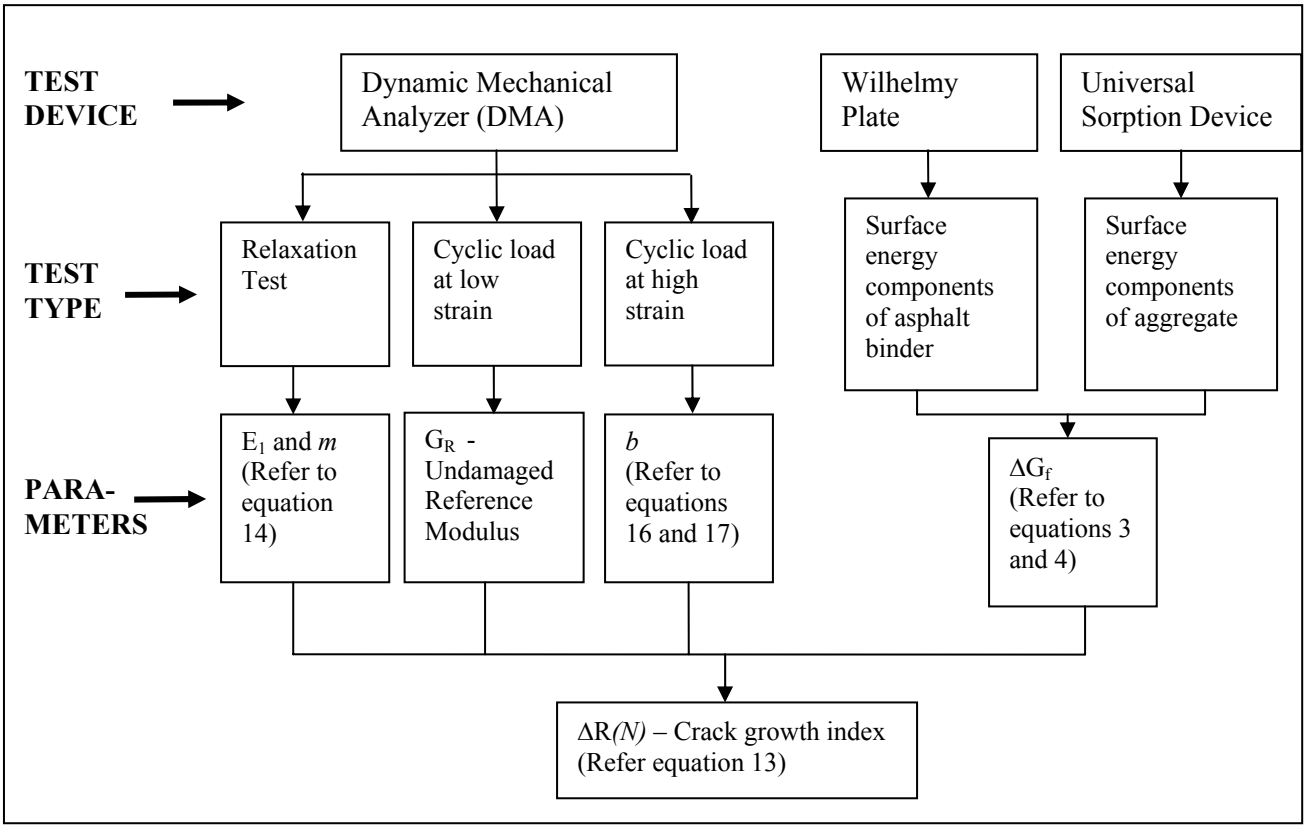

Figure 16. Flow of Steps to Assess Fatigue Cracking Characteristics of Asphalt Mastics.

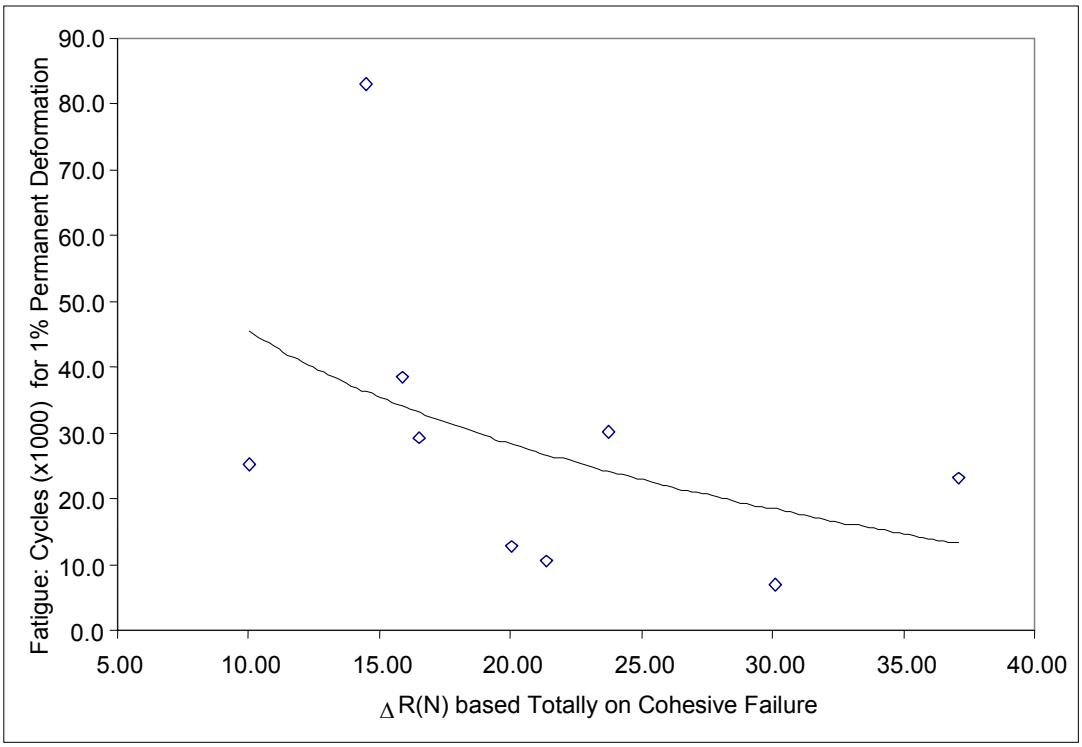

Figure 17(a). Fatigue Life of Asphalt Mixtures Measured in Laboratory vs. ΔR(N) Based Totally on Cohesive Failure.

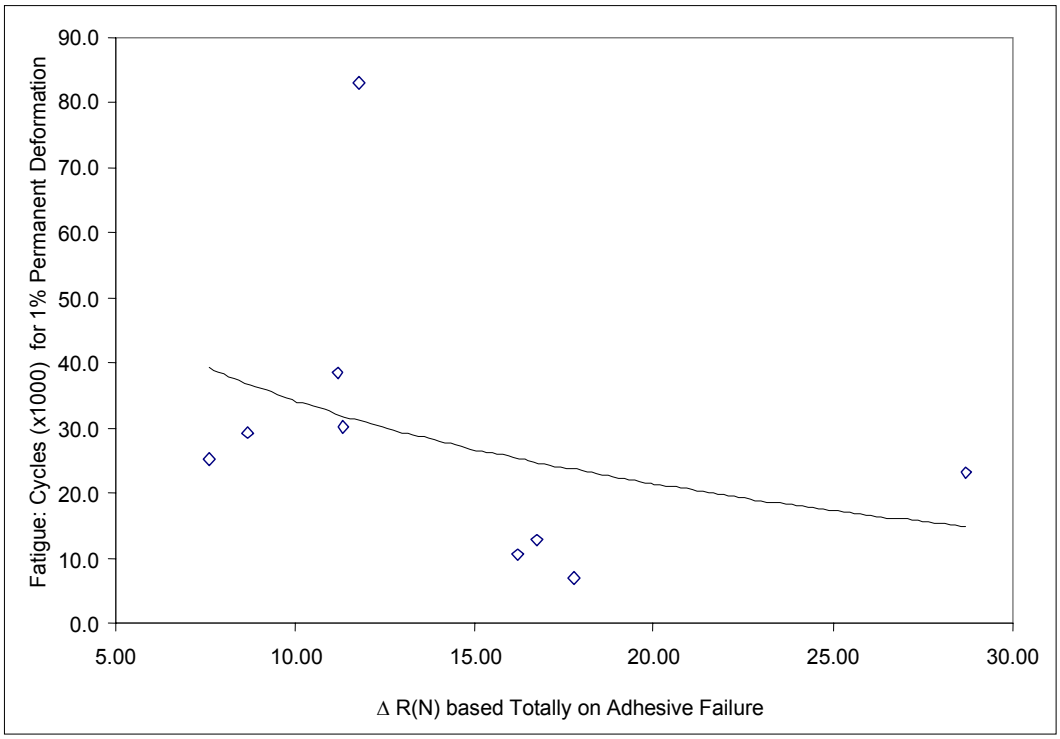

Figure 17(b). Fatigue Life of Asphalt Mixtures Measured in Laboratory vs. ΔR(N) Based Totally on Adhesive Failure.

Table 5 enumerates the fatigue cracking characteristics of the nine asphalt mixtures that were included in this research based on the surface energy measurements made using the Wilhelmy plate method and the USD and tests on mastic samples with the DMA.

Table 5. Fatigue Cracking Characteristics of Nine Asphalt Mixtures.

Mix Design	Properties from testing mastic samples with DMA				Properties from Surface Energy Measurement		ΔR(*N*) – Predicted based on:	
	m	E_1 (x10^6Pa)	G_r (x10^6Pa)	b	ΔG_f (Adhesion)	ΔG_f (Cohesion)	100% Adhesive Failure	100% Cohesive Failure
RA AAB	0.372	37.3	118.0	226	118	27	8.7	16.5
RA AAD	0.360	38.2	98.7	126	70	37	7.6	10.0
RA ABD	0.462	59.9	248.0	231	105	65	11.8	14.5
RK AAB	0.600	20.0	136.0	224	95	27	17.8	30.1
RK AAD	0.670	23.3	145.0	268	69	37	28.7	37.1
RK ABD	0.505	40.2	263.0	272	99	65	16.8	20.1
RL AAB	0.626	17.2	86.1	162	158	27	11.4	23.7
RL AAD	0.448	34.1	118.0	202	83	37	11.2	15.9
RL ABD	0.592	44.1	231.0	314	126	65	16.2	21.4

The cyclic load tests conducted with the DMA were used to establish the fatigue life of the mix. The parameter $N\frac{G_N^*}{G_1^*}$ can also be used to obtain a gross estimate of the fatigue life of the asphalt mastic sample. In this parameter, N is the number of load cycles, G_N^* is the shear modulus at the N^{th} load cycle, and G_1^* is the shear modulus at the first load cycle. As the cyclic test of a mastic sample with a DMA progresses, the value of $N\frac{G_N^*}{G_1^*}$ increases to attain a peak and then drops off. The number of load cycles for the maximum value of this parameter is used to quantify the fatigue life of the mix. Kim et al. *(13)* established that this parameter is a logical approximation of fatigue life and corresponds to the peak value of the phase angle during the DMA test *(14)*.

In order to evaluate the effect of healing on the fatigue life of asphalt mixtures, nine rest periods of four minutes each were applied to each specimen. The rest periods were applied at 2.5, 5, 10, 15, 20, 25, 30, 40, and 50 percent of the lowest fatigue life value, obtained by testing various replicates of that particular mix design without any rest period. The effect of healing was quantified in two ways: first in the form of percentage increase in the measured fatigue life of the mastic and second in the form of percentage decrease in the parameter ΔR(N) determined using equation [12]. The latter was obtained using the same sequence of steps as in the case of mixes without rest periods. The only difference in the case of rest periods was that the parameter b in equations 15 and 16 was determined using the DPSE values after rest periods.

From the results of the nine mixes tested with the DMA, it was found that only mixes with the asphalt binder ABD showed a significant improvement in fatigue life and decrease in the value of $\Delta R(N)$. The work of cohesion for this asphalt binder is 65 ergs/cm^2, whereas the work of cohesion for AAB and ABD are 27.2 and 37.2 ergs/cm^2, respectively. The work of cohesion is the magnitude of work required to fracture the surface of a material to form two surfaces of unit area each. Therefore, cracks in an asphalt binder with a higher magnitude of work of cohesion will have a greater propensity to heal compared to asphalt binders with a lower magnitude of work of cohesion. This is consistent with the observations for the asphalt binders AAB, AAD, and ABD. However, further research is required to model the effect of healing on crack growth characteristics of asphalt mixtures based on the principles of fracture mechanics.

CHAPTER 3
INTERPRETATION, APPRAISAL, AND APPLICATIONS

3.1 GENERAL CONSIDERATIONS IN MEASURING AND INTERPRETING SURFACE ENERGY COMPONENTS

Direct measurement of surface energy components of a solid is rarely feasible. A more efficient way to determine the surface energy components of materials such as asphalt binders and aggregates is to experimentally measure a manifestation of the surface energy of these materials in the form of physical interactions with various probe liquids or vapors. The experimentally measured interactions are related to the surface energy components of the materials using a suitable theory. This section presents a summary of some of the important considerations necessary to apply this methodology to measure the surface energy components of asphalt binders or aggregates and to interpret the test results.

3.1.1 Selection of Appropriate Probe Liquids

According to the GVOC or acid-base theory *(3, 4)*, the surface energy of any material is composed of three components. These are the LW component, the acid component, and the base component. The work of adhesion between the solid and at least three different probe liquids is measured using a suitable experimental technique. The work of adhesion with different liquids is combined using equation (7) to determine the three surface energy components of the solid. Any liquid may be used as a probe if it satisfies the following criteria:

- The three surface energy components of the probe liquid must be known based on the acid-base theory at the test temperature.
- The probe liquid must be chemically homogenous and pure.
- The probe liquid must not interact chemically with the solid surface that is being investigated. For example, the liquid must not dissolve or chemically react with the solid.
- If the probe liquid is used to measure contact angles over a solid surface, then the surface energy of the probe liquid must be greater than the anticipated surface energy of the solid.

For example, consider the selection of probe liquids for measuring the surface energy components of asphalt binders using any contact angle method. There are approximately 60 pure liquids with known surface energy components based on the acid-base theory. However, most of these tend to dissolve asphalt binders to some extent. During this research it was found that five liquids, namely, water, methylene iodide, formamide, glycerol, and ethylene glycol satisfy the aforementioned criteria and can be used with asphalt binders.

Three different probe liquids are required to determine the three unknown surface energy components of any material by measuring their interfacial work of adhesion and solving for the unknown components in equation [7]. Although theoretically correct, an improper choice of liquids combined with small experimental errors can significantly affect the accuracy of the calculated surface energy components *(15)*. For example, consider the contact angle measurement technique used to determine the surface energy components of asphalt binders. If two or more of the three probe liquids have similar surface energy components, then small errors in the measurement of contact angles will magnify the errors in the computed surface energy components of the asphalt binder. This can often lead to inaccuracies and misinterpretation of the material properties. A mathematical measure of this sensitivity is referred to as the condition number. Since the condition number is a function of the surface free energy components of the

selected probe liquids, it can be computed even before conducting the experiments. A large condition number indicates that the calculated results are very sensitive to small experimental errors and vice-versa. Appendix E describes the mathematical methods required to calculate the condition number for any given combination of probe liquids.

The following example further illustrates the significance of condition number and proper selection of probe liquids. Consider the case when water, formamide, and glycerol are used as the only three probe liquids to measure the contact angles of an asphalt binder with the Wilhelmy plate method to determine its surface energy components. The condition number for this set of liquids is 18.6, and therefore the calculated surface free energy components of asphalt binder based on these three probe liquids can accumulate significant errors even if the errors in the measured contact angles are small. If formamide is replaced by methylene iodide, then the condition number reduces to 4.9, which indicates a significantly reduced sensitivity of the computed results to the measured values. Notwithstanding the benefits of making an appropriate selection of the three probe liquids, it is recommended that in order to minimize errors and improve accuracy, as many probe liquids should be used as is feasible for the test. For asphalt binders with the Wilhelmy plate method or sessile drop method, all five probe liquids recommended earlier must be used. For other methods such as USD, where testing with several liquids might not be feasible due to time constraints, it is recommended that liquids with very distinct properties be selected to reduce the condition number. For example, hexane, methyl propyl ketone, and water (with condition number 4.5) may be used with the USD.

3.1.2 Interpretation of Surface Energy Components

The magnitudes of the surface energy components, especially the acid and base components, of the asphalt binders and aggregates must not be interpreted too literally since these are based on a relative scale proposed by GVOC. The breakup of the total surface energy into the LW component and into the polar or acid-base component for various liquids is easily determined by measuring their interfacial tension with nonpolar liquids such as alkanes. For example, the total surface energy of water is 72.8 ergs/cm^2, with a LW component of 21.8 ergs/cm^2 and a polar or acid-base component of 51 ergs/cm^2. GVOC realized that the further breakdown of the polar or acid-base component into the acid and base components was not possible mathematically. This led them to the assumption that the acid and base components for water are equal. Using this assumption with equation [2], the acid and base components of water were each determined to be 25.5 ergs/cm^2. The three surface energy components of water were then used to determine the surface energy components of other liquids by measuring interfacial tensions. Based on their work and this assumption, GVOC presented the three surface energy components for approximately 60 liquids.

The assumption made by GVOC that the acid and base components of water are equal has been criticized in the literature *(15, 16),* and a few other scales have been proposed. Despite the criticism, the scale proposed by GVOC is still popularly used. In summary it must be remembered that because of this assumption, whereas comparisons of bond energies or work of adhesion for different material combinations may be made, the magnitudes of acid and base components of a given material should not be considered as "true" value [16]. This is because the acid and base components of any material are relative to an assumed value of the magnitude of the acid and base components of water.

3.2 CONSIDERATIONS WITH THE USE OF VARIOUS TEST METHODS AND SURFACE ENERGY COMPONENTS OF DIFFERENT MATERIALS

3.2.1 Materials and Tests

Task 4 of this research had two primary objectives. The first was to measure the surface energy components of several different types of asphalt binders and aggregates using the gold standard tests. The gold standard tests for asphalt binders and aggregates are the Wilhelmy plate method and the USD, respectively. The criteria for selecting these methods as gold standards were described earlier in this report. The second objective of Task 4 was to compare the surface energy components of similar materials measured using different test methods. These comparisons also provided valuable information regarding the precision, accuracy, and practical application of each test method. This information was used to recommend test procedures that may be used on a routine basis to measure surface energy components of asphalt binders and aggregates.

The surface energy components of nine different types of asphalt binders from the SHRP, Materials Reference Library MRL were measured using the Wilhelmy plate method. The selected binders represent a wide range of chemical compositions. It was necessary to conduct limited experiments to determine whether factors such as aging of asphalt binders or addition of fillers or liquid antistrip agents affect the surface energies of these materials. In order to do this, three of the neat asphalt binders were modified by means of aging or addition of fillers and liquid antistrip agents and were included in the test matrix. A subset of the neat and modified asphalt binders was then selected for measurement of surface energy components using the other test methods. The exact number and type of asphalt binders selected for each test method varied depending on practical considerations such as the time required for testing, usefulness of the results, and sample preparation requirements. For example, an asphalt binder with hydrated lime filler was not tested with the IGC or AFM since samples for these methods are prepared using a solution of the asphalt binder in toluene, and it was speculated that this solvent might change the way hydrated lime affects the surface energy of the binder.

The surface energy components of five different aggregate types from the SHRP MRL were measured with the USD. In addition to these aggregates, surface energy components of four pure minerals were also measured with the USD. As in the case of asphalt binders, a subset of these materials was included for measurement of surface energy components with the other selected test methods. Tables 6 and 7 present a summary of the selected asphalt binders, aggregates, and the test methods. Appendix I presents a more detailed mineralogical analysis of the aggregates.

Table 6. Summary of Asphalt Binders Tested Using Various Surface Energy Measurement Methods.

Label	Description [17]	Test Method			
		Wilhelmy plate	Sessile drop	A F M	I G C
Neat Asphalt Binders (Description: MRL Code / Crude Oil Source / SHRP PG Grade)					
AAB	AAB-1 / WY Scour / PG58-22	X	X	X	X
ABD	ABD / Ca Valley / PG58-10	X	X	X	X
AAM	AAM-1 / W TX Inter / PG64-16	X	X	X	X
AAF	AAD-1 / Ca Coast / PG58-28	X	X	X	X
AAH	AAH / Rangely / PG58-22	X	--	X	--
AAL	AAL / Cold Lake / PG58-28	X	--	X	--
ABL	ABL-1 / Boscan / PG64-*	X	--	--	--
AAD	AAD-1 / Ca Coast / PG58-28	X	X	X	--
AAE	AAE (blown) / Lloydminster / PG70-22	X	--	X	--
Modified Asphalt Binders (Modification)					
AAB-AG	Aged AAB**	X	X	X	--
AAB-LS	AAB + Limestone filler	X	X	--	--
AAB-HL	AAB + Hydrated lime	X	X	--	--
AAB-LA	AAB + Liquid anti strip agent	X	--	X	X
AAM-AG	Aged AAM**	X	X	--	--
AAM-LS	AAM + Limestone filler	X	X	--	--
AAM-HL	AAM + Hydrated lime	X	X	--	--
AAM-LA	AAM + Liquid antistrip agent	X	--	--	X
ABD-AG	Aged ABD**	X	X	X	--
ABD-LS	ABD + Limestone filler	X	X	--	--
ABD-HL	ABD + Hydrated lime	X	X	--	--
ABD-LA	ABD + Liquid antistrip agent	X	--	X	X
TOTAL		**21**	**14**	**12**	**8**

AFM: Atomic Force Microscopy, IGC: Inverse Gas Chromatography.
* Lower temperature grade not available from the literature.
**Asphalt binder was aged using RTFO and PAV [18, 19].
X indicates that the material was tested with the test method.
-- indicates material was not included for testing with the test method.

Table 7. Summary of Aggregates Tested Using Various Surface Energy Measurement Methods.

Label	Description [20]	Test Method			
		U S D	I G C	Sessile Drop	MC
RA	Granite from Georgia (granite 99%)	X	X	X	--
RK	Basalt from Oregon (basalt 94%)	X	X	X	X
RD	Limestone from Maryland (shaly limestone 53%, limestone 27%, arenaceous limestone 20%)	X	--	X	X
RL	Gulf coast gravel from Texas (chert 59%, arenaceous limestone 18%, granite 11%)	X	--	X	X
RG	Sandstone from Pennsylvania (calcareous sandstone 100%)	X	--	--	X
Albite	Pure mineral samples (99%+ purity) obtained from various sources. Purity was verified using electron microprobe including energy dispersive spectroscopy (EDS).	X	--	--	--
Calcite		X	--	--	--
Microcline		X	--	--	--
Quartz		X	--	--	--
TOTAL		**9**	**2**	**4**	**4**

USD: Universal Sorption Device, IGC: Inverse Gas Chromatography, MC: Micro Calorimeter.
X indicates that the material was tested with the test method.
-- indicates material was not included for testing with the test method.

The following details will be presented for each test method:

- a brief overview of the test method,
- modifications or improvements that were made to customize the test method for measurement of surface energy components of asphalt binders and aggregates,
- the surface energy components for different asphalt binders and/or aggregates including a brief discussion of the results,
- considerations in using the test method or interpreting test results, and
- advantages and limitations of each test method.

3.2.2 Wilhelmy Plate Method

This method is recommended for use as a routine test method to measure the surface energy components of asphalt binders. Appendix B presents the detailed experimental and analytical procedures used to measure contact angles of the asphalt binder with various probe liquids and determine surface energy components of the binder.

Method Overview

The Wilhelmy plate method is used to measure the contact angles of various probe liquids with asphalt binders. The contact angle is measured indirectly by immersing a plate coated with binder into the probe liquid and deriving the angle from the measured force *(21)*. From simple force equilibrium considerations, the difference between weight of a plate measured in air and partially submerged in a probe liquid, ΔF, is expressed in terms of buoyancy of the liquid, liquid surface energy, contact angle, and geometry of the plate. The contact angle

between the liquid and surface of the plate is calculated from this equilibrium as follows:

$$\cos\theta = \frac{\Delta F + V_{im}\left(\rho_L - \rho_{air} g\right)}{P_t \gamma_L^{Tot}} \quad [18]$$

where, P_t is the perimeter of the bitumen coated plate, γ_L^{Tot} is the total surface energy of the liquid, θ is the dynamic contact angle between the bitumen and the liquid, V_{im} is the volume immersed in the liquid, ρ_L is the density of the liquid, ρ_{air} is the density of air, and g is the local acceleration due to gravity.

Figure 18 is a schematic of the Wilhelmy plate device used in this research. Two different contact angles are obtained as the plate advances into the liquid and during the receding process, respectively. Figure 19 illustrates the hysteresis effect obtained during force measurements induced by the difference between advancing and receding modes of measurement. The lines are sloped due to the buoyancy effect.

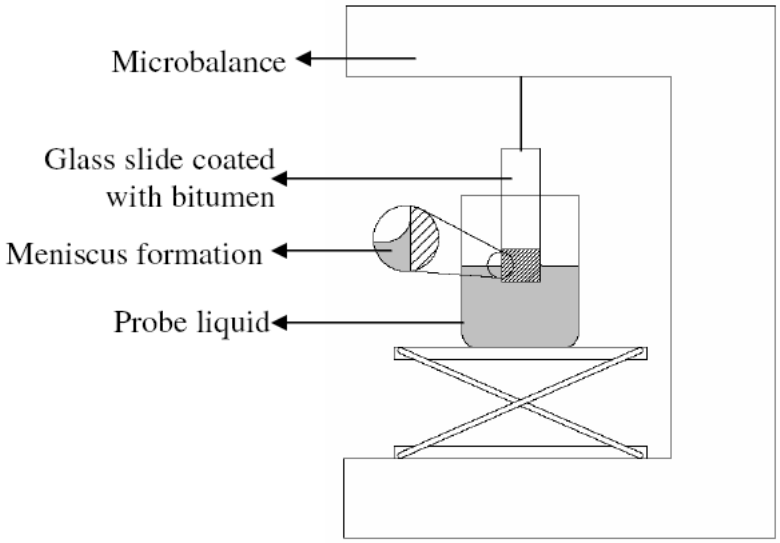

Figure 18. Test Setup for the Wilhelmy Plate Method (6).

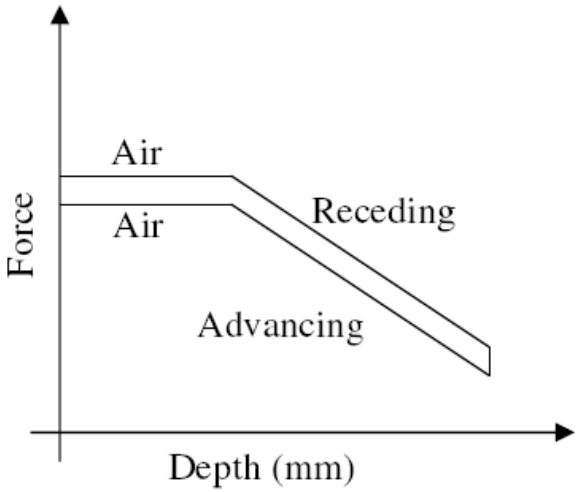

Figure 19. Advancing and Receding Contact Angles from the Wilhelmy Plate Method (6).

Based on the Young-Dupré equation, GVOC *(3, 4)* proposed the following relationship between the Gibbs free energy of adhesion, ΔG_{LS}^{a} ; work of adhesion, W_{LS}; contact angle, θ, of a probe liquid, *L*, in contact with a solid, *S*; and surface free energy components of both the liquid and the solid:

$$W_{LS} = \gamma_L (1 + Cos\ \theta) = 2\sqrt{\gamma_S^{LW} \gamma_L^{LW}} + 2\sqrt{\gamma_S^{+} \gamma_L^{-}} + 2\sqrt{\gamma_S^{-} \gamma_L^{+}} \quad [19]$$

In equation [19], the total and the three surface energy components of the probe liquid are known from the literature, the contact angle is measured using the Wilhelmy plate method, and the three surface energy components of the asphalt binder are unknown. Therefore, contact angles of the asphalt binder with at least three different probe liquids must be measured to generate a set of three equations that can be solved for the three unknown surface energy components. However, in practice it is recommended that redundancy be introduced by measuring contact angles with five different probe liquids. This facilitates examination of the accuracy of the measured contact angles and also improves the overall accuracy of the computed surface energy components.

Method Development

Some of the improvements that were made to the Wilhelmy plate test method during this research for use with asphalt binders are as follows:

- A simple method to prepare samples was developed.
- Two criteria to identify anomalous interactions with any probe liquid were introduced. Such interactions may render the measured contact angles with the probe liquid unsuitable for use with surface energy theory.
- Analytical techniques to quantify the standard deviation in the computed surface energy components based on the errors in the measured contact angles were developed.

Surface Energy Components of Asphalt Binders

In this research, a DCA 315 microbalance with WinDCA software from Thermo Cahn Instruments was used to perform the test, acquire force data, and calculate contact angles. Five probe liquids were selected to determine the advancing and receding contact angles with the selected asphalt binders using the Wilhelmy plate method. This selection was made based on the criteria for selection of probe liquids described earlier. The five probe liquids were methylene iodide (diiodomethane), water, glycerol, formamide, and ethylene glycol.

A criterion to identify contact angle measurements that were not consistent with surface energy theory was developed. Based on this criterion, it was observed that for most of the asphalt binders selected in this study, contact angles measured with formamide were unsuitable for use with equation (20) to determine the surface energy components of the binder. Therefore, the surface energy components of these binders were computed using contact angles with only the remaining four liquids. However, exclusion of contact angles with formamide to determine the surface energy components might not be universally required. Therefore, it is recommended that in practice all five probe liquids be used to measure contact angles with asphalt binders. The accuracy of the measured contact angles can then be verified using the criteria explained later in this section. Contact angles for at least three replicate samples were measured with each probe liquid for each asphalt binder.

Table 8 presents a summary of the surface energy components of the asphalt binders measured using the Wilhelmy plate method and their standard deviations. Appendix E provides more details about the methods used to compute the standard deviations using propagation of errors. The standard deviation in the measured contact angles was typically less than 2°. All measurements were made by a single operator using the same device.

Table 8. Surface Energy Components of Asphalt Binders Using the Wilhelmy Plate Method in ergs/cm^2 at 25°C.

Binder	LW Component		Acid Component		Base Component		Total
	Value	Std. Dev.	Value	Std. Dev.	Value	Std. Dev.	
AAB	13.6	0.7	2.7	0.3	0.0	0.0	13.6
AAD	18.5	0.4	0.1	0.0	0.1	0.1	18.6
AAE	26.1	0.5	2.0	0.2	0.0	0.0	26.1
AAF	21.3	0.7	0.8	0.1	0.0	0.0	21.3
AAH	20.2	0.7	1.4	0.2	0.0	0.0	20.2
AAL	31.3	0.8	0.0	0.0	0.0	0.0	31.3
AAM	24.8	1.2	0.2	0.1	0.0	0.0	24.8
ABD	32.5	1.0	0.4	0.1	0.0	0.0	32.5
ABL	18.5	0.8	1.8	0.3	0.0	0.1	18.8
AAB-AG	16.5	0.2	0.0	0.0	2.9	0.3	16.6
AAB-HL	23.8	0.9	0.9	0.1	0.0	0.0	23.8
AAB-LA	17.8	0.8	2.4	0.4	0.0	0.0	17.8
AAB-LS	22.9	0.3	0.8	0.1	0.0	0.0	22.9
AAM-AG	15.1	0.2	0.7	0.2	2.4	0.7	17.6
AAM-HL	26.2	0.2	0.0	0.0	0.0	0.0	26.2
AAM-LA	19.1	0.3	2.8	0.1	0.0	0.0	19.1
AAM-LS	24.2	0.2	1.2	0.1	0.0	0.0	24.2
ABD-AG	32.3	0.3	0.0	0.0	0.1	0.1	32.3
ABD-HL	31.7	0.5	0.1	0.0	2.7	0.2	32.5
ABD-LA	31.2	0.5	0.0	0.0	0.4	0.1	31.2
ABD-LS	35.2	0.3	0.0	0.0	1.4	0.3	35.2

Important observations related to the data presented in Table 8 are as follows:

- The total surface energy of all asphalt binders varies from 13.6 to 35.2 ergs/cm^2. In another study the total surface tension or surface energies for eight different asphalt binders were reported to be between 22.3 and 30.4 ergs/cm^2 at 60°C measured using a Du Nouy ring tensionmeter *(22)*. Although surface energy of the binders is expected to decrease with a decrease in temperature, the magnitude of this decrease is not very high. Therefore, it can be considered that the total surface energy values for the asphalt binders measured in this research are in agreement with the range of the values reported above.

- The standard deviation of surface energy components is a measure of the precision of this technique. Standard deviations of the surface energy components were typically a small percentage of the total magnitude of the component, especially for the LW component.
- Results suggest that this test method is sensitive to the LW and acid component of different asphalt binders.
- The LW component is the most significant contributor to the total surface energy of the asphalt binders, while the magnitudes of acid and base components are very small. This is consistent with the fact that most asphalt binders are weakly polar materials.
- In most cases the neat asphalt binders had a negligible base component, although this might not be universally true for all asphalt binders. However, an increase in base component was seen for the asphalt binders after aging. Since aging leads to the formation of weak bases and acids such as ketones and sulfoxides, the net effect on the surface energy components due to aging will depend on the initial chemical nature of the asphalt binder and the dynamics of various functional groups during the aging process (WRI) (22).
- Addition of hydrated lime, liquid antistrip agents, or limestone filler had different effects on the surface energy components for different asphalt binders. Since this study was aimed at developing the basic foundations for the application of surface energy measurements, further research to investigate and interpret the effect of aging, fillers, and additives on the surface energy components and performance of asphalt binders is required.

Ensuring Accuracy of Contact Angles

Equation [19] is based on Young's equation for contact angles. In order to use this equation to compute the surface free energy components of a solid, it is important that the experimentally measured contact angles satisfy the requirements necessary for Young's equation to be valid. One of the important requirements is that the probe liquid to be pure and homogenous and that it does not chemically interact with the bitumen. Certain forms of chemical interactions are easily identifiable, such as when the probe liquid dissolves the asphalt binder. However, in some cases complex interactions between the binder and probe liquid might not be apparent and other methods to screen liquids must be used. The following paragraphs describe a method based on a detailed study by Kwok et al. *(23, 24)*.

Kwok, Neumann, and co-workers developed a dynamic method of recording contact angles of liquids as they are dispersed on a solid surface and attain equilibrium. This enabled them to identify liquids that demonstrate anomalous behaviors such as the diffusion of probe the liquid into the solid. They regard contact angle data from such liquids as "meaningless" because such anomalies can alter the surface energy components of the solid surface or the probe liquid or both. They also state that liquids demonstrating such anomalous behavior are in violation of one or more of the assumptions required to apply Young's equation and, therefore, cannot be used to compute surface energy components. In their experimental work, Kwok, Neumann and co-workers *(23, 24 and 25)* used as many as 17 liquids on various polymer surfaces. They used the contact angles measured using various probe liquids to generate a plot of $\gamma_L Cos\theta$ versus γ_L for each solid surface. They reported that in most cases this plot was a smooth curve and that data from the liquids that demonstrate complex interactions with the solid surfaces did not lie on this smooth curve. As a corollary, it can be expected that if a liquid deviates from a

smooth curve plot of $\gamma_L Cos\theta$ versus γ_L, then data from that liquid must not be included for calculation of surface energy components. Some other researchers argue that the plot of $\gamma_L Cos\theta$ versus γ_L might not necessarily be a smooth curve. Deviations of individual points are possible due to polar or acid-base interactions between the solid surface and the liquid.

Notwithstanding either point of view, researchers mathematically derived the contact angles for the five probe liquids recommended in this research using several hypothetical sets of surface energy components with weak acid-base character based on equation [19]. The plot of $\gamma_L Cos\theta$ versus γ_L for these materials was in fact a smooth curve in accordance with the aforementioned criterion. The only exception was the point corresponding to methylene iodide, which indicated some deviation from the smooth curve. Figure 20 illustrates a typical plot derived for a hypothetical asphalt binder with LW component, acid component, and base component of 30, 2, and 0.5 ergs/cm^2, respectively.

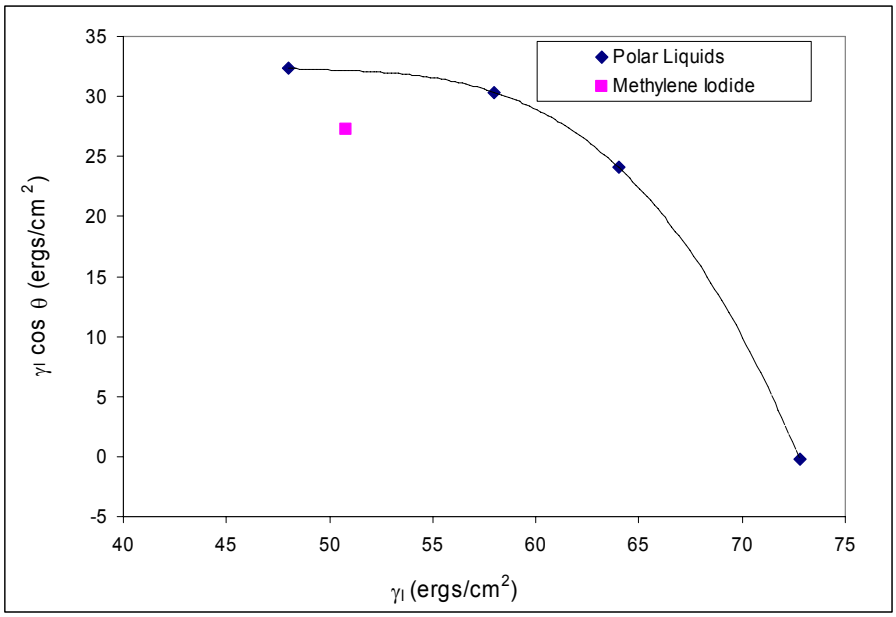

Figure 20. Plot to Examine Validity of Neumann Criteria for Asphalt Binders.

Based on the aforementioned analysis, two indicators are recommended as a criteria by which to identify anomalous interactions of the probe liquid with the binder surface or any errors in measurement. The first is the plot of $\gamma_L Cos\theta$ versus γ_L, which should result in a smooth curve, at least for the four polar probe liquids. Second, the three surface energy components should be determined using a weighted minimization of squares of error method using the data from the five probe liquids. Therefore, if the measured contact angles are accurate and consistent with the surface energy theory, then the magnitude of the sum of squares of errors must be very small.

The Importance of Advancing and Receding Contact Angles

The differences in the advancing and receding contact angle are referred to as contact angle hysteresis. Under ideal conditions, hysteresis should be zero, i.e., the advancing and receding contact angles should be the same for a given solid surface. Contact angles measured using the Wilhelmy plate method almost always demonstrate hysteresis. The causes of

hysteresis and the relevance of advancing and receding contact angles with fracture processes in asphalt binder are discussed in the following paragraphs.

Kwok et al. *(23)* and Kwok and Neumann *(25)* state that physical roughness of the solid surface and chemical heterogeneity are two possible causes for hysteresis. If hysteresis is due to surface roughness, then contact angles obtained from the test are meaningless because they do not satisfy the basic requirement of a smooth solid surface required in the application of Young's equation. On the other hand, if hysteresis is due to chemical heterogeneity of the solid surface, then the measured advancing contact angle can still be considered as a good approximation of the equilibrium contact angle used to calculate surface free energy components *(23)*.

For the Wilhelmy plate method, samples of the asphalt binder are prepared by coating a thin glass slide with molten binder. The sample is prepared at high temperatures where the binder is in a liquid state. As the sample cools, the fundamental intermolecular forces that are responsible for surface energy will ensure that the surface area is minimized. Therefore, samples prepared using this method is not likely to demonstrate roughness at the micro scale. On the other hand, the chemical heterogeneity of asphalt binders is well established. Therefore, it seems reasonable to attribute the hysteresis of contact angles with asphalt binders to chemical heterogeneity rather than physical roughness.

The use of advancing contact angles to calculate the surface free energy components and work of adhesion is supported by the literature *(4, 16)*. However, some work by other researchers *(16, 26)* indicates that the receding contact angles can also be used as an index of surface energy. The receding contact angles are measured when the binder sample is withdrawn from the probe liquid or during the dewetting process of the asphalt binder with the probe liquid. The receding contact angle has been associated with the fracture properties of the material as opposed to the advancing contact angle, which is measured in the wetting process and is associated with the healing characteristics of the material *(8)*.

Advantages and Limitations

The Wilhelmy plate device is available commercially and requires a relatively small capital outlay to prepare the laboratory to accommodate this device. The device is usually accompanied with a user friendly control and analysis software that can be used to conduct the test and analyze results. The test procedure is very simple and requires minimal training. Asphalt binder samples for this test are prepared by immersing a thin glass slide in molten binder and then allowing the coated slides to cool. This affords little potential to alter the chemical state of the binder during the sample preparation process. Preparation of uniform and neat samples may require some skill and practice by the operator.

Another advantage of this test method is that the measured contact angle is an average over an infinite number of boundaries that are created as the sample is very slowly immersed into the probe liquid to a depth of about 5 mm. The advancing and receding contact angles are automatically measured during each test.

In most cases the device does not come equipped with an environmental chamber for stringent temperature control. Therefore, ambient temperature must be in reasonable proximity to the test temperature. This also prevents measurement of contact angles at different test temperatures.

The simplicity of the Wilhelmy plate method combined with relatively low capital outlay makes it an ideal choice for use as a routine test method to measure surface energy components of asphalt binders.

3.2.3 Universal Sorption Device

The USD method is recommended for use as a routine test method to measure the surface energy components of aggregates. Appendix C presents the detailed experimental and analytical procedure to measure adsorption isotherms of various probe vapors with aggregates and determine surface energy components using the USD.

Method Overview

The USD is used to obtain adsorption isotherms of various probe vapors with high-energy solids such as aggregates. An adsorption isotherm is the relationship between the equilibrium mass of the vapor adsorbed on the solid surface and partial vapor pressure of the probe vapor. Figure 21 illustrates a schematic layout of the test equipment and Figure 22 illustrates a typical adsorption isotherm measured using the USD.

The adsorption isotherm is used to compute the SSA of the aggregate using the classical Branauer, Emmett, and Teller (BET) equation *(27)*. The equilibrium spreading pressure, π_e, of a vapor with the aggregate surface is determined from its adsorption isotherm based on the following relationship *(28)*:

$$\pi_e = \frac{RT}{MA}\int_0^{p_0}\frac{n}{p}dp \qquad [20]$$

Where, R is the universal gas constant; T is the test temperature; n is the mass of vapor adsorbed per unit mass of the aggregate at vapor pressure, p; M is the molecular weight of the probe vapor; p_0 is the maximum saturation vapor pressure of the liquid; and A is the SSA of the aggregate.

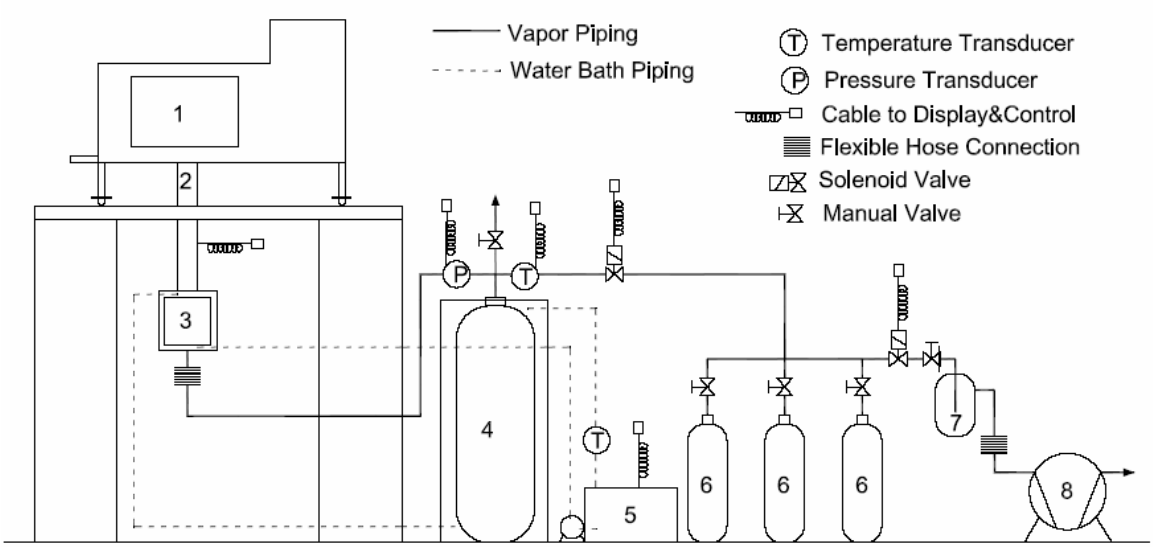

1. Microbalance
2. Magnetic suspension
3. Sample cell
4. Buffer tank
5. Water bath
6. Probe liquid containers
7. Knockout tank
8. Vacuum pump

Figure 21. Schematic Layout of Universal Sorption Device System [6].

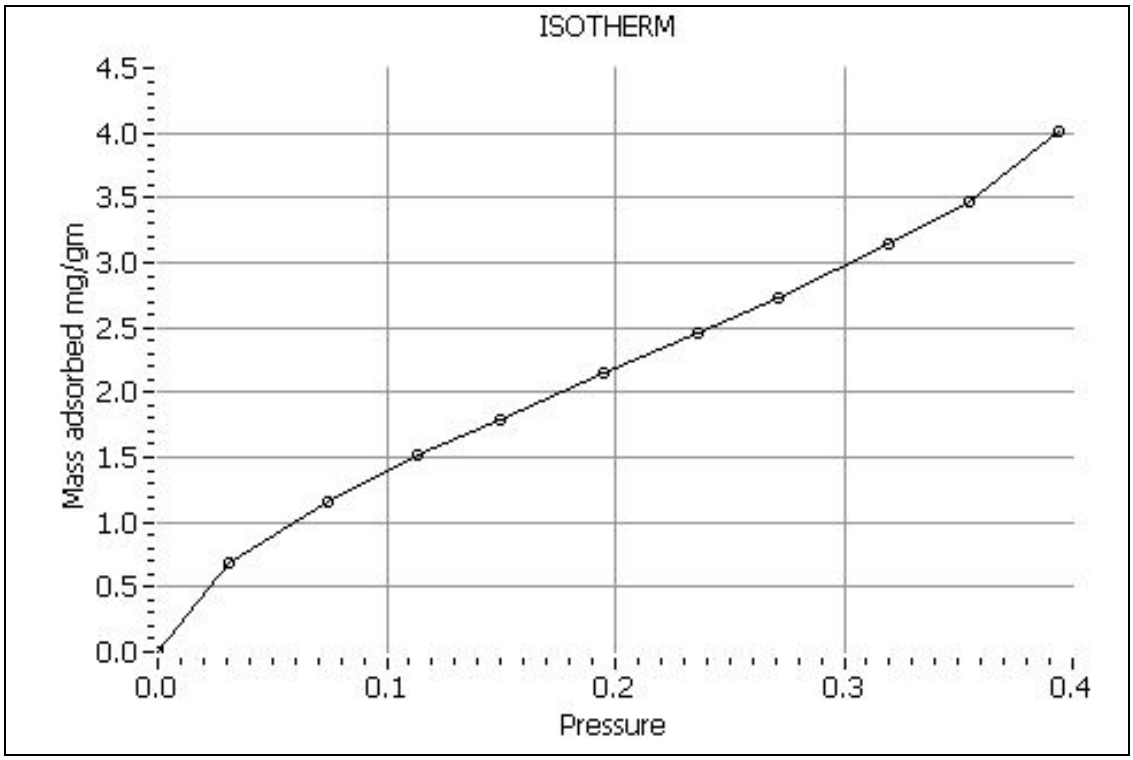

Figure 22. Typical Adsorption Isotherm Measured with the USD (Quartz with n-Hexane)(6).

The spreading pressure between the probe vapor and the solid is related to the surface energy components of the two materials and the total surface energy of the probe vapor using the GVOC theory for the work of adhesion, as follows:

$$\pi_e + 2\gamma_{LV} = 2\sqrt{\gamma_S^{LW}\gamma_L^{LW}} + 2\sqrt{\gamma_S^+\gamma_L^-} + 2\sqrt{\gamma_S^-\gamma_L^+} \quad \textbf{(21)}$$

In equation [21], the three surface energy components of the solid are unknown, the total and three surface energy components of the liquid are known from the existing literature or handbooks, and the spreading pressure between the liquid vapor and solid is measured with the USD. Analogous to the Wilhelmy plate method, the spreading pressure of the aggregate with at least three different probe vapors must be measured in order to compute the three surface energy components of the aggregate using equation [21]. The value of SSA of the aggregates is determined from the adsorption isotherm with n-hexane, which is used as the standard to compute spreading pressures with all three probe vapors. Figure 23 illustrates a flow chart of the tests conducted with the USD and the analysis to determine the surface energy components of the aggregates.

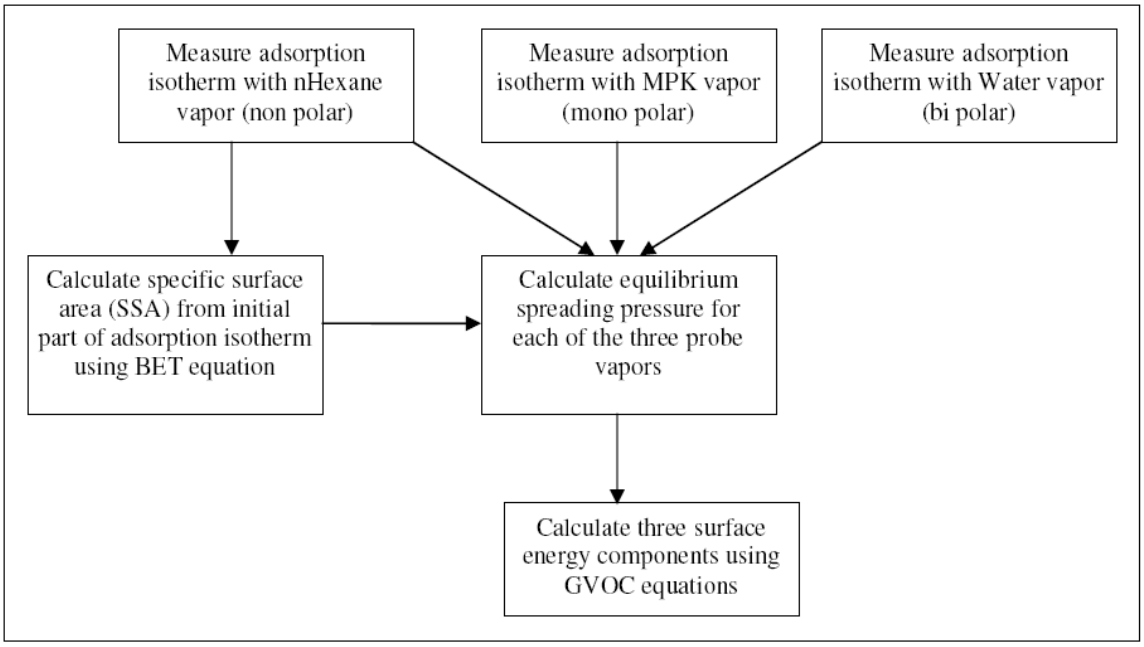

Figure 23. Steps to Determine Surface Energy Components of Aggregates with the USD (6).

Method Development

Some of the improvements to this test method that were made during this research are summarized as follows:

- Measurement of adsorption isotherms is an inherently time consuming procedure. From earlier studies it was observed that lengthy test durations coupled with human errors reduced the precision of measurements from this test. Therefore, a computer-controlled test manifold was developed for use with the magnetic suspension balance and sorption cell furnished by Rubotherm of Germany. Use of the automated test system significantly reduced human error, improved precision, and resulted in optimum testing time.
- SSA of the aggregates is a required input in computing the surface energy components as shown in equation [20]. The SSA of a given sample is not constant but varies depending on the probe vapor and theoretically estimated projected cross sectional area of the probe vapor molecule. This discrepancy was resolved by using a value of SSA measured using n-hexane based on a projected molecular cross sectional area of 52 $Å^2$ over literature *(29)*. More discussion related to SSA is presented later in this section.
- An optimum sample preconditioning time was determined by comparing adsorption isotherms of the same material, after subjecting it to different preconditioning times.
- An analytical method used to compute the standard deviations of surface energy components based on standard deviations of the measured adsorption isotherms were also developed.

Surface Energy Components of Aggregates

The USD used in this research consists of a magnetic suspension balance with a vapor adsorption cell manufactured by Rubotherm of Germany. An indigenously developed computer-controlled manifold was designed to obtain adsorption isotherms suitable for surface energy measurements using the suspension balance and adsorption cell. Three probe liquids were selected to measure the adsorption isotherms and determine the equilibrium spreading pressures

with each aggregate type. These three probe vapors were n-hexane, methyl propyl ketone (MPK), and water. At least three replicate measurements were made with each probe vapor for each aggregate type. Table 9 presents a summary of the surface energy components and their standard deviations for the aggregates and minerals included in this research. SSAs of the aggregates and minerals were also determined as a part of the data analysis from the adsorption tests. Table 10 presents the SSA of the five aggregates and four minerals included in the test matrix. The table also presents the SSA of the five aggregates from the MRL based on the values reported in the literature *(20)*. All tests were conducted by a single operator using the same device.

Table 9. Surface Energy Components of Aggregates Measured Using the USD in ergs/cm^2 at 25°C.

Aggregate	LW Component		Acid Component		Base Component		Total
	Value	Std. Dev.	Value	Std. Dev.	Value	Std. Dev.	
RD: Limestone	44.1	1.25	2.37	1.08	259	18	93.6
RL: Gravel	57.5	4.09	23	4.15	973	39	356.8
RK: Basalt	52.3	4.77	0.64	0.74	164	10	72.8
RA: Granite	48.8	0.49	0	--	412	83	48.8
RG: Sandstone	58.3	4.52	14.6	4.01	855	34	281.5
Mineral: Quartz	37.2	1.0	0.0	--	525	32.2	96.6
Mineral: Albite	47.5	0.5	0.7	0.1	245	10.1	77.1
Mineral: Calcite	67.0	1.6	0.0	--	427	20.8	67.0
Mineral: Microcline	43.9	0.4	0.0	--	239	8.0	46.6

Note: -- Indicates that the standard deviation was not computed since the analytical methods to compute standard deviations are not applicable when the value of the component is 0.

Table 10. SSA of Aggregates and Minerals Reported in m^2/g.

Aggregate	USD (2.36 – 4.75 mm in size)	Micromeritics (2.36 – 4.75 mm in size)	BET MRL (< 1 mm in size) [20]
RD: Limestone	0.26	--	0.72
RL: Gravel	1.06	--	2.41
RK: Basalt	10.54	10.1	15.73
RA: Granite	0.11	0.13	0.19
RG: Sandstone	0.74	--	1.99
Mineral: Quartz	0.05	--	--
Mineral: Albite	0.07	--	--
Mineral: Calcite	0.10	--	--
Mineral: Microcline	0.08	--	--

Note: -- Indicates that either the measurement was not made or the data were not available in the literature.

Important observations from the data presented in Tables 9 and 10 are as follows:

- The total surface energy of all aggregates varies from approximately 50 to 360 $ergs/cm^2$.
- The magnitude of the LW component of surface energy varied from approximately 44 to 70 $ergs/cm^2$. The magnitude of base component of surface energy was the highest and varied from approximately 165 to 975 $ergs/cm^2$. The magnitude of acid component of surface energy was the lowest and varied from 0 to approximately 23 $ergs/cm^2$.
- In most cases the standard deviation of the surface energy component was a small percentage of the value of the component. This indicates that the test method is sufficiently sensitive to surface energy components when comparing them among different types of aggregates.
- From existing literature *(30, 31, 32)* the Lifshitz-van der Waals component of finely divided minerals commonly found in aggregates, such as quartz and calcite, is reported to be between 35 to 80 $ergs/cm^2$. This is consistent with the values determined using the USD.
- The same size fraction of different aggregates can have SSAs that differ by almost two orders of magnitude, ranging from 0.1 m^2/g for RA to 10 m^2/g for RK. However, recent tests with some other aggregates indicate that a more common range for SSA of aggregates is 0.5 to 4 m^2/g. All these values are for the aggregate size passing the #4 sieve and retained on the #8 sieve.
- The SSAs measured with the USD for two different aggregates compared well with the areas obtained for the same size fraction of the aggregates using a standard nitrogen adsorption technique with a commercial device (manufactured by Micromeritics Inc.). The SSAs for the five aggregates measured with the USD also compare well with the values reported for these aggregates in the literature based on BET measurements [20]. The SSAs from the latter source are generally higher than the values from the USD. This is because the SSAs reported in the literature were based on measurement of blends

passing a 1 mm sieve as compared to the aggregates measured in this research, which are between 2.4 and 4.8 mm in size. These comparisons provide a limited validation of the accuracy of measurement of this technique.

Importance of Specific Surface Area

Unlike asphalt binders, aggregate surfaces are very rough and have significant surface features at the micro-scale. Adsorption isotherms are determined by measuring the mass of the vapors adsorbed per unit mass of the aggregates. However, spreading pressures and surface energy components are expressed in units of energy per unit area. Therefore, an important factor in determining the spreading pressure or surface energy components is the SSA of the aggregates.

In this research the BET method proposed by Brunauer, Emmett, and Teller *(33)* was used to determine the SSA of various aggregates. This method is widely accepted and used by various industries to determine the SSA of materials using nitrogen adsorption at 77 K. Figure 24 presents the five types of adsorption isotherms generally encountered *(34)* with porous and nonporous materials. The BET method can be used directly to determine the specific surface areas for Type II and Type III isotherms *(27)*. In general, it was observed that the adsorption isotherms with the aggregates can be classified as one of these two types. However, it is still recommended that users of this method examine and verify the type of isotherm with various aggregates.

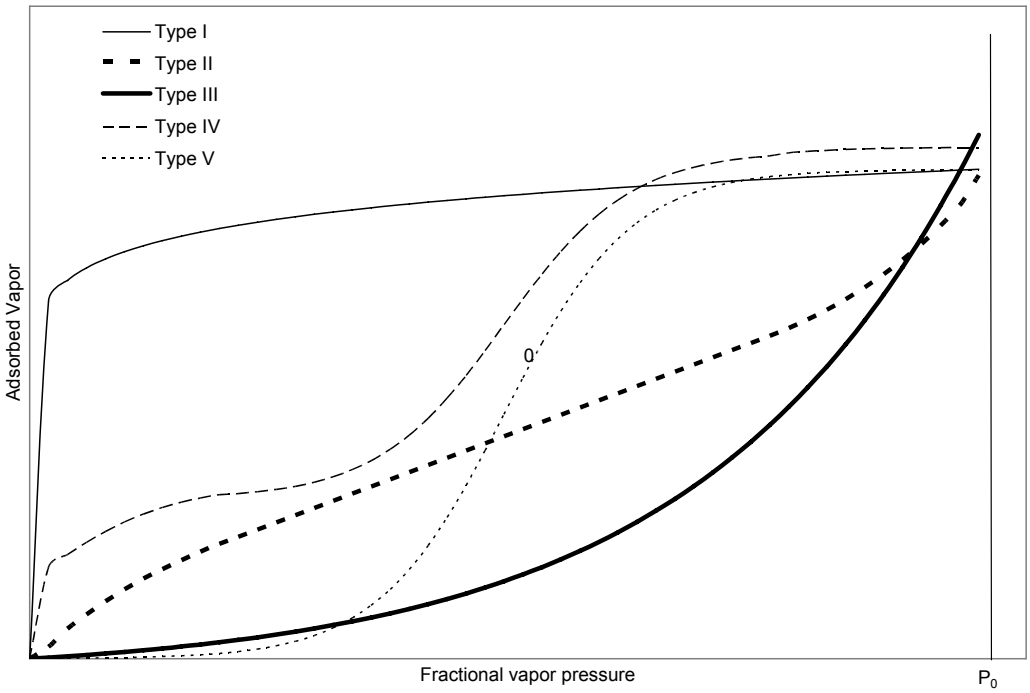

Figure 24. Types of Adsorption Isotherms (27).

The term SSA refers to the surface area per unit mass of the solid. This apparently simplistic definition can be misleading, since SSA depends on the resolution at which the surface area is measured. For example, Figure 25 illustrates the cross section of a hypothetical solid surface at the molecular scale, which is measured using probe molecules of two different sizes.

It is evident that the SSA determined in each case will be different depending on the size of the probe molecule.

An important input to the BET equation is the projected area of the vapor molecule, α. This is typically calculated using the liquid density formula as follows *(35)*:

$$\alpha = f\left(\frac{M}{\rho N_0}\right)^{2/3} \qquad [22]$$

where, f is the packing factor, ρ is the liquid density at the test temperature, and other terms are as previously described. The value of f can be taken as 1.091 if the molecules are considered to be densely packed so as to have 12 nearest neighbors in bulk liquid and 6 in the plane. However, it was observed that use of the liquid density formula to determine the value of α and to obtain SSA of solids does not always provide consistent results among various probe liquids. This could be due to the resolution of the molecule versus the actual surface as shown in Figure 25. Also, the actual effective area occupied by polar vapor molecules adsorbed on polar solid surfaces can differ substantially from the area calculated using equation (23) due to the localized orientation of probe molecules. Therefore, in this research it was recommended that the SSA determined using n-hexane as a probe molecule be used for all computations related to surface energy. The projected cross-sectional area for n-hexane was adopted from the literature *(29)* rather than using the liquid density formula.

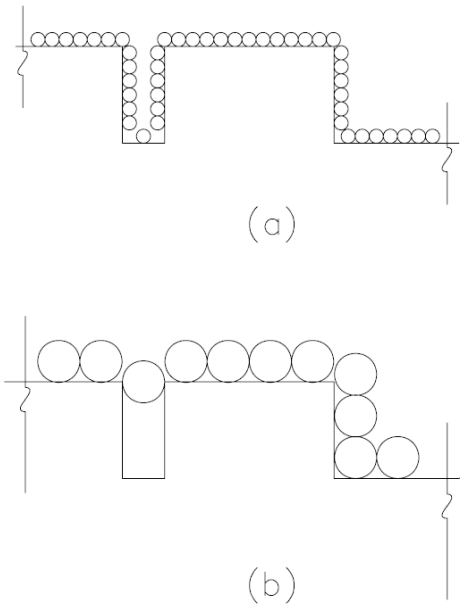

Legend: (a) surface area measured using smaller molecules as measuring unit (b) surface area of the same solid section measured using larger molecules as measuring unit

Figure 25. Dependency of Specific Surface Area on the Size of Probe Molecules(6).

Two important reasons for the use of n-hexane in favor of water or MPK to determine the SSA are as follows. First, n-hexane is a nonpolar molecule and therefore not susceptible to localized orientation as a function of aggregate surface properties. Second, the projected cross-sectional area of n-hexane molecule is larger than the other two probes; therefore, it is likely that any micropores on the aggregate surface that are inaccessible to this molecule will also be inaccessible to the molecules of the asphalt binders. Results based on this recommended procedure are in agreement with the results obtained by using standard nitrogen adsorption methods, as shown in Table 10.

Chemisorption versus Adsorption

Bond strength between two materials due to their surface energies is typically an order of magnitude or smaller than bond strength due to chemical reactions. The two main causes for the development of a bond between two materials are:

- physical adsorption due to their surface energies, and
- chemical adsorption due to formation of a new material from chemical reactions between the two materials at the their interface.

The latter form of adsorption is also referred to as chemisorption. Vapors physically adsorbed on a solid surface can be removed by degassing at normal temperatures, while chemisorbed vapor molecules bond more tenaciously to the solid surface and cannot be removed without the aid of special processes or very high temperatures and a vacuum.

The methodology to measure surface energy of aggregates described in this report is applicable only when the probe vapor molecules are adsorbed due to physical adsorption and not chemisorption. In earlier experiments Cheng *(35)* determined that there was no appreciable difference in the adsorption and desorption characteristics of typical aggregates such as granite, limestone, and gravel using the same probe vapors. Based on these data and similar results from other studies *(36)*, it is considered that the adsorption of the selected probe vapors on typical aggregate surfaces is mostly due to physical adsorption. If aggregates coated with chemically active materials are used for testing, it must be ensured that the probe vapors do not react with the coating.

Advantages and Limitations

Measurement of adsorption isotherms is an inherently time consuming procedure. In this research, a computer-controlled manifold was developed to measure adsorption isotherms with aggregates and determine their surface energy components. The test manifold significantly reduces the time required by the operator to be present during the test, optimizes the test duration, and improves precision of the results. However, a skilled operator with appropriate training is required to conduct the test.

Although all tests in this research were conducted at 25°C, it is possible to use this device to test samples within a temperature range of approximately 10 ^{o} to 70°C with some modification. Also, this device can be used for other applications such as to measure the diffusion of probe vapors into the asphalt binder.

The USD measures properties of clean aggregate surfaces. Because physically adsorbed impurities such as water vapor, etc., are removed during the degassing process, it is not possible to measure the properties of aggregates with partial impurities. An example of such a case would be to measure surface energy components of aggregates with some controlled amount of water adsorbed on its surface.

The theoretical models related to adsorption isotherms, specific surface area, Gibb's free energy, and surface energy components used in the experimental and analytical procedures with the USD are relatively well established in the literature. Therefore, this methodology is considered as the most direct and reliable approach to measure surface energy components of aggregates.

3.2.4 Sessile Drop Method

This method is recommended for the measurement of surface energy components of asphalt binders, although some research may be required to improve the sensitivity of the test method before it can be adopted as a routine test. Appendix D presents the detailed experimental and analytical procedure to measure contact angles of the asphalt binder with various probe liquids and determine its surface energy components using this test method.

Method Overview

The sessile drop method is used to measure static contact angles of probe liquids with any solid surface but is best suited for low-energy surfaces such as asphalt binders. Contact angles are measured directly by dispensing a drop of the probe liquid on the solid surface and capturing an image of the drop. The captured image can be analyzed manually or by using a computer with image processing software to obtain the contact angle of the liquid at the edge of the drop. Figure 26 presents a schematic layout of the setup.

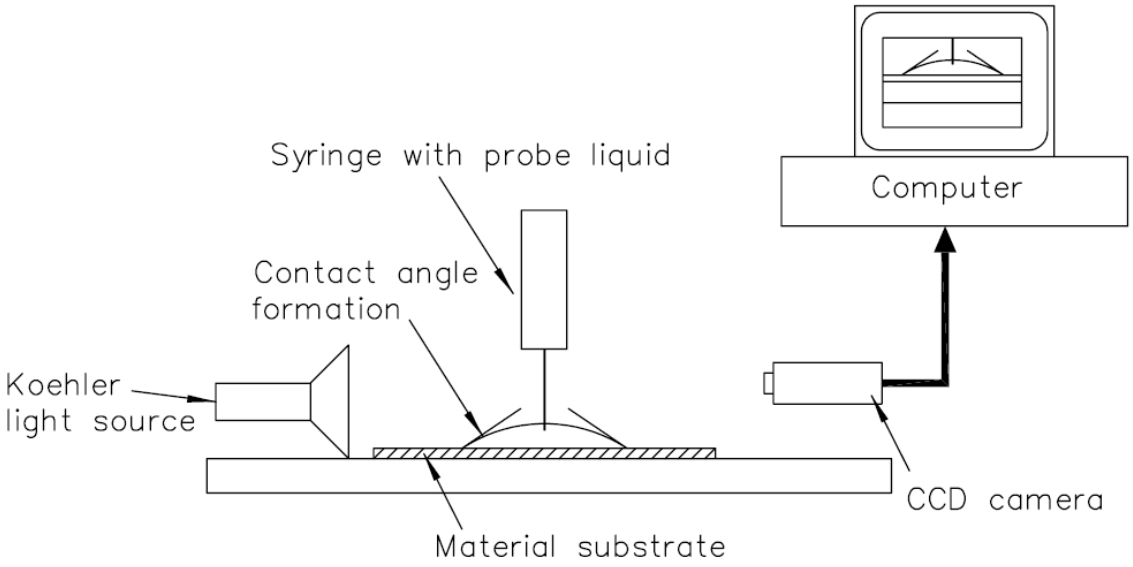

Figure 26. Schematic Layout for the Sessile Drop Method (37).

The contact angles measured by the sessile drop method (static method) are slightly different from the contact angles measured by the Wilhelmy plate method (quasi-static method). However, the analytical tools to interpret the contact angles and compute surface energy components that were developed for the Wilhelmy plate method are also applicable with this technique.

Method Development

Some of the improvements to this test method that were made during this research are summarized as follows:

- An environmental chamber to control sample temperature was developed.
- When a drop of the liquid is dispensed on the solid surface, the contact angle between the liquid and the solid is not necessarily the advancing contact angle. Therefore, a test protocol was developed that adds an appropriate volume of the probe liquid so that the contact angle is stabilized.

Surface Energy Components of Asphalt Binders

In this research, the SEO Contact Angle Analyzer (Phoenix 150) was used to measure contact angles of different probe liquids with asphalt binders or aggregates. The temperature was maintained using a thermoelectric module temperature controller (model: 5C7-195, Oven Industries, Inc.). ImagePro software was used to determine the contact angle of the liquid from the captured image in addition to manual measurements. The five probe liquids used with the Wilhelmy plate method were also used with the sessile drop method to measure the contact angles of asphalt binders. In most cases, contact angles measured with formamide were unsuitable for use with equation [19] to determine the surface energy components. This was based on the criterion used to ensure the accuracy and consistency of contact angles as described in section 3.2.2 for the Wilhelmy plate method. Exclusion of contact angles with formamide to determine surface energy components was consistent with the observations made with the Wilhelmy plate method.

At least three measurements were made for each binder-probe liquid pair. Each measurement was based on the average of the two angles observed on either side of the drop image. Table 11 presents a summary of the surface energy components of the asphalt binders measured using the sessile drop method and their standard deviations. All tests were performed by a single operator on the same device.

Table 11. Surface Energy Components of Asphalt Binders Using Sessile Drop Method in ergs/cm^2 at 25°C.

Binder	LW Component		Acid Component		Base Component		Total
	Value	Std. Dev.	Value	Std. Dev.	Value	Std. Dev.	
AAB	26.7	1.1	0.0	0.0	0.0	0.0	26.7
AAD	31.0	0.8	0.0	0.0	0.0	0.0	31.0
AAF	35.0	0.8	0.0	0.0	0.0	0.0	35.0
AAM	25.3	1.4	0.0	0.0	3.9	1.1	25.3
ABD	35.6	1.3	0.0	0.0	0.3	0.3	35.6
AAB-AG	23.3	1.6	0.0	0.0	2.6	0.8	23.3
AAB-LS	35.1	1.4	0.0	0.0	0.0	0.0	35.1
AAM-AG	22.8	1.1	0.0	0.0	3.6	0.7	22.8
AAM-HL	34.8	1.1	0.0	0.0	0.0	0.0	34.8
AAM-LS	34.3	1.1	0.0	0.0	0.0	0.0	34.3
ABD-AG	32.0	0.5	0.0	0.0	0.3	0.4	32.0
ABD-HL	44.8	0.7	0.0	0.0	0.0	0.0	44.8
ABD-LS	43.2	1.0	0.0	0.0	0.0	0.0	43.2

*Contact angles from different probe liquids for AAB-HL were found to be inconsistent based on criteria described earlier and are not included in this table.

Important observations from the data presented in Table 11 are as follows:

- The total surface energy of all asphalt binders varied from approximately 16 to 45 ergs/cm^2, similar to the range of total surface energy for the asphalt binders, determined using the Wilhelmy plate method.
- The LW component was the most significant contributor to the total surface energy of the asphalt binders. The standard deviation for this component was typically a small percentage of the value of the component.
- The acid and base components of surface energy were negligible for most asphalt binders with the exception of the base component for the three aged asphalt binders, neat AAM, and neat ABD.
- Results indicate that the test method has adequate sensitivity to the LW component but some method improvements may still be required to improve its sensitivity to detect the acid-base components.

Surface Energy Components of Aggregates

Use of the sessile drop method with high-energy surfaces such as aggregates has some theoretical limitations. A more detailed discussion of these limitations is presented later in this section. However, the apparent simplicity of this test method prompted researchers to measure the contact angles with a few aggregates to evaluate the efficacy of this methodology with these materials. Three probe liquids were used to measure the contact angles with the aggregate

surfaces. These were methylene iodide, water, and glycerol. The aggregate samples were first polished to obtain a uniformly smooth and flat surface. The sample was then placed under the syringe and considerable care was taken to ensure that the sample remained horizontal. All measurements were made by a single operator using one device.

Only glycerol and water yielded finite contact angles. No finite contact angles were obtained with methylene iodide. It is not possible to determine the three surface energy components of the solid without contact angles with three different liquids. Therefore, in this case the nonpolar and polar components were determined using the two-component theory as shown in equation [1] in lieu of the three components from the acid-base theory as shown in equation [2]. Table 12 presents the values of these two components for the four aggregates that were included in the test matrix with the sessile drop method.

Table 12. Surface Energy Components of Aggregates Measured Using the Sessile Drop Method in ergs/cm^2 at 25°C.

Aggregate	Non Polar or Dispersive Component		Polar Component	
	Value	Std. Dev.	Value	Std. Dev.
RD: Limestone	48.3	0.3	5.7	0.8
RL: Gravel	48.8	0.6	3.8	1.8
RK: Basalt	48.2	0.9	5.9	2.9
RA: Granite	48.7	1.2	4.0	3.5

From the data presented in Table 12 it appears that this test method is not sensitive to the differences in the LW component or polar component among various aggregate types.

Ensuring Accuracy of Contact Angles

Earlier, two techniques were introduced to ensure the accuracy and consistency of contact angles measured with the Wilhelmy plate method. The first was to examine the plot of $\gamma_L Cos\theta$ versus γ_L for polar probe liquids and ensure that it is a smooth curve. The second was to ensure that the sum of squares of error after determining the three surface energy components using five probe liquids was small. These two techniques can also be used with the sessile drop method to cross-examine the accuracy of the measured contact angles with asphalt binders.

Applicability for Use with Aggregates

The sessile drop method measures the contact angle of various probe liquids with the solid surface. Equation [19] relates the measured contact angle to the surface energy components of these two materials. A more general form of this equation is as follows:

$$\pi_e + \gamma_L(1 + Cos\theta) = 2\sqrt{\gamma_S^{LW}\gamma_L^{LW}} + 2\sqrt{\gamma_S^+\gamma_L^-} + 2\sqrt{\gamma_S^-\gamma_L^+} \quad [22]$$

The term, π_e, refers to the equilibrium spreading pressure of the probe vapor on the solid surface. In case of low energy solids such as polymers and asphalt binders, the equilibrium spreading pressure is generally very small and can be neglected. Therefore, for these type of materials, equation [22] is reduced to equation [19]. However, for high-energy solids, the spreading pressure of the probe vapor on the solid surface is not negligible. In fact, for such

solids the probe liquid usually tends to wet the surface of the solid, resulting in a contact angle measurement of zero degrees. Setting θ as 0 in equation [22] reduces it to equation [21], which is the basic equation to determine surface energy components using adsorption measurements.

In some cases it is possible to measure finite contact angles of probe liquids on aggregate surfaces at room temperature and in an open atmosphere. This is because water molecules and other impurities present in the atmosphere are strongly adsorbed to the clean aggregate surface, lowering its surface energy. Although the contact angles measured on these contaminated surfaces may be regarded as a relative measure of the affinity of the surface to various polar and nonpolar liquids, caution must be exercised in interpreting these contact angles to represent true aggregate surface properties. In general, this procedure is not recommended for aggregates.

Advantages and Limitations

The test equipment for the sessile drop method is commercially available. This device can be set up in the laboratory with a relatively small capital outlay. The test procedure is simple and requires minimal training. Asphalt binder samples are prepared by placing a small piece of the binder on a substrate. The substrate is heated until the binder liquefies and spreads to form an even flat surface, after which it is cooled to the test temperature. There is little alteration to the chemical state of the binder during the sample preparation process. Preparation of aggregate surfaces requires polishing to obtain a smooth surface at a micron scale. This process can alter the natural aggregate surface.

An advantage of this test is that it allows stringent temperature control and therefore facilitates measurement of contact angles at different temperatures. Some method improvements may be required to improve the sensitivity of this device. For example, the contact angle measured right after the liquid is dispensed from the syringe might not correspond to the advancing contact angle, and therefore an additional volume of the probe liquid may have to be added until the drop stabilizes.

The theoretical considerations related to contact angles with high-energy surfaces prevent the application of this method to measure the surface energy components of aggregates. Furthermore, a simple measurement of the contact angles at the aggregate surface is not sufficient, as it does not provide a method to measure the SSA.

The simplicity of this test procedure combined with relatively low capital outlay makes it suitable for measurement of surface energy components of asphalt binders. However, some improvements to the test protocol may be necessary in order to improve the sensitivity of the method to detect the acid and base components.

3.2.5 Inverse Gas Chromatography

This method is recommended to be used as an advanced material characterization tool for asphalt binders and aggregates. Appendix F presents an overview of the experimental and analytical procedure to prepare samples, measure retention times, and compute surface energy components using the IGC.

Method Overview

Conventional gas chromatography is used to separate or investigate a mixture of gases that are passed along with an inert carrier gas through a column of known material. The gas passing through the column interacts with the standard material in it. The total time of interaction results in different retention times for the gas from one end of the column to the other.

The time of interaction, also referred to as the retention time, is characteristic of the gas (mobile phase with unknown properties) and the material in the column (stationary phase with known properties). The principle supporting IGC is very similar to that of gas chromatography with the exception that the mobile phase is the probe vapor with known material properties carried by the inert gas through a column with the stationary phase (asphalt binder or aggregates) with unknown material properties. Figure 27 illustrates a schematic layout for the IGC.

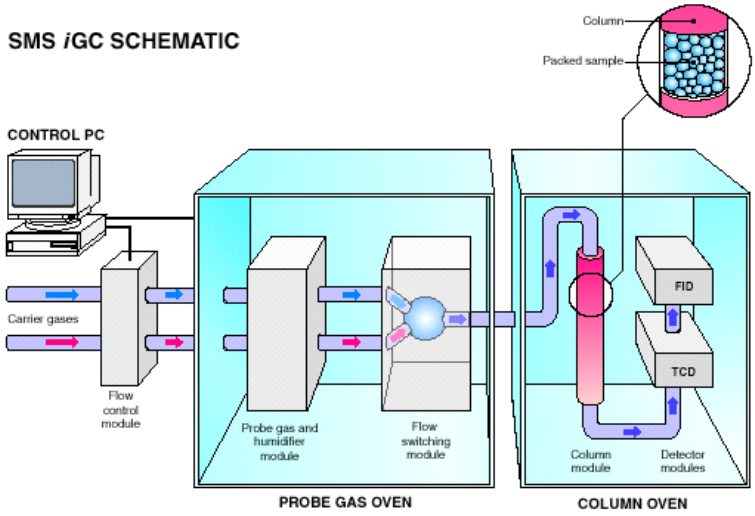

Figure 27. Schematic of SMS-IGC (with permission from SMS).

In a typical experiment, the solid material to be investigated fills the column of the gas chromatograph. For asphalt binders, a fused silica capillary column (30 m long with an inner diameter of 0.53 mm) was coated with the binder dissolved in a toluene solution following Barbour et al. *(38)*. For aggregates, a larger column made of silanized glass with a diameter of about 2 to 3 mm and a length of about 30 -cm was used. The column was filled with the fine aggregate fraction and plugged at each and with silanized glass wool to hold the sample in place.

Small amounts of probe vapors are injected into the column using a gas-tight micro-syringe. The time required for the probe vapors to move out of the column is measured as the difference between the time of injection and the time at which the flame ionization detector (FID) at the end of the column detects the vapor. In this experiment, the time taken for methane to travel through the column is used as a measure of the dead volume. This is based on the assumption that methane has negligible interactions with the solids in the column. The retention time of different probe vapors is measured as the difference of their travel time compared to the travel time of methane, which is used as a datum. Various nonpolar and polar probe vapors are used to measure the retention times and determine the surface energy components of the materials.

Method Development

Improvements to this test method that were made during this research are summarized as follows:

- During the research program a commercially available IGC device was identified. Due to the high capital cost of the equipment it was decided to conduct tests in the manufacturer's laboratory on limited aggregate samples. Simultaneously, a regular gas

chromatograph at Texas A&M University was retrofited to function as an IGC. Comparison of results of a standard material (silica gel) with the results available from the literature indicates that the retrofit gas chromatograph can be successfully used as an IGC.

- Procedures to prepare and precondition asphalt binder samples in capillary columns and aggregate samples in silanized glass columns were developed.
- It was shown that this device can be used to measure surface energy components of asphalt binders and aggregates at different temperatures.

Surface Energy Components of Asphalt Binders using the IGC

The nonpolar probe vapors used in this research to determine the LW component were pentane, hexane, heptane, and octane. The polar probes that were used to determine the acid and base components of surface energy were toluene, chloroform, ethyl acetate, and dichloromethane (DCM). All tests were conducted on the retrofit gas chromatograph at Texas A&M University. Tables 13 presents a summary of the surface energy components of the eight asphalt binders measured in this research.

Important observations from the data presented in Table 13 are as follows:

- The LW component of surface energy for the five asphalt binders varied from approximately 44 to 58 ergs/cm^2. The range of values is slightly higher than the range of values obtained with the Wilhelmy plate method at 25°C. These values are also similar to the range of values reported from other studies at 60°C *(22)*.
- The magnitude of the acid and base components of surface energy are very small compared to the magnitude of the LW component. This is consistent with the results from the Wilhelmy plate method, which also shows the magnitude of acid and base components are small compared to the LW component.
- The values of the acid and base components are dependent on the retention time of the polar probe that is used for the computation.

Table 13(a). Lifshitz-van der Waals Component of Asphalt Binders Measured Using the IGC in ergs/cm^2 at 25°C.

Asphalt Binder	LW Component	
	Value	Std. Dev.
AAB-1	44.1	1.25
AAD-1	57.5	4.09
AAF-1	52.3	4.77
AAM-1	48.8	0.49
ABD	58.3	4.52
AAB-LA	44.5	0.3
AAM-LA	45.0	0.2
ABD-LA	43.5	0.4

Table 13 (b). Acid and Base Component of Asphalt Binders Measured Using the IGC in ergs/cm^2 at 25°C.

Asphalt Binder	Acid Component (Toulene)		Acid Component (Ethyl Acetate)		Base Component (Chloroform)		Base Component (DCM)	
	Value	Std. Dev.	Value	Std. Dev.	Value	Std. Dev.	Value	Std. Dev.
AAB-1	2.6	0.1	0.8	0.02	0.5	0.1	0.4	0.2
AAD-1	3.1	0.1	1.1	0.15	1.2	0.1	0.4	0.1
AAF-1	2.9	0.1	1.1	0.06	0.4	0.05	0.6	0.2
AAM-1	1.7	0.01	0.6	0.01	0.1	0.02	0.01	0.01
ABD	2.3	0.03	1.3	0.04	0.8	0.03	0.3	0.1
AAB-LA	2.1	0.2	0.6	0.001	0.4	0.05	0.1	0.02
AAM-LA	1.5	0.04	0.6	0.07	0.1	0.1	0.2	0.1
ABD-LA	2.1	0.03	1.3	0.01	0.7	0.1	0.3	0.001

- In most cases, addition of liquid antistrip agent had very little impact on the surface energy components when measured with the IGC. This could be due to the small concentrations of the liquid agent that is added to the binder or due to the sample preparation method of coating a capillary column with the binder in toluene solution.
- The standard deviation of the surface energy components was typically a small percentage of the computed value of the component, indicating an acceptable level of precision of this test method.

Surface Energy Components of Aggregates Using the IGC

A commercially available IGC device manufactured by Surface Measurement Systems (SMS) of the United Kingdom (U.K.) was used to measure the surface energy components of aggregates. These tests were conducted at the SMS laboratory in Pennsylvania. Only two aggregates were selected in order to evaluate the efficiency of this test method. The two selected aggregates, RA and RK, represented the smallest and largest specific surface areas in the set of five selected aggregates.

The probe vapors used to measure surface energy components of the aggregates were the same as the probe vapors used to measure the surface energy components of the asphalt binders. However, the free energy of desorption with chloroform and toluene was small compared to the free energy of desorption with ethyl acetate and DCM. Therefore, only the latter two were used to determine the acid and base components of the aggregate, respectively. Table 14 presents the surface energy components of the two aggregates measured using the IGC.

Table 14. Surface Energies of Aggregates Measured Using the IGC in ergs/cm^2 at 25°C.

Aggregate	LW Component		Acid Component (Ethyl Acetate)		Base Component (DCM)		Total
	Value	Std. Dev.	Value	Std. Dev.	Value	Std. Dev.	
RK: Basalt	107.5	--	124.6	--	236.6	--	450.9
RA: Granite	53.7	--	73.6	--	149.9	--	263.7

Note: -- Standard deviations in surface energy components were not computed since only averaged data were available. The coefficient of variation of the measured response (retention time) was typically in the range of 0.5 to 8 percent.

Important observations from the data presented in Table 14 are as follows:

- The magnitude of all three surface energy components is approximately in the range of 50 to 340 ergs/cm^2. This is not unusual since aggregates are high-energy materials.
- For each aggregate the magnitude of the base component was the highest compared to the other two components. This observation is consistent with the trend seen in results from the USD.

Test Conditions and Impact on Measured Properties

The IGC is used to measure the retention time of various probe vapors when passed through a sample column. The retention time is a function of the surface free energies of probe vapor and the solid material being investigated in the column. The test is usually conducted under infinitely diluted conditions, i.e., the amount of probe vapor injected is very small compared to the volume of carrier gas (inert gas such as helium) that flows through the column. This condition is necessary to apply some of the equations that relate retention time to the surface properties of these materials. The small quantity of probe vapor injected into the column may not be adequate to interact with the entire surface of the material being investigated. As a result, interaction between the probe vapors and the solid surface will be limited to only the high-energy spots on the surface of the solid in the column. Therefore, if the solid that is being investigated is chemically heterogeneous, which is often true in the case of asphalt binders and aggregates, the retention time measured may correspond to only the high-energy functional groups that are present on the surface of the material.

A possible solution to circumvent the limitations of the infinitely diluted conditions is to use an alternative technique referred to as the finite concentration method. In this technique the probe vapor is added in incremental concentrations and the retention volume for each probe vapor at different concentrations is obtained. Also, the theoretical treatment of the results from this test is different from the method described above. One of the motivating factors to investigate this test method for the measurement of surface energy components of aggregates is that tests could be conducted in a much shorter time compared to the USD. Use of the finite concentration technique, which requires more testing time than the conventional infinite dilution method, weighs against the benefit of this protocol. Further research is required in order to investigate application of the finite concentration method for asphalt binders and aggregates.

In some cases interaction between the probe vapor molecules and highly polar molecules of the solid may be so strong that the probe molecules might take an unduly long period of time to be eluted from the column, affecting the precision of the measured retention time.

Advantages and Limitations

The IGC can be procured commercially or a conventional gas chromatograph may be used to function as an IGC with slight modifications. Only one manufacturer of commercially available IGC devices could be found during this research. Also, the capital cost of this equipment is very high. Skilled operators with adequate training are required to use this device. Aggregate samples (typically sizes below 1 mm) can be used after cleaning without the need of any special preparation with this test procedure. However, asphalt samples are prepared by passing a solution of asphalt binder in toluene through a capillary column using nitrogen gas. This process may change the chemical components or their distribution in the binder compared to its natural state.

The IGC requires less testing time to determine the surface energy components of aggregates when compared to the USD. Also, this device is very sensitive to polar species in asphalt binders or active functional groups on aggregate surfaces. However, the infinitely diluted test condition casts some potential limitations on its application for routine surface energy measurement. Despite this limitation, it is envisioned that this device can be used as an advanced research tool to investigate the effects of temperature, chemically active modifiers, and different preconditioning procedures on the surface energy components of asphalt binders and aggregates.

3.2.6 Atomic Force Microscopy

This method is recommended for use as an advanced material characterization tool for asphalt binders. Appendix G presents an overview of the experimental and analytical procedure to prepare samples, measure retention times and compute surface energy using AFM.

Method Overview

AFM is used to measure the force-distance curve when a glass bead tip cantilever is brought into close proximity to the surface of the asphalt binder. A laser beam reflects off the cantilever and is detected by a position-sensitive photodetector. This is used to measure the deflection in the cantilever and hence the force to which it is subjected. Figure 28 illustrates a schematic of AFM tip deflection measurement.

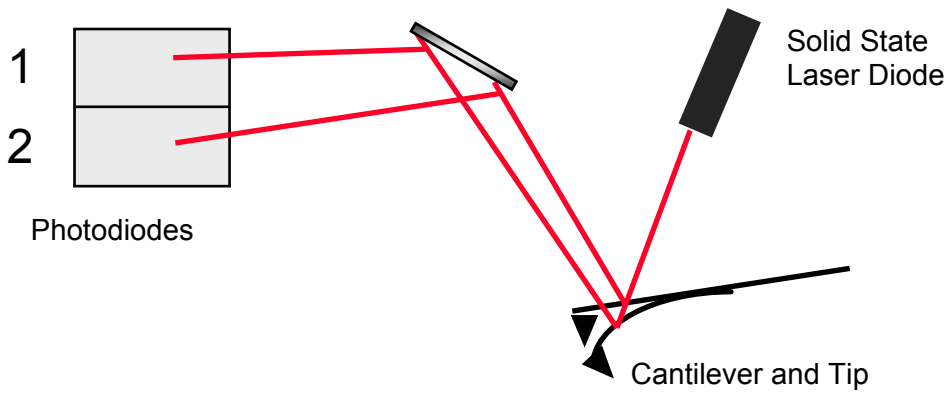

Figure 28. General AFM Tip Deflection Measurement.

The externally applied loading force, the jump-to-contact force, and the pull-off force are each extracted from the force curve measurements (Figure 29), such that adhesion is

characterized in terms of the work required to detach the glass-bead cantilever tip from the asphalt thin-film surface after the application of various levels of external loading applied at different rates. The work of adhesion, W_{adh}, is determined using the spring constant, k, of the cantilever; the vertical distance, D, between the minimum of the retraction curve and the horizontal line of data after the minimum point; and the radius, R, of the cantilever tip, using equation [23].

$$\gamma = \frac{1}{2} W_{adh}(dyne/cm) = \frac{D(nm) * k(nN/nm)}{4\pi R(\mu m)} \qquad [23]$$

Plots for both the tip deflection and load force (x-axis) versus 0.5 times the work of adhesion (y-axis) (Figure 30) are extrapolated to zero on the x-axis. This value represents the equilibrium surface tension at the temperature at which the measurement was made.

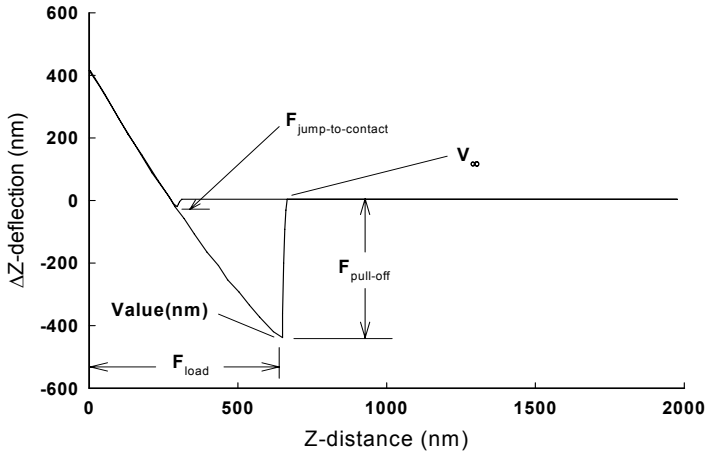

Figure 29. Force Curve Plot for AFM.

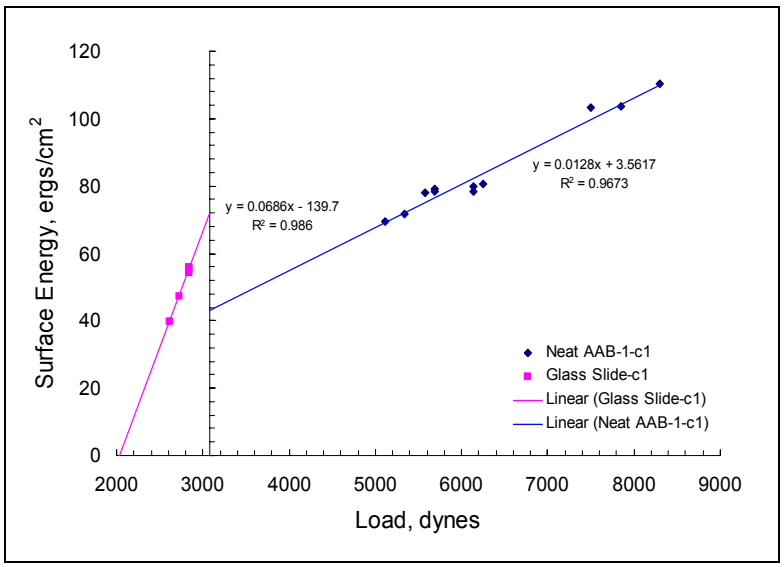

Figure 30. Typical Load vs. Surface Energy Plot.

Surface Energy Components of Asphalt Binders

In this research, a Digital Instruments MultiMode™ scanning probe AFM was used. A glass-bead tip cantilever was used to obtain force curves for various asphalt binders. Table 15 presents the LW component of surface energy for various asphalt binders measured using AFM.

Table 15. Surface Energies of Asphalt Binders Measured Using the AFM in ergs/cm^2 at 25°C.

Asphalt	Total Surface Energy
AAB	43.25
ABD	47.40
AAM	50.15
AAF	44.60
AAH	46.50
AAL	48.20
AAD	40.40
AAE	48.30
AAB-AG	44.0
ABD-AG	49.10
ABD-LA	45.90

Important observations from the data presented in Table 15 are as follows:

- The range of the LW component of surface energy varied from approximately 40 to 50 ergs/cm^2, in proximity of the range of values for this component determined using other test methods.
- Estimating the precision of measurements from this technique is not straightforward. However, Appendix G presents a section on the general analysis of errors from this technique. Based on the errors from various sources, typically a variation of 3 to 6 ergs/cm^2 (6 to 12 percent coefficient of variation) in the surface energy components is possible.
- The jump to contact force for asphalt binders modified with a liquid antistripping agent was considerable, indicating strong interactions between the tip and the modified asphalt surface.
- In order to measure the acid and base components of the asphalt binder, the tip of the glass bead cantilever may be modified by active mono-layers of polar materials. However, further research is required to be able to derive all three surface energy components using this methodology.

Advantages and Limitations

Several different types of AFM are available commercially. Although the capital outlay required to set up some of the basic AFM is not very high, a skilled operator with extensive training is required to be able to obtain the force-distance curves and determine the surface

energy components of the asphalt binder. Asphalt binder samples are prepared by dispensing a drop of the solution of asphalt binder in toluene solution on a glass substrate. This process might alter some of the binder properties compared to its initial state.

An advantage of this test method is its ability to measure properties at a nano-scale. This enables identification of different phases within the asphalt binder and the specific properties of each phase, instead of the representative average obtained from other test methods. However, this advantage becomes a disadvantage if a larger length scale for surface energy measurement is required, such as is the case when principles of fracture mechanics are applied. Use of functionalized cantilever tips with the AFM can also provide valuable information about the polar groups in asphalt binders. Research in this area is currently in progress.

Although application of AFM to measure surface energy components of asphalt binders is not envisaged in the near future, this device is strongly recommended as an important material characterization tool for advanced research related to the properties of asphalt binders.

3.2.7 Micro Calorimeter

This method is recommended for use as a rapid test to obtain estimates of the surface energy components of aggregates. However, results from this test method demonstrate a systematic error. Further research can help eliminate the systematic error and make this approach more useful as a routine test to measure the surface energy components of aggregates.

Method Overview

A micro calorimeter is used to measure the total heat of immersion or enthalpy of immersion of an aggregate when it is immersed in a probe liquid. In this research a differential isothermal micro calorimeter was used. Figure 31 illustrates the schematic layout of the differential micro calorimeter.

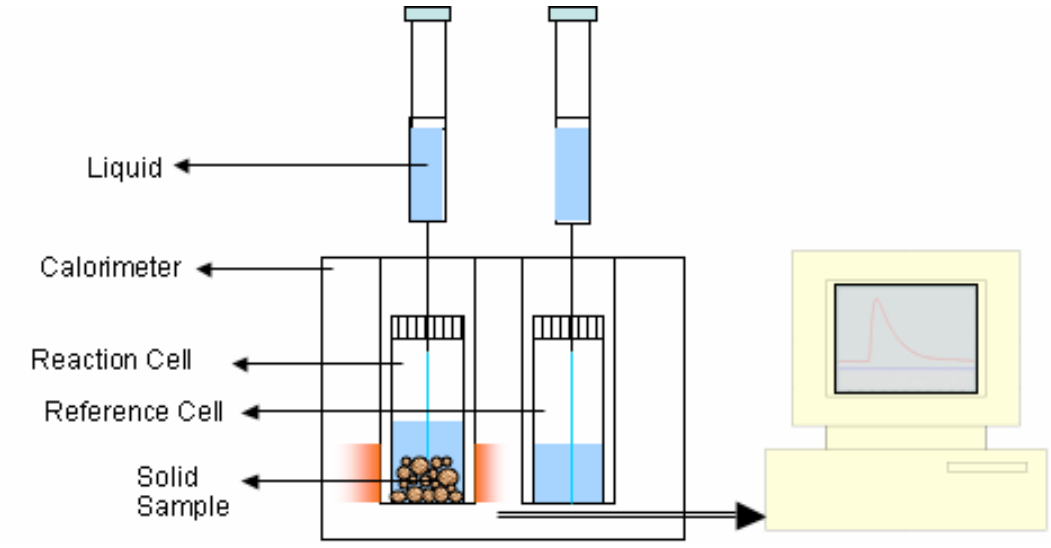

Figure 31. Schematic Layout of the Micro Calorimeter.

In the absence of chemical reactions, the enthalpy of immersion represents the reduction in total energy of the system due to the total surface energies of the two materials. If the interfacial surface free energy at the aggregate-liquid interface is represented by γ_{AL}, and surface

free energy of the clean solid surface is represented by γ_A, then, based on the above explanation, the change in free energy of the system due to immersion ΔG_{imm} is given by:

$$\Delta G_{imm} = \gamma_{AL} - \gamma_A \quad \textbf{[24]}$$

The right-hand side of equation [24] can be replaced by the surface free energy components of the solid and liquid using the GVOC theory. Further, based on the classic Gibbs free energy equation, ΔG_{imm} can be replaced by the enthalpy of immersion, ΔH_{imm}, and entropy of immersion, ΔS_{imm}, to obtain the following equation:

$$\Delta H_{imm} - T\Delta S_{imm} = \gamma_L - 2\sqrt{\gamma_A^{LW}\gamma_L^{LW}} - 2\sqrt{\gamma_A^+\gamma_L^-} - 2\sqrt{\gamma_A^-\gamma_L^+} \quad \textbf{[25]}$$

In equation [25] the subscript "A" refers to the aggregate and "L" refers to the liquid and other terms are as described previously.

Douillard et al. *(32)* determined the heats of immersion and adsorption isotherms for various pure minerals with different probe liquids. Based on the comparisons of adsorption isotherms and heats of immersion, they demonstrated that the entropy term $T\Delta S_{imm}$ in equation [25] can be approximated as 50% of the magnitude of the enthalpy term ΔH_{imm} at 25°C. Since aggregates are composed of minerals, which belong to the same class of materials used by Douillard et al., it is reasonable to extend this approximation to heats of immersion with aggregates. If a calorimeter is used to measure enthalpy of immersion, ΔH_{imm}, of a solid immersed in a probe liquid with known surface free energy components, and the approximation that the entropy term is 50% of the magnitude of the enthalpy term is used, then the only unknowns in equation [25] are the three surface free energy components of the solid. Analogous to the Wilhelmy plate method and USD, measuring enthalpy of immersion with three probe liquids generates a set of three equations that are solved to determine the three surface free energy components of the aggregate.

Recent Developments

Some of the developments to use the micro calorimeter for measurement of surface energy components of aggregates are as follows:

- A simple sample preparation and preconditioning method was developed. Since degassing of sample requires more time than the test, an independent degassing unit that allows degassing of more than one sample at a time was developed. This also significantly reduced the time for engaging the micro calorimeter to test each sample.
- Analysis methods to derive the surface energy components by measuring their heat of immersion in different probe liquids were developed.
- A methodology to measure the total energy of adhesion between asphalt binders and aggregates at their mixing and compaction temperatures was also developed.

Surface Energy Components of Aggregates

In this research a differential isothermal micro calorimeter manufactured by OmniCal Inc. was used. The device is accompanied by user friendly software to measure the heat flow and determine the total heat of immersion. Three probe liquids, heptane, chloroform, and benzene, were used to measure the surface energy components of the aggregates. In addition to these tests, the heat of immersion of the aggregates with water was also measured to assess the relative affinity of the aggregates to water. The SSAs of aggregates must be known in order to complete the surface energy calculations. In this research, SSA of the size fraction of the

aggregates that were measured with the micro calorimeter were measured using the USD. In practice, this value can be obtained from simple nitrogen adsorption tests with the aggregate. Table 16 presents the surface energy components of the aggregates measured using the micro calorimeter.

Table 16. Surface Energy Components of Aggregates Measured Using the Micro Calorimeter in ergs/cm^2 at 25°C.

Aggregate	LW Component		Acid Component		Base Component	
	Value	Std. Dev.	Value	Std. Dev.	Value	Std. Dev.
RD	52	3.4	11	0.0	469	24.0
RG	48	1.0	162	3.6	920	52.7
RK	18	0.4	16	0.6	154	0.7
RL	38	3.4	42	1.0	1652	78.4

Important observations from the data presented in Table 16 are as follows:

- The LW component of surface energy varies from 18 to 52 ergs/cm^2. This range of values is slightly broader than the range determined using the USD.
- The magnitude of acid component of surface energy is small compared to magnitude of the base component, with the exception of RG. Also, the base component of surface energy was the highest among all three components. This observation is consistent with the results from the USD and the IGC. Also, the order of magnitude of the base component is the same as obtained with these two test methods.
- The standard deviation of the surface energy components was typically a small percentage of the value. This suggests that the test method is sensitive to the surface energy components for different types of aggregates.

Change in Aggregate Surface Energy Due to Aging

In this research the micro calorimeter was also used to evaluate the effect aging surface properties of the aggregate. As described previously, the aggregates used in this research were obtained from the Materials Reference Library (MRL), Reno, Nevada. These aggregates were in storage for over 10 years in the materials library. Therefore, it is reasonable to consider that the surface properties of the aggregates that were received directly from the materials library represent an aged condition. In order to obtain the surface properties of the fresh aggregates, large aggregate particles (larger than 12.5 mm) were crushed to obtain the size fraction passing the number 100 sieve and retained on the number 200 sieve. This process created a significantly large proportion of freshly crushed aggregate surface in the aggregate sample. The crushed aggregate sample was immediately transferred to vacuum sealed polyethylene bags and stored at 4°C prior to testing. The micro calorimeter was used to measure the heats of immersion of various probe liquids on the freshly crushed aggregate sample. Two aggregate types, RD and RK were used for these tests. No specific trends in the heat of immersion with mono polar acid or base probe liquids were observed due to aging differences for these two aggregates. In most cases the change in the heat of immersion due to aging was not significant. This is not unusual since freshly crushed high energy surfaces (such as aggregates) are reported to accumulate

surface contamination within few seconds after exposure to atmosphere *(1)*. Further, research is required to evaluate the effect of different aging methodologies, such as accumulation and oxidation of organic debris, on the surface energy components of aggregates.

Advantages and Limitations

The micro calorimeter is a commercially available device and requires a relatively small capital outlay for laboratory setup. A degassing station to degas and prepare the samples for testing was developed in this research to improve the time efficiency of the test method. The test procedure is simple and requires minimal training. Clean aggregate samples (passing #100 sieve and retained on #200 sieve) are used without any special preparation procedure for this test.

An advantage of this test method is that tests can be conducted on aggregate samples either in air, in a vacuum, or in intermediate states. This is in contrast to the sessile drop method and the USD. The sessile drop method measures the properties of aggregate in air when there can be significant amount of water vapor adsorbed on the aggregate surface. Aggregates used in the hot mix plant rarely have this type of a surface. The USD measures properties of the aggregates in a complete vacuum after almost all physically adsorbed molecules are removed from the surface. In some cases, researchers or application engineers may be interested in testing the properties of aggregates with a specific amount of moisture retained on their surfaces. The micro calorimeter can be used to measure heats of immersion and determine surface properties of aggregates with different initial conditions. The micro calorimeter can also be used to conduct immersion tests over a broad range of temperatures.

Other applications of a micro calorimeter include the direct measurement of total energy of adhesion between aggregates and asphalt binders at the mixing and compaction temperature. This device can also be used to quantify the affinity of water for different aggregates in terms of the heat of immersion of aggregates in water.

A limitation of this device is that the SSA of the size fraction of the aggregate tested must be known in order to determine surface energy components of the aggregate. Furthermore, the assumption that the contribution of entropy is a set value (50%) establishes a potential systematic error in the surface energy measurements. This probably can be corrected by measuring enthalpy at different temperatures and backcalculating entropy.

The simplicity and short test durations are key advantages of this test method. In order to use this method as a routine test method for measurement of surface energy components of aggregates, further research is required to eliminate the systematic errors due to the contribution of entropy.

3.3 SURFACE ENERGY COMPONENTS FROM DIFFERENT TEST METHODS

As described earlier in this report, direct measurement of surface energy of solids or their components is not feasible. A more practical method to determine the surface energy components is to experimentally measure a physical property that is a manifestation of the surface free energy between two materials. The surface energy components of solids are determined by applying appropriate theories and models to the physically measured property.

While comparing surface energy components of the same material determined using two or more methods, consideration must be given to the fact that each test method has different sources of experimental and systematic errors and is based on a different theory. For example, consider the comparison between surface energy components of an aggregate measured using the USD with the surface energy components of the same aggregate measured using IGC. The USD

measures adsorption isotherms that are used to determine the equilibrium spreading pressure, which is related to the surface energy components of the aggregate and probe vapors. IGC measures retention times of small quantities of probe vapors carried using an inert gas (infinitely dilute condition) through a column of the sample. The retention times are used to compute the free energy of desorption of the probe molecules, which are then related to the surface energy components of the aggregate and probe vapors. The infinitely diluted condition of probe vapors in IGC prevents measurement of averaged representative properties of the sample in the column. However, this method is highly sensitive to the presence of strongly polar molecules and may be advantageous in identifying, for example, aggregates with mineral interfaces that might initiate debonding, so-called "hot spots." The surface energy components from both these methods for the same material may not necessarily agree.

3.3.1 Asphalt Binders

The four test methods selected to measure the surface energy components of asphalt binders are the Wilhelmy plate method, the sessile drop method, inverse gas chromatography, and atomic force microscopy. The Wilhelmy plate method and sessile drop method measure contact angles of probe liquids with the asphalt binder in a static and dynamic mode, respectively. IGC measures the retention time of probe vapors when they pass through a capillary column coated with asphalt binder, and AFM measures the force-distance curves of a glass bead tip cantilever in close proximity to the surface of the asphalt binder.

All methods, except for AFM, can be used to determine the three surface energy components of the asphalt binders. At the time this report was written, research for using AFM to determine the acid and base components of surface energy for asphalt binders was still in progress. Also, the properties of asphalt binders measured using the AFM are representative of relatively smaller areas and on a nanometer scale.

Asphalt samples used in IGC are prepared by coating a capillary column by passing asphalt binder solution in toluene using dry nitrogen gas. Typically, the capillary column is about 30 m long in the form of a coil. Although the area of the asphalt binder exposed to the probe vapor is significant, the concentration of the probe vapor in the carrier gas itself is very low. Since the asphalt binder is a chemically heterogeneous material, the probe vapor molecules interact with only the higher energy areas of the asphalt binder. As a result, the surface energy component measured by IGC is usually higher and representative of the most active species on the surface.

Compared to AFM or IGC, the sessile drop and Wilhelmy plate methods measure more representative general properties of the binder surface. The unique modes of measurement of IGC and AFM compared to the sessile drop method or the Wilhelmy plate method preclude direct comparison of the surface energy components from the former two test methods with the latter two. However, results from all four test methods indicate that the LW component is the most significant contributor to the surface energy of asphalt binders. The value of this component varies from 14 to 50 ergs/cm^2, which is common for low-energy materials such as asphalt binders and polymers. Also, the acid and base components from all test methods are very small, ranging from 0 to 3.9 ergs/cm^2. This is in agreement with the fact that asphalt binders are weakly polar materials.

Both the Wilhelmy plate method and the sessile drop method measure contact angles of probe liquids with asphalt binders. In the Wilhelmy plate method, a glass slide coated with asphalt binder is suspended from a microbalance. The mass of the slide is recorded as the slide is

slowly immersed to about 5 mm depth in the probe liquid and retracted back to its initial condition. The contact angle is computed from force equilibrium conditions as identified in equation [19]. The contact angle obtained with the Wilhelmy plate method is representative of the infinite number of boundaries between the liquid and the solid that are created as the slide is immersed in the probe liquid. In the sessile drop method, contact angles are measured by capturing an image of the drop of the probe liquid on the solid surface. Figure 32 illustrates a typical example of the image of the drop obtained from this method. Two contact angles are obtained from the two diametrically opposite ends of the image of the drop.

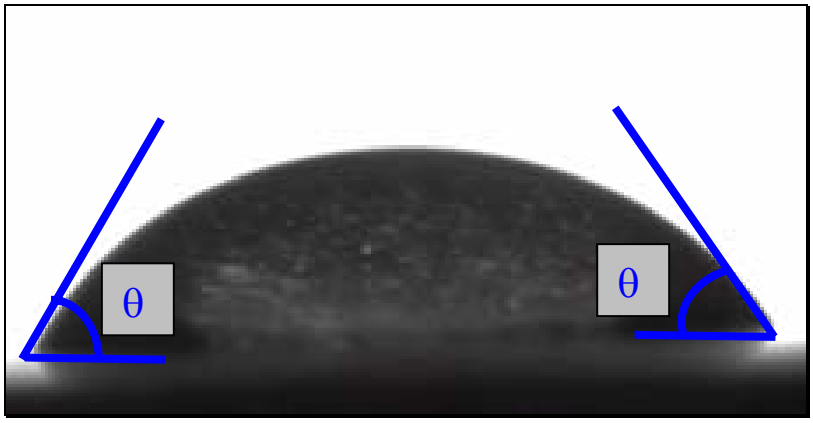

Figure 32. Typical Image of Sessile Drop for Contact Angle Measurement.

The surface energy components of asphalt binders from the Wilhelmy plate method and the sessile drop method are determined from contact angle measurements. Both test methods produced results for the LW component with adequate precision. Figure 33 illustrates a comparison of these results. The comparison also reflects a bias in the results due to the differences in the methodologies used to measure contact angles with these two methods.

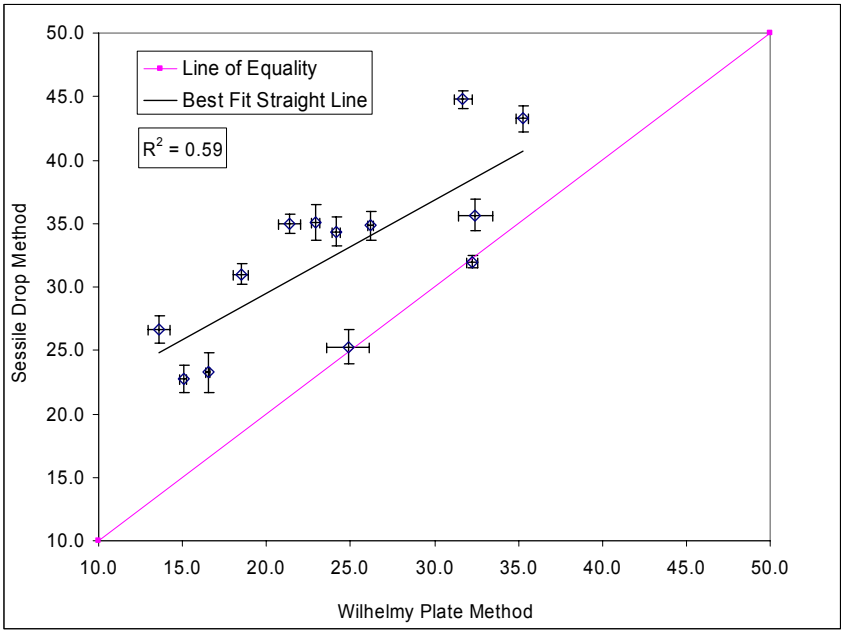

Figure 33. Comparison of the Lifshitz-van der Waals Component of Asphalt Binders Measured using the Wilhelmy Plate Method with the Sessile Drop Method in ergs/cm^2 at 25°C.

The base component measured using the Wilhelmy plate method and the sessile drop method was negligible for almost all asphalt binders with two exceptions. Asphalts AAD and ABD showed small values of the base component with the Wilhelmy plate method and the sessile drop method. The only neat asphalt binder that had a significant base component with the sessile drop method and negligible base component with the Wilhelmy plate method was AAM. In case of the three aged asphalt binders, the base component was of significant magnitude when determined by either test method. There was, however, a significant time interval between when the contact angle was measured for neat AAM with the Wilhelmy plate method when the contact angle for AAM was measured with the sessile drop method. Since AAM is susceptible to aging, it is speculated that the large difference in base component from the two test methods could be due to this factor.

The Wilhelmy plate method measured a significant value for the acid component for most asphalt binders, neat and modified. However, the sessile drop method indicates a negligible value of the acid component for all asphalt binders. This could be due to the differences in test methodologies to obtain contact angles coupled with sensitivity of the test methods. For example, in the sessile drop method the point of equilibrium advancing contact angles is determined by dispensing the drop and adding volume to it until the drop is at a point where extension of its interface with the aggregate surface is imminent. It is speculated that some further research on improvement of method sensitivity and use of more sensitive instruments can alleviate this problem.

3.3.2 Aggregates

The four test methods that were selected to measure the surface energy components of aggregates were the universal sorption device, sessile drop method, inverse gas chromatography, and micro calorimeter. Each of these methods measures a unique form of physical interaction due to the surface energies of the materials. The USD measures adsorption isotherms of probe vapors with the aggregate surface, the sessile drop method measures contact angles of probe liquids on a smooth aggregate surface, IGC measures retention time of probe vapors as they pass through a column filled with the aggregate sample, and the micro calorimeter measures the heat of immersion when aggregate samples are immersed in a probe liquid. All four test methods can be used to determine the three surface energy components of the aggregate. The size, preparation, and initial condition of the aggregate is different for each test method.

With the exception of the sessile drop method, no special sample preparation is required for these tests. For the sessile drop method, a piece of aggregate approximately 12.5 mm in size must be polished to obtain a smooth and flat surface. The probe liquid is dispensed on the aggregate surface to measure the contact angle at the interface. For the other three test methods, an appropriate size fraction of the aggregate is obtained by dry and wet sieving the aggregates as obtained from the source. Aggregate passing the #4 sieve and retained on the #8 sieve, and passing the #100 sieve and retained on the #200 sieve are used with the USD and the micro calorimeter, respectively. Aggregate sizes smaller than about 3 mm may be used with IGC. Since surface free energy is an intrinsic material property, it is unlikely to change with the size of the material. This can be regarded as generally true, unless the size fraction of the aggregate is extremely small so that the effect of differences in surface energies of edges compared to the surface energies of faces predominates *(21)*.

The difference is the size range of aggregates used with each test method probably do not significantly affect the measured surface energy components. The aggregates are degassed under high temperatures and a vacuum before being tested with the USD or the micro calorimeter. This process removes a significant fraction of water and other molecules that are physically adsorbed on the aggregate surface at room temperature and in an open atmosphere. These adsorbed molecules significantly lower the surface energy of the aggregates. A similar effect is achieved in IGC by purging a dry inert gas at very high temperatures prior to measuring the interaction between the gas and the aggregate. In contrast, the sessile drop method measures the contact angles of the aggregates in an open atmosphere, where the surface energy is significantly lowered due to adsorption of water molecules or molecules from the probe liquid on the aggregate surface. In fact, in most cases measurement of a finite contact angle is only possible when the surface energy of the aggregate is reduced due to surface contamination. The aggregates that are coated with bitumen in a hot mix plant are subjected to very high temperatures just prior to mixing. This facilitates removal of moisture from the aggregate surface. Therefore, the aggregate surface measured with the USD, micro calorimeter, or IGC provides a better representation of the surface properties of interest as compared to the measurement made with the sessile drop method. Of course, a case can be made for having the capability of measuring the impact of a modest amount of moisture or organic contamination on the aggregate surface.

The theoretical models used with IGC are valid only when the probe molecules are present in the inert carrier gas in an infinitely dilute condition, i.e., the concentration of probe vapors in the inert gas is extremely low. Since aggregate surfaces are typically heterogeneous, the probe vapor molecules interact with only high-energy functional groups on the aggregate surface. Therefore, the surface energy components of aggregates derived using IGC are representative of the highly polar species on the surface and not an average representation of the aggregate surface at a micro-scale. This also explains why surface energy components measured using IGC are in general higher when compared to the other methods. Analogous to the measurement of asphalt binders, this limitation of IGC precludes comparison of results from this test method with other test methods.

The USD and the micro calorimeter both test the surface properties of aggregates in a vacuum. The former test method measures adsorption isotherms, while the latter measures heats of immersion. The adsorption isotherm is used to obtain the equilibrium spreading pressure, which is related to the Gibbs free energy and surface energy components of the materials. The micro calorimeter measures the total heat of immersion, which is the sum of Gibbs free energy of immersion and the entropy of immersion. Since surface energy components of the aggregate are related to the Gibbs free energy, either the entropy of immersion must be measured in a different experiment or estimated from theoretical considerations. In this research, the contribution of entropy at 25°C was estimated to be about 50% of the measured enthalpy based on the literature. However, this approximation may introduce a bias when the results are compared with the USD.

With the exception of the acid component of RG, the order of magnitude of each of the surface energy components obtained from the USD and the micro calorimeter are the same. Results also indicate that the micro calorimeter provides a broader range of values for the LW component when compared to the USD. The base component of the aggregates measured using the USD and the micro calorimeter show similar trends. An important application of surface energy components is not to rank aggregates based on their surface energy components, but to calculate the work of adhesion and work of debonding for different combinations of asphalt

binders and aggregates. For example, the energy parameters ER_1 and ER_2 are used to quantify the moisture sensitivity of any combination of asphalt binder and aggregate based on their surface energy components. Figures 34 and 35 illustrate a comparison of these two parameters determined using the Wilhelmy plate method and the USD versus the values determined using the Wilhelmy plate method and the micro calorimeter. The comparison is made for all four aggregates that were tested using the micro calorimeter and three asphalt binders AAB, AAD, and ABD. These figures demonstrate that although there is a bias in the results with the micro calorimeter, the trends of these energy parameters for different combinations of materials are similar irrespective of the method of measurement. Further research related to entropy measurement or its more refined estimation will help improve the accuracy and overall efficiency of this method for use on a routine basis to measure surface energy components.

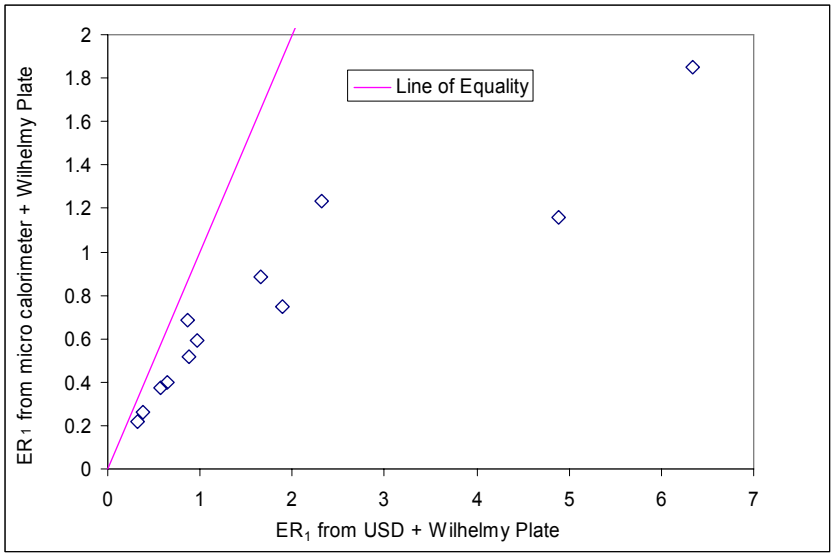

Figure 34. Comparison of ER_1 Derived from USD vs. ER_1 Derived from Micro Calorimeter.

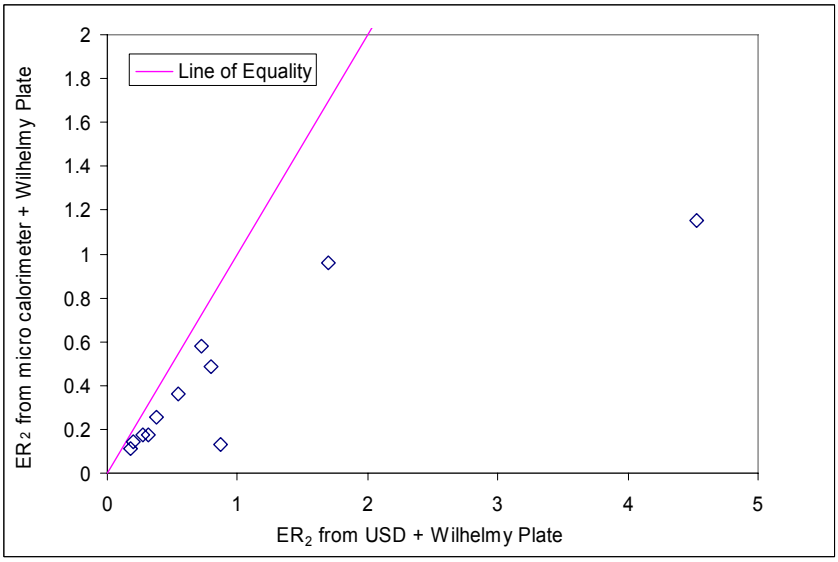

Figure 35. Comparison of ER_2 Derived from USD vs. ER_2 Derived from Micro Calorimeter.

3.4 CONSIDERATIONS IN USING SURFACE ENERGY METHODS TO SELECT MATERIALS FOR ASPHALT MIXTURES

Surface energy of asphalt binders and aggregates can be used to select materials that promote better performing asphalt mixtures. The relationship between surface energy of these materials with the moisture sensitivity of the asphalt mixture is straightforward and also well established in the literature. Surface energy is a fundamental material property that can also be combined with other material properties using principles of fracture mechanics and mechanistic models to predict the crack growth and healing characteristics of asphalt mixtures. This section presents a discussion related to both these applications.

3.4.1 Moisture Damage

Four energy parameters were introduced earlier in this report to quantify the moisture sensitivity of any given combination of asphalt binder and aggregate. Although all four parameters are derived using the surface energy components of these materials, they are independent measures of the moisture sensitivity of the mix. A combination of asphalt binder and aggregate with a higher value of any of the energy parameters will be more resistant to moisture damage compared to a combination with a lower value of the energy parameter. Tables 17 through 20 present the values for these four parameters for all 45 possible asphalt mixtures based on the combinations of the nine neat asphalt binders and five aggregates included in this research.

Table 17. Energy Parameter ER_1 for Different Material Combinations.

Bitumen	RA	RK	RL	RD	RG	Range
AAB	2.05*	6.34*	0.87*	2.32	0.97	0.87 – 6.34
ABD	1.34*	4.88*	0.57*	1.66	0.65	0.57 – 4.88
AAM	1.00	3.13	0.44	1.24	0.50	0.44 – 3.13
AAF	1.32	4.12	0.58	1.59	0.66	0.58 – 4.12
AAH	1.61	5.23	0.70	1.91	0.79	0.70 – 5.23
AAL	0.79	2.65	0.33	1.03	0.39	0.33 – 2.65
ABL	1.74	5.41	0.77	2.04	0.86	0.77 – 5.41
AAD	0.69*	1.90*	0.33*	0.88	0.38	0.33 – 1.90
AAE	2.23*	9.87*	0.89*	2.63	1.02	0.89 – 9.87
Range	0.69 – 2.23	1.9 – 9.87	0.33 – 0.89	0.88 – 2.63	0.38 – 1.02	Overall 0.33 – 9.87

* Indicates mixes selected for laboratory testing to evaluate impact of surface energy.

Table 18. Energy Parameter ER_2 for Different Material Combinations.

Bitumen	RA	RK	RL	RD	RG	Range
AAB	1.57*	4.53*	0.72*	1.70	0.80	0.72 – 4.53
ABD	0.51*	1.67*	0.27*	0.54	0.31	0.27 – 1.67
AAM	0.44	1.27	0.23	0.48	0.26	0.23 – 1.27
AAF	0.76	2.15	0.38	0.84	0.43	0.38 – 2.15
AAH	1.02	3.00	0.50	1.11	0.55	0.5 – 3.0
AAL	0.16	0.60	0.09	0.16	0.10	0.09 – 0.6
ABL	1.16	3.30	0.58	1.27	0.64	0.58 – 3.3
AAD	0.32*	0.87*	0.18*	0.38	0.20	0.18 – 0.87
AAE	1.32*	5.19*	0.61*	1.42	0.68	0.61 – 5.19
Range	0.16 – 1.57	0.6 – 5.19	0.09 – 0.72	0.16 – 1.7	0.1 – 0.8	Overall 0.09 – 5.19

* Indicates mixes selected for laboratory testing to evaluate impact of surface energy.

Table 19. Energy Parameter SSA*ER_1 for Different Material Combinations.

Bitumen	RA	RK	RL	RD	RG	Range
AAB	0.21*	65.81*	0.87*	0.60	0.72	0.21 – 65.81
ABD	0.13*	50.65*	0.57*	0.43	0.48	0.13 – 50.65
AAM	0.10	32.49	0.44	0.32	0.37	0.10 – 32.49
AAF	0.13	42.77	0.58	0.41	0.49	0.13 – 42.77
AAH	0.16	54.29	0.70	0.50	0.58	0.16 – 54.29
AAL	0.08	27.51	0.33	0.27	0.29	0.08 – 27.51
ABL	0.17	56.16	0.77	0.53	0.64	0.17 – 56.16
AAD	0.07*	19.72*	0.33*	0.23	0.28	0.07 – 19.72
AAE	0.22*	102.45*	0.89*	0.68	0.75	0.22 – 102.4
Range	0.07 – 0.22	19.72 – 102.4	0.33 – 0.89	0.23 – 0.68	0.28 – 0.75	Overall 0.07-102.4

* Indicates mixes selected for laboratory testing to evaluate impact of surface energy.

Table 20. Energy Parameter SSA*ER_2 for Different Material Combinations.

Bitumen	RA	RK	RL	RD	RG	Range
AAB	0.17*	47.75*	0.76*	0.44	0.59	0.17 – 47.75
ABD	0.06*	17.60*	0.29*	0.14	0.23	0.06 – 17.60
AAM	0.05	13.39	0.24	0.12	0.19	0.05 – 13.39
AAF	0.08	22.66	0.40	0.22	0.32	0.08 – 22.66
AAH	0.11	31.62	0.53	0.29	0.41	0.11 – 31.62
AAL	0.02	6.32	0.10	0.04	0.07	0.02 – 6.32
ABL	0.13	34.78	0.61	0.33	0.47	0.13 – 34.78
AAD	0.04*	9.17*	0.19*	0.10	0.15	0.04 – 9.17
AAE	0.15*	54.70*	0.65*	0.37	0.50	0.15 – 54.70
Range	0.04 – 0.17	6.32 – 54.70	0.10 – 0.76	0.04 – 0.44	0.07 – 0.59	Overall 0.04 – 54.70

* Indicates mixes selected for laboratory testing to evaluate impact of surface energy.

Several important observations can be drawn from these tables and are as follows:

- By measuring the individual surface energy components of the asphalt binder and the aggregate (in this case surface energies of 14 different materials) it is possible to develop a matrix of energy ratios for all the possible asphalt mixtures (in this case 45) based on different combinations of these materials.
- A wide range of values exists for any one of the energy parameters for different combinations of asphalt binder and aggregate.
- For any given aggregate type, the energy parameters vary significantly depending on the type of asphalt binder and vice-versa.
- Based on these parameters it cannot be generalized that a particular asphalt binder is prone to stripping without taking into consideration the aggregate with which it is being mixed. For example, the asphalt binder AAD may have a very low value of ER_1 when mixed with aggregate RL indicating a poor performing mix. But the same asphalt binder has a considerably higher value of ER_1 when mixed with aggregate RK. The same argument also holds good for aggregates.

Nine of the 45 combinations of asphalt binders and aggregates were selected for mixture testing in the laboratory. Section 2.6.2 presents the details of the comparison between the energy parameters and moisture sensitivity of asphalt mixtures based on laboratory testing. Some of important considerations in interpreting these results are as follows:

- These results are based on a limited number of mixes but mixes that demonstrate a wide range of energy parameters. Different energy parameters show different strengths of correlation with moisture sensitivity and different levels of moisture sensitivity of the mixes measured in the laboratory. Although some parameters might appear to have better correlation than others, these results must not be construed as conclusive for retaining or excluding one or any of these parameters for all future work. Also, all four parameters can be determined if the surface energy components of the asphalt binder, aggregate and the specific surface area of the aggregate are known.

- All selected mixtures had the same aggregate gradation and were designed and compacted in a similar manner in order to minimize variability due to extraneous (other than surface free energy) factors such as air void distribution and mixture volumetrics.
- The results demonstrate how surface energy components of asphalt binders and aggregates may be used to eliminate moisture sensitive mixes.
- Only neat asphalt binders were selected for these mixes. The impact of addition of active fillers such as hydrated lime, liquid antistrip agents, and other chemically active compounds on the surface energy components of asphalt binders and eventually on their moisture sensitivity still needs to be established. This is part of the proposed future work plan, as described in Chapter 4.
- The four energy parameters can best serve as a material selection tool, although a specific threshold value can only be recommended after an extensive investigation of various mixes and their performance. Appropriate selection of materials cannot compensate for moisture induced damage due to other factors such as open air void structure of the mix or poor construction practices and, etc.
- Surface energy components can be used to predict performance of mixes in addition to being used as a material selection tool. In order to do so, mechanistic models based on principles of fracture mechanics that account for material properties such as surface energy must be used. The following section on fatigue presents an example of such a model.
- The energy parameters were derived by measuring surface properties with the USD on aggregates passing the #4 sieve and retained on the #8 sieve. Although asphalt mixtures contain aggregates over a wide range of sizes, it is unlikely that the surface energy and hence the energy parameters will be significantly affected by the aggregate size. This is because surface energy is an intrinsic material property and is independent of geometry. This is generally true unless the aggregate size fraction is so small that the differences in edge and face surface energies become significant. Aggregate particles of such small sizes are more likely to be considered a part of the mastic phase and not independent particles adhered to by the binder.
- The specific surface areas used in the last two energy parameters are derived from measurement of aggregates passing the #4 sieve and retained on the #8 sieve with the USD. SSAs of different size fractions of the same aggregate will be different. However, the trends in the SSA between different size fractions of aggregates are likely to be similar for any given size fraction.

3.4.2 Fatigue Cracking

A model to determine the crack growth behavior of asphalt mixtures was proposed in section 2.4.2 of this report. This model incorporates the effect of important material properties to predict the crack growth behavior in asphalt mixtures. Examples of material properties required as model input data are work of adhesion determined using the surface energy of asphalt binders and aggregates and the undamaged modulus of the material. Material properties other than the surface energy components of asphalt binders and aggregates are obtained by conducting some simple tests using the DMA on asphalt mastic samples. Table 3 in section 2.5.2 presents a comparison of the predicted fatigue cracking characteristics of the asphalt mixture using this model with actual performance of the mix in field. Table 5 in section 2.6.3 demonstrates how

this model can be employed to determine the crack growth characteristics of various mixes. Some of the important considerations in using this model are as follows:

- The term ΔG_f in equation [12] used in this case is the adhesive bond energy, which has the same magnitude as the work of adhesion between the asphalt binder and the aggregate. Fatigue cracking in asphalt mixtures can be in the form of adhesive cracks, i.e., cracks formed at the interface of the asphalt binder and the aggregate or cohesive cracks, i.e., cracks formed within the asphalt binder. The actual nature of cracks will depend on the film thickness *(8)* of the asphalt binder over the aggregate. Thinner films are prone to adhesive failure while thicker films are prone to cohesive failure. Further research is required to incorporate the effect of different film thickness and hence the mode of failure from adhesive to cohesive in the term ΔG_f. This will still require the use of surface energy components of the asphalt binder and the aggregate.
- In this research, the benefit of rest periods during testing for healing of the mixes was accounted for in terms of the parameter b from DMA tests. This parameter, along with the undamaged material properties of the mastic, was used with the adhesive bond energy ΔG_f in equation [12] to demonstrate the use of material properties to assess the fatigue characteristics of mixes with rest period. According to the literature *(39)*, asphalt binders undergo short-term and long-term healing, which depends on its surface energy components. Although this research demonstrates the application of surface energy and concomitant bond strengths to predict the fatigue cracking characteristics of asphalt mastics subjected to rest periods, further research is required to expand on the relationship between surface energy and healing characteristics of these materials.
- Higher adhesive bond strengths between asphalt binders and aggregates can cause an increase in the stiffness of the asphalt mixture. While an increase in stiffness of the mix might increase its susceptibility to fatigue cracking, higher adhesive or cohesive bond strengths will also tend to increase the amount of external work required for fatigue cracks to propagate.

CHAPTER 4
CONCLUSIONS AND SUGGESTED RESEARCH

4.1 GENERAL CONCLUSIONS

In this research various methods by which to measure surface energy components of asphalt binders and aggregates were evaluated based on the expectation that the selected methodology will ultimately be used for routine screening and selection of material for optimum performance of asphalt pavements. This research also provides a limited validation of the relationship between surface energy of these materials and the performance of asphalt mixtures. The following section presents the general conclusions from this research related to these two aspects.

4.1.1 Methods to Measure Surface Energy of Asphalt Binders

Four candidate methods were used to measure the surface energy components of asphalt binders. The Wilhelmy plate method and the sessile drop method are recommended for use on a routine basis to measure the surface energy components of asphalt binders using at least five probe liquids. Some further research is required with the latter test method in order to improve its sensitivity to the acid and base components of the asphalt binders. IGC and AFM can be used as advanced material characterization tools to characterize surface properties of asphalt binders. These recommendations are based on criteria such as precision of the test method, ability to measure the three surface energy components, ability to measure a representative surface area of the sample, and practical considerations such as capital outlay and expertise and experience required from the operator in order to conduct each type of test.

4.1.2 Methods to Measure Surface Energy of Aggregates

Four candidate methods were used to measure the surface energy components of aggregates. The USD is recommended for use on a routine basis to measure the surface energy components of aggregates. The use of a micro calorimeter to measure the surface energy components of aggregates entails making an assumption for the contribution of entropy. Further research with this test method can improve the accuracy of results and render it useful as a routine test method to measure the surface energy components of aggregates. The IGC can be used for advanced material characterization and to measure specific surface properties of aggregates and pure minerals. These recommendations are based on criteria such as precision and accuracy of the test method, ability to measure a representative area of the sample, and practical considerations such as expertise required to conduct each type of test.

4.1.3 Application of Surface Energy to Select Materials for Asphalt mixtures

Four energy parameters, based on the work of adhesion between asphalt binder and aggregate, work of debonding when water displaces binder from the aggregate, wettability, and specific surface area of the aggregate, were evaluated in this research to select materials for asphalt mixtures that are resistant to moisture damage. These energy parameters can be computed for all possible combinations of different asphalt binders and aggregates if the surface energy components of these materials are known. In general, parameters demonstrated good correlations with the moisture sensitivity of nine different asphalt mixtures measured in the laboratory.

Surface free energy of asphalt binders and aggregates and concomitant works of adhesion or cohesion are important material properties that can be used with the principles of fracture mechanics to model the crack growth behavior and healing characteristics of asphalt mastics. Other important material properties that relate to the crack growth behavior in asphalt mastic can be obtained from simple tests conducted using a DMA. In this research it was demonstrated that material properties derived from surface energy measurements and tests with the DMA can be used to determine the crack growth behavior in mastic samples. Limited correlation of results based on this approach with the qualitative performance of field mixes was also demonstrated.

4.2 SUGGESTED RESEARCH

The various aspects related to measurement and use of surface energy to select materials for asphalt mixtures covered in this research were:

- selection and development of appropriate test methods to measure surface energy components of asphalt binders and aggregates,
- identification of parameters based on principles of thermodynamics and fracture mechanics that relate the surface energy of these materials to the performance of asphalt mixtures,
- measurement of the surface energy components for a suite of asphalt binders and aggregates, and
- limited validation of the relationship between the selected parameters and field or laboratory performance of asphalt mixtures.

The results of this research provide an important skeletal structure for the implementation of surface energy measurement methodology for selection and specification of materials for asphalt pavements. Additional testing, verification, and refinement is required in each of the aforementioned aspects of this research. This will facilitate development of specification type recommendations based on a larger database of material properties that include surface energy measurements and long-term field performance under specific traffic and environmental conditions. This section presents a work plan for future studies to achieve this objective.

4.2.1 Effect of Temperature on Surface Energy

In this research most surface energy measurements were made at 25°C. Typically, surface energy of a material decreases slightly with an increase in temperature. The working hypothesis in this research was that the trends in change of surface energy components of various materials with temperature are similar. Nevertheless, it is important to quantify the effect of temperature on the surface energy components of asphalt binders and aggregates in future studies.

4.2.2 Surface Energy of Asphalt Binders

Surface energy components of various unmodified asphalt binders were measured in this research. Surface energy components of a limited number of asphalt binders modified by aging, addition of liquid antistrip agents, and fine filler material were also determined. The objective of measuring the surface energy components of modified asphalt binders was to determine if the test methods are sensitive enough to detect the differences in surface energy due to these modifications. In some cases, such as addition of liquid antistrip agents, the concentration of the additive and its effect on the surface energy components is very small. A more detailed study is

required to establish the relationship between addition of chemically active modifiers, surface energy components of the binder, and performance of the asphalt mixtures.

The presence of functional groups or chemically active materials in asphalt binders is the foundation of the adhesive bond with aggregate surfaces. The effect of these groups on the surface energy of asphalt binders must be investigated in more detail by using base asphalt binders that are modified by addition of various model compounds that represent various functionalities in asphalt binders. This information can greatly enhance the understanding of the mechanisms of adhesion between the asphalt binder and aggregate and also provide information to make intelligent decisions such as how to modify various types of asphalt binders and improve their performance.

4.2.3 Surface Energy of Aggregates

Surface energy components of various aggregates and pure minerals were measured in this research. Although the methodology to use sorption measurements with the USD to measure surface energy components of aggregates has a sound theoretical basis, this method is inherently time consuming. Various other approaches were introduced in this research to obtain rapid estimates of surface energy components of aggregates. Further work that is required to advance these approaches is described below.

A micro calorimeter can be used as an efficient tool to estimate the surface energy components of various aggregates. However, the contribution of entropy must be approximated, which reflects on the accuracy of the results obtained from this method. Measuring the enthalpy of immersion at more than one temperature can alleviate this drawback. Studies to further develop this methodology and implement it for use on a routine basis are recommended.

The surface energy of aggregates can also be estimated using a numerical model that requires the quantitative mineralogical composition and the surface energy components of the minerals as input data. In order to develop this model, a large database of surface energy components of various aggregates and pure minerals is required. It is recommended that a centralized database of aggregate mineralogy from various sources and surface energy components be maintained to achieve this objective.

Surface energy of aggregates is a function of the different mineral groups present on its surface. Generically similar aggregates can have widely different surface energies depending on the exact mineralogical composition of the aggregate. However, it is possible that the surface energy components of a particular aggregate from a given source remain similar irrespective of the batch or location within the quarry. For example, limestone aggregates may have significantly different surface energy components depending on the source and exact mineralogical composition of the aggregate. However, limestone aggregates from the same quarry or geological location may have similar surface energy components. If this is true, representative surface energy components of aggregates from a given source need only to be measured periodically. Studies to investigate the changes in surface energy of materials from different sources within the same quarry are needed to address this important question.

Another important consideration in the surface energy of aggregates is the initial state of the aggregate when tests are conducted. The USD and micro calorimeter measure the surface energy of aggregates in a vacuum where a negligible amount of water is present on the aggregate surface. It is important to determine the real state of the aggregate at mixing and compaction temperatures. This is especially important in applications such as warm mix asphalt, where the surface energy of the aggregate may be reduced due to the presence of water molecules on its

surface. It is recommended that future studies be undertaken to measure the surface energy components of aggregates with different initial states.

Chemically active minerals such as limestone may interact with certain functional groups from the asphalt binder to form compounds at the interface. The formation of these bonds in some systems contributes to the binder-aggregate adhesion in addition to the surface energy of the materials. The micro calorimeter can be deployed to measure the heat of immersion of different asphalt binder and aggregate systems and used in conjunction with the surface energy components of these materials to identify the presence of chemical interactions in various asphalt binder and aggregate systems. Further studies must also include testing of various asphalt binder and aggregate systems, especially modified binders, to evaluate the effect of chemical interaction on adhesion.

4.2.4 Application of Surface Energy to Predict Performance of Asphalt mixtures

The scope and limitations of surface energy to select materials and predict performance must be understood by its end user. To better understand this, consider the Performance Grade (PG) system of classifying asphalt binders. Selection of the appropriate PG asphalt binder based on the climatic conditions where the pavement is being constructed is an important step in the material selection process. However, selection of the correct PG binder does not preclude other important tests such as the dynamic modulus test to evaluate the overall mixture properties. Similarly, use of the energy parameters must be regarded as a material selection tool only. In order to better assess the fracture and plasticity characteristics of the mix in wet and dry conditions, surface energy of the asphalt binder and aggregates must be used in conjunction with other material properties such as those obtained by tests with the DMA, using a mechanistic model, to predict the performance of the asphalt mixture as a whole.

Based on the aforementioned explanation it is recommended that future studies be aimed at developing the application of surface energy using a two-pronged approach. First, the surface energy components of a large collection of aggregates and asphalt binders must be measured and concomitant energy parameters must be calculated and compared with long-term field performance of pavements. Comparisons must be made on similar types of mixes with the objective of deriving a threshold value of energy parameters that can be used to select materials that yield an acceptable performance of the asphalt pavement. Second, surface energies of materials must be integrated with other material properties of the asphalt binder, aggregate, or mastic using mechanistic models to predict the performance of asphalt mixtures. A database of pavements with known performance, traffic, environmental conditions, and mixture properties can be used to validate or calibrate this model.

4.3 SUMMARY OF WORK PLAN FOR FUTURE

The following is a summary of the work plan for future studies related to the implementation of surface energy to select materials for asphalt pavements:

- Quantity of effect of temperature on surface energy components.
- Evaluate the effect of liquid antistrip agents and active fillers on the surface energy component of asphalt binders and performance of asphalt mixtures.
- Evaluate the influence of various functional groups in asphalt binders on its surface energy using model compounds.
- Refine the use of a micro calorimeter to measure surface energy components of aggregates.

- Develop a database of aggregate surface energy components and evaluate the effect of location in the quarry on the surface energy of aggregates.
- Develop a database of surface energy components of various pure minerals commonly found in aggregates.
- Compare heats of immersion of different aggregate-binder systems measured with the micro calorimeter with the work of adhesion of the systems derived from their surface energy components.
- Develop a database of similar mixes with known long-term field performance and compare the energy parameters of the materials used in these mixes to derive a threshold value that enables selection of materials for durable mixes.
- Develop mechanistic models that incorporate surface energy of asphalt binder and aggregate along with other material properties to predict the performance of asphalt mixtures and calibrating the model based on field data.

REFERENCES

1. Adam, N. K., The Physics and Chemistry of Surfaces - Third Edition, Oxford University Press. (1940) 436 pages.

2. Fowkes, F. M., "Determination of Interfacial Tensions, Contact Angles and Dispersion Forces in Surfaces by Assuming Additivity of Intermolecular Interactions in Surfa," *Journal of Physical Chemistry*, Vol. 66 (1962) 382 pages.

3. van Oss, C. J., Chaudhury, M. K., and Good, R. J., "Interfacial Lifshitz-van der Waals and Polar Interactions in Macroscopic Systems," *Chemical Reviews*, Vol. 88 (1988) pp. 927-941.

4. Harkins, W. D., and Cheng, Y. C., "The Orientation of Molecules in Surfaces. VI. Cohesion, Adhesion, Tensile Strength, Tensile Energy, Negative Surface Energy, Interfacial Tension, and Molecular Attraction," *Journal of the American Chemical Society*, Vol. 43 No. 1 (1920) pp. 35-53.

5. Bhasin, A., "Development of Methods to Quantify Bitumen-Aggregate Adhesion and Loss of Adhesion Due to Water," Ph.D. Dissertation, Texas A&M University, College Station, (2006) p. 146.

6. Kim, Y. R., Little, D. N., and Lytton, R. L., "Fatigue and Healing Characterization of Asphalt Mixes," *Journal of Materials in Civil Engineering (ASCE)*, Vol. 15 (2003) pp. 75-83.

7. Schapery, R. A., "Correspondence Principles and a Generalized J Integral for Large Deformation and Fracture Analysis of Viscoelastic Media," *International Journal of Fracture*, Vol. 25 (1984) p. 195-223.

8. Lytton, R. L., "*Adhesive Fracture in Asphalt Concrete Mixes*," in *Chapter in Book Edited by J. Youtcheff,* Submitted for Publication 2004.

9. Masad, E., Branco, V. T. C., Little, D. N., and Lytton, R. L., "A Unified Method for the Dynamic Mechanical Analysis of Sand Asphalt Mixtures", Submitted for the 82nd Annual Meeting of the Association of Asphalt Paving Technologists, (2007).

10. Zollinger, C., "Application of Surface Energy Measurements to Evaluate Moisture Susceptibility of Asphalt and Aggregates," Ph.D. Thesis, Texas A&M University, College Station, Texas, (2005) 133 pages.

11. Masad, E., Branco, V. T. C., Little, D. N., and Lytton, R. L. "Fatigue Damage: Analysis of Mastic Fatigue Damage Using Stress Controlled and Strain Controlled Test," Submitted to International Journal of Pavement Engineering, 2006, In review.

12. Witczak, M. W., Kaloush, K., Pellinen, T., Basyouny, M. E., and Von Quintus, H., "Simple Performance Test for Superpave Mix Design," *NCHRP Report No. 465*, Transportation Research Board, National Research Council, Washington, DC (2002) 105 pages.

13. Kim, Y. R., Little, D. N., and Song, I., "Effect of Mineral Fillers on Fatigue Resistance and Fundamental Material Characteristics," *Transportation Research Record,: Journal of the Transportation Research Board*, Vol. 1832 (2003) p. 1-8.

14. Reece, R., "Properties of Aged Asphalt Binder Related to Asphalt Concrete Fatigue Life," Journal of the Association of Asphalt Paving Technologist, Vol. 66, (1997), pp. 604 - 632.

15. Della Volpe, C., and Siboni, S., "Some Reflections on Acid Base Solid Surface Free Energy Theories," *Journal of Colloid and Interface Science*, Vol. No. 195 (1997) pp. 121-136.

16. Della Volpe, C. and Siboni, S., "Acid Base Surface Free Energies of Solids and the Definition of Scales in the Good van Oss Chaudhury Theory," *Journal of Adhesion Science and Technology*, Vol. 14 No. 2 (2000) pp. 235-272.

17. Jones, D. R., "SHRP Materials Reference Library: Asphalt Cements: A Concise Data Compilation," Report No. SHRP-A-645 Strategic Highway Research Program Washington, D.C. (1993) 28 pages.

18. "Effect of Heat and Air on a Moving Film of Asphalt (Rolling Thin-Film Oven Test) Test Method T-240," American Association of State Highway and Transportation Officials, Washington, D.C. (2003) pp. 679 - 683.

19. "Practice for Accelerated Aging of Asphalt Binder Using Pressurized Aging Vessel (PAV) Practice PP1," American Association of State Highway and Transportation Officials, Washington, D.C. (2005).

20. Robl, T. L., Milburn, D., Thomas, G., Groppo, J., and O'Hara, K., "The SHRP Materials Reference Library Aggregates: Chemical, Mineralogical, and Sorption Analyses," Report No. SHRP-A/UIR-91-509, Strategic Highway Research Program, Washington, D.C. (1991) 88 pages.

21. Adamson, A. W., and Gast, A. P., Physical Chemistry of Surfaces Sixth ed. John Wiley & Sons, Inc. (1997) 784 pages.

22. Western Research Institute, "Fundamental Properties of Asphalts and Modified Asphalts, Volume I: Interpretive Report," *FHWA-RD-99-212*, Western Research Institute, Laramie, WY, (2001) 460 pages.

23. Kwok, D. Y., Gietzelt, T., Grundke, K., Jacobasch, H. J., and Neumann, A. W., "Contact Angle Measurements and Contact Angle Interpretation. 1. Contact Angle Measurements by ADSA and a Goniometer Sessile Drop Technique". *Langmuir*, Vol. No. 13 (1997) pp. 2880-2894.

24. Kwok, D. Y., Leung, A., Lam, C. N. C., Li, A., and Wu, R., "Low-Rate Dynamic Contact Angles on Poly(methyl methacrylate) and the Determination of Solid Surface Tensions," *Journal of Colloid and Interface Science*, Vol. No. 206 (1998) pp. 44-51.

25. Kwok, D. Y. and Neumann, A. W., "Contact Angle Measurements and Criteria for Surface Energetic Interpretation," *Contact Angle, Wettability, and Adhesion*, Vol. 3, (2003) pp. 117-139.

26. Jacobasch, H. J., Grundke, K., Schneider, S., and Simon, F., "Surface Characterization of Polymers by Physio-Chemical Measurements," *Journal of Adhesion*, Vol. 48 (1995) pp. 57-73.

27. Gregg, S. J., and Sing, K. S. W., "Adsorption, Surface Area and Porosity," Academic Press (1967) 371 pages.

28. Jura, G., and Harkins, W. D., "Surfaces of Solids XI. Determination of the Decrease of Free Surface Energy of a Solid by an Adsorbed Film," *Journal of American Chemical Society*, Vol. 66 (1944) pp. 1356-1361.

29. McClellan, A. L., and Harnsberger, H. F., "Cross-sectional Areas of Molecules Adsorbed on Solid Surfaces," *Journal of Colloid and Interface Science*, Vol. No. 23 (1967) pp. 577-599.

30. Bilinski, B., and Chibowski, E., "The Determination of the Dispersion and Polar Free Surface Energy of Quartz by the Elution Gas Chromatography Method," *Powder Technology*, Vol. No. 35 (1983) pp. 39-45.

31. Bilinski, B., and Holysz, L., "Some Theoretical and Experimental Limitations in the Determination of Surface Free Energy of Siliceous Solids," *Powder Technology*, Vol. 102 (1999) pp. 120-126.

32. Douillard, J. M., Zoungrana, T., and Partyka, S., "Surface Gibbs Free Energy of Minerals: Some Values," *Journal of Petroleum Science and Engineering*, Vol. 14, (1995) pp. 51-57.

33. Brunauer, S., Emmett, P. H., and Teller, E., "Adsorption of Gases in Multimolecular Layers," *Journal of American Chemical Society*, Vol. 60, No. 2 (1938) pp. 309-319.

34. Brunauer, S. and Copeland, L. E., "Physical Asorption of Gases and Vapors on Solids," *Symposium on Properties of Surfaces*, Los Angeles, California, Proceedings (1962) pp. 59-79.

35. Cheng, D., "Surface Free Energy of Asphalt-Aggregate System and Performance Analysis of Asphalt Concrete," Ph.D. Thesis, Texas A&M University, College Station, Texas, (2002) 167 pages.

36. Chen, C. H., and Dural, N. H., "Chloroform Adsorption on Soils," *Journal of Chemical Engineering Data*, No. 47 (2002) pp. 1110-1115.

37. Bose, A, "Measurement of Work of Adhesion between Asphalt and Rock," University of Rhode Island Internal Report to Texas A&M University, March 2006, 23 pages.

38. Barbour, A. F., Barbour, R. F., and Petersen, J. C., "A Study of Asphalt-Aggregate Interactions Using Inverse-Liquid Chromatograph," *Journal of Applied Chemistry and Biotechnology*, Vol. 24, No. 11 (1974). pp. 645-654.

39. Lytton, R. L., Chen, C. W., and Little, D. N., "Microdamage Healing in Asphalt and Asphalt Concrete, Volume III: A Micromechanics Fracture and Healing Model for Asphalt Concrete," *FHWA-RD-98-143*, Texas Transportation Institution, College Station, TX, (2001) 72 pages.

APPENDIX A

BACKGROUND TO THE MEASUREMENT OF SURFACE ENERGY

BACKGROUND TO THE MEASUREMENT OF SURFACE FREE ENERGY

In the context of measurement of surface free energy (or simply surface energy), it is important to emphasize the difference between liquid and solid surfaces. For liquids, the terms surface "tension" and surface "free energy" are used interchangeably, are dimensionally equivalent, and numerically equal *(1)*. Since the surface free energy of a liquid is equal to its surface tension, it can be readily obtained through direct mechanical means, such as detachment. Other methods are based on measurement of contact angles, and shapes of bubbles and drops. Adamson and Gast *(2)* describe several classic techniques including the Capillary Rise method, the Wilhelmy Plate method, the Maximum Bubble Pressure method, the du Nöy Ring method, the Drop Weight method, the Pendant Drop method, and the Sessile Drop method.

For solids, however, the application of the surface tension concept becomes less clear. Solid surface characteristics such as reduced mobility of atoms and molecules, and varying surface morphology give rise to a heterogeneous, or direction dependent, solid surface tension phenomenon, which is not easy to convey. The concept of surface energy is therefore more appropriate to solid surfaces *(1)*. Stretching of solids not only involves a large expenditure of work associated with elastic and sometimes plastic deformation, but also changes the surface structure. Direct mechanical measurement of solid surface energy has therefore been limited to a few solids like mica and diamond where surface stretching is avoided during cleavage, and the work of cleaving yields surface free energy. Surface "tension" values for solids have also been derived from empirical relationships by measuring their liquid phase surface tensions *(2)*. Modern texts on adhesive science, suggest that indirect methods of obtaining solid surface energy, especially the contact angle approach, are widely used. Force microscopy is a technique which has been used to measure intrinsic adhesion forces directly *(3)*.

The literature suggests that the first fundamental studies on asphalt-aggregate adhesion were recorded in the early 1920s where surface tension of asphalt was recognized as an important property. The du Nöy ring method and pendant drop method were used to measure surface tension of asphalt *(4)*. Adhesive failure induced by water entering the paving mix, referred to as moisture damage, or simply stripping is a national problem which has focused national attention on adhesive and cohesive bond strength. Efforts to resolve adhesion problems in bituminous mixtures led to the establishment of 'The Committee on Interfacial Surface Tension' *(5)*. The most significant outcome of research during this period was identification of chemical compounds that could be used as adhesion promoters between bitumen and aggregate. Although the stripping phenomenon was known to be related to interfacial tension between aggregate and bitumen in the presence of water, attempts to formulate these as an equation were generally unsuccessful. Pavement engineers chose to use tests such as the boiling water test (Riedel-and-Wieber test), the wash test, swell test, and eventually wet-dry mechanical tests to assess water susceptibility of bituminous mixtures *(6)*.

The fact that surface tension was fundamentally related to the asphalt-aggregate adhesive bond continued to stimulate research in this area. Thelen *(7)* proposed a test to determine the contact angles of asphalt drops on smooth aggregate surfaces. A lamp and lens system was used to project an image of the drop onto a screen where the contact angle could be measured with a straight edge and protractor. This method, generally known as the sessile drop method, is widely used in the field of adhesion science, and technologically advanced imaging systems are commercially available today. Interest in the application of surface free energy to the adhesion

problem was renewed with the proposal of Fowkes *(8)* that surface energy can be divided into independent components and with subsequent development of refined theories such as the one by Van Oss et al *(9)*. These ideas where applied in fundamental research on asphalt-aggregate adhesive bonds. Ardebrant and Pugh *(10)* measured contact angles of water drops on polished aggregate surfaces by a goniometer telescope (basically a telescope equipped with a protractor), facilitated by incorporating two immiscible hydrocarbon fluids. Bose *(11)* proposed a system to obtain the surface energy components of asphalt and aggregates utilizing the sessile drop method and selected probing liquids. Elphingstone *(12)* and Cheng et al *(13)* determined the surface energy of several asphalts using the Wilhelmy plate method. In this method an asphalt-coated plate is dipped into three solvents with known surface energy components and contact angles for each of these liquids are obtained. The so-called wicking method can be used to obtain the contact angles of powders through capillary rise of a liquid through a compacted powder sample, and is based on the Washburn equation.

Micro calorimetry is a technique that was used in research on asphalt-aggregate interaction by Ensley and co-workers. Essentially, aggregates are brought into contact with asphalt and the energy released during interaction, and over time, is measured with a sensitive micro calorimeter *(14-16)*. In the context of the current research, Malandrini *et al (17)* and Médout-Maréne *et al (48)* describe the link between immersion enthalpies and surface energy components. Yildirim *(49)* proposed an alternative way to obtain the surface energy components of powdered talc from contact angles obtained through heats of immersion.

During the Strategic Highway Research Program (SHRP), Curtis and her co-workers investigated asphalt-aggregate interactions by the adsorption and desorption of asphalt from toluene solution circulated through an aggregate column. The adsorbance of the asphalt solution was monitored by visible spectroscopy. Adsorption isotherms are usually developed from the data to obtain important thermodynamic parameters such as monolayer surface coverage and Gibbs free energy *(20, 21)*. Within this group of techniques specific or net retention times or volumes of a probe medium eluted through a chromatographic column are obtained. Inverse Gas Chromatography (IGC) is gaining increasing popularity in many disciplines due to its sensitivity, speed, accuracy and simplicity *(22)*. This technique has been used to obtain information about surface energetic and acid/base properties of solid surfaces of minerals, such as calcium carbonate *(22)*, as well as polymers *(23)*.

Similar to the dynamic sorption devices described above, vacuum gravimetric static and vacuum volumetric static sorption techniques can also be used to obtain these thermodynamic parameters. Li *(24)* used a vacuum gravimetric static technique to measure the adsorption of different organic solvents onto aggregates used in pavement layers with a highly sensitive magnetic suspension balance. From adsorption isotherms, equilibrium spreading pressures were calculated, which in turn were used to calculate surface energies and their components according to the theory described in Section 3.1. Cheng et al *(13)* also used this technique, referred to as a Universal Sorption Device (USD), to obtain surface energies of different aggregates. In addition they utilized this device to determine water diffusion through thin asphalt films. Volumetric static sorption devices, and the previously described Inverse Gas Chromatography device, are commonly used in the pharmaceutical, food science and other industries and are commercially available.

Direct measurement of intrinsic adhesion forces became a reality with the advent of scanning probe microscopy in the early 1980s. Of these techniques, the most well-known is undoubtedly that of Atomic Force Microscopy (AFM). AFM is powerful and has great potential,

and it has been used extensively to measure surface morphology of polymers and other materials on a molecular scale. However, it can also be used to measure intrinsic surface forces through the interaction of the fine tip and the surface. In this technique the deflection of a cantilever of a few hundred microns in length is detected by the reflection of a laser from the top of the cantilever. The deflection is used to calculate the force for a known spring constant of the cantilever *(25)*. Studies on asphalt surface morphology and surface energy have been conducted by Pauli *et al (26)*. When this technique is used to measure forces between a chemically functionalized tip and a substrate, this technique can be categorized as Chemical Force Microscopy. This application has the ability to derive the surface energy components of a material. The use of functionalizing tips with self-assembling mono-layers is well-established *(27)*. The Interfacial Force Microscope (IFM) is another device, specifically developed to measure surface forces and works on the basis of a self-balancing force-feedback system, rather than deflection-based force sensors as in the case of AFM.

REFERENCES

1. Myers, D., Interfaces and Colloids, Part 1: Some General Concepts about Interfaces, Cheresources, Inc. (2002) http://www.cheresources.com/interfaces2.shtml

2. Adamson, A. W. and Gast, A. P., Physical Chemistry of Surfaces, 6th Edition, John Wiley & Sons, Inc., NY (1997) pp. 742.

3. Pocius, A. V., Adhesion and Adhesives Technology: An Introduction, Carl Hanser Verlag, NY (1997) pp. 84 – 91.

4. Endesbey, V.A., Griffen, R.L., and Sommer, H.J., "Adhesion between Asphalts and Aggregates in the Presence of Water." *Journal of Association of Asphalt Paving Technologists,* Vol. 16 (1947) p.

5. Dow, A.W., "Report of Committee on Interfacial Surface Tension between Aggregate and Asphalt." *Proceedings of the Association of Asphalt Paving Technologists*, Vol. 5 (1933) p.22.

6. Krchma, L.C., and Loomis, R.J., " Bituminous-Aggregate Water Resistance Studies." *The Association of Asphalt Paving Technologists*, Chicago, Illinois, Vol. 15 (1943) pp. 153-187.

7. Thelen, E., "Surface Energy and Adhesion Properties in Asphalt Systems." *Thirty seventh Annual Meeting of the Highway Research Board*, Washington, D.C., Bulletin 192 (1958) pp. 63-74.

8. Fowkes, F.M., (1964), "Attractive Forces at Interfaces", *Ind. Eng. &. Chem.,* Vol. 56, No. 12 (1964) pp 40-52.

9. Van Oss, C.J., Chaudhury, M.K., and Good, R.J., "Interfacial Lifshitz-van der Waals and Polar Interactions in Macroscopic Systems." *Chemical Review*, Vol. 88 (1988) p. 927.

10. Ardebrant, H., and Pugh, R.J., "Wetting Studies on Silicate Minerals and Rocks used in Bituminous Highways." *Colloids and Surfaces*, Vol. 58 (1991) pp 111-130.

11. Bose, A., "Measurement of Work of Adhesion Between Asphalt and Rock." *Internal Report*, Department of Chemical Engineering, University of Rhode Island, Kingston, RI (2002), pp 6.

12. Elphingstone, G.M., Adhesion and Cohesion in Asphalt-Aggregate Systems. PhD. Dissertation, Texas A&M University, College Station, TX (1997) 95 pp.

13. Cheng, D., Little, D.N., Lytton, R.L., and Holste, J.C., "Use of Surface Free Energy of Asphalt-Aggregate Systems to Predict Moisture Damage Potential." *Journal of Association of Asphalt Paving Technologists*, Vol. 71 (2002).

14. Ensley, E.K., Petersen, J.C., and Robertson, R.E., (1984), "Asphalt-Aggregate Bonding Energy Measurements by Microcalorimetric Methods." *Thermochimica Acta*, 77 (1984) pp 95-107.

15. Ensley, E.K. and Sholz, H.A., "A Study of Asphalt-Aggregate Interactions by Heat of Immersion." *Journal of the Institution of Petroleum*, Vol. 58, No. 560 (1972) pp. 95-101.

16. Ensley, E.K. (1973), "A Study of Asphalt-Aggregate Interactions and Asphalt Molecular Interactions by Microcalorimetric Methods: Postulated Interaction Mechanisms." *Journal of the Institution of Petroleum*, Vol. 59, No. 570 (1973) pp. 279-289.

17. Malandrini, H., Clauss, F., Partyka, S., and Douillard, J.M. "Interactions between Talc Particles and Water and Organic Solvents." *J. Colloid Interface Sci.,* 194 (1997) pp.183-193.

18. Médout-Maréne, V., Belarbi, H., Thomas, P., Morato, F., Guintini, J.C., Douillard, J.M., Thermodynamic Analysis of Immersion of a Swelling Clay." *J. Colloid Interface Sci.*, 202 (1998) pp. 139-148

19. Yildirim, I., Surface Free Energy Characterization of Powders. PhD Dissertation, Mining and Minerals Engineering, Faculty of the Polytechnic Institute and State University, Blacksburg, Virginia, (2001) 225 pp.

20. Curtis, C.W., Terrel, R.L., Perry, L.M., Al-Swailmi, S., Brannan, C.J., "Importance of Asphalt-Aggregate Interactions in Adhesion." *Journal of Association of Asphalt Paving Technologists*, 60 (1991), p. 476

21. Curtis, C.W., "Investigation of Asphalt-Aggregate Interactions in Asphalt Pavements." *Am. Chem. Soc. Div. Fuel*, Vol. 37 (1992) pp.

22. Ahsan, T. and Taylor, D.A., "The influence of Surface Energies of Calcium Carbinate Minerals on Mineral-Polymer Interaction in Polyolefin Composites" *Fundamentals of Adhesion and Interfaces*, Edited by L.P. DeMejo, D.S. Rimai, and L.H. Sharpe, Gordon and Breach Science Publishers, The Netherlands (1999) pp. 69-79.

23. Uhlman, P. and Schneider, S., "Acid-Base Surface Energy Characterization of Grafted Polyethylene using Inverse Gas Chromatography." *Journal of Chromatography A*, 969, (2002) pp. 73-80

24. Li, W., "Evaluation of the Surface Energy of Aggregate Using the Chan Balance." *Final Report of Cahn Balance Thermogravimetry Gas Adsorption Experiments*, Texas A&M University, Chemical Engineering Department, College Station, TX (2002) 34 pp.

25. Niemantsverdriet, J.W., Spectroscopy in Catalysis, An Introduction, Second Completely Revised Edition, Wiley-VCH Verlag GmbH, D-69469 Weinheim (2000).

26. Pauli, A.T., Grimes, W., and S.C. Huang, S.C., "*Fundamental Properties of Asphalt and Modified Asphalt: Mastic/Asphalt Thin Film Behavior*." Subtask 12-2, Draft Final Report, Contract DFTH61-99C-00022. FHWA, USA (2003)

27. Beach, E.R., Tormoen, G.W., and Drelich, J., "Pull-off Forces Measured between Hexadecanethiol Self-Assembled Monolayers in Air using an Atomic Force Microscope: Analysis of Surface Free Energy." *J. Adhesion Sci. Technol.,* Vol. 16, No. 7 (2002) pp 845-868.

APPENDIX B

PROPOSED TEST METHOD TO USE A WILHELMY PLATE DEVICE TO DETERMINE SURFACE ENERGY COMPONENTS OF ASPHALT BINDERS

Disclaimer

"The proposed test methods are recommendations of the NCHRP Project 9-37 staff at Texas Transportation Institute. These methods have not been approved by NCHRP or by any AASHTO Committee of formally accepted for the AASHTO specifications."

PROPOSED TEST METHOD TO USE A WILHELMY PLATE DEVICE TO DETERMINE SURFACE ENERGY COMPONENTS OF ASPHALT BINDERS

1. Scope

1.1 This test method covers the procedures for preparing samples and measuring contact angles using the Wilhelmy plate device to determine the three surface energy components of asphalt binders.

1.2 This standard is applicable to asphalt binders that do not contain particulate additives such as crumb rubber.

1.3 This method must be used in conjunction with the manual for mathematical analysis to determine surface energy components from contact angle measurements or the computerized spreadsheets that were developed to carry out this analysis.

1.4 *This standard may involve hazardous material, operations, and equipment. This standard is not intended to address all safety problems associated with its use. It is the responsibility of the user of this procedure to establish appropriate safety and health practices and to determine the applicability of regulatory limitations prior to its use.*

2. Referenced Documents

2.1 AASHTO Standards
T40 Sampling of Bituminous Materials

3. Definitions

3.1 *Surface Energy* γ, or surface free energy, of a material is the amount of work required to create unit area of the material in vacuum. The total surface energy of a material is divided into three components, namely, the Lifshitz-van der Waals component, the acid component, and the base component.

3.2 *Contact Angle* - θ, refers to the equilibrium contact angle of a liquid on a solid surface measured at the point of contact of the liquid-vapor interface with the solid.

3.3 *Advancing Contact Angle*, within the context of this test, refers to the contact angle of a liquid with the solid surface as the solid surface is being immersed into the liquid.

3.4 *Receding Contact Angle*, within the context of this test, refers to the contact angle of a liquid with the solid surface as the solid surface is being withdrawn from the liquid.

3.5 *Probe Liquid*, within the context of this test, refers to any of the pure, homogeneous liquids that do not react chemically or dissolve with asphalt binders and are used to measure the contact angles with the binder. The three surface energy components of the probe liquid must be known at the test temperature from the literature.

3.6 *Mixing Temperature*, within the context of this test, refers to the temperature at which the viscosity of the asphalt binder is approximately 0.170 Pa's, or any other temperature that is prescribed or determined by the user for use as the mixing temperature with aggregates to prepare hot mix asphalt.

4. Summary of Method

4.1 A glass slide coated with the asphalt binder and suspended from a microbalance is immersed in a probe liquid. From simple force equilibrium conditions the contact angle of the probe liquid with the surface of the asphalt binder can be determined. The analysis to obtain the contact angle is carried out using software accompanying the device.

4.2 Contact angles measured with different probe liquids are used with equations of work of adhesion to determine the three surface energy components of the asphalt binder.
4.3 Figure B-1 presents a schematic of the Wilhelmy plate device.

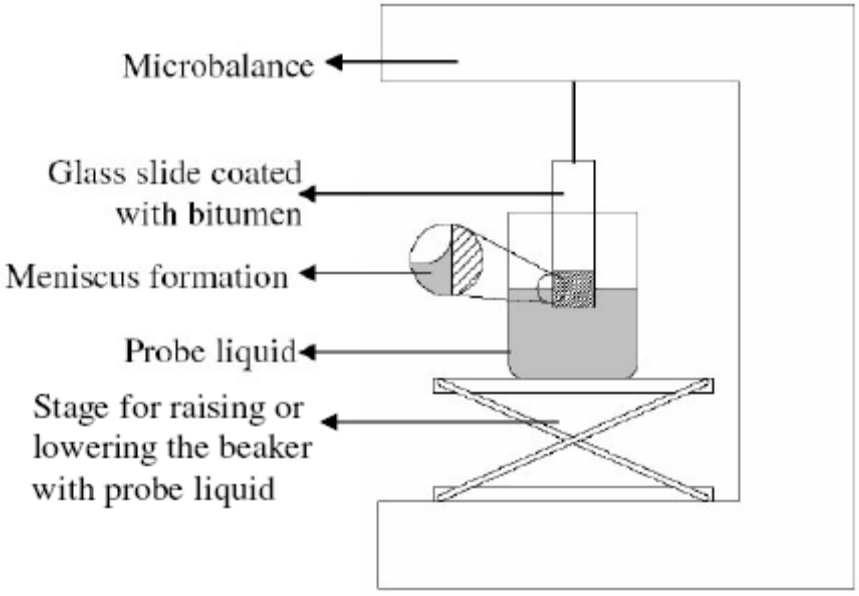

Figure B-1. Schematic of the Wilhelmy Plate Device.

5. Significance and Use

5.1 Surface energy components of asphalt binders are important material properties that are related to the performance of hot mix asphalt. Surface energy components of asphalt binders can be used to determine the total surface energy and cohesive bond strength of this material. The cohesive bond strength of asphalt binders is related to the work required for microcracks to propagate within the asphalt binder in an asphalt mix, which is related to the fatigue cracking characteristics of the mix.
5.2 Surface energy components of asphalt binders can also be combined with the surface energy components of aggregates to compute the work of adhesion between these two materials and the propensity for water to displace the asphalt binder from the asphalt binder-aggregate interface. These two quantities are related to the moisture sensitivity of the asphalt mix.

6. Apparatus

6.1 Wilhelmy plate device – This device comprises a microbalance with a motor-controlled stage that can be raised or lowered at desired speed to immerse a slide with asphalt binder in the probe liquid in advancing mode and to withdraw the slide from the probe liquid in receding mode.
6.2 Data acquisition and analysis software to collect the data and determine the contact angles.
6.3 An oven capable of heating up to 150°C is required to heat asphalt binders for sample preparation. Microscope glass slides (24 mm x 60 mm no. 1.5) are required to serve as substrates for the asphalt binder and a vernier caliper to measure the dimensions of the slide. A heating plate with temperature control is required for maintaining the temperature of the asphalt binder during the sample preparation process.

6.4 The tests are conducted at 25±1°C. If the room temperature is significantly different from the test temperature, then an appropriate environmental chamber may be required to house the apparatus.

6.5 A slotted slide holder is required to hold the finished asphalt binder slides.

7. Sampling

7.1 Obtain a representative sample of the asphalt binder according to procedure T40. Approximately 50 g of asphalt binder stored in a small metallic container is required for this test.

8. Preparation of Test Samples

8.1 Heat the container with asphalt binder in an oven to the mixing temperature for about 1 hour and place it over a heating plate. Set the temperature of the heating plate so that the asphalt binder remains at the mixing temperature. Stir the liquid asphalt binder from time to time throughout the sample preparation process.

8.2 Pass the end of the glass slide intended for coating six times on each side through the blue flame of a propane torch to remove any moisture (Figure B-2). Dip the slide into the molten bitumen to a depth of approximately 15 mm (Figure B-3). Allow excess binder to drain from the plate until a very thin (0.18 to 0.35 mm) and uniform layer remains on the plate. The thickness of asphalt binder must be uniform on both sides of the slide throughout its width and for at least 10 mm from the edge that will be immersed in the probe liquid. A thin coating is required to reduce variability of the results. Turn the plate with the uncoated side downward (Figure B-4) and carefully place it in the slotted slide holder (Figure B-5). If necessary, the heat-resistant slide holder with all the coated slides is placed in the oven after coating for 15 to 30 seconds to obtain the desired smoothness. Place the binder-coated plates in a desiccator overnight.

Figure B-2. Glass Slide Dried Before Immersion by Passing it Over a Propane Flame.

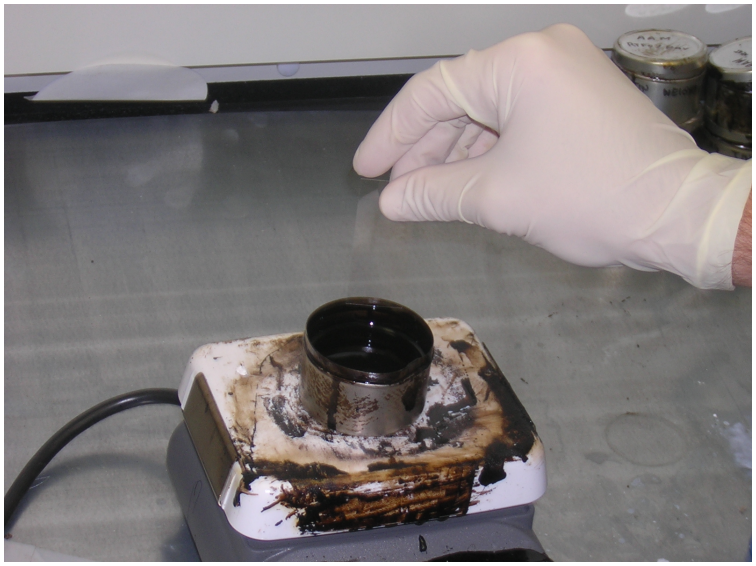

Figure B-3. Clean Glass Slide Dipped in Molten Asphalt Binder to Create Coating.

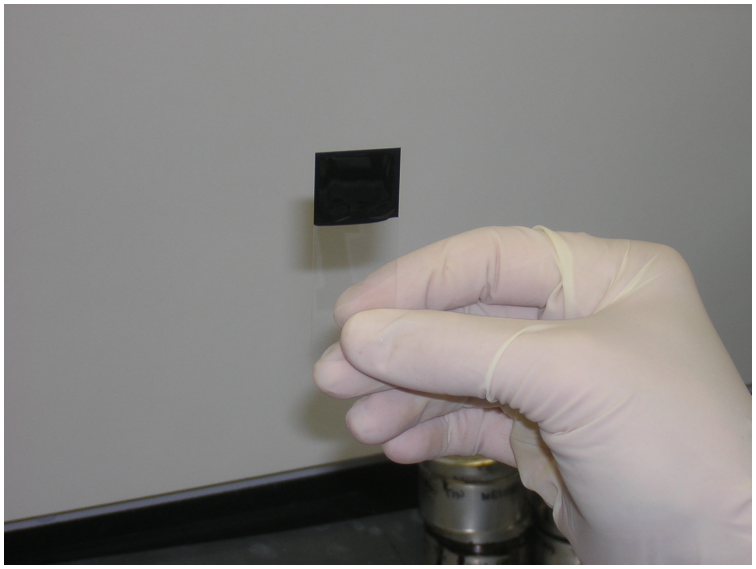

Figure B-4. Glass Slide Coated with Asphalt Binder for Testing with the Wilhelmy Plate Device.

Figure B-5. Finished Slides Stored on Slotted Holder in Desiccator Prior to Testing.

9. Procedure

9.1 User must ensure that the microbalance is calibrated in accordance with the manufacturer specifications prior to the start of test.

9.2 One asphalt binder coated slide is removed from the desiccator at a time. Measure the width and thickness of the asphalt binder slide to an accuracy of 0.01 mm to calculate its perimeter. The measurements must be made just beyond 8 mm from the edge of the slide to avoid contamination of the portion of coating that will be immersed in the probe liquid.

9.3 Suspend the glass slide coated with asphalt binder from the microbalance using a crocodile clip. Ensure that the slide is horizontal with respect to the base of the balance. Fill a clean glass beaker with the probe liquid to a depth of at least 10 mm and place it on the balance stage. Raise the stage manually to bring the top of the probe liquid in proximity to the bottom edge of the slide (Figure B-6).

9.4 During the test, the stage is raised or lowered at the desired rate via a stepper motor controlled by the accompanying software. A rate of 40 microns per second is recommended to achieve the quasi-static equilibrium conditions for contact angle measurement. The depth to which the sample is immersed in the probe liquid is set to 8 mm. Larger depths up to 15 mm may be used if the thickness of asphalt coating on the slide is uniform. The weight of the slide measured by the microbalance is recorded continuously by the software accompanying the device during the advancing (stage is raised to dip the slide) and receding (stage is lowered to retract the slide from the liquid) process.

9.5 At least five probe liquids are recommended for use with this test. These are water, ethylene glycol, methylene iodide (diiodomethane), glycerol, and formamide. All reagents must be high-purity grade (>99%). Contact angles must be measured for at least three replicates with each probe liquid for each asphalt binder.

9.6 Since methylene iodide is a light-sensitive material, cover the beaker containing methylene iodide with black tape to reduce the effect of light.

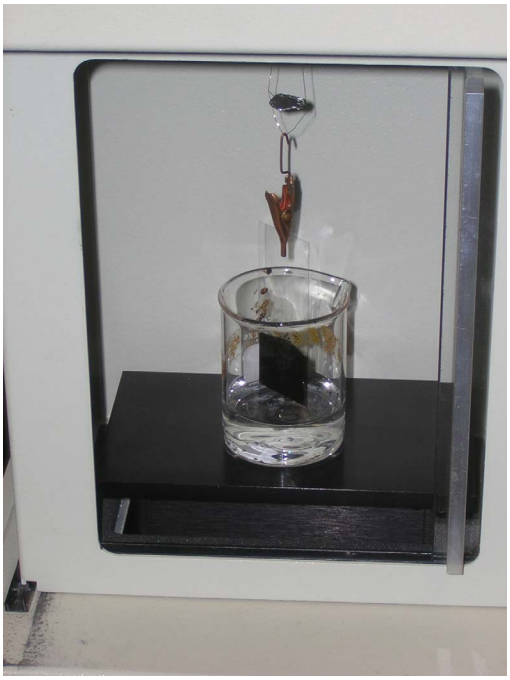

Figure B-6. Asphalt Binder Sample Suspended from Microbalance for Immersion in Probe Liquid.

9.7 Dispose the probe liquid in the beaker after testing with three asphalt binder slides, and use a fresh sample of the probe liquid for each different type of binder. Store all probe liquids in air tight containers and do not use after prolonged exposure to air in open-mouthed beakers.

9.8 Tests must be completed within 24 to 36 hours from the time of preparation of the slides.

10. Calculations

10.1 From simple force equilibrium considerations, the difference between weight of a plate measured in air and partially submerged in a probe liquid (ΔF) is expressed in terms of buoyancy of the liquid, liquid surface energy, contact angle, and geometry of the plate. The contact angle between the liquid and surface of the plate is calculated from this equilibrium as:

$$\cos\theta = \frac{\Delta F + V_{im}\left(\rho_L - \rho_{air} g\right)}{P_t \gamma_L^{Tot}} \qquad \textbf{(B.1)}$$

where, P_t is the perimeter of the bitumen coated plate, γ_L^{Tot} is the total surface energy of the liquid, θ is the dynamic contact angle between the bitumen and the liquid, V_{im} is the volume immersed in the liquid, ρ_L is the density of the liquid, ρ_{air} is the air density, and g the local acceleration due to gravitation. The accompanying software requires the density of the liquid, total surface tension of the liquid, dimensions of the sample, and local acceleration due to gravity as inputs to compute the contact angle using the force measurements from the microbalance.

10.2 Buoyancy correction based on slide dimensions and liquid density can introduce unwanted variability into the resulting contact angles. To eliminate these effects, the accompanying software performs a regression analysis of the buoyancy line and

extrapolates the force to zero depth. The user must select a representative area of the line for regression analysis (Figure B-7). The software reports the advancing and receding contact angles based on the area selected using the aforementioned equation.

10.3 If the force measurements are not smooth, i.e., if sawtooth-like force measurements are observed due to slip-stick behavior between the probe liquid and the asphalt binder, then report this along with the advancing and receding contact angles.

10.4 The typical standard deviation of the measured contact angle for each pair of liquid and asphalt binder based on measurements with three replicate slides is less than 2°.

10.5 The contact angle of each replicate and probe liquid is used with the surface energy analysis workbook that conducts the required analysis to determine the three surface energy components of the asphalt binder and the standard deviations of these components. This workbook also verifies the accuracy and consistency of the measured contact angles and integrates data from other test methods such as the surface energy components of aggregates to determine various parameters of interest that are related to the performance of asphalt mixes.

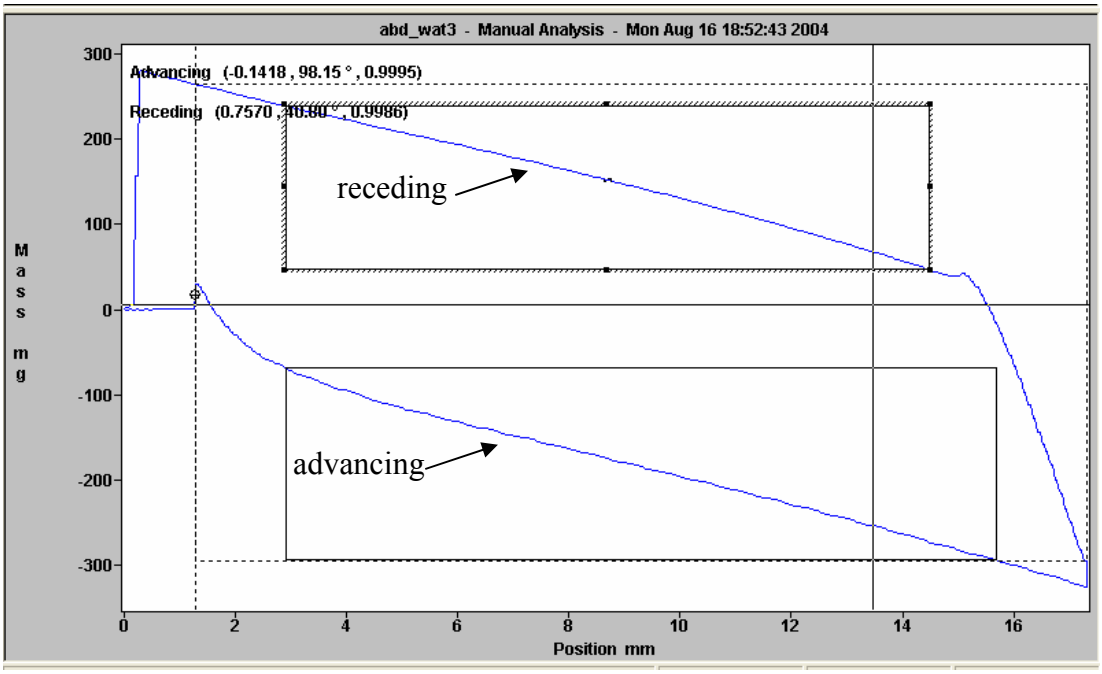

Figure B-7. Selection of Representative Area to Determine Advancing and Receding Contact Angles.

APPENDIX C

PROPOSED TEST METHOD TO USE A SORPTION DEVICE TO DETERMINE SURFACE ENERGY COMPONENTS OF AGGREGATES

Disclaimer

"The proposed test methods are recommendations of the NCHRP Project 9-37 staff at Texas Transportation Institute. These methods have not been approved by NCHRP or by any AASHTO Committee of formally accepted for the AASHTO specifications."

PROPOSED TEST METHOD TO USE A SORPTION DEVICE TO DETERMINE SURFACE ENERGY COMPONENTS OF AGGREGATES

1. Scope

1.1 This test method covers the procedures for preparing samples and measuring adsorption isotherms using a sorption device with an integrated Surface Energy Measurement system (SEMS) to determine the three surface energy components of asphalt binders.

1.2 This standard is applicable to aggregates that pass through a 4.75 mm sieve (# 4) and are retained on a 2.36 mm sieve (# 8).

1.3 This method must be used in conjunction with the manual for mathematical analysis to determine surface energy components from spreading pressures or the computerized spreadsheets that were developed to carry out this analysis.

1.4 *This standard may involve hazardous material, operations, and equipment. This standard is not intended to address all safety problems associated with its use. It is the responsibility of the user of this procedure to establish appropriate safety and health practices and to determine the applicability of regulatory limitations prior to its use.*

2. Referenced Documents

2.1 AASHTO Standards

T2 Practice for sampling aggregates

3. Definitions

3.1 *Surface Energy* γ , or surface free energy, of a material is the amount of work required to create unit area of the material in vacuum. The total surface energy of a material is divided into three components, namely, the Lifshitz-van der Waals component, the acid component, and the base component.

3.2 *Equilibrium spreading pressure* - π_e, is the reduction in surface energy of the solid due to adsorption of vapors at its saturation vapor pressure on the surface of the solid.

3.3 *Probe Vapor*, within the context of this test, refers to vapors from any of the pure, homogeneous liquids that do not chemically react or dissolve with aggregates and are used to measure the spreading pressure with the aggregate. The three surface energy components of the probe vapor must be known at the test temperature from the literature.

3.4 *Relative Vapor Pressure,* within the context of this test, refers to the ratio of the pressure of the vapor to its saturation vapor pressure and can vary from 0 (complete vacuum) to 1 (saturation vapor pressure).

3.5 *Adsorption Isotherm,* of a vapor with an aggregate is the relationship between the equilibrium mass of vapor adsorbed per unit mass of the aggregate and the relative vapor pressure of the vapors at a constant temperature.

4. Summary of Method

4.1 Clean aggregate samples are degassed under high temperature and vacuum in an air-tight sorption cell. Vapors of probe liquids are introduced into the sorption cell in controlled and gradually incremental quantities to achieve different relative pressures. The equilibrium mass of the vapor adsorbed to the solid surface is recorded for each relative pressure to obtain the adsorption isotherm. The adsorption isotherm is used to compute the equilibrium spreading pressure of the probe vapor with the aggregate.

4.2 Equilibrium spreading pressure with different probe vapors is used with equations of work of adhesion to determine the three surface energy components of the aggregate.

5. Significance and Use

5.1 Surface energy components of aggregates are important material properties that are related to the performance of hot mix asphalt. Surface energy components of aggregates can be combined with the surface energy components of asphalt binders to quantify the work of adhesion between these two materials and the propensity for water to displace the asphalt binder from the asphalt binder-aggregate interface. These two quantities are related to adhesive fracture properties and moisture sensitivity of the asphalt mix.

6. Apparatus

6.1 A sorption device integrated with the SEMS comprising an air-tight adsorption cell, a magnetic suspension balance that measures the mass of the sample in the sorption cell in non contact mode, a manifold with vacuum pump, temperature control, probe liquid containers with appropriate valves and controls to regulate the flow of vapors into the sorption cell, and associated software for test control and analysis (Figure C-1). The microbalance must have a precision of 10 μg with a capacity to weigh at least 50 g.

6.2 Temperature of the sorption cell, piping that carries vapors, and a buffer tank is maintained using a water bath that is automatically controlled by the SEMS software.

6.3 An oven capable of heating up to 150°C is required to prepare aggregate samples before testing.

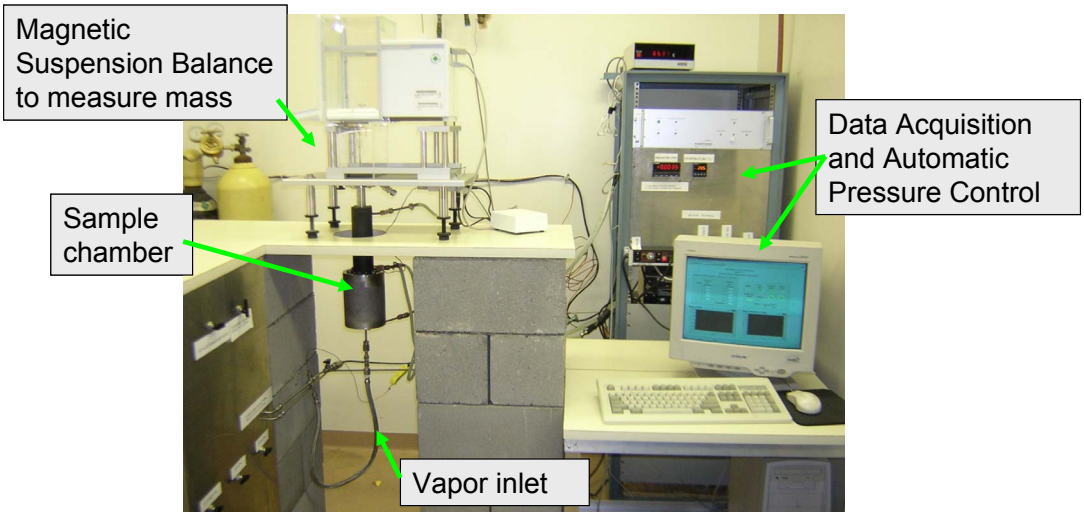

Figure C-1. Universal Sorption Device.

7. Sampling

7.1 Obtain a representative sample of the aggregate according to procedure T2. Sieve the sample to obtain about 100 g of aggregates passing a 4.75 mm sieve (#4) and retained on a 2.36 mm sieve (#8).

8. Preparation of Test Samples

8.1 Thoroughly wash about 25 g of the aggregate in a 2.36 mm sieve with deionized or distilled water. The quality of water used for cleaning of aggregates must be comparable to the quality of water used for gas chromatography. Place the clean aggregate sample in an oven at 150°C for 8 hours, and thereafter transfer it to a desiccator at room temperature for at least 8 hours before testing.

9. Procedure

9.1 The samples are held in a wire mesh basket during the test. Rinse the basket with acetone and air dry. Transfer the aggregate sample to the basket (Figure C-2) and suspend the basket from the hook underneath the suspension balance (Figure C-3). Seal the sorption cell with the coupling with the suspension balance using a viton O-ring (Figure C-4). A metal jacket connected to a water bath is used around the sorption cell to maintain temperature (Figure C-5).

9.2 In order to obtain stable and consistent readings with the magnetic suspension balance it is necessary that the sample basket and magnetic suspension coupling are in vertical and horizontal alignment with each other. Activate and deactivate the magnetic suspension coupling repeatedly until stable and consistent readings are observed. This is an indication that the basket is aligned. This process, referred to as centering of balance, can also be automatically executed with the "Horizontal Centering" module of the SEMS software (Figure C-6).

Figure C-2. Basket with Aggregate Sample for Testing with the USD.

Figure C-3. Sample Basket Suspended from the Magnetic Suspension Balance.

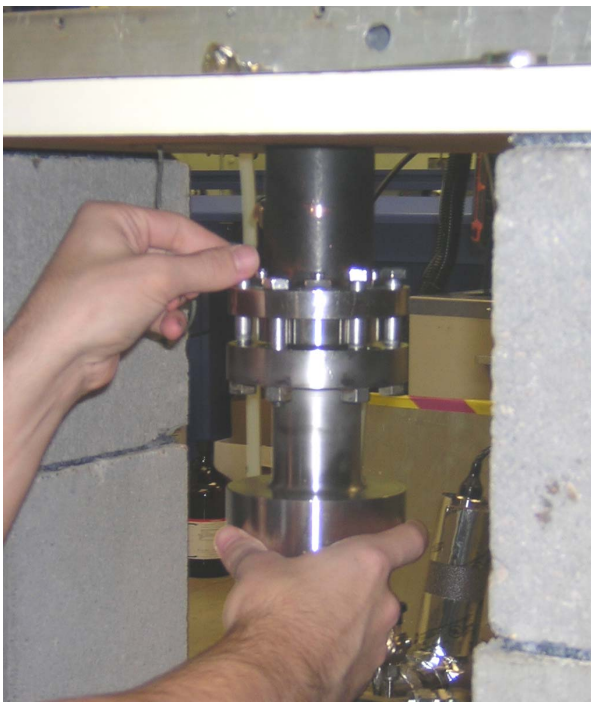

Figure C-4. Adsorption Cell Raised and Sealed with Sample Basket Inside.

Figure C-5. Temperature Jacket Raised to Cover Adsorption Cell.

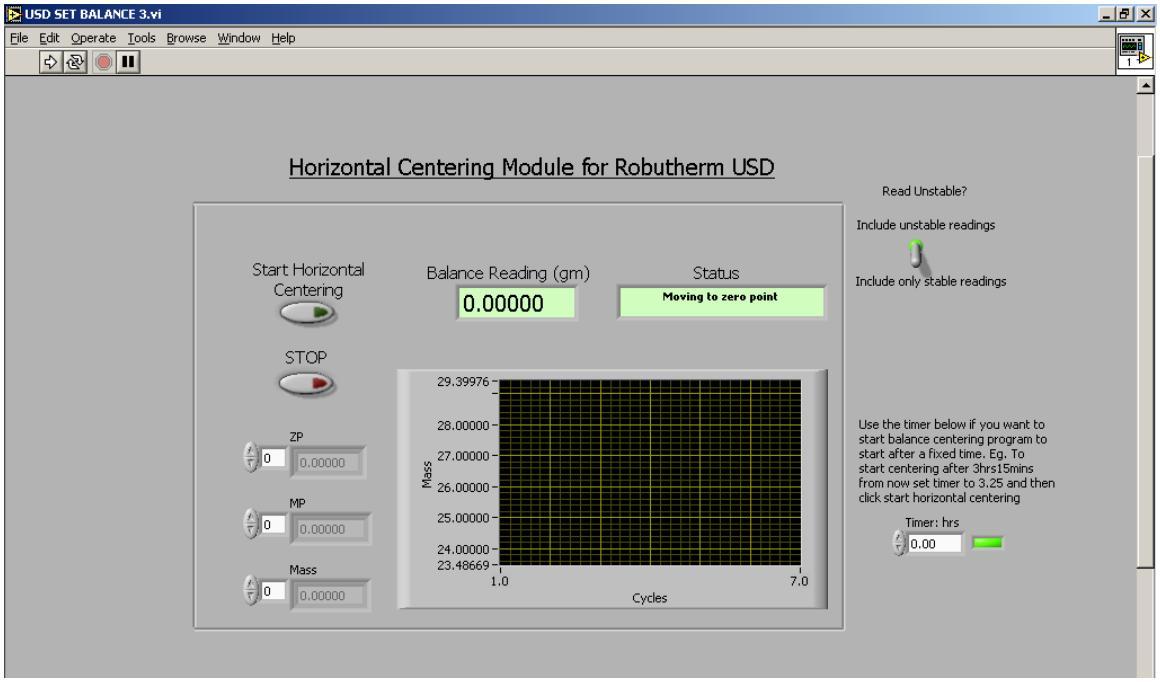

Figure C-6. Auto Centering Module in SEMS Software.

9.3 Degas the sample and the test manifold by drawing vacuum from the system using a mechanical vacuum pump. After the first 2 hours of degassing at 70°C, reduce the temperature of the manifold to 25°C (test temperature) and continue degassing for another 4 hours. The pressure in the cell must be maintained below 20 millitorr during the last 4 hours of degassing. The temperature and degassing times can be controlled manually or automatically using the "Degassing" module of the SEMS software (Figure C-7). Monitor the mass of the sample for the last 1 hour of the degassing time to ensure that it is stable. If the mass continues to decrease it indicates that the sample is still loosing physically adsorbed particles from its surface and more degassing time is required.

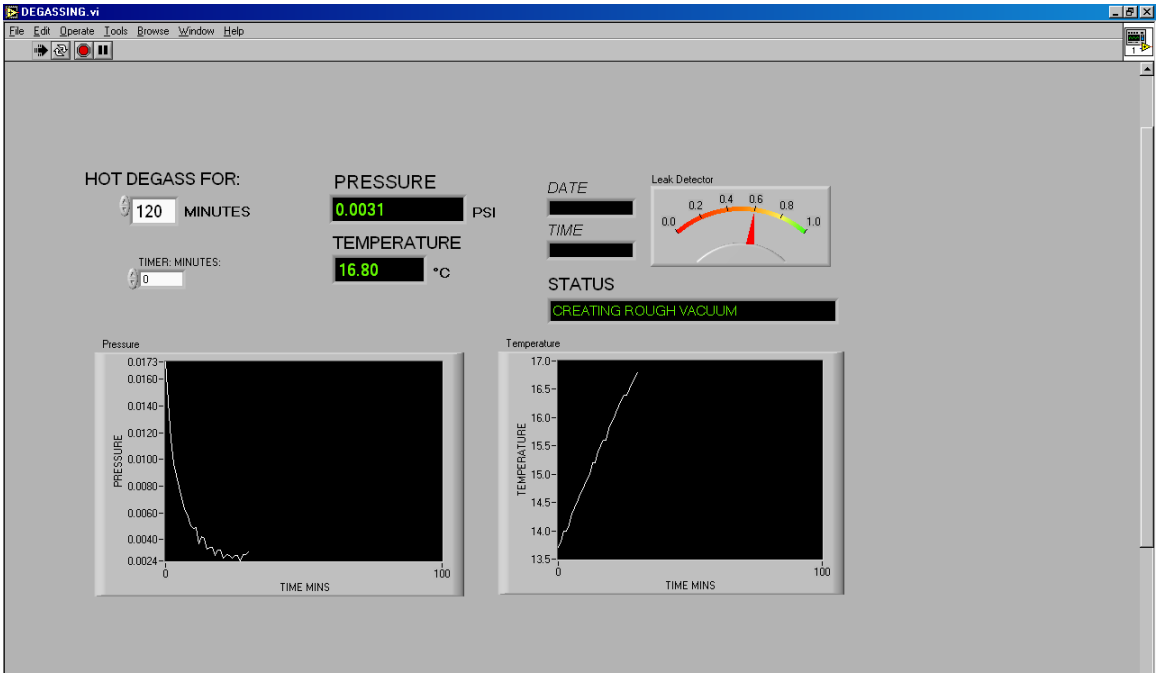

Figure C-7. Degassing Module in SEMS Software.

9.4 After completion of degassing isolate the vacuum pump from the adsorption system. Monitor the pressure of the system for a few minutes to ensure that there is no significant leak. Typically, a leak that allows the system pressure to increase by more than 40 millitorr per hour is unacceptable. In such cases, retighten and replace the seal with the sorption cell and repeat the degassing process.

9.5 Activate the "Adsorption Test" module of the SEMS software to control and execute the adsorption test (Figure C-8). Provide the necessary inputs to the software, such as volume of aggregate (computed by dividing the mass of the aggregate by its density) and probe vapor to execute the test. Other inputs such as name and description of the sample, name and location of the summary and raw data file for saving results, and minimum equilibrium time for each increment of relative pressure are also required. A minimum time of 15 minutes for equilibrium of each increment is recommended. Start the test from the SEMS software. A mechanical isolation valve is used between

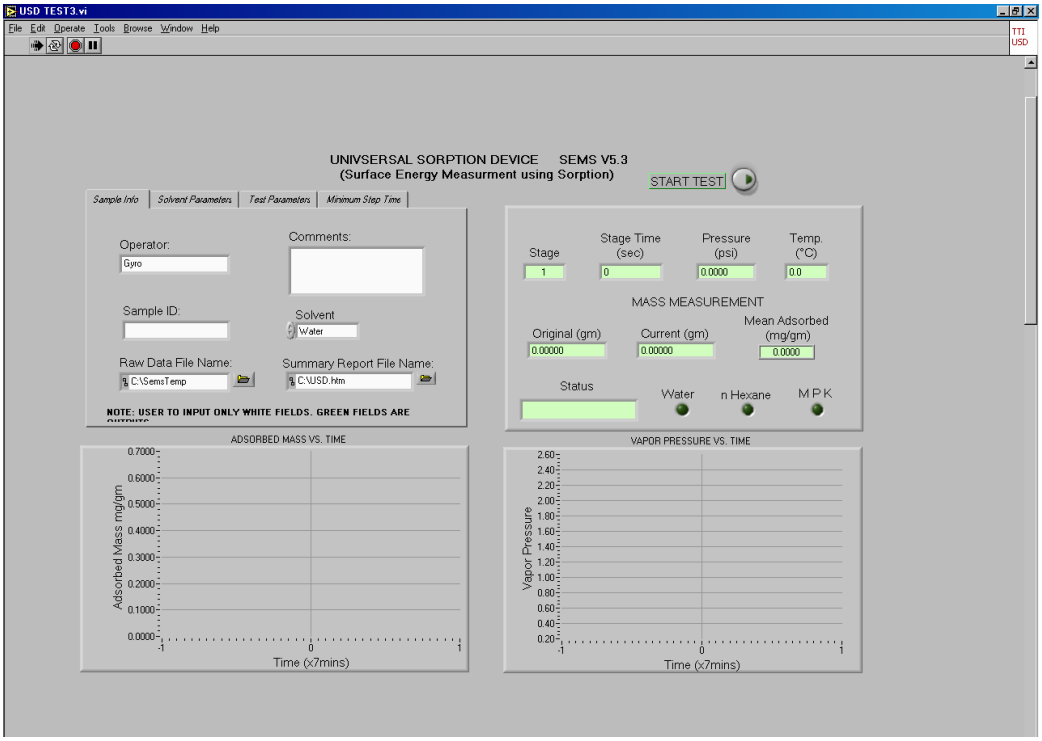

Figure C-8. Adsorption Test Module in SEMS Software.

each of the probe liquid tanks and the system to prevent accidental exposure of the system to the probe vapors. Open the valve corresponding to the probe vapor for the test. Close this valve after completion of the test and before changing or degassing samples.

9.6 The test is controlled and data are acquired using the SEMS software. The software regulates valves to dose probe vapors into the system in 10 steps to achieve an increment of 0.1 in the relative pressure with each step. The mass of the sample is continuously acquired during this process by the SEMS software. The software computes the mass of vapor adsorbed in real time as the difference in the mass of sample at any time from the mass of the sample in vacuum after applying for corrections due to buoyancy. The software also corrects for any drift in the measurements due to the magnetic suspension coupling. Each increment of relative pressure is applied by the software after the mass of the sample comes into equilibrium due to adsorption of vapors from the previous increment, or after the minimum time for equilibrium is achieved, whichever is later. The test is complete after the saturation vapor pressure of the probe liquid is achieved in 10 increments and the equilibrium mass of vapor adsorbed is recorded for each increment.

9.7 Three probe vapors are recommended for this test. These are water, methyl propyl ketone (MPK), and hexane. All reagents must be high-purity grade (>99 percent). After the filling the respective liquid tanks in the manifold for the first time, degas the tanks to remove any air trapped during the process of refilling. Typically, 100 ml of n-hexane lasts for approximately 15 tests, and 100 ml of MPK and water last for 60 tests.

10. Calculations

10.1 After completion of all 10 increments in vapor pressure the software reports a summary of final results that includes the adsorption isotherm, specific surface of the aggregate with BET equations, and spreading pressure based on the specific surface area and the adsorption isotherm (Figure C-9).

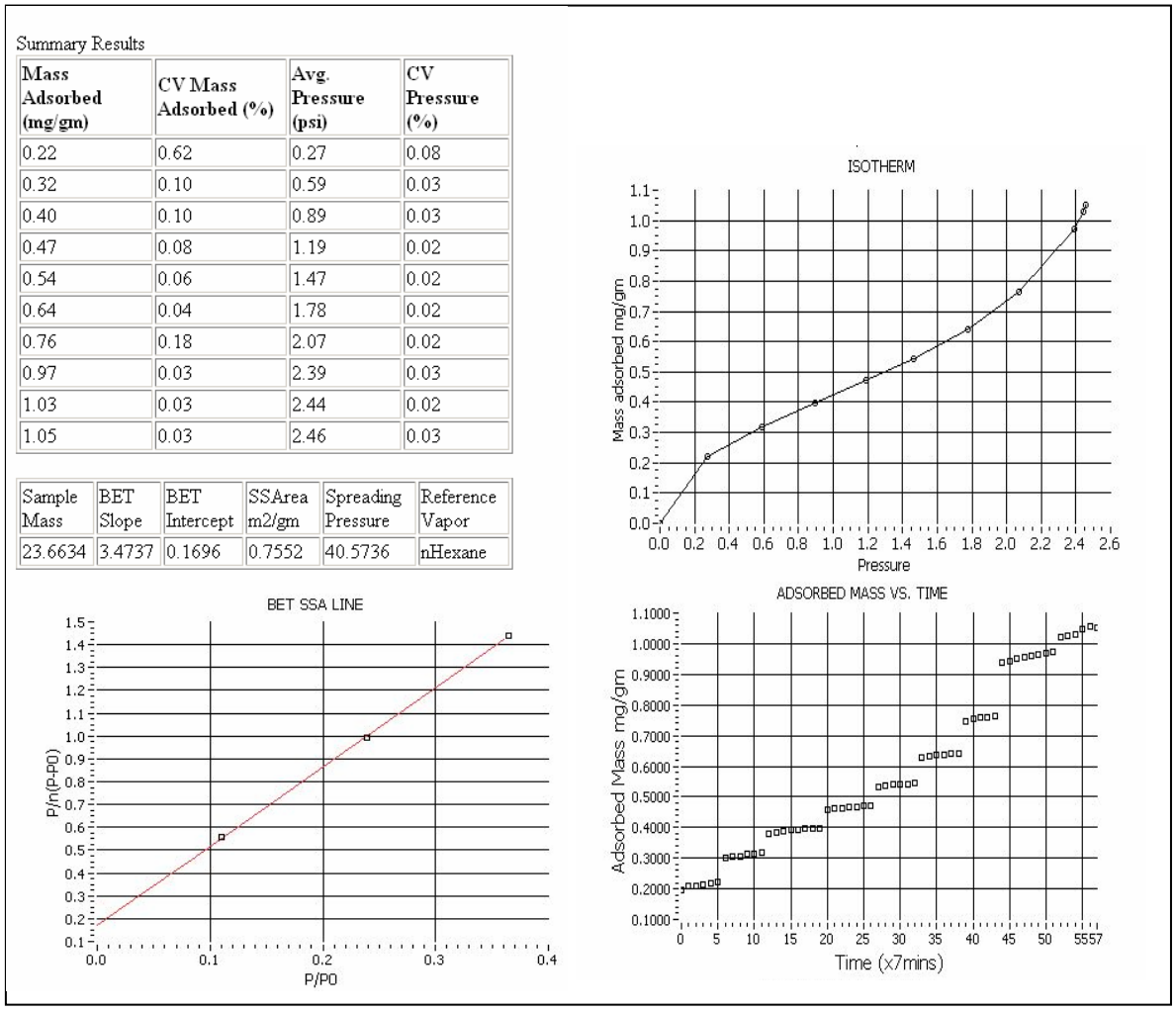

Summary Results

Mass Adsorbed (mg/gm)	CV Mass Adsorbed (%)	Avg. Pressure (psi)	CV Pressure (%)
0.22	0.62	0.27	0.08
0.32	0.10	0.59	0.03
0.40	0.10	0.89	0.03
0.47	0.08	1.19	0.02
0.54	0.06	1.47	0.02
0.64	0.04	1.78	0.02
0.76	0.18	2.07	0.02
0.97	0.03	2.39	0.03
1.03	0.03	2.44	0.02
1.05	0.03	2.46	0.03

Sample Mass	BET Slope	BET Intercept	SSArea m2/gm	Spreading Pressure	Reference Vapor
23.6634	3.4737	0.1696	0.7552	40.5736	nHexane

Figure C-9. Results Reported by SEMS Software.

10.2 The typical coefficient of variation (standard deviation / average) for the spreading pressure for each pair of probe vapor and aggregate based on three replicate measurements is about 15%.

10.3 Although the SEMS software reports specific surface areas and spreading pressures for each test, certain corrections must be applied in order to obtain the correct specific surface area and spreading pressures that can be combined to determine the three surface energy components. Therefore, the adsorption isotherms for each of the three probe vapors reported by SEMS are used with the surface energy analysis workbook

that conducts the required analysis to determine the specific surface area and the three surface energy components of the aggregate and the standard deviations of these components. This user friendly workbook also integrates data from other tests such as the surface energy components of asphalt binders to determine various parameters of interest that are related to the performance of asphalt mixes.

APPENDIX D

PROPOSED TEST METHOD TO USE A SESSILE DROP DEVICE TO DETERMINE SURFACE ENERGY COMPONENTS OF ASPHALT BINDERS

Disclaimer

"The proposed test methods are recommendations of the NCHRP Project 9-37 staff at Texas Transportation Institute and University of Rhode Island. These methods have not been approved by NCHRP or by any AASHTO Committee of formally accepted for the AASHTO specifications."

PROPOSED TEST METHOD TO USE A SESSILE DROP METHOD TO DETERMINE SURFACE ENERGY COMPONENTS OF ASPHALT BINDERS

1. Scope

1.1 This test method covers the procedures for preparing samples and measuring contact angles using the sessile drop method to determine the three surface energy components of asphalt binders.

1.2 This standard is applicable to asphalt binders that do not contain particulate additives such as crumb rubber.

1.3 This method must be used in conjunction with the manual for mathematical analysis to determine surface energy components from contact angle measurements or the computerized spreadsheets that were developed to carry out this analysis.

1.4 *This standard may involve hazardous material, operations, and equipment. This standard is not intended to address all safety problems associated with its use. It is the responsibility of the user of this procedure to establish appropriate safety and health practices and to determine the applicability of regulatory limitations prior to its use.*

2. Referenced Documents

2.1 AASHTO Standards
T40 Sampling of Bituminous Materials

3. Definitions

3.1 *Surface Energy* γ, or surface free energy, of a material is the amount of work required to create unit area of the material in vacuum. The total surface energy of a material is divided into three components, namely, the Lifshitz-van der Waals component, the acid component, and the base component.

3.2 *Contact Angle* - θ, refers to the equilibrium contact angle of a liquid on a solid surface measured at the point of contact of the liquid-vapor interface with the solid.

3.3 *Probe Liquid*, within the context of this test, refers to any of the pure, homogeneous liquids that do not react chemically or dissolve with asphalt binders and are used to measure the contact angles with the binder. The three surface energy components of the probe liquid must be known at the test temperature from the literature.

3.4 *Mixing Temperature*, within the context of this test, refers to the temperature at which the viscosity of the asphalt binder is approximately 0.170 Pa's, or any other temperature that is prescribed or determined by the user for use as the mixing temperature with aggregates to prepare hot mix asphalt.

4. Summary of Method

4.1 A probe liquid is dispensed over a smooth horizontal surface coated with asphalt binder. The image of the drop of liquid formed over the surface of the binder is captured using a camera. Contact angles are obtained by analyzing the image manually or using software.

4.2 Contact angles measured with different probe liquids are used with equations of work of adhesion to determine the three surface energy components of the asphalt binder.

4.3 Figure D-1 presents a schematic of the sessile drop device.

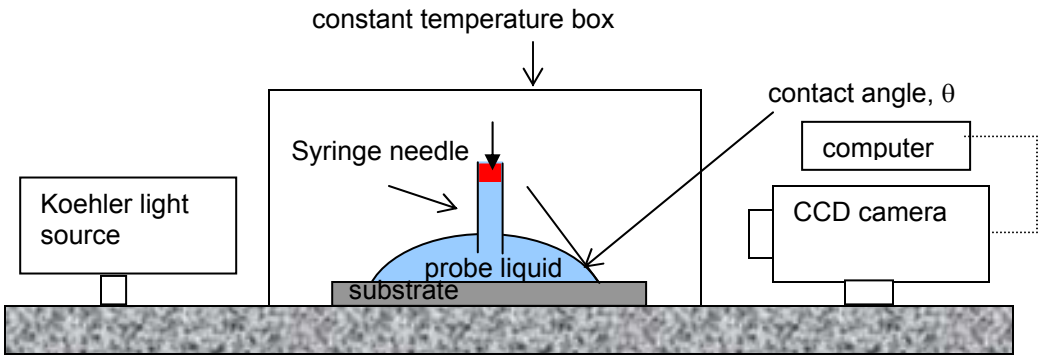

Figure D-1. Schematic of the Sessile Drop Method.

5. Significance and Use

5.1 Surface energy components of asphalt binders are important material properties that are related to the performance of hot mix asphalt. Surface energy components of asphalt binders can be used to determine the total surface energy and cohesive bond strength of this material. The cohesive bond strength of asphalt binders is related to the work required for microcracks to propagate within the asphalt binder in an asphalt mix, which is related to the fatigue cracking characteristics of the mix.

5.2 Surface energy components of asphalt binders can also be combined with the surface energy components of aggregates to compute the work of adhesion between these two materials and the propensity for water to displace the asphalt binder from the asphalt binder-aggregate interface. These two quantities are related to the moisture sensitivity of the asphalt mix.

6. Apparatus

6.1 Sessile drop system – A sessile drop system comprises a microsyringe and a CCD camera (charge-coupled device) to create and capture images of sessile drops, respectively.

6.2 Image analysis software is required to determine contact angles from captured images. Alternatively, contact angles can also be determined from manual measurements on the drop images.

6.3 An oven capable of heating up to 150°C is required to heat asphalt binders for sample preparation. Glass slides or thin aluminum sheets are required to serve as substrates for the asphalt binder.

6.4 An environmental control system using a thermoelectric module is optional to conduct tests at temperatures other than room temperature.

7. Sampling

7.1 Obtain a representative sample of the asphalt binder according to procedure T40. Heat the asphalt binder is to the mixing temperature, stir it thoroughly, and transfer to smaller containers approximately 50 mL in capacity. Fifteen containers are required

to prepare a sample of asphalt binder to test three replicates with five probe liquids. These containers will be heated only once more to prepare samples for testing.

8. Preparation of Test Samples

8.1 Clean the surface of the glass slide or aluminum sheet that is used as a substrate for the asphalt binder.

8.2 Heat the container with asphalt binder in an oven to the mixing temperature. Stir the liquid asphalt binder in the container and pour a small quantity on the substrate. The quantity of asphalt poured must be adequate to form an area of approximately 5 cm x 5 cm in size.

8.3 This binder sample is stored in a desiccator and allowed to cool to room temperature.

9. Procedure

9.1 Place the substrate with the asphalt binder in between the light source and the camera. If a thermoelectric temperature control module is used, then place the sample over the module which is fixed at the proper location between the light source and the camera. A transparent glass cover may also be used to reduce thermal flow with the atmosphere. Set the temperature of the module is set to the test temperature and allow the sample to remain at this temperature for at least an hour before starting the test.

9.2 Rinse the micro syringe with the probe liquid. Position the tip of the micro syringe needle approximately 5 mm away from the top of the sample. Dispense a small drop of the probe liquid from the syringe. As more volume of the probe liquid is added, the drop on the asphalt binder surface expands to a point when its interfacial boundary with the binder surface just begins to expand. Stop addition of probe liquid at this point and capture an image of the drop using the CCD camera.

9.3 At least five probe liquids are recommended for use with this test. These are water, ethylene glycol, methylene iodide (diiodomethane), glycerol, and formamide. All reagents must be high-purity grade (>99 percent). Contact angles must be measured for at least three replicates with each probe liquid for each asphalt binder.

9.4 When methylene iodide is used as a probe liquid, cover the light source with a red film because methylene iodide is a light-sensitive material and must not be exposed or stored in light for prolonged duration.

9.5 Store all probe liquids in air tight containers and do not be use after prolonged exposure to air.

10. Calculations

10.1 Analyze each sessile drop image to obtain two contact angles (Figure D-2). Report the average of these two contact angles as the contact angle for that specific replicate and probe liquid combination.

10.2 The typical standard deviation for the contact angle measured for each pair of probe liquid and asphalt binder based on tests with three replicates is less than 5°.

10.3 The contact angle of each replicate and probe liquid is used with the surface energy analysis workbook that conducts the required analysis to determine the three surface energy components of the asphalt binder and the standard deviations in these components. This workbook also verifies the accuracy and consistency of the measured contact angles and integrates data from other test methods such as the surface energy components of aggregates to determine various parameters of interest that are related to the performance of asphalt mixes.

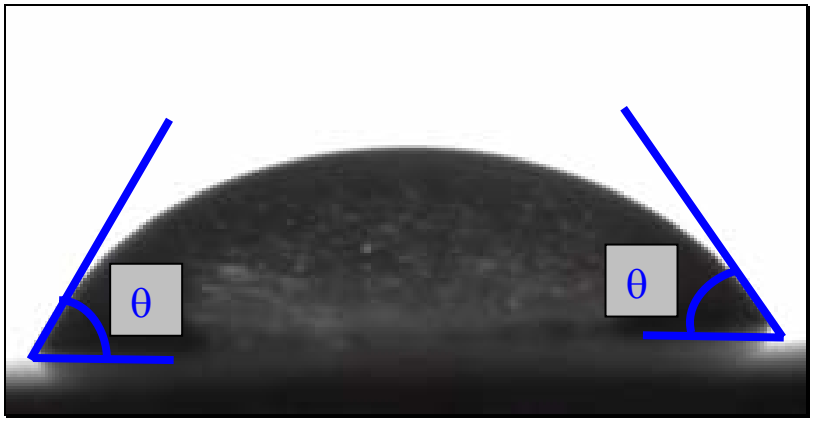

Figure D-2. Typical Image of Sessile Drop for Contact Angle Measurement.

APPENDIX E

MANUAL FOR STATISTICAL AND MATHEMATICAL ANALYSIS

MANUAL FOR STATISTICAL AND MATHEMATICAL ANALYSIS

This manual presents the mathematical analyses required to achieve the following:

- determine the condition number of any selected set of probe liquids,
- determine the surface energy components with standard deviations from contact angle measurements with various probe liquids with asphalt binders including checking for the accuracy of the measured contact angles,
- determine the surface energy components with standard deviations from adsorption isotherms of various probe liquids with aggregates, and
- determine various energy parameters related to moisture sensitivity using the surface energy components of asphalt binders and aggregates.

Spreadsheets using Microsoft Excel© were developed in this research to carry out various types of analysis related to the measurement and application of surface free energy. The spreadsheets are user friendly and all the analyses reported in the following section are built into these spreadsheets.

E.1 COMPUTING SURFACE ENERGIES FROM CONTACT ANGLES

The surface energy component of a solid surface is determined by measuring its contact angles with various probe liquids. Typically more than three liquids are recommended to determine the three surface energy components of the solid. This section presents two different methods to determine the surface energy components and standard deviations of the solid when three or more than three liquids are used. The first method uses singular value decomposition following Della Volpe and Siboni (*1, 2)* and the second method uses weighted least squares.

E.1.1 Equations for Work of Adhesion

Based on the Young-Dupre' equation (neglecting the spreading pressure), work of adhesion is expressed as follows:

$$w = W_{adhesion} / 2 = 0.5\gamma(1 + Cos\theta) \qquad \textbf{[E.1]}$$

where, γ is the total surface free energy of the probe liquid and θ is the contact angle of the probe liquid on the surface of the solid being investigated.
For a set of probe liquids, this equation is expressed as:

$$0.5\gamma_{li}(1 + Cos\theta_i) = \sqrt{\gamma_{li}^{LW}\gamma_s^{LW}} + \sqrt{\gamma_{li}^{+}\gamma_s^{-}} + \sqrt{\gamma_{li}^{-}\gamma_s^{+}} \qquad \textbf{[E.2]}$$

where, γ is the total surface free energy, γ^{LW} is the Lifshitz-van der Waals component of surface free energy, γ^{-} is the Lewis acid component of surface free energy, γ^{+} is the Lewis base component of surface free energy, subscript *li* refers to the i^{th} liquid, where *i* is equal to the number of probe liquids being used, and subscript *s* refers to the solid surface.

If the actual number of liquids used is *m*, then the system of linear equations generated based on the above equations is shown below:

$$\mathbf{A\ x = B}, \qquad \textbf{[E.3]}$$

where,

$$A = \begin{bmatrix} \sqrt{\gamma_{l1}^{LW}} & \sqrt{\gamma_{l1}^{+}} & \sqrt{\gamma_{l1}^{-}} \\ ..... & ..... & ..... \\ \sqrt{\gamma_{lm}^{LW}} & \sqrt{\gamma_{lm}^{+}} & \sqrt{\gamma_{lm}^{-}} \end{bmatrix}_{mx3}, \qquad \textbf{[E.4]}$$

$$x = \begin{bmatrix} \sqrt{\gamma_{s}^{LW}} \\ \sqrt{\gamma_{s}^{-}} \\ \sqrt{\gamma_{s}^{+}} \end{bmatrix}_{3x1}, \qquad \textbf{[E.5]}$$

$$B = 0.5 \begin{bmatrix} \gamma_{li}(1+Cos\theta_1) \\ ..... \\ \gamma_{li}(1+Cos\theta_m) \end{bmatrix}_{mx1} \qquad \textbf{[E.6]}$$

Three distinct cases can occur:
Case 1: When m < 3, the number of equations generated is less than the number of unknowns and hence the set of equations becomes indeterminate,
Case 2: When m = 3, the number of equations is exactly equal to the number of unknowns and the equations can be solved. In this case the matrix **A** is a square matrix and the vector 'X' containing the square roots of the unknown components of the solid can be solved if **A** is non-singular as follows:

$$\mathbf{x} = \mathbf{A}^{-1}\mathbf{B} \qquad \textbf{[E.7]}$$

Case 3: When m > 3, then the number of equations available is more than the unknowns and the system becomes over determinate. It is easy to see that the matrix A would no longer be a square matrix and it will not be possible to directly determine the inverse of the matrix. Other tools to get the best solution for this scenario will have to be used and are discussed later in this section.

E.1.2 Sensitivity to Choice of Liquids and Importance of Condition Number

If the surface energy components of the selected probe liquids are very close to each other, the calculated surface free energy components of the solid (asphalt binder or aggregate) will become unduly sensitive to the measured physical property. This is more important in cases when only a limited set of liquids is being used to estimate the surface energy components of the solid. A simplified demonstration of a similar effect is given as follows.

Consider a case where a value *y* is measured using different probes with characteristic *x*. The calculated parameter of interest is the slope of *y* vs. *x*. If two probes with very similar values of *x* are selected then the measured value of *y* might not be very different. This theoretically small difference is compounded by experimental error, which could be relatively large. As a result the calculated value of slope can have a large variability. This is illustrated in Figure E.1, where probes 1 and 2 with hypothetical values of *x* as 1 and 2, respectively, are used to measure a physical property *y*. With only these two points on the graph the variability in the slope (which is the parameter of interest computed using *x* and *y*) can be very large. However, if a third probe is used with the value of *x* as 10, which is significantly different from the values of the other two probes, and assuming that the variability of the measured parameter *y* is the same in this range, it can easily be seen that the variability in the calculated slope is reduced.

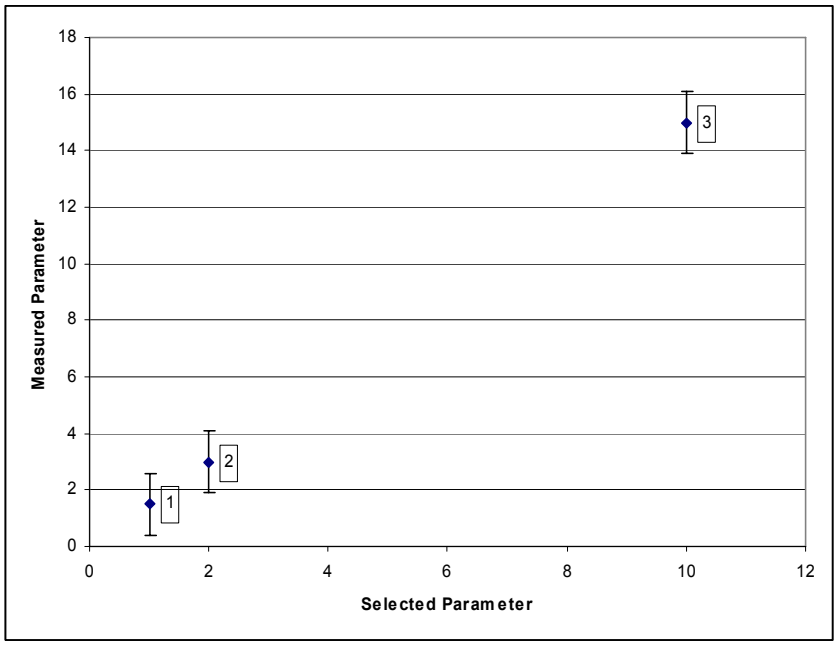

Figure E-1 Demonstration of Effect of Choice of Probes on Calculated Values.

Mathematically, this scenario can be represented as follows:

$$Slope = \frac{y_2 - y_1}{x_2 - x_1} \qquad \textbf{[E.8]}$$

It is evident that if x_2 - x_1 is very small its reciprocal would be very large, in turn implying that the error in measuring y_2 and y_1 is amplified by a very large number.

The above illustration is a simplification of what could happen as a consequence of a poor choice of liquids, especially when a limited set of liquids is to be used to determine the surface properties. In the present case, liquids must be selected so that the calculated surface energies represent reasonable estimates of the true value with minimum error. A mathematical measure of this is the condition number of the selected set of liquids. The smaller the condition number the less sensitive are the calculated results to the experimental error. The method to obtain the condition number for any given set of probe liquids is presented in section E.1.4.

E.1.3 Error Propagation

As shown in equation (E.1), w is a function of γ and θ. By the propagation of error formulas, an estimate $\hat{w}$ of the true value of w, and the standard deviation of $\hat{w}$ can be obtained as follows *(3)*:

$$\hat{w} = 0.5\gamma\left(1 + \cos\bar{\theta}\right) \qquad \textbf{[E.9]}$$

$$\mathrm{var}\left(\hat{w}\right) = \sigma_{\hat{w}}^2 = \sigma_{\gamma}^2\left[\frac{\partial w}{\partial \gamma}\right]^2 + \sigma_{\bar{\theta}}^2\left[\frac{\partial w}{\partial \theta}\right]^2 + 2\sigma_{\gamma\theta}\left[\frac{\partial w}{\partial \gamma}\right]\left[\frac{\partial w}{\partial \theta}\right] \qquad \textbf{[E.10]}$$

$$\sigma_{\hat{w}} = \sqrt{\mathrm{var}\left(\hat{w}\right)} \qquad \textbf{[E.11]}$$

where, γ is the total surface free energy value of the liquid available from literature, $\bar{\theta}$ is the average contact angle from *r* replicate measurements, σ_{γ}^2 is the variance of γ, $\sigma_{\bar{\theta}}^2$ is the variance of $\bar{\theta}$ expressed in radians, $\sigma_{\gamma\bar{\theta}}$ is the covariance of γ and $\bar{\theta}$, and the square brackets denote that the derivatives within the brackets are to be evaluated at the mean of γ and of θ, respectively.

When the random errors in measurements of γ and θ are assumed to be independent, $\sigma_{\gamma\bar{\theta}} = 0$ and equation [E.10] is reduced to the following form:

$$\sigma_{\hat{w}}^2 = \sigma_{\gamma}^2\left[\frac{\partial w}{\partial \gamma}\right]^2 + \sigma_{\bar{\theta}}^2\left[\frac{\partial w}{\partial \theta}\right]^2 \qquad \textbf{[E.12]}$$

The value of σ_{γ}^2 is obtained from the literature. A reasonable approximation of σ_{γ} is 0.1 ergs/cm^2 if the exact values are not available. The value of $\sigma_{\bar{\theta}}^2$ is, however, unknown and it is estimated as (1/*r*)*variance of *r* replicate measurements of θ. That is:

$$\hat{\sigma}_{\bar{\theta}}^2 = \frac{1}{r}\hat{\sigma}_{\theta}^2 = \frac{1}{r}\frac{1}{(r-1)}\sum_{k=1}^{r}\left(\theta_k - \bar{\theta}\right)^2 \qquad \textbf{[E.13]}$$

Also, note from equation [E.1] that

$$\frac{\partial w}{\partial \gamma} = 0.5(1+\cos\theta), \qquad \textbf{[E.14]}$$

and

$$\frac{\partial w}{\partial \theta} = -0.5\gamma\sin\theta. \qquad \textbf{[E.15]}$$

Thus the estimates,

$$\left[\frac{\partial w}{\partial \gamma}\right] = 0.5\left(1+\cos\bar{\theta}\right) \qquad \textbf{[E.16]}$$

and

$$\left[\frac{\partial w}{\partial \theta}\right] = -0.5\sin\bar{\theta}\,. \qquad \textbf{[E.17]}$$

Using equations [E.12], [E.13], [E.16], and [E.17], the propagated variance of error in the work of adhesion can be calculated for each liquid as follows:

$$\hat{\sigma}_{\hat{w}}^2 = \sigma_{\gamma}^2\left\{0.5\left(1+\cos\bar{\theta}\right)\right\}^2 + \frac{1}{r}\frac{1}{(r-1)}\sum_{k=1}^{r}\left(\theta_k - \bar{\theta}\right)^2\left\{-0.5\gamma\sin\bar{\theta}\right\}^2 \qquad \textbf{[E.18]}$$

E.1.4 Determining Condition Number and Surface Energy Components Using Singular Value Decomposition Method

In the case when more than three liquids are used, the system of equations becomes over-determinate and matrix **A** is a *m* x 3 rectangular matrix. The singular value decomposition

(SVD) technique can be used to solve such as system of equations. The SVD technique can also be used to calculate the condition number of the selected liquids (even without any contact angle measurements) to assess if the choice of liquids is appropriate for calculating the surface free energy components of the solid. The SVD is based on a linear algebra theorem that states that any *m* x *n* matrix **A** where *m* > *n* can be represented as follows:

$$\mathbf{A} = \mathbf{U}\,\mathbf{W}\,\mathbf{V}^{T} \qquad \textbf{[E.19]}$$

where, **U** is a *m* x *n* orthogonal matrix, **W** is a *n x n* diagonal matrix, and $\mathbf{V}^{T}$ is a *n x n* orthogonal matrix *(4)*. In the present case *n* = 3, since there are three unknown components of surface free energy and *m* = number of probe liquids being used.

The condition number of the matrix **A** is defined as the ratio of the largest to the smallest diagonal element in the **W** matrix. Typically, a condition number above 10 can render solutions sensitive to the errors in the measured physical property. This may result in inaccurate or erroneous solutions, for example, a solution where square roots of the surface free energy components are negative.

The inverse of the matrix **A** is obtained as follows:

$$\mathbf{A}^{+} = \mathbf{V}\,[\mathrm{diag}\,(1/w_j)]\,\mathbf{U}^{T} \qquad \textbf{[E.20]}$$

where, $\mathbf{A}^{+}$ is referred to as the Moore-Penrose inverse. Now, equation (E.20) is used with equation (E.7) to calculate **x**, which is a vector comprising the square roots of the three surface free energy components as follows:

$$\mathbf{x} = \mathbf{V}\,[\mathrm{diag}\,(1/w_j)]\,\mathbf{U}^{T}\,\mathbf{B} \qquad \textbf{[E.21]}$$

In order to take into account the different error variances in work of adhesion for different probe liquids, the matrices **A** and **B** are changed as follows:

$$A' = \begin{bmatrix} \frac{\sqrt{\gamma_{l1}^{LW}}}{\sigma_1} & \frac{\sqrt{\gamma_{l1}^{+}}}{\sigma_1} & \frac{\sqrt{\gamma_{l1}^{-}}}{\sigma_1} \\ \ldots\ldots & \ldots\ldots & \ldots\ldots \\ \frac{\sqrt{\gamma_{lm}^{LW}}}{\sigma_m} & \frac{\sqrt{\gamma_{lm}^{+}}}{\sigma_m} & \frac{\sqrt{\gamma_{lm}^{-}}}{\sigma_m} \end{bmatrix}_{mx3}, \qquad \textbf{[E.22]}$$

$$B' = 0.5\begin{bmatrix} \frac{\gamma_{l1}(1+Cos\theta_1)}{\sigma_1} \\ \ldots\ldots\ldots\ldots \\ \frac{\gamma_{lm}(1+Cos\theta_m)}{\sigma_m} \end{bmatrix}_{mx1} \qquad \textbf{[E.23]}$$

where, $\hat{\sigma}_1$ through $\hat{\sigma}_m$ are the estimates of the propagated error standard deviations in the work of adhesion of the *m* liquids calculated using equation [E.18].

The matrix **A´** is referred to as the design matrix. **x** is calculated using the design matrix **A´** and vector **B´** in place of **A** and **B** using the same procedure as described earlier. The SVD matrices must be generated for **A´** and not **A** to calculate **x** when the errors are to be included.

The variance in the estimate of the parameters of vector **x**, x_1 through x_3, which represent the square roots of the three surface free energy components, are estimated from the following equation when SVD is used:

$$\hat{\sigma}_{x_i}^2 = \sum_{j=1}^{n} \left(\frac{V_{ij}}{w_j} \right)^2 \text{ for } i = 1, 2, 3 \ . \qquad \textbf{[E.24]}$$

The surface energy components are calculated by squaring the individual values of the vector **x.** The variance estimate of the errors in the surface free energy components is obtained by propagation of errors as follows:

$$\hat{\sigma}_{x_i^2}^2 = \hat{\sigma}_{x_i}^2 \left[\frac{\partial x_i^2}{\partial x_i} \right]^2 = \left[2x_i \right]^2 \hat{\sigma}_{x_i}^2 = 4x_i^2 \hat{\sigma}_{x_i}^2 \qquad \textbf{[E.25]}$$

E.1.5 Determining Surface Energy Components Using Least Squares

The singular value decomposition method is used to compute the surface energy components with standard deviations and the condition number for a set of probe liquids. Since condition number of probe liquids depends only on the properties of the probe liquids and not the measured contact angles, once an appropriate set of liquids is selected it might not be necessary to repeat the computations for condition number. A simpler method to determine the surface energy components and their standard deviations using contact angles with three or more than three probe liquids is presented here. For the materials tested in this research, results from both these methods were found to be very similar in most cases.

The matrices **A´** and **B´** are determined as described in the previous section using equations [E.22] and [E.23]. These matrices are used with equation [E.7], which is modified as follows:

$$\mathbf{E = A'x - B'} \qquad \textbf{[E.26]}$$

where, **E** is a column matrix referred to as the error matrix based on assumed initial values of **x**. An iterative solution method can be used to determine the value of **x** such that sum of squares of the values of the error matrix **E** are minimized. This value of **x** represents square roots of the three surface energy components of the solid.

The standard deviations of the surface energy components may be obtained from equation [E.25]. The term $\hat{\sigma}_{x_i}^2$ is obtained as follows:

$$\hat{\sigma}_{x_i}^2 = c_{ii} \qquad \textbf{[E.27]}$$

where, c_{ii} are diagonal elements of the $(\mathbf{A'}^{T}\mathbf{A'})^{-1}$ matrix.

E.1.6 Important Considerations during Analysis

The measured contact angles must not be in violation of any of the requirements for applying Young-Dupre equation in order to determine the surface energy components of the solid. There are two methods to check this. First a plot of $\gamma_l \cos\theta$ versus γ_l based on the total surface energies of the probe liquids and the measured contact angles with any given asphalt binder must follow a smooth curve, at least for the four polar probe liquids. Second, when the

minimization of sum of squares of errors is used to determine the surface energy components, magnitude of the residual error must be small.

In some cases, the square root of the surface energy component of **x** may be a negative number. It is very important that this number not be squared and reported as the surface energy component of the solid. If the magnitude of the negative number is large, then accuracy of the contact angles with the probe liquids must be examined closely. If the magnitude is small, then the negative value may be due to small experimental errors or redundancy. In such cases the value of the square root of the component must be set to zero. A constrained weighted least squares method can also be used to improve the accuracy of the results. This method is similar to the minimization of squares of error method, except that in this method a constraint that the value of x_i must be greater than or equal to zero is applied while minimizing the sum of squares of errors.

E.2 COMPUTING SURFACE ENERGIES FROM SPREADING PRESSURES

The sequence of calculations to determine the surface energy components using spreading pressures is the same as the procedure used to determine surface energy components using contact angles. The only difference is in the work of adhesion formula, which in this case is:

$$w = W_{adhesion} / 2 = \gamma + 0.5\pi_e \qquad \textbf{[E.28]}$$

where, γ is the total surface free energy of the probe liquid and π_e is the equilibrium spreading pressure of a probe vapor on the surface of the solid being investigated. Equation [E.3] remains the same where only the definition of **B** changes to accommodate spreading pressure instead of contact angle:

$$\mathbf{A\ x = B}, \qquad \textbf{[E.29]}$$

where,

$$A = \begin{bmatrix} \sqrt{\gamma_{l1}^{LW}} & \sqrt{\gamma_{l1}^{+}} & \sqrt{\gamma_{l1}^{-}} \\ ..... & ..... & ..... \\ \sqrt{\gamma_{lm}^{LW}} & \sqrt{\gamma_{lm}^{+}} & \sqrt{\gamma_{lm}^{-}} \end{bmatrix}_{mx3}, \qquad \textbf{[E.30]}$$

$$x = \begin{bmatrix} \sqrt{\gamma_{s}^{LW}} \\ \sqrt{\gamma_{s}^{-}} \\ \sqrt{\gamma_{s}^{+}} \end{bmatrix}_{3x1}, \qquad \textbf{[E.31]}$$

$$B = \begin{bmatrix} \gamma_{l1} + 0.5\pi_1 \\ ..... \\ \gamma_{lm} + 0.5\pi_m \end{bmatrix}_{mx1} \qquad \textbf{[E.32]}$$

Also, the error propagation in *w,* given by equations [E.12], [E.13], [E.16], and [E.17] is modified as follows:

$$\sigma_{\hat{w}}^2 = \sigma_\gamma^2\left[\frac{\partial w}{\partial \gamma}\right]^2 + \sigma_\pi^2\left[\frac{\partial w}{\partial \pi}\right]^2 \quad \textbf{[E.33]}$$

Where, γ is the total surface free energy value of the liquid available from literature, and $\bar{\pi}$ is the average spreading pressure from *r* replicate measurements, σ_γ^2 is the variance of γ, and $\sigma_{\bar{\pi}}^2$ is the variance of $\bar{\pi}$. The value of σ_γ^2 is obtained from the literature. A reasonable approximation of σ_γ is 0.1 ergs/cm^2 if the exact values are not available. The value of $\sigma_{\bar{\pi}}^2$ is, however, unknown and is estimated as (1/*r*)*sample variance of *r* replicate measurements on π. Also, from equation [E.23] for this case:

$$\left[\frac{\partial w}{\partial \gamma}\right] = 1, \quad \textbf{[E.34]}$$

and

$$\left[\frac{\partial w}{\partial \pi}\right] = 0.5 \quad \textbf{[E.35]}$$

The propagated variance of error in the work of adhesion can be calculated for each liquid as follows:

$$\hat{\sigma}_{\hat{w}}^2 = \sigma_\gamma^2 + (0.5)^2 \frac{1}{r}\frac{1}{(r-1)}\sum_{k=1}^{r}(\pi_k - \bar{\pi})^2 \quad \textbf{[E.36]}$$

All other steps to calculate **x** remain the same as in the case of determining **x** from contact angles.

E.3 COMPUTING ENERGY PARAMETERS

This section provides a summary of some of the important thermodynamic parameters that can be computed from the surface energy components of the asphalt binder and the aggregate.

E.3.1 Work of Cohesion

The work of cohesion of a material, *B*, is computed as:

$$W_{BB} = 2\gamma_B = 2\gamma_B^{LW} + 4\sqrt{\gamma_B^+\gamma_B^-} \quad \textbf{[E.37]}$$

where, γ_B is the total surface free energy of the material and the superscripts *LW*, +, and - represent the Lifshitz-van der Waals or dispersive component, the Lewis acid component, and the Lewis base component, respectively.

E.3.2 Work of Adhesion

The work of adhesion between two materials, *A* and *B*, is computed as:

$$W_{AB} = 2\sqrt{\gamma_A^{LW}\gamma_B^{LW}} + 2\sqrt{\gamma_A^+\gamma_B^-} + 2\sqrt{\gamma_A^-\gamma_B^+} \quad \textbf{[E.38]}$$

where, the subscripts *A* and *B* represent the two materials and other terms are as described before.

E.3.3 Work Required to Displace a Material from its Interface with Another

If a material W displaces a material B from its interface with another material A, then the work required for this process to occur is:

$$W_{ABW} = \gamma_{AW} + \gamma_{BW} - \gamma_{AB} \quad \textbf{[E.39]}$$

where, the subscripts *A*, *B*, and *W* represent the three materials and γ_{ij} the interfacial energy between any two materials *i* and *j* determined from their respective surface energy components as follows:

$$\gamma_{ij} = \gamma_i + \gamma_j - 2\sqrt{\gamma_i^{LW}\gamma_j^{LW}} - 2\sqrt{\gamma_i^+\gamma_j^-} - 2\sqrt{\gamma_i^-\gamma_j^+} \quad \textbf{[E.40]}$$

E.3.4 Energy Parameters Related to Moisture Sensitivity of the Asphalt Binder – Aggregate Combination

Four energy parameters were recommended as independent measures of the moisture sensitivity of any combination of asphalt binder and aggregate in an asphalt mix. These parameters can be determined using the surface energy components of the asphalt binders, aggregates, and water using the above equations as follows:

$$ER_1 = \left| \frac{W_{AB}}{W_{ABW}^{wet}} \right| \quad \textbf{[E.41]}$$

where, the subscripts *A*, *B*, and *W* refer to aggregate, asphalt binder, and water, respectively. W_{AB} and W_{ABW}^{wet} are determined using equations (E.38) and (E.39), respectively.

$$ER_2 = \left| \frac{W_{AB} - W_{BB}}{W_{ABW}^{wet}} \right| \quad \textbf{[E.42]}$$

where, the subscripts *A*, *B*, and *W*, refer to aggregate, asphalt binder, and water. W_{BB}, W_{AB}, and W_{ABW}^{wet} are determined using equations [E.37], [E.38] and [E.39], respectively.

The other two energy parameters are the products of ER_1 and ER_2 with the specific surface area of the aggregate expressed in m^2/g.

A combination of asphalt binder and aggregate with a higher value of energy ratio will have a better resistance to moisture damage as compared to a combination of asphalt binder and aggregate with a lower value of energy ratio, when other mixture properties are similar.

E.4 ILLUSTRATIVE EXAMPLE

This section presents an illustrative example of how to determine which one of two given unmodified asphalt binders will result in an asphalt mixture that is more resistant to moisture damage when used with a particular aggregate (considering all other properties of the two mixtures are similar) based on surface energy measurements. This exercise is to demonstrate the application of the tools developed in this research but is not intended to replace any standard testing procedure. Also, this example is for material selection only. Overall prediction of

mixture performance requires a comprehensive evaluation of various other mixture properties including surface free energy.

The materials provided are asphalt binders A and B, and aggregate R. The following steps are executed to achieve the objective of this exercise.

E.4.1 Computing Surface Energy Components of Materials from Test Data

1. Use the Wilhelmy plate method to measure the contact angles of both the asphalt binders with each of the five probe liquids following the procedure shown in Appendix B. Use the USD to measure the spreading pressure of three probe vapors with the aggregate following the procedure shown in Appendix C. At least three replicates of each material must be tested with each probe liquid or vapor. It is not necessary to check the condition number if the liquids recommended in Appendices A and B are used.
2. Table E.1 and E.2 present results from these tests.

Table E.1. Contact Angles Measured with Wilhelmy Plate Device (degrees).

Asphalt Binder	Probe Liquid	Replicate 1	Replicate 2	Replicate 3	Average	Sample Standard Deviation
A	Water	91.90	92.59	89.06	91.18	1.08
	Formamide	79.31	79.38	79.87	79.52	0.18
	Glycerol	86.14	85.55	85.23	85.64	0.27
	Methylene Iodide	67.77	68.38	67.76	67.97	0.21
	Ethylene Glycol	67.93	68.50	69.10	68.51	0.34
B	Water	88.73	89.48	88.90	89.04	0.23
	Formamide	78.15	79.83	78.42	78.80	0.52
	Glycerol	83.13	83.64	83.76	83.51	0.19
	Methylene Iodide	62.72	62.41	62.44	62.52	0.10
	Ethylene Glycol	62.63	62.70	64.12	63.15	0.49

Table E.2. Spreading Pressures and Specific Surface Areas Reported by SEMS Software with the Universal Sorption Device.

Parameter	Probe Vapor	Replicate 1	Replicate 2	Replicate 3	Average	Sample Standard Deviation
Spreading Pressure ($ergs/cm^2$)	n Hexane	40.09	37.91	43.40	40.46	1.60
	MPK	55.51	50.77	47.62	51.30	2.29
	Water	157.85	146.60	137.58	147.35	5.86
Specific Surface Area (m^2/gm)	n Hexane	0.74	0.65	0.75	0.71	0.03
	MPK	1.31	1.49	1.38	1.39	0.05
	Water	1.93	1.95	2.15	2.01	0.07

3. The surface energy components of the probe liquids or vapors based on the acid-base theory are known from the literature and are shown in Table E.3. The standard deviations in the surface energy components of these probe liquids or vapors can also be found from the literature. In the absence of specific data, the standard deviation in the total surface energy component can be considered to be 0.1 ergs/cm^2.

Table E.3. Surface Energy Components of the Probe Liquids or Vapors (ergs/cm^2).

Probe Liquid / Vapor	γ^{LW}	γ^{+}	γ^{-}	γ^{Total}
Water	21.80	25.50	25.50	72.80
Formamide	39.00	2.28	39.60	58.00
Glycerol	34.00	3.92	57.40	64.00
Methylene Iodide	50.80	0.00	0.00	50.80
Ethylene Glycol	29.00	1.92	47.00	48.00
Hexane	18.40	0.00	0.00	18.40
Methyl propyl ketone (MPK)	21.70	0.00	19.60	21.70

4. The three surface energy components of the asphalt binders are computed as follows. First a plot of $\gamma_l \cos\theta$ versus γ_l is generated for each of the two asphalt binders. Figures E.1 and E.2 present this plot for the two asphalt binders. From these plots ensure that the points corresponding to the four polar probes lie on a smooth curve. Note that the point lying outside the general trend on these plots corresponds to the non polar liquid (methylene iodide). If any of the polar probes deviates from a smooth trend then it is recommended that the measurements for that probe be repeated. If the problem persists then other possibilities such as a chemical interaction between the probe and the binder must be investigated.

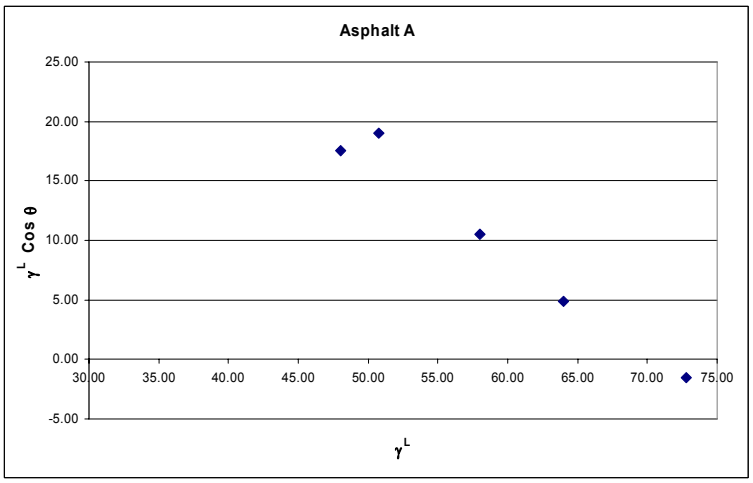

Figure E.1. Plot of $\gamma_l \cos\theta$ versus γ_l for Asphalt Binder A to Check Data Consistency.

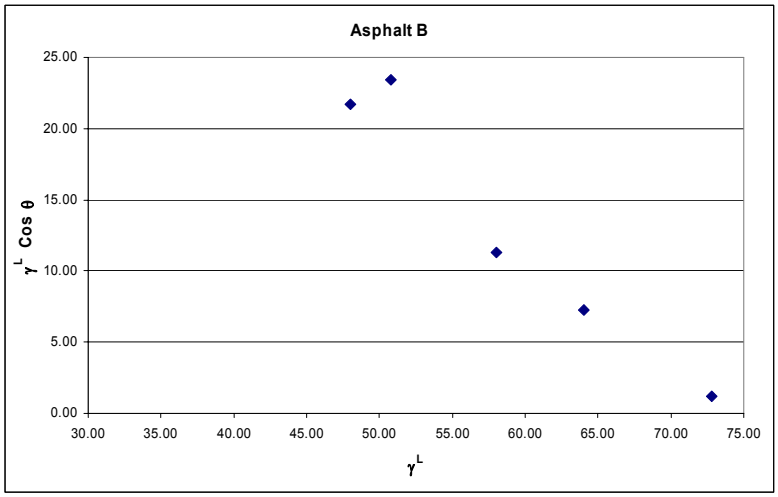

Figure E.2. Plot of $\gamma_l \cos\theta$ versus γ_l for Asphalt Binder B to Check Data Consistency.

5. Determine the matrix **A** using data from the table E.3 with equation E.4. This matrix is valid for both asphalt binders.

$$\mathbf{A} = \begin{bmatrix} 4.67 & 5.05 & 5.05 \\ 6.24 & 1.51 & 6.29 \\ 5.83 & 1.98 & 7.58 \\ 7.13 & 0 & 0 \\ 5.39 & 1.39 & 6.86 \end{bmatrix} \quad \textbf{[E.43]}$$

6. Determine the matrix B using data from the tables E.1 and E.3 with equation E.6 for each of the two asphalt binders.

For asphalt binder A, $\mathbf{B} = 0.5 \begin{bmatrix} 71.30 \\ 68.55 \\ 68.86 \\ 69.85 \\ 65.58 \end{bmatrix}$ **[E.44]**

For asphalt binder B, $\mathbf{B} = 0.5 \begin{bmatrix} 74.02 \\ 69.27 \\ 71.23 \\ 74.24 \\ 69.68 \end{bmatrix}$ **[E.45]**

7. Use equation E.18 to compute σ_1 through σ_5 for each of the five probe liquids for each asphalt binder. The value of σ_γ can be approximated as 0.1 if data for the probe liquids

is not available. All other inputs for this equation are available from tables E.1 and E.3. As an illustration the value of σ_1 for asphalt binder A is computed below. Note that the value of θ used in equation E.18 must be expressed in radians after appropriate conversion from the data in table E.1.

$$(\sigma_1)^2 = (0.1)^2\{0.5(1-0.02059)\}^2 + \frac{1}{3}\frac{1}{2}\left[(1.60-1.59)^2+(1.62-1.59)^2+(1.55-1.59)^2\right]\{-0.5(72.8)0.9978\}^2 \quad \text{or}$$

$$\sigma_1 = 0.6878 \quad \textbf{[E.46]}$$

8. Compute the **A**' and **B**' matrices for the two asphalt binders using equations E.22 and E.23 with the values of σ_1 through σ_5 computed in the previous step for the respective binders. Thus, the **A**' and **B**' matrices for asphalt binder A are:

$$\mathbf{A'} = \begin{bmatrix} 6.79 & 7.34 & 7.34 \\ 59.06 & 14.28 & 59.51 \\ 36.93 & 12.54 & 47.99 \\ 65.54 & 0 & 0 \\ 36.31 & 9.34 & 46.22 \end{bmatrix} \quad \textbf{[E.47]}$$

$$\mathbf{B'} = \begin{bmatrix} 51.83 \\ 324.17 \\ 218.10 \\ 321.18 \\ 221.08 \end{bmatrix} \quad \textbf{[E.48]}$$

Similarly, the **A**' and **B**' matrices for asphalt binder B are:

$$\mathbf{A'} = \begin{bmatrix} 30.53 & 33.02 & 33.02 \\ 23.53 & 5.69 & 23.71 \\ 48.28 & 16.39 & 62.74 \\ 86.14 & 0 & 0 \\ 27.56 & 7.09 & 35.09 \end{bmatrix} \quad \textbf{[E.49]}$$

$$\mathbf{B'} = \begin{bmatrix} 242.05 \\ 130.49 \\ 294.94 \\ 448.61 \\ 178.31 \end{bmatrix} \quad \textbf{[E.50]}$$

9. The matrix **x**, represents the square roots of the three surface energy components of the asphalt binder as shown in equation E.5. Compute the values of the column matrix x using any iterative solution method such that sum of squares of values of the column matrix **E** from equation E.26 is minimized. The "Solver" feature of Microsoft® Excel can be used for this iterative procedure. For asphalt binder A,

$$\mathbf{x} = \begin{bmatrix} 4.87 \\ 1.68 \\ 0.36 \end{bmatrix} \quad \textbf{[E.51]}$$

For asphalt binder B,

$$\mathbf{x} = \begin{bmatrix} 5.20 \\ 2.34 \\ 0.16 \end{bmatrix} \quad \textbf{[E.52]}$$

10. Compute the surface free energy components of each asphalt binders as the squares of the **x** matrix. Thus, the Lifshitz-van der Waals, acid and base components for asphalt binder A are 23.75, 0.13, and 2.83 ergs/cm^2, respectively. Similarly, the Lifshitz-van der Waals, acid and base components for asphalt binder A are 27.07, 0.02, and 5.46 ergs/cm^2, respectively.

11. In order to determine the standard deviations in the computed surface energy components, determine the $(\mathbf{A'}^T\mathbf{A})^{-1}$ matrix for each asphalt binder. The three diagonal elements of this matrix represent the variance of the square roots of the surface energy components (Lifshitz-van der Waals, base and acid component, respectively) as shown in equation E.27. For asphalt binder A this matrix is,

$$\left(\mathbf{A'}^T\,\mathbf{A'}\right)^{-1} = \begin{bmatrix} 0.0021 & -0.0002 & -0.0017 \\ -0.0002 & 0.0465 & -0.0120 \\ -0.0017 & -0.0120 & 0.0055 \end{bmatrix} \quad \textbf{[E.53]}$$

For asphalt binder B this matrix is,

$$\left(\mathbf{A'}^T\,\mathbf{A'}\right)^{-1} = \begin{bmatrix} 0.0016 & -0.0002 & -0.0013 \\ -0.0002 & 0.0124 & -0.0043 \\ -0.0013 & -0.0043 & 0.0036 \end{bmatrix} \quad \textbf{[E.54]}$$

12. For asphalt binder A, the standard deviation in the surface energy component is computed using the results in E.51 and E.53 with equation E.25 as show below.
For Lifshitz-van der Waals component,

$$\sigma^{LW} = \sqrt{4(4.87)^2(0.0021)} = 0.45\,\text{ergs/cm}^2 \quad \textbf{[E.55]}$$

For base component,

$$\sigma^{-} = \sqrt{4(1.68)^2(0.0465)} = 0.72 \text{ ergs/cm}^2 \quad \textbf{[E.56]}$$

For acid component,

$$\sigma^{+} = \sqrt{4(0.36)^2(0.0055)} = 0.05 \text{ ergs/cm}^2 \quad \textbf{[E.57]}$$

13. The same procedure is followed to determine the standard deviation in the Lifshitz-van der Waals, acid, and base components of asphalt binder B as 0.42, 0.02, and 0.52 ergs/cm^2, respectively

14. In order to determine the surface energy components of the aggregate, the spreading pressures recorded by the USD in table E.2 are used. Based on the protocols developed in this research, the spreading pressures must be computed using the specific surface area of the aggregate determined using nHexane as a probe with a molecular cross sectional area of 56A^2 in lieu of the calculated projected cross sectional area of 39A^2. In order to do so, for each probe vapor obtain the product of the spreading pressure reported in table E.2 with its respective specific surface area (SSA). Compute the correct SSA for nHexane by multiplying the reported SSA of nHexane with a factor of 56/39. Finally, for each probe vapor divide the product of the spreading pressure and the SSA with the corrected SSA. Table E.4 below presents these steps.

Table E.4. Obtaining Corrected Spreading Pressures (ergs/cm^2).

Parameter	Probe Vapor	Replicate 1	Replicate 2	Replicate 3	Average	Sample Standard Deviation
Spreading Pressure (ergs/cm^2)	n Hexane	40.09	37.91	43.40	40.46	1.60
	MPK	55.51	50.77	47.62	51.30	2.29
	Water	157.85	146.60	137.58	147.35	5.86
SSA (m^2/gm)	n Hexane	0.74	0.65	0.75	0.71	0.03
	MPK	1.31	1.49	1.38	1.39	0.05
	Water	1.93	1.95	2.15	2.01	0.07
Spreading Pressure x SSA	n Hexane	29.60	24.55	32.64	28.93	2.36
	MPK	72.72	75.65	65.71	71.36	2.95
	Water	304.65	285.87	295.81	295.44	5.42
Corrected SSA = SSA of nHexane x 56/39	nHexane	1.06	0.93	1.08	1.02	0.05
Corrected Spreading Pressure = Spreading Pressure x SSA /Mean corrected SSA	n Hexane	28.92	23.99	31.90	28.27	2.31
	MPK	71.07	73.92	64.21	69.73	2.88
	Water	297.70	279.35	289.06	288.71	5.30

15. Determine the matrix **A** using data from the table E.3 with equation E.4.

$$\mathbf{A} = \begin{bmatrix} 4.29 & 0.0 & 0.0 \\ 4.66 & 0.00 & 4.43 \\ 4.67 & 5.05 & 5.05 \end{bmatrix} \quad \textbf{[E.58]}$$

16. Determine the matrix B using data from the tables E.3 and E.4 with equation E.32.

$$\mathbf{B} = \begin{bmatrix} 32.53 \\ 56.56 \\ 217.33 \end{bmatrix} \quad \textbf{[E.59]}$$

17. Similar to step 7 for asphalt binders, use equation E.36 to compute σ_1 through σ_3 for each of the three probe vapors. The value of σ_γ can be approximated as 0.1 if data for the probe liquids is not available. All other inputs for this equation are available from tables E.3 and E.4. The values of σ_1, σ_2, and σ_3 for the aggregate are 0.68, 1.05, and 3.52 ergs/cm^2, respectively.

18. Compute the **A**' and **B**' matrices for the aggregate as in the case of asphalt binders using the values of σ_1 through σ_3 computed in the previous step. Thus, the **A**' and **B**' matrices are,

$$\mathbf{A'} = \begin{bmatrix} 6.327 & 0.0 & 0.0 \\ 4.45 & 0.0 & 4.23 \\ 1.33 & 1.43 & 1.43 \end{bmatrix} \quad \textbf{[E.60]}$$

$$\mathbf{B'} = \begin{bmatrix} 47.98 \\ 54.03 \\ 61.72 \end{bmatrix} \quad \textbf{[E.61]}$$

19. The matrix **x**, represents the square roots of the three surface energy components of the aggregate as shown in equation E.29. Since there are only three probe vapors and three unknowns, compute the value of **x** directly using equation E.7 as shown below.

$$\mathbf{x} = \mathbf{A'}^{-1}\mathbf{B} = \begin{bmatrix} 0.158 & 0 & 0 \\ 0.019 & -0.236 & 0.6993 \\ -0.166 & 0.236 & 0 \end{bmatrix} \begin{bmatrix} 47.98 \\ 54.03 \\ 61.72 \end{bmatrix} = \begin{bmatrix} 7.58 \\ 31.31 \\ 4.79 \end{bmatrix}$$

20. Compute the surface free energy components of the aggregate as the squares of the **x** matrix. Thus, the Lifshitz-van der Waals, acid and base components for the aggregate are 57.5, 23.0, and 980.5 ergs/cm^2, respectively.
21. The standard deviations of the surface energy components can be computed in the same manner using the inverse of **A'A** matrix as described before.

E.4.2 Computing and Interpreting Thermodynamic Parameters Using Surface Energy Components

22. Work of cohesion for each of the asphalt binders is computed using equation E.37. The work of cohesion for binders A and B are 49.93 and 55.47 ergs/cm^2, respectively. A higher work of cohesion indicates that more work is required to fracture the material.
23. Use equations E.37 through E.42 to compute ER_1 and ER_2. These parameters are independent measures of moisture sensitivity and are computed for each combination of asphalt binder and aggregate. Two additional parameters that can be calculated are $ER_1 * SSA$ and $ER_2 * SSA$, where *SSA* is the specific surface area of the aggregate (size fraction passing #4 sieve and retained on #8 sieve). Since only aggregate is used in the present example the last two parameters will be proportional to the first two parameters.
24. A higher value of ER_1 indicates better resistance to moisture damage. Typically this value can range from 0.3 to 10.0 depending on the surface energy components of the asphalt binder and the aggregate. In this case the values of ER_1 for the combination of asphalt binder A with aggregate R and asphalt binder B with aggregate R, are 0.463 and 0.435, respectively. Based on this parameter the asphalt binder A is likely to have better resistance to moisture damage than binder B when used with aggregate R, although this difference may not be very significant.
25. A higher value of ER_2 indicates better resistance to moisture damage. Typically this value can range from 0.1 to 5.0 depending on the surface energy components of the asphalt binder and the aggregate. In this case the values of ER_2 for the combination of asphalt binder A with aggregate R and asphalt binder B with aggregate R, are 0.257 and 0.216, respectively. Based on this parameter the asphalt binder A is likely to have better resistance to moisture damage than binder B when used with aggregate R, which is consistent with the observation made using the previous parameter.
26. Relative comparison of the energy parameters derived using surface energy measurements indicates that binder A will perform better than binder B in terms of moisture resistance when used with aggregate R. However, in general the value of both the energy parameters is low indicating poor resistance to moisture damage for both these material combinations. Therefore, some type of treatment to the asphalt binder or aggregate may be necessary to improve the resistance of the mixture to moisture damage

The user is reminded that the above illustration compares mixtures based on a single material property, i.e., surface energy. This illustration is most suitable as a tool by which to select material combinations that will result in an asphalt mixture that is more resistant to moisture damage. In order to predict performance of asphalt mixtures, a more comprehensive evaluation of various other material properties, such as the distribution of air voids in the mixture, including surface energy is required for robust performance prediction of the asphalt mixture.

REFERENCES

1. Della Volpe, C. and Siboni, S., "Acid Base Surface Free Energies of Solids and the Definition of Scales in the Good van Oss Chaudhury Theory," *Journal of Adhesion Science and Technology*, Volume 14 No.2, (2000), pp. 235-272.

2. Della Volpe, C., and Siboni, S., " Some Reflections on Acid Base Solid Surface Free Energy Theories*," Journal of Colloid and Interface Science*, Volume 195, (1997), pp. 121-136.

3. Ku, H., "Notes on the Propagation of Error Formulas", *Journal of Research of National Bureau of Standards - C*, Engineering and Instrumentation, Volume 70C No.4, (1966), pp. 263-273.

4. Press, W.H., Flannery, B.P., Teukolsky, S.A., and Vetterline, W.T., "Numerical Recipes the Art of Scientific Computing," Cambridge University Press, (1988).

APPENDIX F

TEST METHOD TO USE AN INVERSE GAS CHROMATOGRAPH TO MEASURE SURFACE PROPERTIES OF AGGREGATES AND ASPHALT BINDERS

TEST METHOD TO USE AN INVERSE GAS CHROMATOGRAPHY TO MEASURE SURFACE PROPERTIES OF AGGREGATES AND ASPHALT BINDERS

Inverse gas chromatography (IGC) was used in this research to determine the surface energy components of asphalt binders and aggregates. Section 3.2.5 of the main report presents an overview of this technique along with the results for two different types of aggregates and eight different types of asphalt binders. This appendix presents details of the sample preparation procedure, test protocol, and analysis methods used to determine the surface energy components of aggregates or asphalt binders using IGC following Hefer *(1)*.

Only one manufacturer, Surface Measurement Systems (SMS) of the U.K. was found to commercially manufacture IGC devices. Due to the high capital outlay required for the purchase of this device it was decided to conduct tests on the aggregates using the IGC device at a laboratory of SMS in Allentown, Pennsylvania. Conventional gas chromatographs can also be easily retrofit to function for IGC. In this research, an existing HP5980 gas chromatograph at Texas A&M University was modified to work as an IGC. The asphalt binders were characterized using this device.

F.1 SAMPLE PREPARATION

In a typical test using IGC, small concentrations of the probe vapor are passed through a column using an inert gas. The column contains the solid material (asphalt binder or aggregate) for which the surface energy components are to be determined. The time taken for the probe vapor to travel through the column depends on the interaction between the solid phase in the column and the probe molecules. Different columns are required for use with aggregates and asphalt binders. The following section describes the types of column suitable for each material and the sample preparation techniques.

F.1.1 Aggregates

Glass columns were used in these experiments, although stainless steel columns can also be used. Glass columns are silane treated to make them more inert, while supreme grade stainless steel (SS304) columns are also commonly used. Glass columns cost about $10 each and stainless steel about $3.50 each (based on 300 mm column length). Both these options are relatively inexpensive when compared to long coiled capillary columns used in analytical chromatography, which can range between $75 and more than $500 each. The advantage of glass columns is that it is easier to exercise control when packing the sample into the column. The standard SMS-*i*GC oven provides two straight 6.35 mm (¼ inch) outer diameter (OD) columns that are 300 mm in length. The inner diameter (ID) can be up to 4 mm for these columns. Stainless steel columns of 6.35 mm (¼ inch) OD usually have an ID of 5.3 mm but are more difficult to pack especially when small quantities of material are used.

In order to prepare columns with aggregate samples, first glass wool was inserted into one end of the column. The desired sample mass was then loaded into the column through a funnel while the column was kept vertical. For fine powders, a vibratory stand was available to ensure continuous packing, which results in better peak separation during the test. Alternatively, a simple fill-and-tap method can also be used. The sample was then secured by inserting glass wool at the open end. A special tool or simple wire conveniently configured can be used for this

purpose. The glass wool was also silanized to make it less reactive, similar to the silanized glass column.

F.1.2 Asphalt Binders

The methodology to prepare columns for testing asphalt binders was adapted from the original method developed and published by Western Research Institute [2]. Untreated Fused silica capillary columns with dimensions of 15 m × 0.25 mm (Sigma-Aldrich, Supelco), were used in these experiments. Approximately 1g of bitumen was diluted in 10 mL toluene to produce a 10% solution. A rinsing kit (Sigma-Aldrich, Supelco) consisting of a 25 mL plastic-coated (pressure safe) glass reservoir with a screw-on stainless steel inlet-outlet unit is the key apparatus in the coating process. The solution was transferred to the 25 ml vial and one end of the column inserted into the solution. The solution was pushed through the column with dry nitrogen by applying a pressure of approximately 35 kPa. The column rinsing assembly is illustrated in Figure F.1.

After about six to seven coils of the transparent capillary column were filled, the inlet of the column was pulled out of the solution and the bitumen solution was pushed through the remainder of the column by nitrogen pressure. This process was repeated two more times to ensure adequate coating of the column walls. No significant coloring of the column occurred due to the thin film produced. After the final purge, the pressure was increased to approximately 200 kPa and the water bath turned on. This initial drying process was allowed to continue for 60 minutes at 40°C.

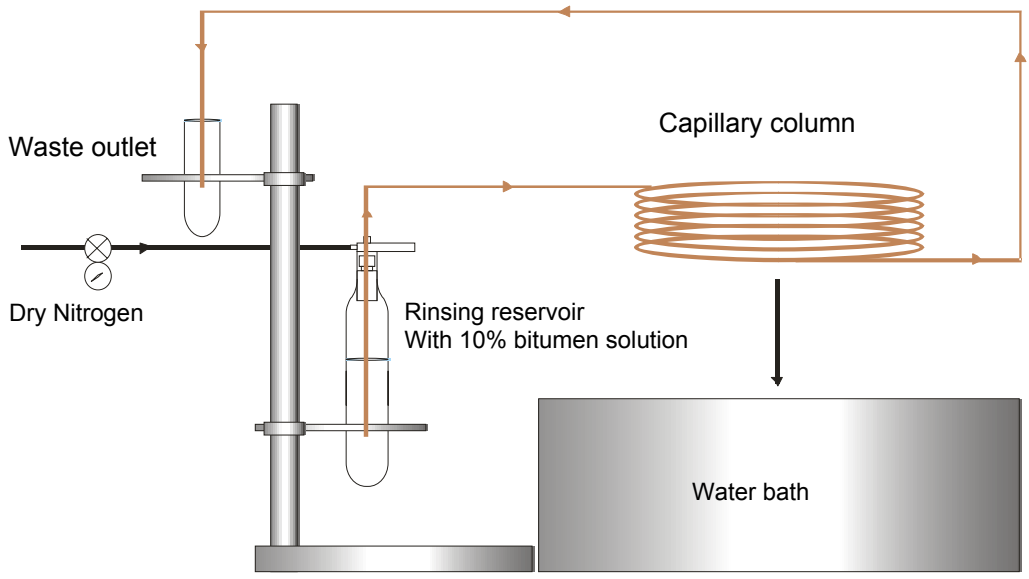

Figure F-1. Column Rinse Assembly (1).

F.2 TEST PROCEDURE

The test procedure to measure the surface energy components of asphalt binders using IGC is described in this section. This same procedure can also be extended to test the surface

energy components of aggregates with only difference of using a glass or stainless column packed with aggregates in place of the capillary column coated with the asphalt binder.

A HP5890 Series II gas chromatograph (GC) equipped with electronic pressure control (EPC) and a flame ionization detector (FID) was used in this study. ChemStation software was used for experimental setup, control, and data capture. The inlet and outlet temperatures were set to 175˚C and 250˚C, respectively. The bitumen column was installed in the GC oven and conditioned for an hour at 130˚C before testing. The temperature program lowered the temperature to the test temperature of 25˚C after conditioning. The column flow was set to 1.5 mL/min, corresponding to a column head pressure on the order of 70 kPa, and the total flow (or injection-spit flow) was set to 15 mL/min. Operating in split mode allowed injection of minute amounts of the probe vapor with a syringe by removing some of the injected sample before elution through the column, thereby increasing the resolution.

The probe molecules were injected manually with gas-tight glass microsyringes (Sigma-Aldrich, Hamilton). High-purity chemicals (high-pressure liquid chromolography [HPLC} grade) purchased from Sigma-Aldrich, USA, were used. A mixture of normal alkanes, including normal pentane, hexane, heptane, octane and nonane was made with methane as the reference probe. Approximately 0.1μL of the mixture in liquid form was injected into the system. Methane is considered as an inert hydrocarbon and its retention time serves as a measure of the dead volume of the column. In addition to the series of n-alkanes, polar probes with known surface energy components were required in these experiments. Two probes with acidic character, namely chloroform and dichloromethane, and two probes with basic character, namely toluene and ethyl acetate, were used. One replicate consisted of a sequence of the n-alkane mixture followed by individual injections of each of the polar probes. A 5-minute conditioning time at 130˚C was sufficient between sequences to remove all excess gas from the system.

F.3 ANALYSIS OF RESULTS

An important assumption in the application of IGC to study adsorption processes is that the solute equilibrium conditions are achieved between the mobile and stationary phase. These conditions are achieved at infinite dilution of the adsorbate and therefore zero coverage of the surface. Under these conditions the adsorbate can be considered to behave as an ideal gas, which becomes important in the following approach to the analysis. The retention time, t_R, of the adsorbates interacting with the surface allows determining the net retention volume, V_N. This quantity is obtained from the following relationship:

$$V_N = j/m \cdot F \cdot \left(t_R - t_M\right) \cdot \frac{T}{273.15} \qquad \textbf{[F.1]}$$

In equation (F.1), j is the dimensionless James-Martin compressibility factor, correcting for the pressure drop in the column, expressed by [3, 4]:

$$j = \frac{3}{2} \cdot \frac{\left(p_i / p_0\right)^2 - 1}{\left(p_i / p_0\right)^3 - 1} \qquad \textbf{[F.2]}$$

where, p_i and p_o represent the column input and outlet pressures, respectively, t_m is the dead time, accounting for column characteristics, or essentially any volume other than that of the sample. The latter is usually determined by an “inert” hydrocarbon, usually methane, through the column.

Some researchers use air and record an air peak. The flow rate of the carrier gas (F), usually helium, the test temperature (T), and sample mass (m) are also provided for in this equation. V_N is the quantity from which all thermodynamic quantities can be determined. A common relationship between this volume and the Gibbs free energy of adsorption (ΔG in kJ/mol) is provided by the following relationship:

$$\Delta G = RT \ln(V_N) \quad \textbf{[F.3]}$$

In order to obtain the Lifshitz-van der Waals (LW) component of surface energy, nonpolar vapors need to be eluted through the column. Normal alkanes, from pentane (C_5H_{14}) up to decane ($C_{10}H_{22}$) are commonly used for this purpose. Each of the retention times obtained for these solutes is used to calculate the free energy utilizing equation (F.3). For the series of n-alkanes with progressive increase in molecular weight, plotting the free energies against some molecular descriptor of the solutes (e.g., molecular weight, partial pressure etc.) enables one to obtain a straight line. The slope of this line is associated with the LW component of the surface energy (γ^{LW}). For the theory adopted in this research, the LW component of the free energy (ΔG^{LW} in mJ/m^2 or ergs/m^2, both the same value) is expressed by the Barthelot geometric mean, which can be traced back to first principles based on the Lifshitz theory:

$$\Delta G^{LW} = 2\left(\gamma_l^{LW}\right)^{\frac{1}{2}}\left(\gamma_s^{LW}\right)^{\frac{1}{2}} \quad \textbf{[F.4]}$$

where, l and s traditionally represent liquid (solute in this case) and solid, respectively. This equation when expressed in kJ/mol is:

$$\Delta G^{LW} = aN_A 2\left(\gamma_l^{LW}\right)^{\frac{1}{2}}\left(\gamma_s^{LW}\right)^{\frac{1}{2}} \quad \textbf{[F.5]}$$

where, a is the cross-sectional area of the solute, and N_A is Avogardo's number (6.0221 x 10^{23} species per mol). Therefore, ΔG^{LW} can be plotted against $a\left(\gamma_l^{LW}\right)^{\frac{1}{2}}$. Figure F-2 was compiled from measurements made on amorphous silica (silica "gel") and illustrates this technique. The LW component of surface energy in mJ/m^2 is then given by:

$$\gamma_s^{LW} = \left(\frac{slope}{2N_A}\right)^2 \quad \textbf{[F.6]}$$

Elution of monopolar basic and monopolar acid solutes enable determining the acid and the base components of surface energy, respectively. When a polar molecule interacts with the surface, specific interactions (mainly due to acid-base interactions) and nonspecific interactions (mainly due to LW forces), take place simultaneously. It is therefore assumed that the LW and acid-base (AB) contributions to the total free energy are additive. Accordingly,

$$\Delta G = \Delta G^{LW} + \Delta G^{AB} \quad \textbf{(F.7)}$$

This separation is seen at a position above the alkane line where the molecular descriptor of the polar molecule corresponds to that of a hypothetical n-alkane as illustrated in Figure F-2.

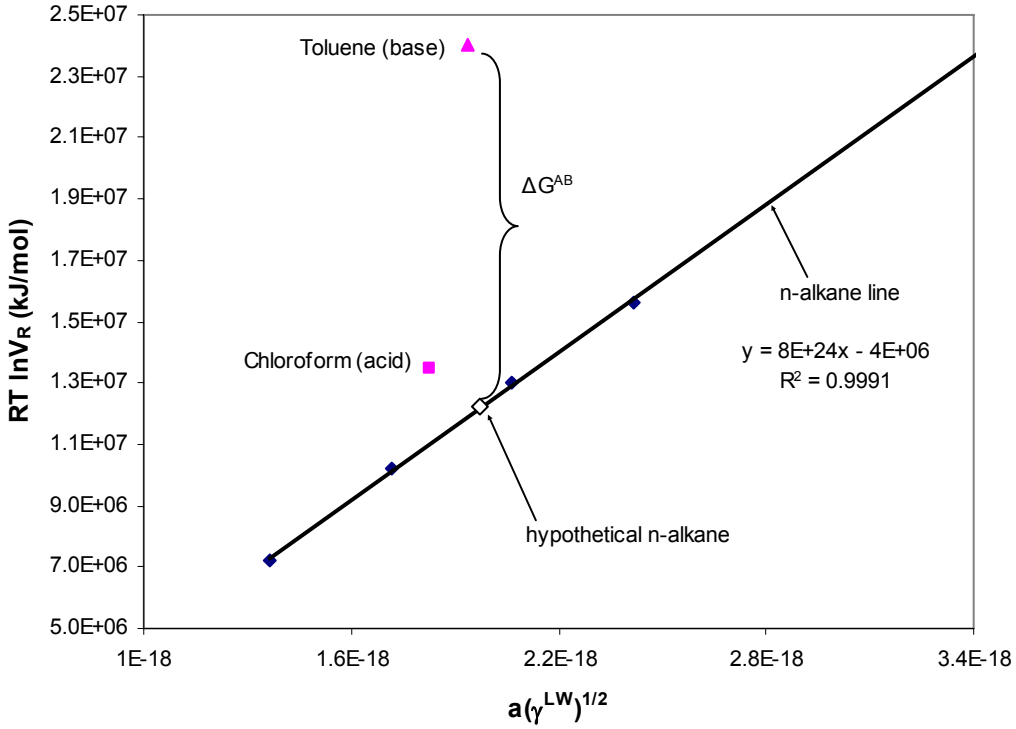

Figure F-2 Plot of Free Energies Obtained from n-Alkanes and Polar Solute (1).

Using the approach by van Oss, Good, and Chaudhury adopted in this research, the acid-base contribution of the free energy can be expressed in terms of the known surface energy components of the solute and that of the surface under consideration,

$$\Delta G^{AB} = aN_A 2\left[\left(\gamma_l^+\gamma_s^-\right)^{\frac{1}{2}} + \left(\gamma_l^-\gamma_s^+\right)^{\frac{1}{2}}\right] \qquad \textbf{[F.8]}$$

Therefore, if the acid (+ , electron acceptor) and base (- , electron donor) surface energy components of the two mono-polar solutes are known, and if either γ^+ or γ^- equals zero in each case, then the unknown surface energy components can be calculated alternately.

REFERENCES

1. Hefer, A., "Adhesion in Bitumen-Aggregate Systems and Quantification of the Effects of Water on the Adhesive Bond," Ph.D. Thesis in Civil Engineering, Texas A&M University, (2004) College Station, Texas.

2. Western Research Institute, "Fundamental Properties of Asphalts and Modified Asphalts Volume II Final Report New Methods," FHWA-RD-99-213, Western Research Institute, (2001), Laramie, WY.

3. Skoog, D.A. and Leary, J.J., "Principles of Instrument Analysis," 4th ed. Saunders College Publishing (1992), New York, New York.

4. Condor, J., and Young, C., "Physiochemical Measurement by Gas Chromatography," John Wiley and Sons, (1979), London, UK.

APPENDIX G

TEST METHOD TO USE AN ATOMIC FORCE MICROSCOPE TO MEASURE SURFACE PROPERTIES OF ASPHALT BINDERS

TEST METHOD TO USE AN ATOMIC FORCE MICROSCOPE TO MEASURE SURFACE PROPERTIES OF ASPHALT BINDERS

This section presents two procedures for preparing an asphalt thin-film sample and measuring the film thickness with a Filmetrics F-20 light-scattering device. The procedure to measure the dispersive component of surface energy of an asphalt thin film using two different instruments, a Digital Instruments MultiMode™ Scanning Probe Microscope and a Quesant Q-Scope 250 AFM is also described.

G.1 SAMPLE PREPARATION: SOLVENT-CASTING AND SOLUTION SPIN-CASTING OF ASPHALT THIN-FILMS

Measurement of asphalt thin-film sample surface energies is based on determining the "pull-off" force between a cantilever tip and a sample surface by atomic force microscopy. Asphalt sample thin films, measured to be 1000-4000 nm thick, were prepared by weighing 0.1155 ± 0.0003 g of each asphalt sample into individual 20 mL vials supplied with Teflon-lined caps. To each sample a 2.00 mL aliquot of a good solvent (toluene in the present case) for dissolving asphalt was added to each of the vials using a 2.500 ± 0.025 mL syringe. Solutions were capped under argon and allowed to sit overnight to ensure complete dissolution of the sample asphalt. Thin films were then prepared by placing a 12.5 mm diameter cover slide in a fume hood, placed on a level surface. Using a 0.05 ± 0.001 mL syringe, a 0.025 mL aliquot of the solution was deposited onto each cover slide, and the solvent was allowed to evaporate overnight in a nitrogen gas-purged bell jar.

Asphalt thin films (Figures G.1 and G.2) are often found to form a thick ring (position 1) around the outside of the film, with a thin layer (position 2) on the inside of the film that is slightly thicker at the center of the film. The height of the outer ring may vary for different asphalts based on the viscosity of the asphalt and the asphalt solution concentration initially prepared. A Filmetrics F-20 thin-film light-scattering device (Figure G.3), Filmetrics, Inc. F-20, was used to measure the thickness of each film measured at three to four different positions on the cover slide. Film thicknesses are determined by the F-20 by observing the interference pattern of the reflected light through the sample and substrate, reflected back into the measuring probe. Figure G.3 depicts one such measurement conducted for the asphalt AAD, solvent-cast onto a stand microscope glass slide. Input parameters required for these measurements include the initial guess of the film thickness (estimate), the estimated or known refractive index of the material thin film, and the composition of the substrate. Several measurements of the film thickness at each position and goodness of fit of the reflectance wave were recorded by varying the refractive indices around the initial estimated value. Each successive film-thickness measurement following the initial guess was then used as the next guess in the remaining measured values from the previous measurement. In this fashion, a sweep of the refractive indices, based on the highest value of goodness of fit, determined the actual film thickness to the great accuracy.

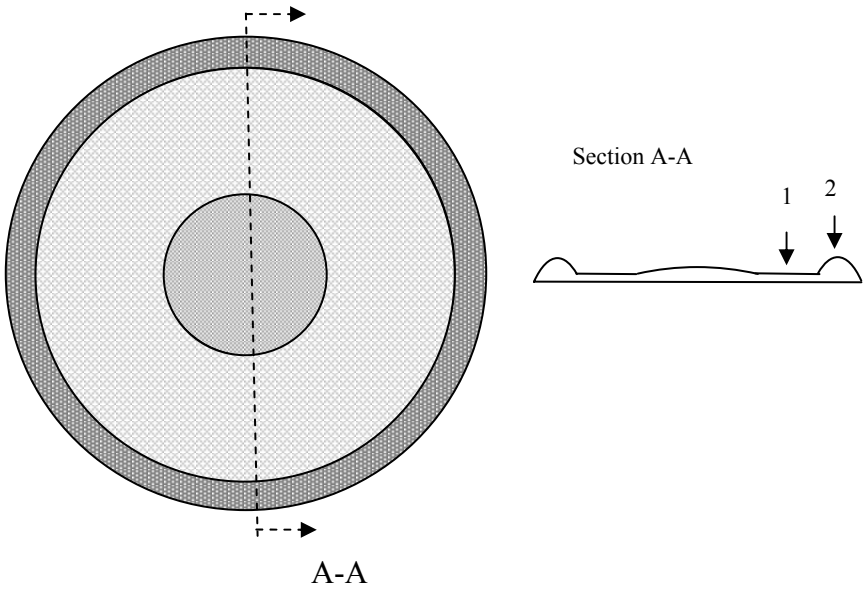

Figure G.1. Pictorial of an Asphalt Film Pattern and Film-Thickness Variation after Solvent Casting.

Figure G.2. Solvent Cast Procedure where a 0.025 mL Aliquot of a 0.0578 ± 0.0002 g (asphalt/mL) Toluene is Deposited onto a 12.5 mm Diameter Glass Disc Slide.

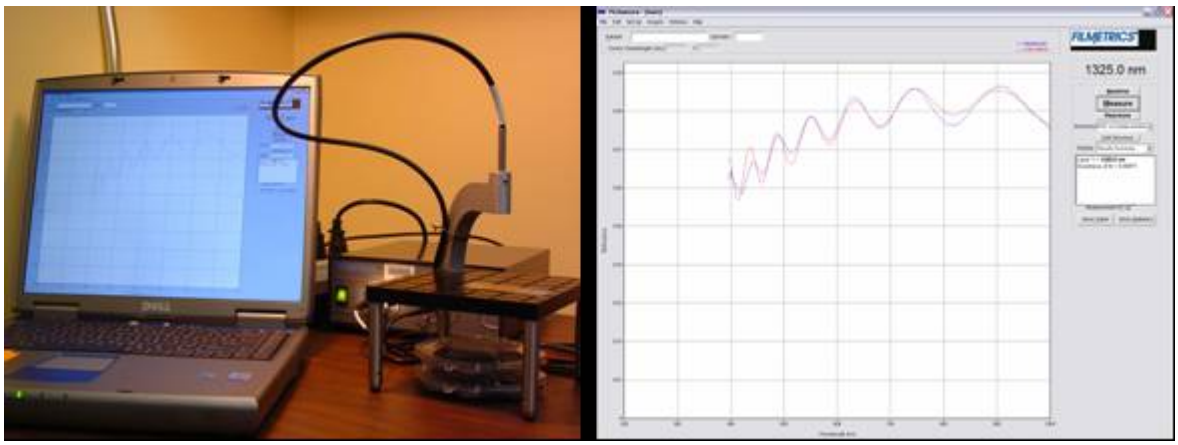

Figure G.3 An F-20 Filmetrics Thin-Film Analyzer (left), and Interference Spectrum of a Thin Film (right).

Sample thin films were also prepared by spin casting the asphalt, prepared as an asphalt-toluene solution; onto standard (soda lime) glass microscope slides (Figure G.4). Asphalt solutions were prepared as 0.4000 ± 0.0005 g of asphalt dissolved in 3.00 ± 0.01 mLl of HPLC-grade toluene, which were allowed to stand overnight in nitrogen gas-purged sealed vials prior to spin casting. Asphalt solutions were spin cast, using an ICL Roto-Film™ film maker (Figure G.4), on pre cleaned standard 75 mm x 25 mm x 1 mm soda lime glass slides, each spun at a rate of 600 rpm to develop the film. By slowly depositing approximately 2-3 μL of the solution from a 25 or 50 μL syringe onto a spinning slide, uniform films were obtained. The slides were allowed to dry overnight in a nitrogen gas-purged bell jar. Film thickness and refractive index measurements were conducted using an F-20 Thin-Film Measuring Device by placing the spin-cast plated films on the F-20 stage using the same method as described above. Film thicknesses were found to vary between 0.8 and 1.4 μm, with the exception of asphalt AAK-1 = 3.1 μm.

Figure G.4. An ICL Roto-Film Thin-film Casting Device (left), and a Series of Images (right) of the Progression of a Film as it Forms During the Spin Casting Process.

G.2 TEST PROCEDURE AND ANALYSIS

G.2.1 Force Curve Measurements Employing a DI-MultiMode AFM

Force-distance measurements of asphalt thin films were conducted under ambient conditions using a two-step process. In the first of these two steps, a bare glass cover slide and cantilever were loaded into the AFM instrument for calibration purposes. The Digital Instruments MultiMode™ scanning probe microscope was set up to operate in "contact" mode. Cantilevers having a spring constant, k = 14 N/m, and tip diameter, d = 10 μm diameter Novascan™ was placed into the cantilever holder then placed into the SPM laser photodiode head. Initial settings of the SPM were as follows; Z-scan start = 100 nm, Z-scan size = 1 μm, scan rate = 1.0 Hz, sensitivity = 0.0258 V/nm, set point = –0.4 V. The instrument was then engaged, first with a blank glass cover slide, then with a sample thin-film. The initial settings were varied appropriately to first obtain a calibration force curve (blank glass slide). Several force curves were then obtained for the calibration slide, as well as for each sample, where a new cantilever was calibrated and used each time with each new sample. Occasionally, the same cantilever was used to make measurements with one or two different samples and at two or three different spots of the same sample.

To evaluate force-distance measurements, raw detected-tip deflection data, which are stored by the instrument directly in binary format in least significant bits (LSB), are converted to distance values reported in units of nanometers. The first step of this conversion relies on the use of the following equation:

$$Value(V) = \frac{Value(LSB)}{32767} * Full\ volt\ range(V) \qquad \textbf{[G.1]}$$

Equation (G.1) is used to convert the detected-tip deflection data, reported in LSB units, to data reported in units of volts. The full volt range of measurements reported in volts, and the "Value" of these measurements reported in units of LSB both relate to the actual deflection of the cantilever during the process of attachment, then detachment at the sample-tip interface, as measured by the quad-photodiode detector. These values may be found in the parameter list that is stored along with all of the raw data available for a given measurement. These data values, reported in units of volts, are then converted to nanometers as:

$$Value\ (nm) = \frac{Value\ (V)}{Detector\ \ Sensitivit\ y(V\ /\ nm)} * Zstep \qquad \textbf{[G.2]}$$

where, the detector sensitivity data (an adjustable gain setting of the instrument which relates the detected deflection to the actual tip-deflection of the cantilever) is reported in units of volts/nm and the Z-step values are unitless. The deflection data are then multiplied by the Z step parameter to account for the computer's scaling of the data. This gives the data values of tip deflection (plotted on the y-axis of a force-distance curve) in nanometers. To obtain the Z-position values (plotted on the x-axis of a force-distance curve), the total Z-range of the cantilever was initially set to move and this range is divided by the number of data points produced by the measurement.

These last two equations, equations (G.1) and (G.2) are used to calibrate the tip deflection data by converting the Value data, in LSB units, to Z-distance values reported in units of nanometers. From the Z-distance data, two points are chosen to define a vertical displacement, D, the pull-off distance, used to calculate the work of adhesion. The first point of interst, labeled "Value," is for convenience. This "Value" point corresponds the minimum point on the retraction curve just before pull-off. The second data point, V_∞, is the deflection value after pull-off; this point corresponds to the straight line to the right of the pull-off region, at which point the tip is no longer in contact with the surface. The vertical distance, *D*, reported in nanometers is then determined using the two tip-deflection data points just described as follows:

$$D = Value - V_\infty \qquad \textbf{[G.3]}$$

The work of adhesion, W_{adh}, is then determined using the spring constant, *k*, corresponding to the cantilever used; the vertical distance, D, between the minimum of the retraction curve and the horizontal line of data after the minimum point; and the radius, *R*, of the cantilever tip (Figure G-5) as follows:

$$\gamma = \frac{1}{2} W_{adh}\ (dyne\ /\ cm) = \frac{D\ (nm) * k\ (nN\ /\ nm)}{4\pi R\ (\mu m)} \qquad \textbf{[G.4]}$$

In the present study the software package; SPIP, "Scanning Probe Image Processor" for MS Windows 98/NT/2K/Me/XP, (version 3.2.11.0, by Image Metrology A/S, Sep. 3 2004, All

Rights Reserved, Demonstration license) was used to automatically derive and display force-distance data measured using the DI MultiMode AFM microscope, reported in Z-position (nm), x-axis, versus force (nN), y-axis.

The applied load force, the jump-to-contact force, and the pull-off force were each extracted from force curve measurements (Figure G-5), such that adhesion was characterized in terms of the force required to detach the glass micro-bead cantilever tip from the asphalt thin-film surface after the application of various levels of external loading were applied to the sample at different rates, sensitivities, and setpoint values. Each sample test only required about 20-30 minutes, and some times much less time, to acquire a complete data set.

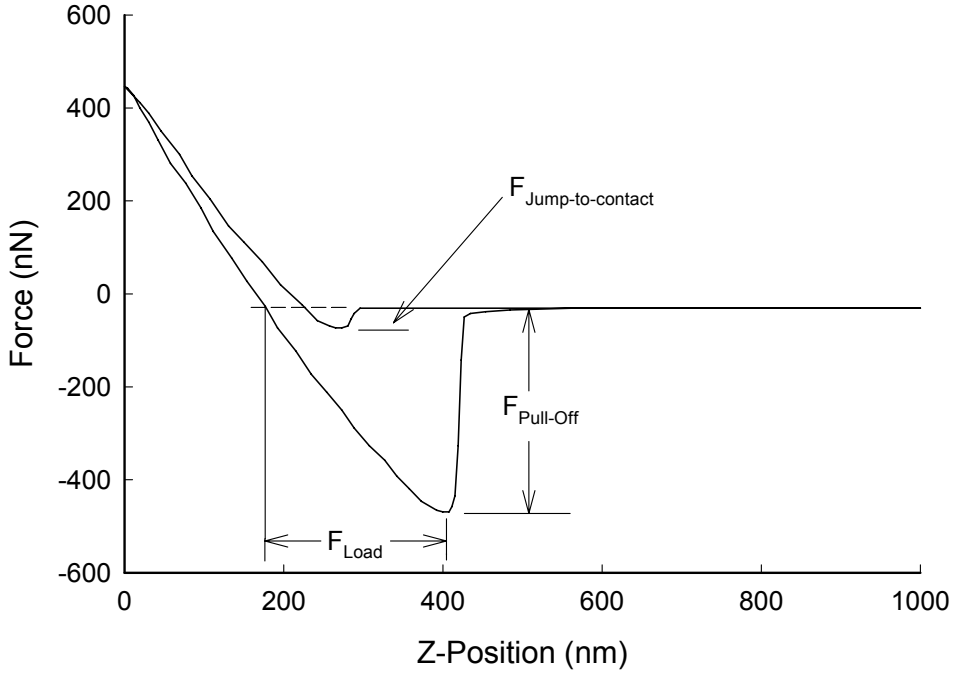

Figure G.5. Force Curve Plot Depicting Applied Loading Force, F_{Load}, Jump-to-Contact Force, $F_{Jump\text{-}to\text{-}contact}$, and Pull-Off-Force, $F_{pull\text{-}off}$, the Minimum Point on the Retraction Curve, Just Before Pull-Off.

Individual data points of load and pull-off force were derived for each measurement using SPIP, where the cantilever spring constant was used as an input parameter to automatically calculate and display pull-off force in force-distance curves. In turn, load force data for each measurement was derived from the force versus Z-position plots by measuring the Z-distance (actual distance the cantilever moves during the attachment and pull-off process), then multiplying this value by the spring constant.

Plots of load versus surface energy (pull-off force/$4\pi R$, R = 5 μm) were constructed for each sample set, along with the glass slide values for a given cantilever. Glass slide Load versus surface energy data were extrapolated forward to a load value corresponding to 72 ergs/cm^2 (capillary water interaction between tip and slide), and asphalt sample load versus surface energy data were subsequently extrapolated backward to this same minimum load. The surface energy

corresponding to this minimum load is reported as the surface energy of the sample. In a few specific cases, where the sample-extrapolated surface energy extended past the glass slide minimum load at 72 ergs/cm^2, the lowest observed surface energy (or average of points) was taken as the desired value. Figure G.6 illustrates a load versus surface energy plot for one sample tested.

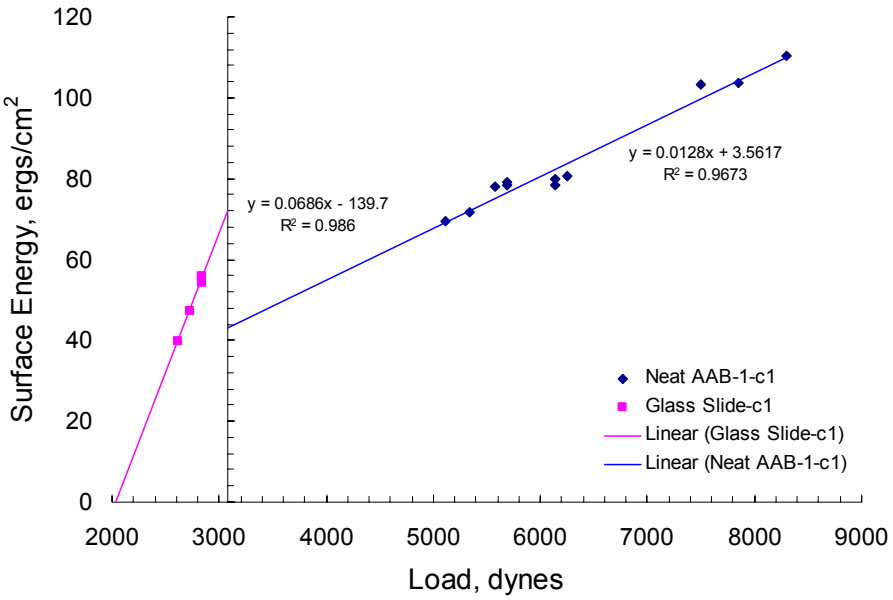

Figure G.6. Load versus Surface Energy Plot for Cantilever #1: Glass Slide Calibration and Neat AAB-1.

G.2.2 Force Curve Measurements Employing a Quesant Q-Scope 250 AFM

Surface energies of the eight SHRP asphalts, measured by AFM, are derived based on contact mechanics models referred to as the Johnson-Kendell-Roberts (JKR) contact theory and the DMT (Derjaguin-Muller-Toporov) theory. Force curves were measured using a Quesant Q-Scope 250 AFM, operated such that surface energy could be measured as a function of contact load at a slow sampling frequency (rate at which the cantilever approaches the sample surface), where a minimum in the contact load corresponds to the equilibrium surface energy at a given temperature. To accomplish this, the cantilever's distance of travel is decreased or increased to advance the tip upward or downward, respectively, relative to the surface, in order to decrease or increase the contact load. A force versus displacement "force curve" is then recorded for each step-up or step-down series of measurements, constituting a measure of the mechanical advancing and receding surface energies, in addition to the equilibrium surface energy. It has been observed that by employing cantilevers with 5 μm diameter glass bead tips attached to the end of the cantilever (Novascan Technologies, Inc.) that repeatable force curves for these types of materials may be obtained.

Values of the work of adhesion, W_{adh}, are calculated from force-curve data based on the nominal spring constant of the cantilever suggested by the manufacturer, k; the vertical distance,

D, measured from the minimum point of the retraction curve to the horizontal line after the minimum point (or pull-off distance or force); and the radius of the cantilever tip, *R*:

$$\gamma = \frac{1}{2} W_{adh} = \frac{kD}{4\pi R} \qquad \textbf{[G.5]}$$

Several measurements of the pull-off distance (which is automatically converted to force values by entering the force constant into the AFM software) were made at different locations on the sample films as a function of stepping up or down, in series, the cantilever for a predetermined setpoint force. The values of surface energy (derived from pull-off force data) were then reported as the value at load = 0 nN when the data were plotted in terms of surface energy versus load force.

G.2.3 Error Analysis

The mean differential in surface energy based on equation [G.5] may be evaluated as

$$\gamma \pm d\gamma = \frac{Dk}{4\pi R} \pm \sqrt{\sum_i \left(\frac{\partial}{\partial x_i} (\gamma(x_i)) dx_i \right)^2} \qquad \textbf{[G.6]}$$

where, the variation in surface energy is derived as

$$\begin{aligned} d\gamma &= \sqrt{\sum_i \left(\frac{\partial}{\partial x_i} (\gamma(x_i)) dx_i \right)^2} \\ &= \frac{1}{4\pi R} \sqrt{(kdD)^2 + (Ddk)^2 + \left(\frac{-DkdR}{R} \right)^2} \end{aligned} \qquad \textbf{[G.7]}$$

In general, the variance in the measured value of D is assumed to be less than 1%, i.e., dD = 0.01D, if the instrument is calibrated properly, and the variance in the tip radius is assumed to be 5% or less, i.e., dR = 0.05R, but the variance in the spring constant may be as high as 20%. Given these values, force distance measurements made over small distances; small D (20-60 nm) with the same cantilever for several samples, with consistent cleaning of the tip in between measurements should give surface energy values within $\pm d\gamma = 3 - 6$ ergs/cm^2.

REFERENCE

1. Pauli, A.T., et al., *Surface Energy Studies of Asphalts by AFM.* American Chemical Society Division of Fuel Chemistry Preprints, (2003) Volume 48 No.1, pp. 14-18.

APPENDIX H

TEST METHOD TO USE A MICRO CALORIMETER TO MEASURE SURFACE PROPERTIES OF AGGREGATES

TEST METHOD TO USE A MICRO CALORIMETER TO MEASURE SURFACE PROPERTIES OF AGGREGATES

A micro calorimeter was used in this research to measure the heat of immersion of aggregates in different probe liquids and determine their surface energy components. Section 3.2.7 of the main report presents an overview of this technique along with results for four different aggregate types and an analysis and discussion of the results. This appendix presents details of the sample preparation procedure, test method, and analysis methods to measure surface energy components of aggregates using the micro calorimeter following Bhasin *(1)*.

H.1 MATERIALS

Samples of aggregates passing the #100 sieve and retained on the #200 sieve were obtained from the source. The aggregates were thoroughly washed using deionized or distilled water in the #200 sieve followed by a final rinse using HPLC-grade water. The cleaned aggregate sample was dried for 12 to 16 hours in an oven at 150°C. The aggregate was allowed to cool to room temperature and stored in clean glass air-tight containers. A small portion of the dried aggregate was retained for measurement of specific surface area. In this research the specific surface area of the aggregate was measured using the USD using BET equations. However, in practice a standard nitrogen adsorption method with BET equations can also be used.

H.2 SAMPLE PREPARATION

The aggregate samples were preconditioned in a 16 mL glass vial. These vials also served as the reaction cells when the sample was placed in the micro calorimeter. The vials have open top polypropylene caps with a polytetrafluoroethylene (Teflon) PTFE-silicone septa to provide an air-tight seal. Mass of the empty vial and septa was recorded, and approximately 8 g of the aggregate sample was added to the vial and sealed. A syringe with a 27-gauge needle was passed through the septa. Vacuum was drawn in the vial by connecting the syringe to a vacuum pump. The vial was placed in an aluminum block over a heater that was set to maintain the sample temperature at 150°C during the degassing process. The aggregate sample in the vial was subjected to this temperature and a vacuum of less than 300 millitors for 4 hours.

After degassing, the needle connected to the vacuum pump was swiftly withdrawn from the vial. The PTFE-silicone seal helps retain the sample in the vial under vacuum even after the needle is withdrawn. The sample vial was allowed to cool to the test temperature, and mass of the dry aggregate was obtained as the difference of the mass of the vial + sample after degassing and the empty vial before degassing. An empty vial was preconditioned in exactly the same manner as the vial with the sample to serve as the reference.

Each pair of sample and reference cell was tested together with the micro calorimeter. A degassing station was developed that allowed preparation of up to two pairs of samples for testing. All samples were tested within 24 hours of degassing.

H.3 TEST PROCEDURE

An isothermal differential micro calorimeter was used in this study to measure the heats of immersion of aggregate samples with different probe liquids. The micro calorimeter was manufactured by OmniCal Inc., of USA. The instrument was accompanied by a proprietary data acquisition and analysis package to measure heat flow during the test and compute the total heat of immersion.

The vial with the sample was placed in the reaction cell and the empty vial was placed in the reference cell. Four syringes of 2 mL capacity were each filled with the probe liquid. Two of these syringes were positioned on top of the reaction vial and two on top of the reference vial. Accompanying software with the instrument recorded the differential heat flow between the two cells with an accuracy of 10 μW.

After thermal equilibrium was reached, which took about 30 to 40 minutes from the time the vials were placed in the calorimeter, the syringes were pushed simultaneously through the PTFE-silicone seal and the probe liquid was injected into both cells. Since differential heat between the two cells is recorded, heat generated due to the process of piercing the seal and injection is compensated during measurement. The net heat measured in the cell is due to,

(i) enthalpy of immersion in the reaction cell, and
(ii) difference in heat of vaporization of the probe liquid on account of the difference in free volume of the reaction and reference cell.

After injecting the probe liquids, the two cells were allowed to return to thermal equilibrium with each other. This process took about 30 to 45 minutes and was identified by monitoring the heat flow between the two cells. The test was stopped at this point and the data were saved and analyzed using the accompanying software. At least two replicates were tested for each aggregate-probe liquid pair. The three probe vapors used to determine the three surface energy components of the aggregates were heptane, benzene, and chloroform. These chemicals were all HPLC-grade procured from Sigma-Aldrich, USA. In addition to these three probe vapors, heat of immersion with water was also measured. This provided a relative measure of the affinity of different aggregates to water.

H.4 ANALYSIS OF RESULTS

Heat flow between the sample and reference cell was recorded using software that accompanied the micro calorimeter. Under ideal conditions, the heat flow between the reference and reaction cell must be zero. However, because of the differences in the specific heats of the sample and reaction cell and other environmental conditions, a small amount of heat flow between the two cells is possible. When the two cells are in thermal equilibrium, this heat flow is constant and can be easily identified by a horizontal line on the chart that records heat flow over time. Figure H.1 illustrates a typical example of the heat flow from the reaction to the reference cell during an immersion experiment. The figure shows the initial and final datum of equilibrium and the point at which heat flow increases due to the injection of the probe liquid. The area under this curve between the two equilibrium points is integrated to obtain the total heat of immersion or enthalpy of immersion of the aggregate in the probe liquid. The software accompanying the instrument allows the user to select pre-and post-test equilibrium points and provides the total heat of immersion by computing the area under the curve between the two points.

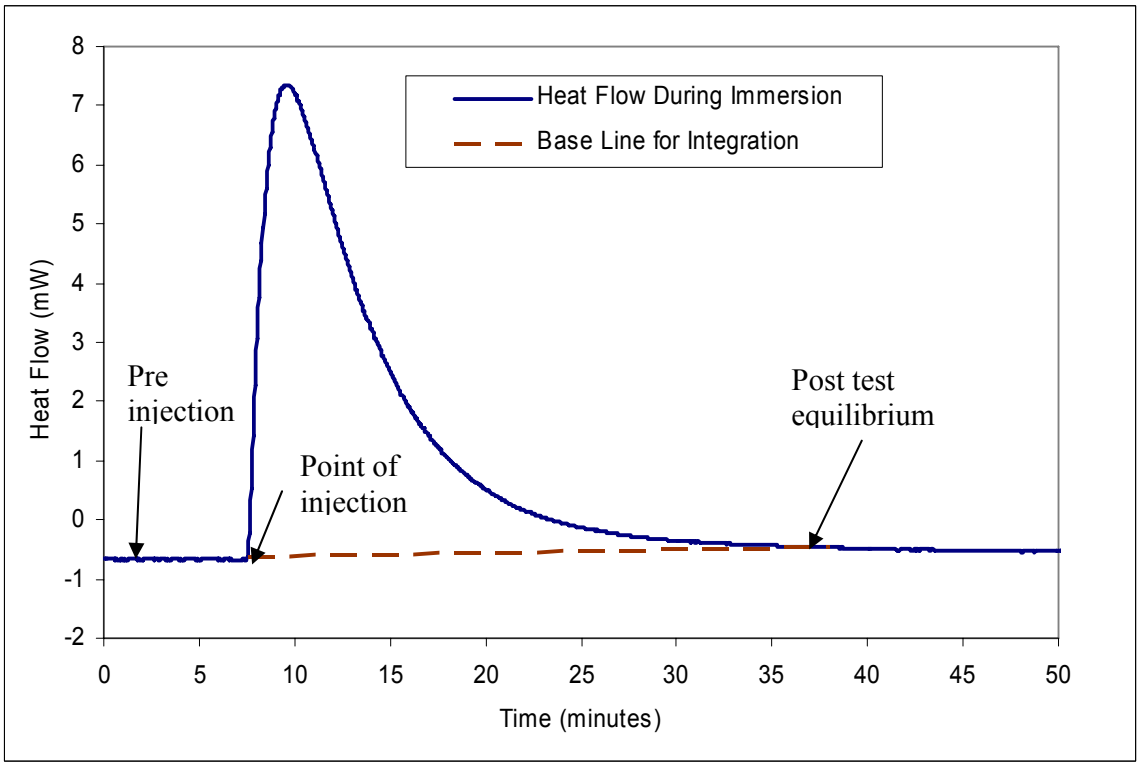

Figure H-1. Typical Heat Flow Curve Recorded with the Micro Calorimeter.

The net enthalpy of immersion, ΔH_{imm}^{net}, in ergs/cm^2 was calculated from the measured enthalpy of immersion, $\Delta H_{imm}^{measured}$, in millijoules, using the following equation:

$$\Delta H_{imm}^{net} = \frac{\left(\Delta H_{imm}^{measured} - H_{vap}^{correction}\right)}{M\ A} \qquad \textbf{[H.1]}$$

where, M is the dry mass of the aggregate sample in grams, A is the specific surface area of the aggregate in m^2/g, and $H_{vap}^{correction}$ is the correction for the differences in heat of vaporization between the reaction and the reference cell in millijoules. The necessity and rationale for the last correction term is as follows. The free volume under vacuum in the reaction cell and the reference cell are different due to presence of the sample in the former. As a result, when probe liquids are injected in both cells a small fraction of the probe liquid vaporizes instantly to achieve saturation, absorbing heat in the process. Since the free volume in the sample cell is less, the amount of probe that vaporizes and hence the heat of vaporization will also be less compared to the reference cell.

The relationship between the measured enthalpy of immersion and surface energy components of the probe liquid and solid is as follows:

$$\Delta H_{imm}^{net} - T\Delta S_{imm} = \gamma_L - 2\sqrt{\gamma_A^{LW}\gamma_L^{LW}} - 2\sqrt{\gamma_A^{+}\gamma_L^{-}} - 2\sqrt{\gamma_A^{-}\gamma_L^{+}} \qquad \textbf{[H.2]}$$

where, ΔS_{imm} is the entropy of immersion, T is the test temperature, γ_L is the total surface energy of the probe liquid, the superscripts LW, +, and – represent the Lifshitz-van der Waals, acid, and base components of surface energy, respectively, and the subscripts L and A represent

the probe liquid and aggregate, respectively. Douillard et al. [2] determined the heats of immersion and adsorption isotherms for various pure minerals with different probe liquids. Based on the comparisons of adsorption isotherms and heats of immersion, they demonstrate that the entropy term, $T\Delta S_{imm}$, in equation (H.2) can be approximated as 50% in magnitude of the enthalpy term ΔH_{imm} at about 25°C. Based on this assumption, equation (H.2) is reduced to the following form for tests at 25°C:

$$0.5\Delta H_{imm}^{net} = \gamma_L - 2\sqrt{\gamma_A^{LW}\gamma_L^{LW}} - 2\sqrt{\gamma_A^{+}\gamma_L^{-}} - 2\sqrt{\gamma_A^{-}\gamma_L^{+}} \quad \textbf{[H.3]}$$

Heats of immersion from three different probe liquids were used with equation (H.3) to generate a set of three equations that were solved to obtain the three unknown surface energy components of the aggregates. Equation (H.3) is an approximation of equation (H.2) at 25°C. Research is under way to develop a simple methodology to account for the entropy effect and eliminate the need for using an approximation.

REFERENCES

1. Bhasin, A., "Development of Methods to Quantify Bitumen-Aggregate Adhesion and Loss of Adhesion Due to Water," Ph.D. Dissertation in Civil Engineering. (2006), Texas A&M University, College Station, Texas.

2. Douillard, J.M., Elwafir, M., and Partyka, S., "Surface Interactions between Silica Particles and Water and Organic Solvents," *Journal of Colloid and Interface Science*, (1994) Volume 164, pp. 38-244.

APPENDIX I

MECHANICAL TESTS TO EVALUATE LABORATORY PERFORMANCE OF ASPHALT MIXES AND MATERIAL PROPERTIES OF ASPHALT MASTICS

MECHANICAL TESTS TO EVALUATE LABORATORY PERFORMANCE OF ASPHALT MIXES AND MATERIAL PROPERTIES OF ASPHALT MASTICS

The objective of Task 5 was to provide limited validation of the relationship between laboratory performance of asphalt mixes and the surface energy components of its constituent materials. Two types of mechanical tests were conducted on selected asphalt mixes. The first type of tests were conducted on whole asphalt mixes in dry and moisture conditioned state. The second type of tests were conducted on asphalt mastic samples (asphalt binder + aggregates passing a #16 sieve) using a dynamic mechanical analyzer (DMA). This appendix presents details of these tests that were conducted to accomplish the objectives of Task 5. Section 2.6 of this report presents a summary of the results from these tests.

I.1 MECHANICAL TESTS ON ASPHALT MIXES

I.1.1 Mix Designs and Sample Preparation

Surface energy measurements from Task 4 were used to calculate the energy parameters related to performance of asphalt mixes. This information was used to select twelve candidate asphalt-aggregate combinations that represented various degrees of resistance to moisture damage and fatigue cracking. These mixes use four asphalt binders (AAB, ABD, AAD, and AAE) and three aggregates (RA, RK, and RL).

Figure I.1 shows the aggregate gradation used for all twelve mix designs. The optimum asphalt content was determined using the Superpave design method with a Superpave Gyratory Compactor (SGC) at 125 design gyrations and 4% air voids. The test samples were prepared using the SGC in a 101 mm diameter mold. Two of the mechanical tests included in this study were in the direct tension mode. Based on the literature, the minimum recommended aspect ratio (diameter/height) for samples subjected to direct tension tests is 1:2 *(1)*. Also, the minimum diameter of the cylindrical sample must be at least four times the size of the largest aggregate in the mix. Therefore a test specimen with 75 mm diameter and 150 mm height was rationalized to be appropriate. The finished test specimen was obtained by coring and sawing a 100 mm diameter and 175 mm high sample compacted using the SGC. The number of gyrations of the SGC was adjusted to achieve a target air void of 7 ± 0.5% for the finished sample (after coring and sawing). Samples with air voids that did not fall in this range were discarded. Extreme care was exercised during sawing and coring operations to ensure proper sample geometry.

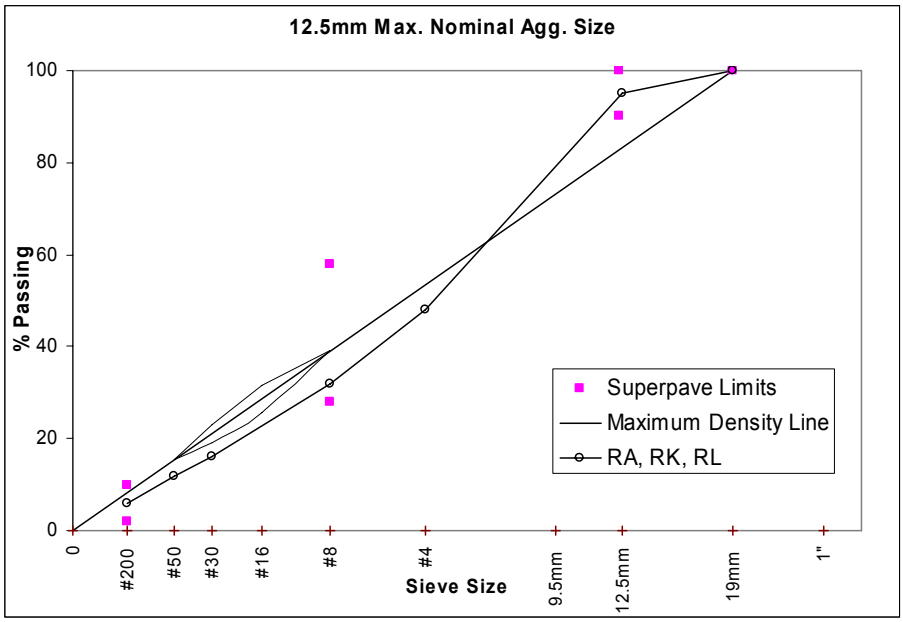

Figure I.1. Aggregate Gradation for All Mixes.

I.1.2 Mechanical Tests and Parameters

Three types of mechanical tests were conducted on the dry and moisture conditioned asphalt mix samples. One of these tests was in compression mode and the other two were in direct tension mode. Direct tension mode was selected since the effect of stripping would be most evident in this mode. At least two replicates of both dry and moisture conditioned samples were tested for each of the twelve mix designs. All mechanical tests were conducted at a temperature of about 25 ± 1°C. Aluminum plates with fixtures to connect them to the universal testing machine were glued to both ends of the sample using epoxy glue to enable testing in direct tension mode. Each sample was attached with three linear variable displacement transformers (LVDTs) with a maximum range of 1.8 mm to record permanent and resilient deformation. The LVDTs were mounted at a distance of 25 mm from either face of the sample with a total gauge length of 100 mm. Figure I-2 shows the setup for conducting the tension tests with a sample that failed in tension after a dynamic creep test in tension.

The first mechanical test was the dynamic modulus test in compression. This test was conducted using a haversine loading with a frequency of 10 Hz. The stress level was kept to a minimum to avoid any permanent sample damage. Each sample was tested for 200 load repetitions. The samples were then allowed to rest for a minimum of 30 minutes prior to further testing. The parameter of interest from this test is the ratio of the dynamic modulus of the moisture conditioned sample to the dry sample.

The second type of test was the dynamic modulus test in tension. The sample was connected to the loading arm from the top and gripped using a mechanical chuck at the bottom via the aluminum end plates. Proper alignment of the sample was ensured during this process. The loading arm was continuously adjusted during the process of fixing the sample to ensure that the sample was not prestressed. The dynamic modulus in tension was also conducted using a haversine loading with a frequency of 10 Hz and 200 load repetitions. The parameter of interest from this test is the ratio of the dynamic modulus in tension of the moisture conditioned sample to the dry sample.

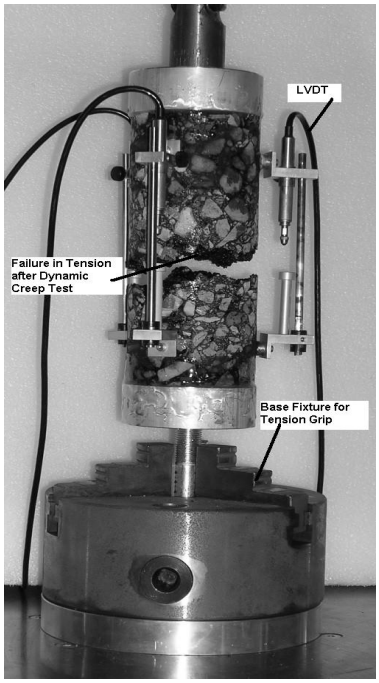

Figure I.2. Test Setup and Sample Failure for Dynamic Creep Test (Tension).

The third test immediately followed the second test. In this test the dynamic haversine loading was continuously applied at a high stress level until the sample failed in tension. In most cases failure of the sample was from the middle. Resilient strain and permanent deformation of the sample was continuously recorded during the test. Figures I-3 and I-4 show typical loading and response from the dynamic creep test in tension. The parameter of interest from this test is the ratio of the fatigue life of the moisture conditioned sample to the dry sample. Figure I-4 shows the reduction in modulus of the mix with increasing number of load cycles normalized by the modulus of the first load cycle.

From the dynamic creep test, the parameters of interest were the accumulated permanent strain in the sample as well as the reduction in modulus of the sample with increasing number of load cycles. In order to collect data for these parameters, LVDTs with smaller range and greater sensitivity were used. However, due to practical limitations, these LVDTs could not record data until complete sample failure for all samples. Therefore for this research, the fatigue life of the mix is defined as the number of load cycles required to attain 1% permanent strain.

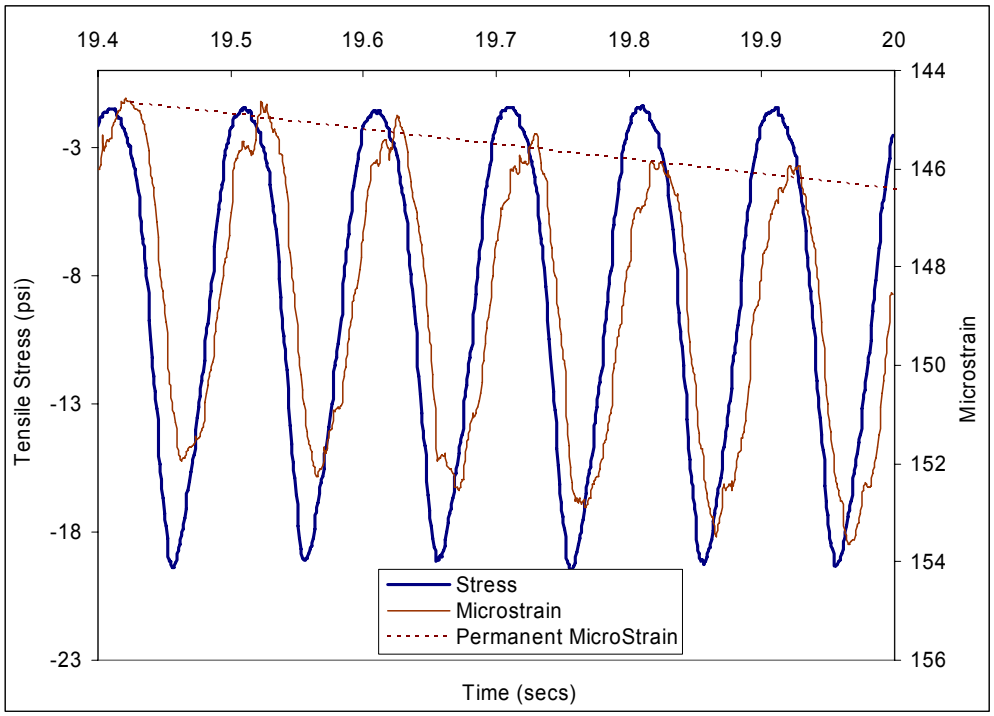

Figure I.3. Typical Loading and Average Response from Dynamic Creep Test without Rest Period.

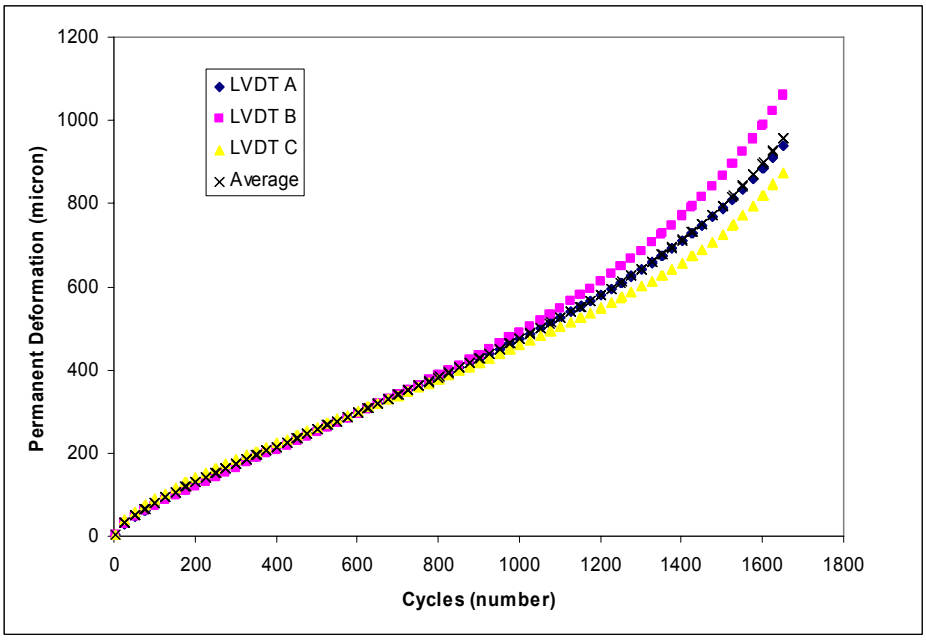

Figure I.4. Curve Showing Accumulated Permanent Strain Versus Load Cycles.

I.1.3 Moisture Conditioning

Samples were moisture conditioned by submerging them in deionized water under vacuum to achieve a saturation level between 70 and 80%. This took about 2 minutes in most cases. After achieving target saturation, the samples were kept submerged under deionized water for 24 hours at 50°C. The samples were then removed from the water and air dried for 24 hours prior to testing. The samples retained a saturation level between 25 and 30% at the time of testing. Testing of the moisture conditioned samples was completed within 24 to 36 hours after removal from the water. Figure I-5 shows the failure plane of a moisture conditioned sample after a dynamic creep test in tension.

Figure I.5. Failure Plane of Moisture Conditioned Sample after Dynamic Creep Test.

I.2 MECHANICAL TESTS ON ASPHALT MASTICS

I.2.1 Mix Designs and Sample Preparation

The cylindrical specimens for testing with the dynamic mechanical analyzer (DMA) were designed and prepared according to the procedure following Zollinger *(2)*. The asphalt mastic comprised the asphalt binder mixed with fine aggregate (passing sieve #16). Figure I.-6 illustrates the gradation of fine aggregates for all mastic samples.

Preparation of specimens for testing with the DMA is very similar to the procedure followed for preparing asphalt mixes. The percentage of asphalt binder was set to 8.9% by weight of the mix based on a procedure by Kim et al., *(13)*. The aggregates and the binder were mixed at the mixing and compaction temperature using a mechanical mixer. The loose mixture was placed in a convection oven for 2 hours at the compaction temperature for short-term aging. After aging, the mix was compacted using a 152 mm diameter mold in the SGC to a height of 75 mm and target air void content of 13%.

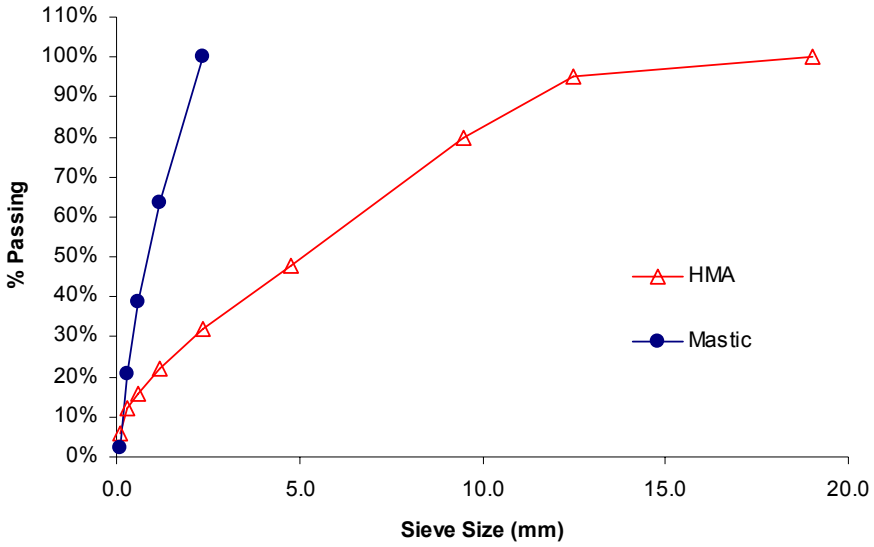

Figure I.6. Aggregate Gradation for Asphalt Mastics.

The samples were allowed to cool to room temperature. Each side of the specimen (top and bottom) was trimmed to obtain a sample height of 50 mm. Approximately 30 specimens of 12 mm were obtained by coring a 152 mm compacted sample (Figure I-7). The 12 mm mastic samples were labeled according to their position in the main sample (Figure I-8) in order to ensure that there was no excessive variability in air voids due to their location. The maximum specific gravity of the loose mix, bulk specific gravity of the samples, and the actual air void content of each 12 mm sample was determined in a manner similar to the asphalt mixes. The air void content of the samples was ensured to be within 13 ± 1 percent.

Figure I.7. SGC Compacted Sample and 12 mm Sample for DMA Testing.

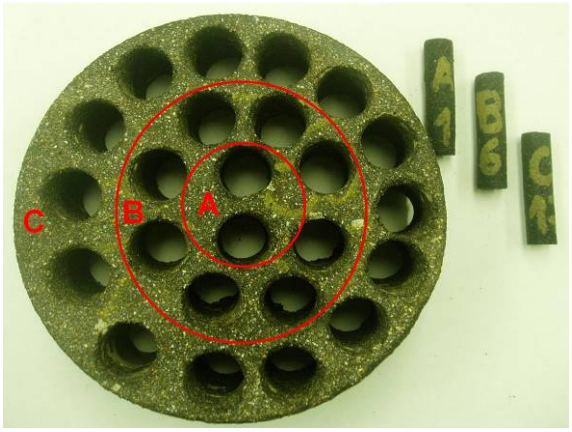

Figure I.8. The Three Regions in the 152 mm Sample.

I.2.2 Testing with the DMA

The DMA test is conducted by fixing the lower end of the mastic sample and applying a strain or stress-controlled torque at the top end of the sample and measuring the stress or strain response. Figure I-9 illustrates the DMA test setup. When used with cyclic load tests, the shear modulus, G*, and phase angle, ϕ, at different load cycles are recorded by the software accompanying the DMA device. Three types of tests were conducted with the DMA to obtain the necessary inputs to predict crack growth characteristics of the mastic as described in section 2.4.2 of this report. The first type of test was a relaxation test conducted by applying a strain of 0.0065 percent on the sample for a duration of 5 minutes. This is required to obtain the relaxation parameters, *m* and $E_{1,}$ which are described in the main report. The second type of test was a strain-controlled cyclic load test conducted by applying a small strain of 0.0065 percent in a sinusoidal wave form at 10 Hz frequency for approximately 500 cycles to obtain the undamaged reference modulus and phase angle of the material. This test was followed by the third test, which was conducted by applying a larger strain of 0.2 percent in a sinusoidal wave form at 10 Hz frequency until the sample failed. Results from this test were combined with the results from the previous test for each sample to obtain the dissipated pseudo-strain energy and fatigue life of the mastic.

The fatigue life of the mastic sample was measured using the following parameter:

$$N\frac{G_N^*}{G_1^*} \qquad \textbf{[I.1]}$$

where, N is the number of load cycles, G_N^* is the shear modulus at the N^{th} load cycle, and G_1^* is the shear modulus at the first load cycle. Figure I.10 illustrates a typical response curve that is obtained from the data with the DMA test.

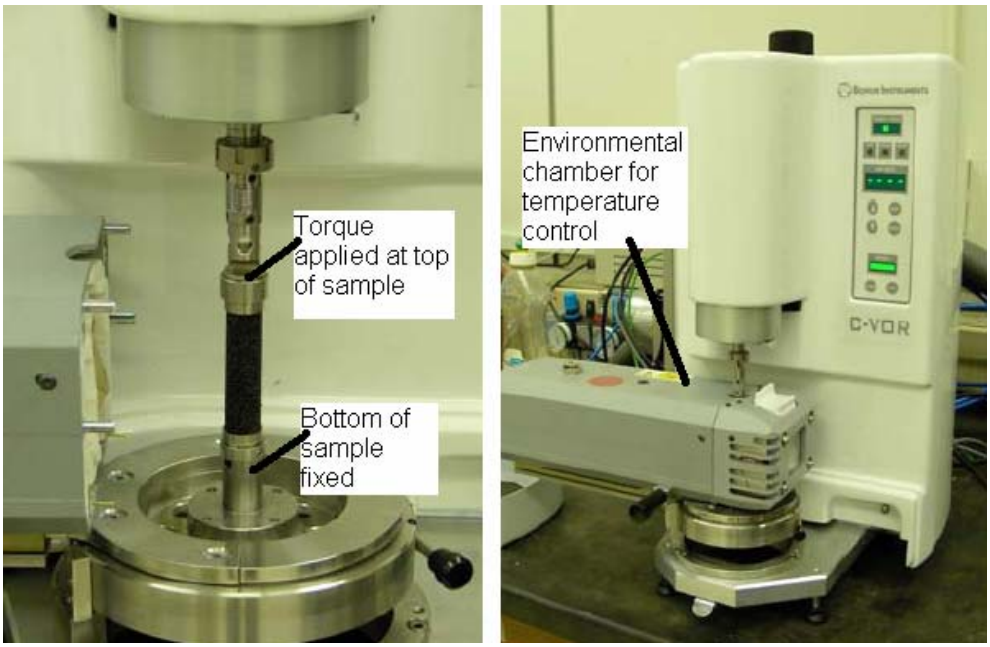

Figure I.9. Sample and Test Setup for DMA.

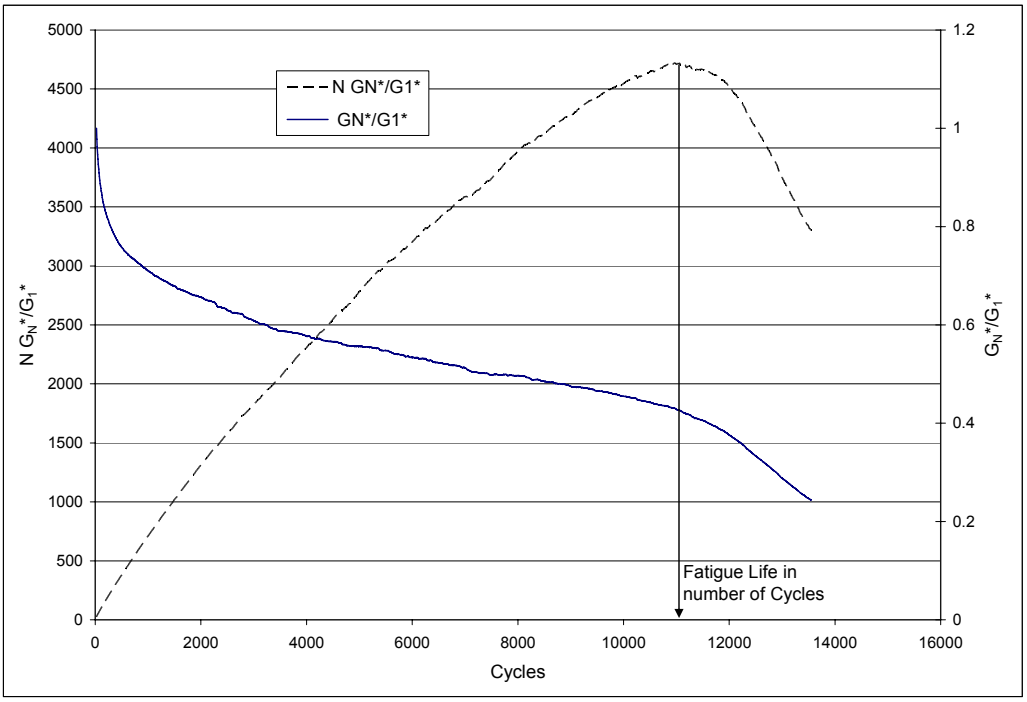

Figure I.10. Typical Response Curve from DMA Test.

REFERENCES

1. Chehab, G.R., O'Quinn, E., and Kim, Y.R., "Specimen Geometry Study for Direct Tension Test Based on Mechanical Tests and Air Void Variation in Asphalt Concrete

Specimens Compacted by SGC," *Transportation Research Record*, Transportation Research Board, Volume 1723, (2000), pp. 125-132.

2. Zollinger, C., "Application of Surface Energy Measurements to Evaluate Moisture Susceptibility of Asphalt and Aggregates," Ph.D. Thesis in Civil Engineering, Texas A&M University, (2005), College Station, Texas.

3. Kim, Y.R., Little, D.N., and Lytton, R.L., "Fatigue and Healing Characterization of Asphalt Mixes," *Journal of Materials in Civil Engineering*, American Society of Civil Engineering, Volume 15, (2003), pp. 75-83.

APPENDIX J

MINERALOGICAL INVESTIGATION OF AGGREGATES

MINERALOGICAL INVESTIGATION OF AGGREGATES

Four aggregates (RA, RK, RD, and RL) were analyzed using the Electron Microprobe (EM) Laboratory in the Department of Geology and Geophysics. The aggregate RG was not analyzed due to non availability of appropriate size of this aggregate to prepare thin sections at the time of testing. The EM laboratory is shown in Figure J.1. The laboratory comprises a Cameca SX50 fully automated four-spectrometer electron microprobe integrated with a Princeton Gamma-Tech (PGT) Imix energy-dispersive X-ray spectrometer system.

While energy-dispersive spectroscopy (EDS) is used for qualitative analyses, automated wavelength-dispersive spectroscopy (WDS) is used for quantitative elemental analysis of properly prepared polished samples at a spatial resolution of a few microns. WDS can be used to determine the concentrations of up to tens of chemical elements with an accuracy as high as ±1% of the amounts present. In addition to these capabilities, the microprobe can also obtain digital secondary and back-scattered electron images as well as elemental distribution maps at magnifications up to 5000X.

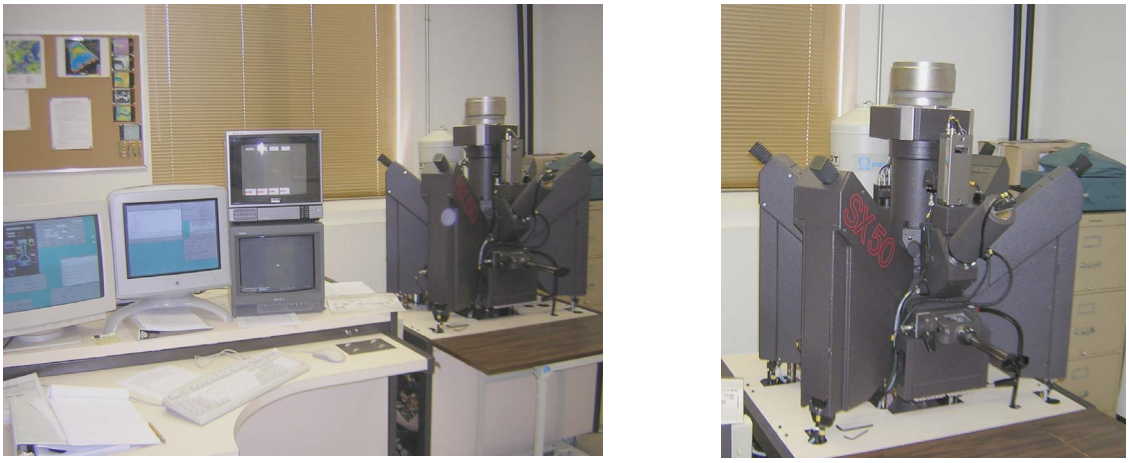

Figure J.1. Electron Microprobe Laboratory.

J.1 MATERIALS AND SAMPLE PREPARATION

In order to complement information available from the Material Reference Library (MRL) on the selected materials, used during the Strategic Highway Research Program (SHRP), specimens for microprobe analyses were selected by inspection with the help of an experienced geoscientist.

The specimens were cut with a diamond saw to obtain one flat side, which could then be glued onto glass slides for manufacturing of thin sections. The cut samples were further processed to thin sections of approximately 30 μm thick (required for optical microscopy) polished to a smoothness of 0.3 μm (required for electron microprobe analysis). Photos of the scanned thin sections are shown in Figure J.2.

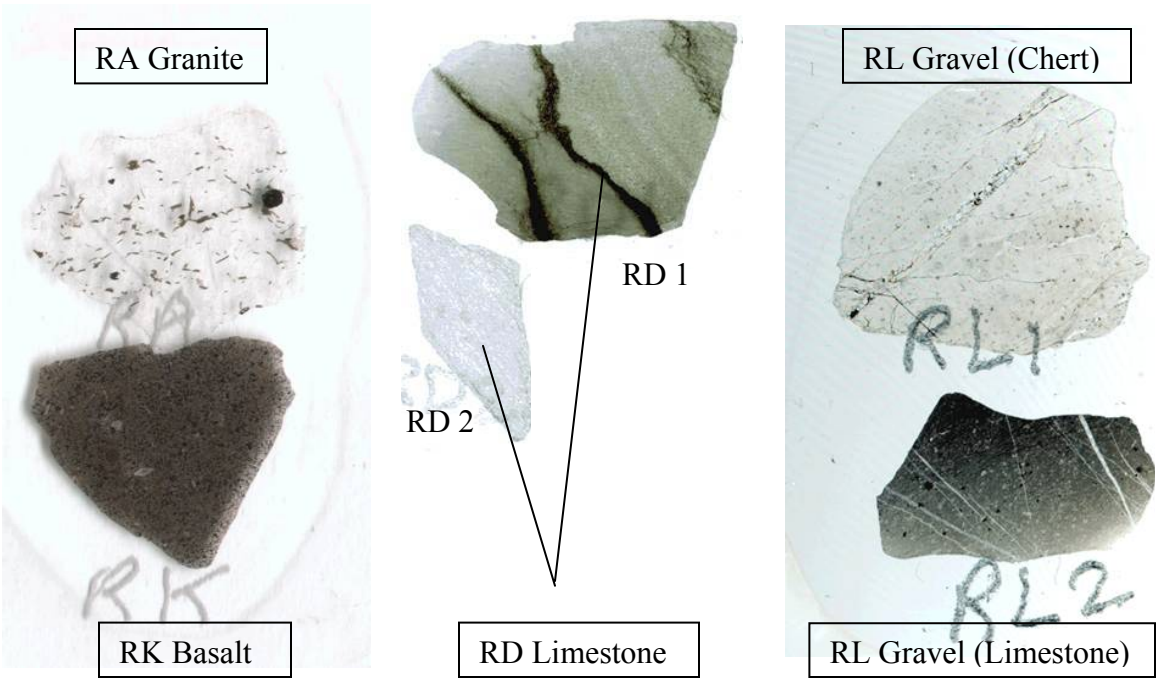

Figure J.2. Thin Sections of Aggregate Specimens.

Eleven minerals were identified and specimens collected which was a first attempt in relating the minerals in the selected aggregates to reference minerals. These minerals were epoxy mounted in a 25 mm phenol ring and polished to microprobe smoothness. Figure J.3 illustrates the mounted minerals. Biotite and muscovite micas were also analyzed but there was no need to polish these surfaces due to natural smooth cleavage planes provided by mica minerals. Quartz and calcite were not analyzed due to the known high purity of the selected reference minerals. Both thin sections and mounted mineral specimens were coated with a layer of approximately 100 to150Å thick carbon to prevent charge build-up during electron bombardment.

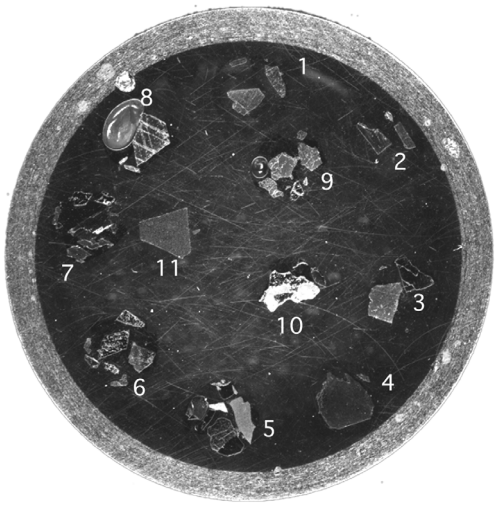

Figure J.3. Minerals mounted in epoxy: 1. Microcline; 2. Albite; 3. Andesine; 4. Labradorite; 5. Olivene; 6 Augite; 7 Hornblende; 8. Ilmenite; 9. Magnetite; 10. Hematite; 11. Dolomite.

J.2 OPTICAL MICROSCOPY

Thin sections were explored using optical microscopy. It was not the objective in this part of the study to give a detail account of minerals based on their optical properties, as these details would be accurately and efficiently obtained utilizing the electron microprobe. Optical microscopy merely served as the first step to a closer look at the aggregates. The images provide a glimpse into the complexity of these materials, especially with the focus on different surface features that can take part in the formation of strong or weak adhesive bonds.

The first two images represent RA Granite. Figure J.4 is an image obtained when light is transmitted through the sample without polarization. Grain boundaries are clearly visible. Dark, elongated grains represent mica, while other minerals are difficult to distinguish. Figure J.5 is the same area as shown above, but with a cross-polarization filter applied. Different minerals are clearly visible due to their different optical properties. In this particular image, grains with parallel line patterns are typical of plagioclase feldspar, which exhibits twinning in one direction. Crosshatched patterns can be attributed to potassium feldspars, known to have twinning in two directions. This is but one cross-polarization position and not all minerals can be identified effectively from this photo.

The fine-grained nature of the basalt is easily observed from Figure J.6, with an enlarged image presented in Figure J.7. The dark-brown circle represents a cay-filled cavity. More of these regions are present which indicates traces of decomposition. The large light crystals are the same as the little light ones, probably plagioclase feldspar.

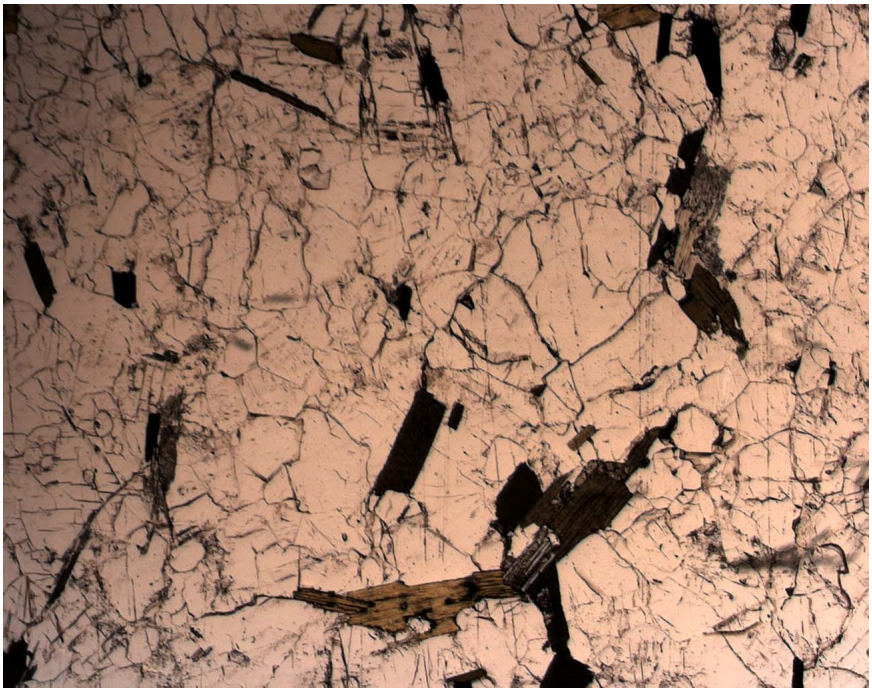

Figure J.4. (2.5X plane transmittance): RA Granite.

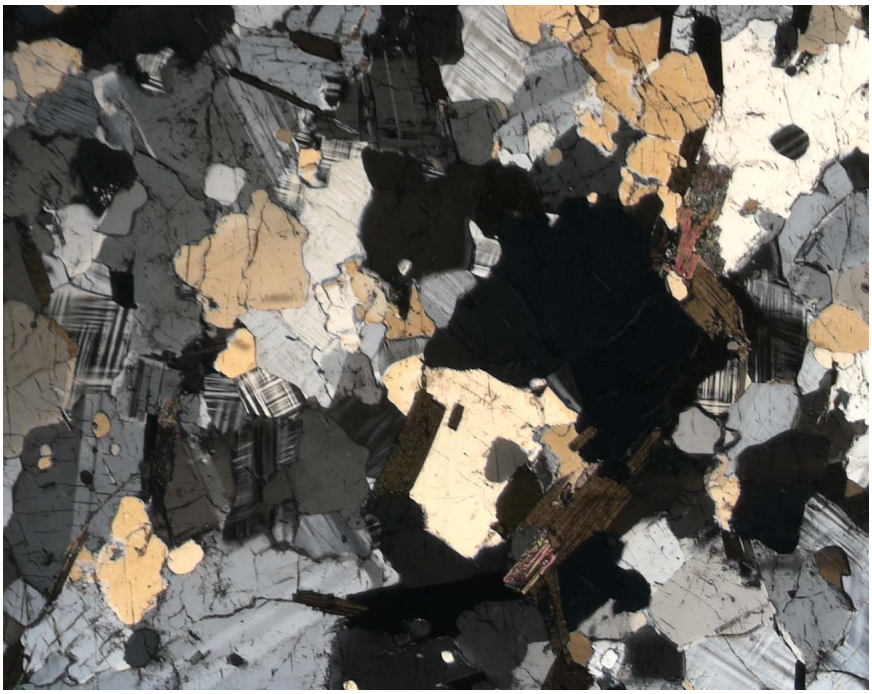

Figure J.5. (2.5X Cross-polarized): RA Granite.

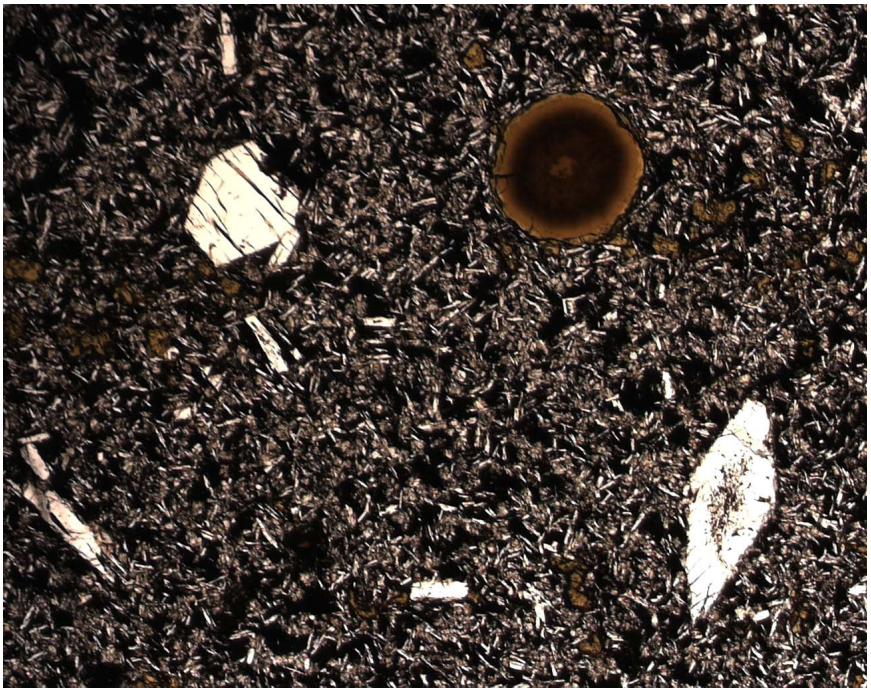

Figure J. 6. (2.5X Plane):RK Basalt.

Figure J.7. (10X Plane):RK Basalt.

The two optical images of RD limestone (Figures J.8 and J.9) show that the RD1 and RD2 represent fine and coarser grain limestone, respectively. The image presented as Figure J.8 captures an area where a dark vein occurs, most likely due to trace amounts of impurities.

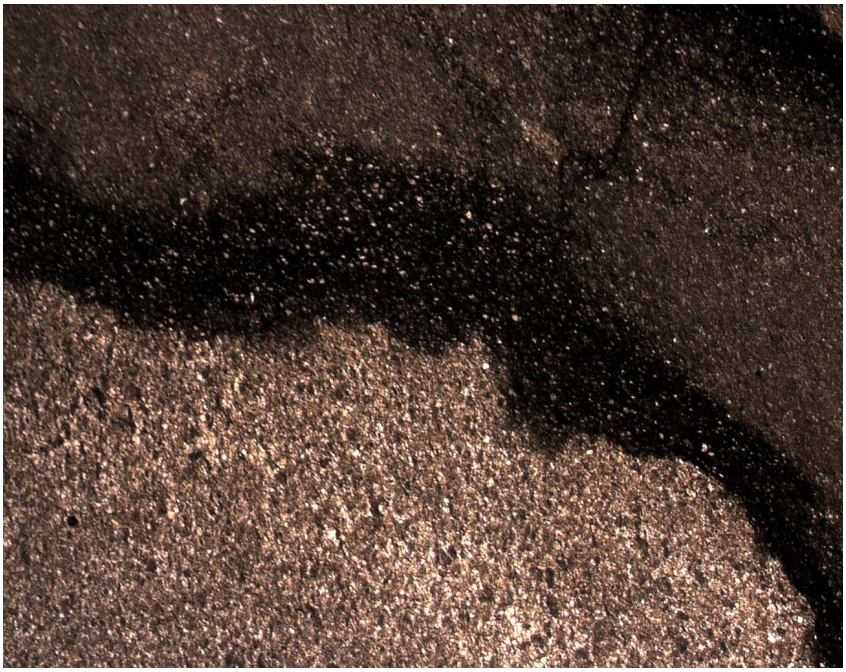

Figure J.8. (2.5X Plane): RD Limestone, RD1.

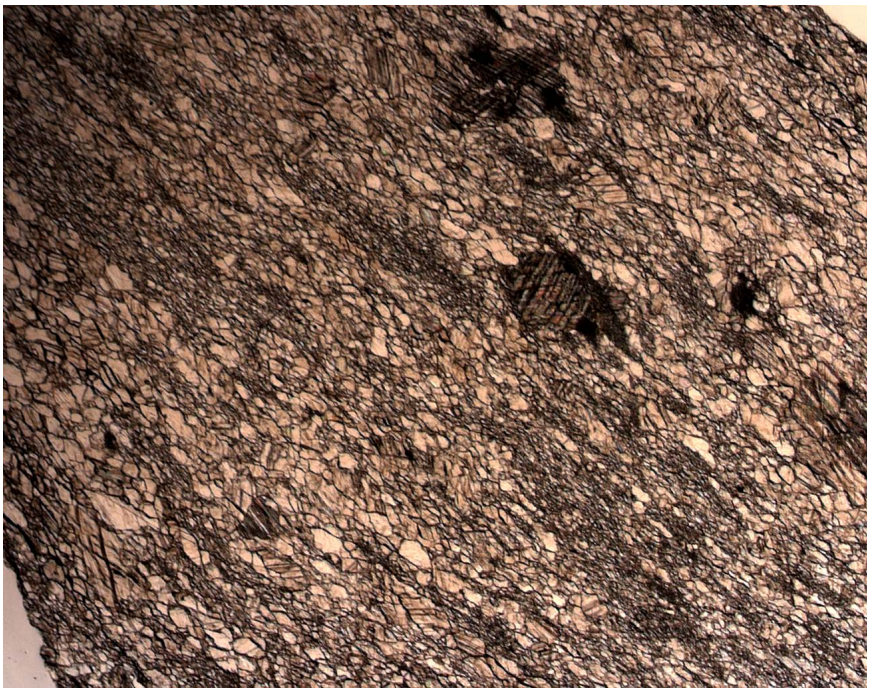

Figure J.9. (2.5X Plane): RD Limestone, RD2.

The optical image of RL gravel, RL1, in general shows that grains are not easily distinguishable, which is typical for microcrystalline quartz, i.e. chert. Larger grains are present in veins (Figures J.10 and J.11). Interesting fossils are present in RL2, limestone gravel, depicted in Figure J.12.

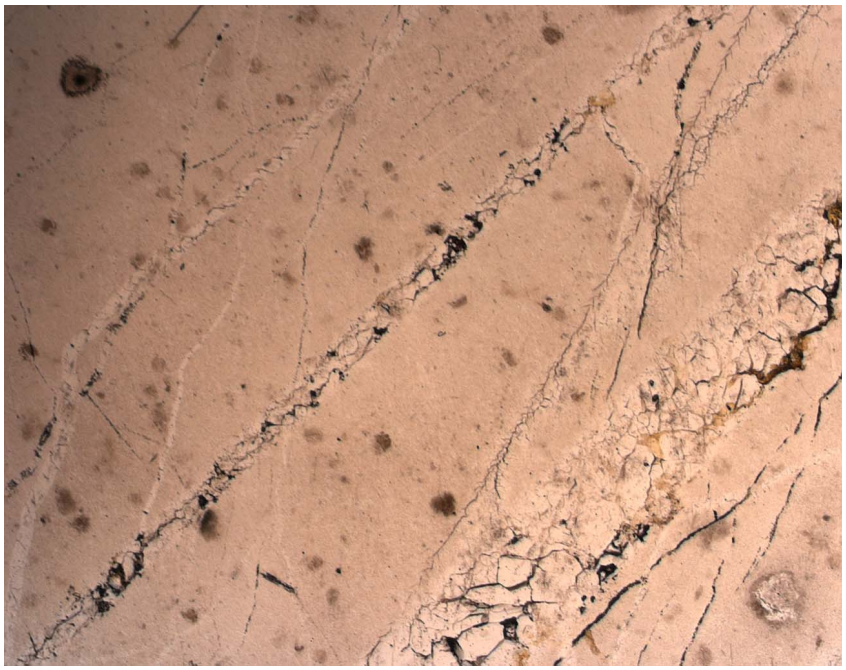

Figure J.10. (2.5X Plane): RL Gravel, Chert (RL1).

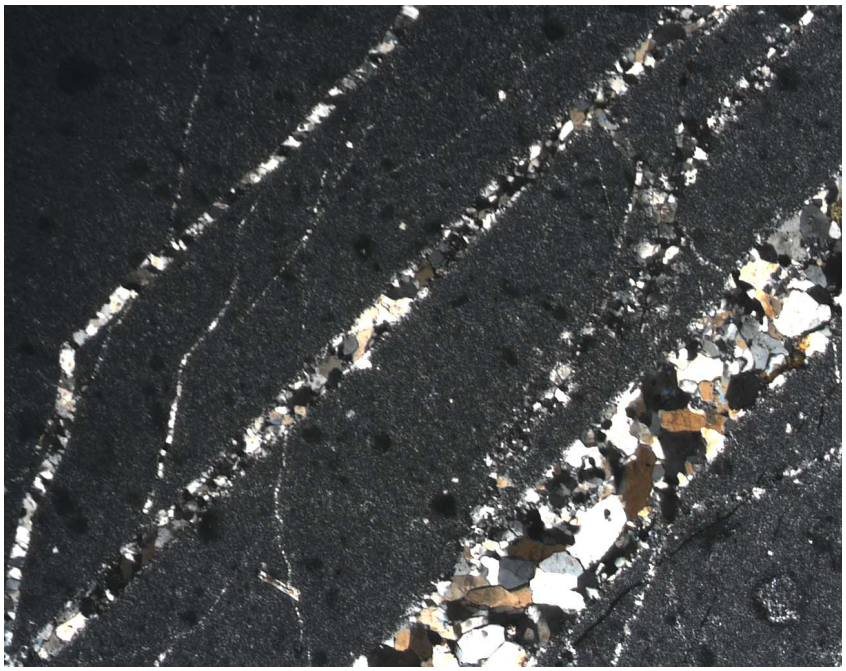

Figure J.11. (2.5X Cross-Polarized): RL Gravel, Chert (RL1).

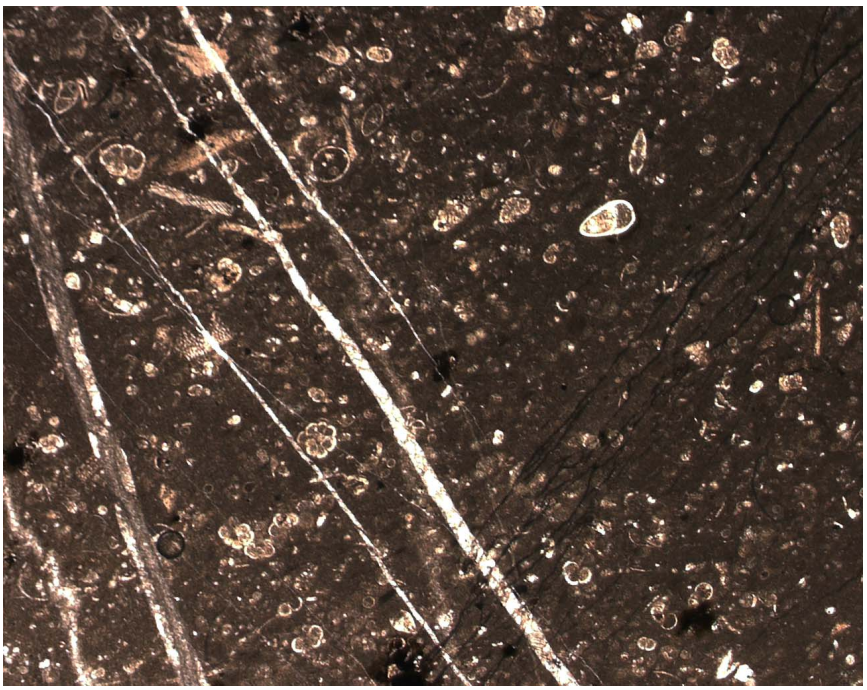

Figure J.12. (2.5X Plane): RL Gravel, Limestone (RL2).

J.3 QUALITATIVE ANALYSES

Scanned thin sections and digital secondary electron images produced by the scanning electron microscope were used to navigate the aggregate samples. After determining general regions, back-scattered electron images were used to establish final positions for qualitative analyses utilizing energy dispersive X-ray spectroscopy (EDS).

Routine scanning electron microscopy (SEM) uses secondary electrons generated from the top surface atoms to show topography of surface features a few nm across. Backscattered electrons are also generated, and images produced show the spatial distribution of chemical elements within the top micron of the sample. Contrast images, or chemical phases, are determined by the atomic number of the particular element responsible for the elastic backscattering of the electrons. A higher atomic number produces a higher intensity of backscattered electrons, and therefore a brighter image. If the mineral phases are readily distinguishable and elements identified, these images can be used to obtain area percentages of the minerals present by employing imaging software. X-ray mapping by wavelength-dispersive spectroscopy readily identifies elements, is accurate and takes care of potential ambiguity associated with mapping by BSE. This feature was applied to RA granite and is discussed later in this section.

EDS is commonly used due to its speed and simplicity. When the sample is bombarded by the focused electron beam, electrons are knocked out of their shells. A resulting electron vacancy is filled by an electron from a higher shell and X-rays are emitted to balance the energy difference between the two electrons. These X-ray energies are characteristic of the elements that produced it. The EDS system detects all X-ray energies simultaneously and accepts a wide solid angle of X-ray emission. It is for this reason that EDS is fast and ideal for survey spectra when the sample is totally unknown. The EDS microanalysis system collects the X-rays, sorts, and plots them by energy and automatically identifies and labels the elements responsible for the peaks in the energy spectrum.

J.3.1 RA Granite

The BSE image of RA granite is presented below (Figure J.13). An elemental X-ray map was composed using wavelength-dispersive spectroscopy (WDS) due to the difficulty to distinguish between some of the chemical phases. Since X-ray mapping is essentially a detail WDS analysis, further surveying would be redundant. Only minor unknown phases were detected using EDS. Iron oxides [Fe,O] and apatite [Ca,P] occur in small amounts.

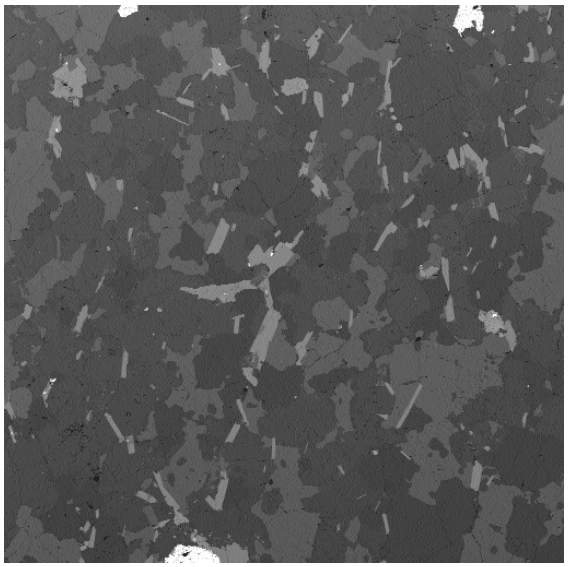

Figure J.13. BSE image of RA Granite.

J.3.2 RK Basalt

The BSE image for a region on RK basalt is shown in Figure J.14. This is the same region shown in the optical microscopy digital image. EDS surveys indicate inconsistency in the dark areas which represent fine material of mixed composition comprising silica, alumina as well as other elements, which represents mostly clayey type materials. The latter are signs of decomposition of the basalt. EDS suggests that small bright areas are ilmenite [Fe,O,Ti]; light gray areas represent pyroxene [Si, O, Al, Fe, Ca], most likely augite; and darker grey areas of plagioclase feldspar [Si, O, Na, Al, Ca].

The energy dispersive spectrum for pyroxene is depicted in Figure J.15.

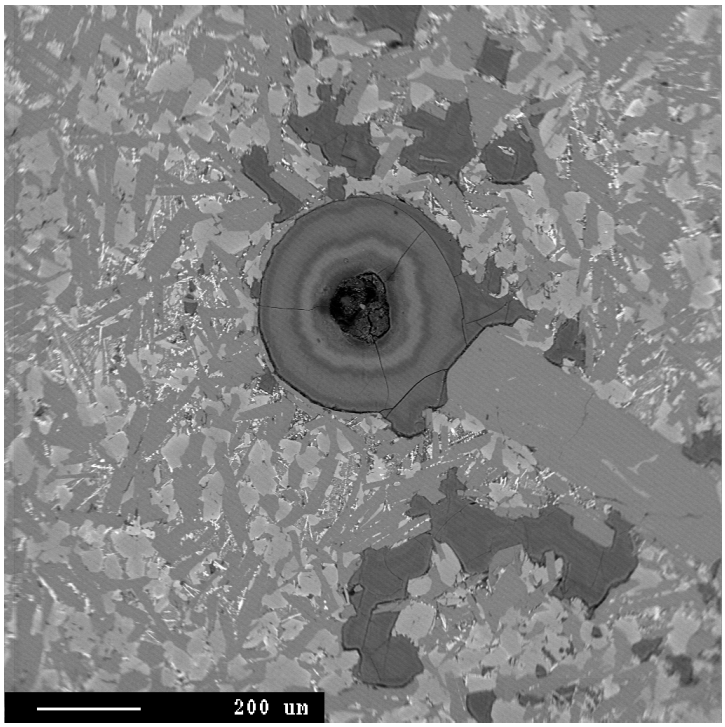

Figure J.14. BSE image (66X) of RK Basalt.

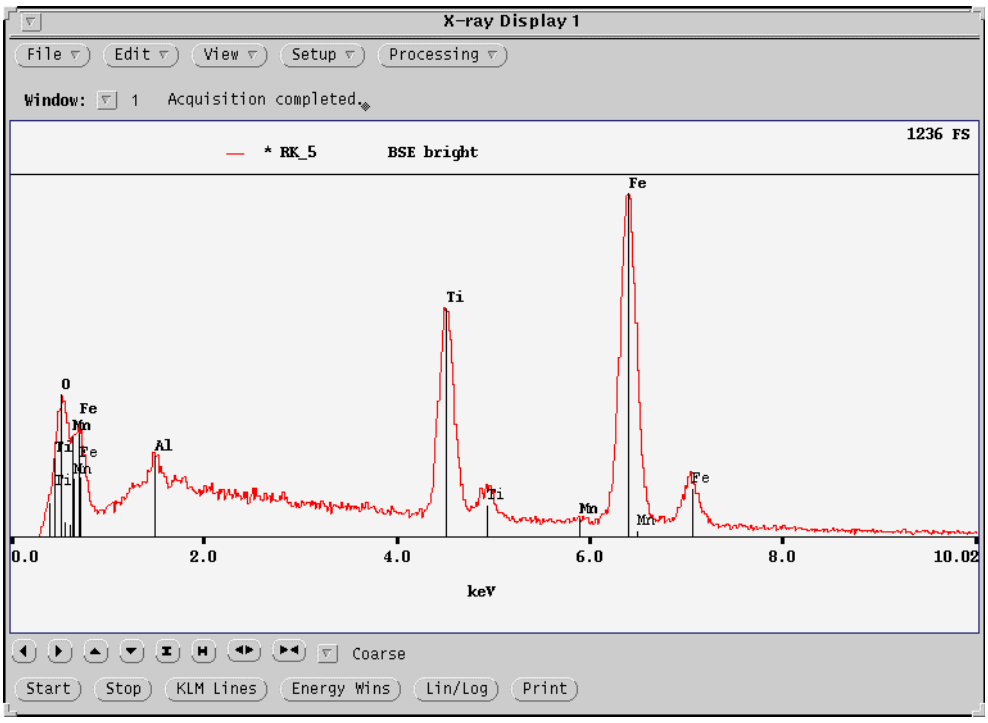

Figure J.15. EDS of bright BSE areas on RK Basalt.

J.3.3 RD Limestone

Two primary limestone types were identified within aggregate RD and accordingly included for analysis. RD1 and RD2 are indicated on the thin sections presented in Figure J.1. RD1 exhibits characteristic dark veins which represent areas that contain impurities. A number of images were captured on RD1. Figure J.16 is a BSE image taken within a dark vein over a 200 μm^2 area.

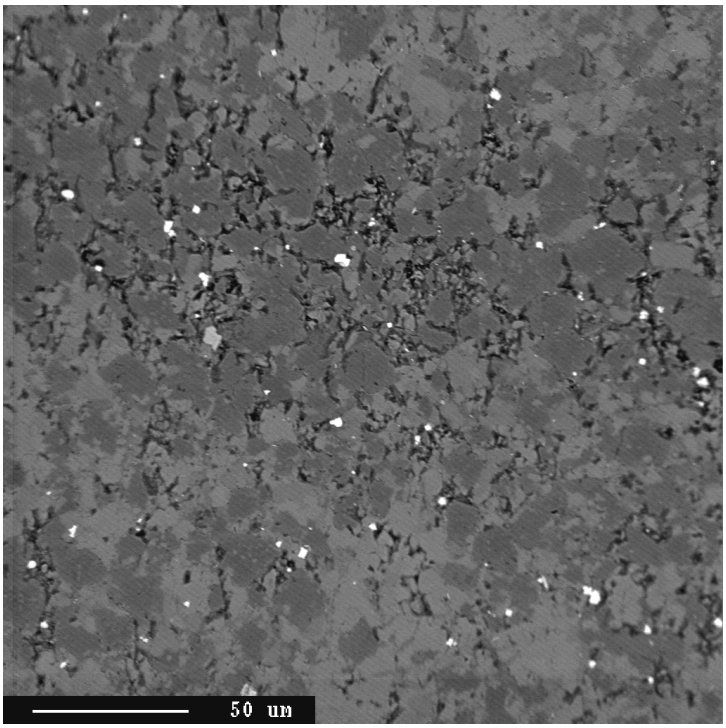

Figure J.16. BSE image (400X) within dark vein of RD1.

EDS surveys reveal that in addition to calcite, RD1 also contains a fair amount of dolomite (dark grey, larger grains) which are concentrated within the vein areas. An area EDS of these areas also indicates the presence of Al and Mg silicates, presumably clay impurities. Organic matter can also be present in these areas. Pyrite (FeS_2) is represented by the bright spots occurring primarily within the veins. The EDS for dolomite is presented in Figure J.17, characterized by the abundance of both calcium and magnesium. As can be expected, RD2 contains calcite as the primary phase. Small amounts of quartz and clay [Si, O,Al] are present but constitutes less than 1% of the sample area.

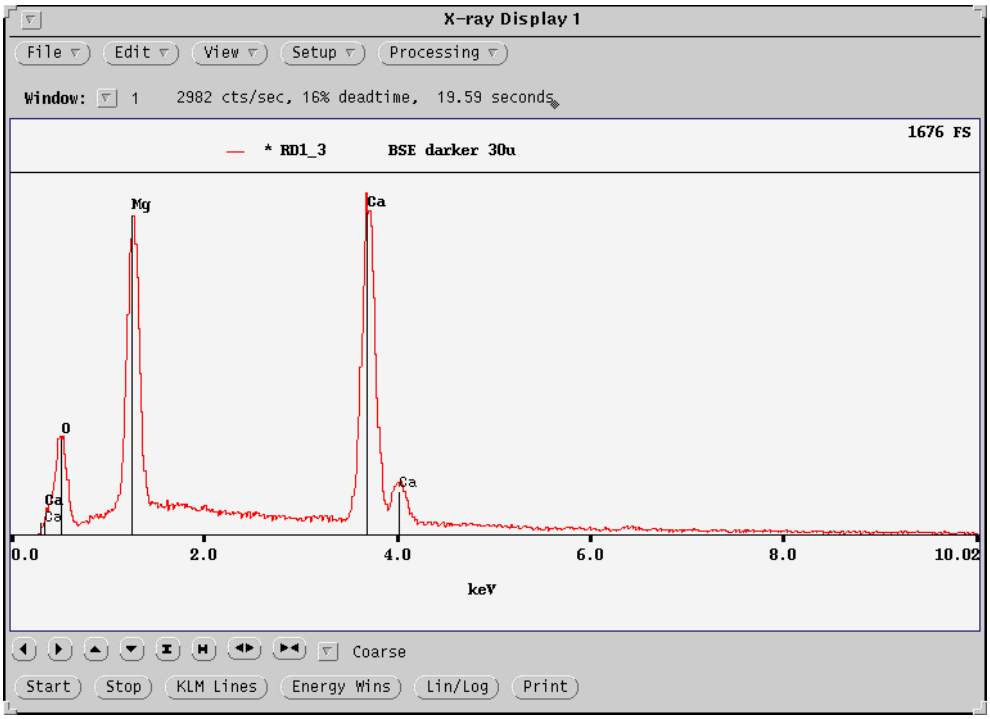

Figure J.17. EDS of Darker Gray Grains in RD1.

J.3.4 RL Gravel

The primary types of aggregate constituting RL gravel are chert (RL1) and limestone (RL2). The chert is homogeneous with trace amounts of impurities. Naturally, the major phase is silica and no further investigation was required. White bright BSE areas of barium sulfate [Ba,S,Al,Si] and less bright phases of iron rich chlorite [Fe,Al,Si,O] were detected.

A BSE image of the limestone gravel is presented in Figure J.18. Apart from the major phase, calcite, a dark grey phase of albite is present in this image. EDS confirmation of pure albite (no calcium) is presented in Figure J.19 as an example for this aggregate. A less bright minor phase of apatite [Ca,P], and brightest phase (diamond shape) of iron oxide are also present in this aggregate and noticeable in the figure.

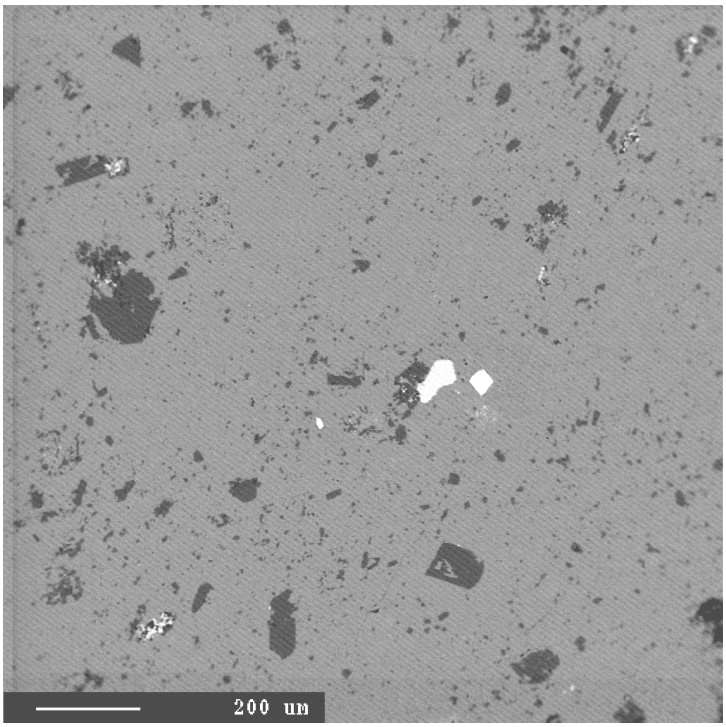

Figure J.18. BSE Image (66X) of RL2.

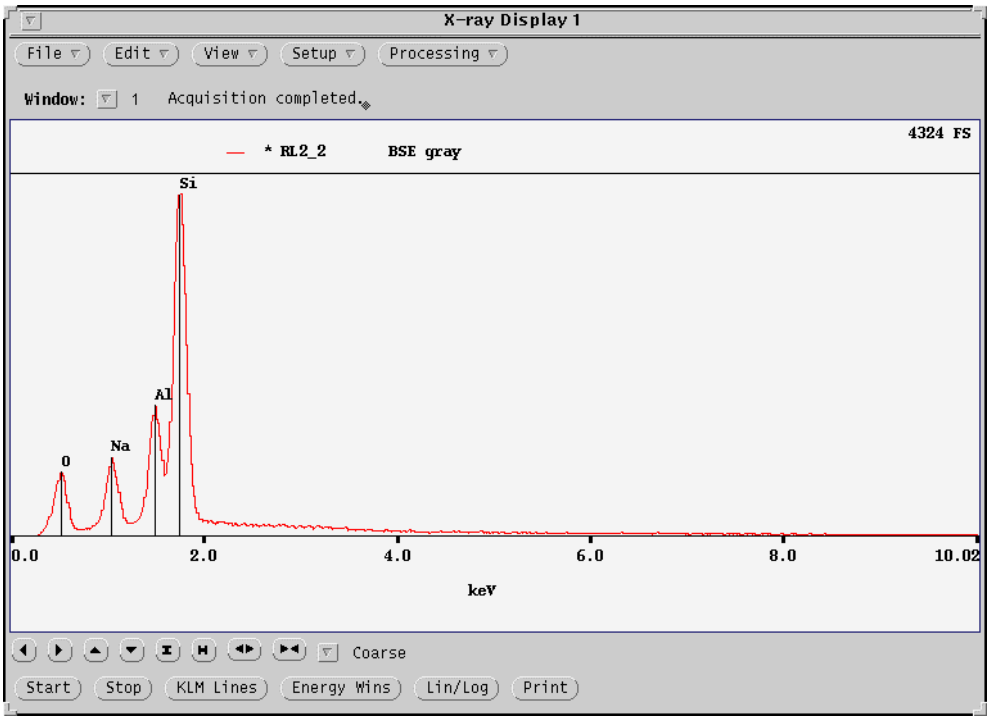

Figure J.19. Albite present in RL2,Limestone Gravel.

J.4 QUANTITATIVE ANALYSES

Points for qualitative analyses were established after a general survey using EDS, as described above. Wavelength dispersive spectroscopy (WDS) was then employed to accurately determine the composition of minerals present, which we refer to as quantitative analysis. While EDS collects and displays the X-ray spectrum for the whole energy range, WDS only measures at a single wavelength at a time and consequently takes longer. The microprobe introduced previously, however, has four wavelength dispersive spectrometers that can measure simultaneously. WDS offers important and critical refinement of EDS data, for example: at least an order of magnitude better sensitivity; resolution of severely overlapping spectrum peaks for improved elemental specificity; and more accurate quantitative analysis in general. Detail results from these analyses are presented in the Appendix, while a summary of each aggregate is presented below.

In addition to determining the composition of minerals present, mapping of the minerals through imaging software will also be presented. While the latter can be accomplished with a combination of well distinguishable BSE images and EDS or WDS single point analyses, certain cases cannot be easily mapped this way. The collection of X-rays utilizing WDS by moving the stage while bombarding the sample with a focused electron beam, results in clean X-ray maps.

J.4.1 RA Granite

The minerals analyzed for reference purposes were potassium feldspar, microcline (1); three plagioclase feldspars, namely albite (2), andesine (3), and labradorite (4); amphibole (7), hornblende; biotite mica and muscovite mica (not included in with the other minerals in the mineral mount). Analyses of the microlcline sample indicated that in addition to the primary phase of potassium feldspar, albite is present as a second phase. Despite this finding, the potassium as well as the sodium feldspar phases compare well to those present in RA granite. The albite reference mineral contains potassium and chlorine rich (5-10%) impurities, not considered suitable as a reference mineral and will be replaced. No other plagioclase feldspars are present in RA granite. Results confirmed the identity of biotite mica in RA granite with no amphiboles or muscovite mica present. Minor phases of iron oxides were identified in RA granite.

This aggregate was identified as a suitable candidate for WDS X-ray mapping as discussed previously. The spectrometers were set-up to detect X-ray wavelengths over a 1cm x 1cm area for: iron (Fe), representing biotite mica; potassium (K), representing K-feldspar; sodium (Na), representing plagioclase; and silicon (Si), representing the quartz as well as feldspars. These images are shown in Figure J.20. Imaging software was used to superimpose individual images and a suitable legend selected to represent different minerals. This image was used to establish the area percentages represented by the different minerals in RA granite. The final image is depicted in Figure J.21.

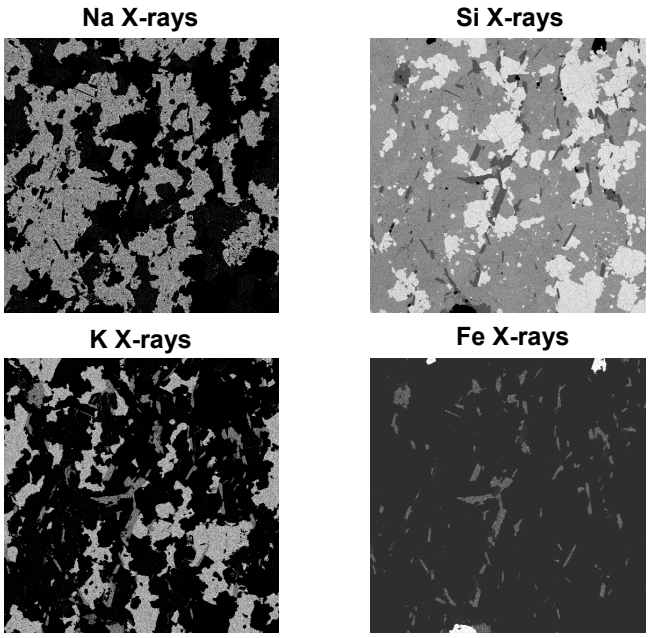

Figure J.20. Individual X-ray Maps.

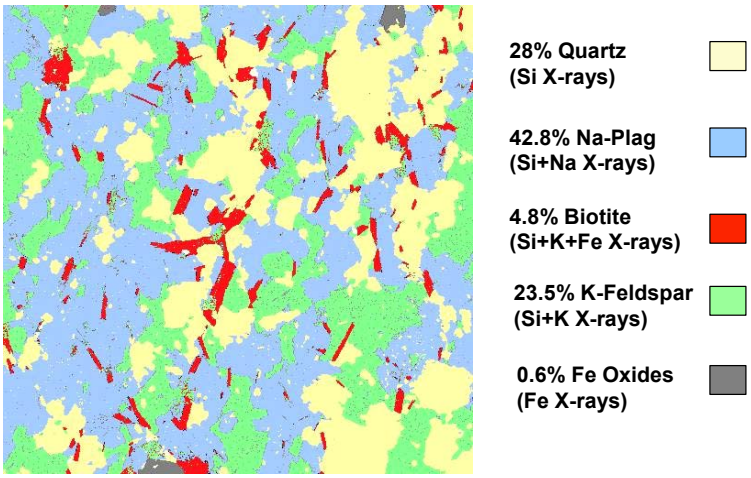

Figure J.21. X-ray map of RA Granite and Estimated Mineral Content Based on Area %.

J.4.2 RK Basalt

An indication of the elements present in different phases of BSE images was obtained by EDS. The reference minerals initially selected for WDS analysis were the three plagioclase feldspars (2, 3, 4) outlined above; pyroxene, augite (6); and amphibole (7). Individual points were selected for WDS analysis of the minerals present in aggregate RK based on several BSE

images. Results, appended, indicate that the feldspar present in this aggregate is a marginal labradorite/ bytownite with an approximately ratio of 30% sodium plagioclase (albite) to 70% calcium plagioclase (anorthite). The presence of augite was confirmed and the reference mineral compares reasonably well according to the oxide percentages obtained. The clayey inclusions were also measured and variable results obtained which suggests that these areas may contain chlorite, smectite, or even serpentine. Table J.1 presents the estimated mineral percentages in RK basalt based on BSE images, EDS, and WDS results.

Table J.1. Estimated Mineral Composition of RK, Basalt.

Mineral	Area %
Plagioclase feldspar (labradorite/bytownite)	56
Pyroxene (augite)	36
Iron oxides (ilmenite)	3
Clayey material	4
Other	1

J.4.3 RD Limestone

The primary phase of both RD1 and RD2 is essentially pure calcite. Minor impurities of quartz and clay occur within RD2 and no further analysis was carried out. RD1 on the other hand includes an important second phase of dolomite concentrated in the vein areas as depicted in the thin sections and discussed previously. An estimate of area percentages based on these areas would not be representative. Nevertheless, dolomite content in the vein areas was found to vary between approximately 30 and 50 %, while it is typically 6% in other areas.

J.4.4 RL Gravel

EDS indicated that the chert (RL1) is essentially comprises pure silica and no further testing was conducted. The limestone (RL2) comprises of two major phases, namely calcite and albite, and minor minerals such as iron oxide and apatite, which represent less than 1% of the area. Table J.2 presents the estimated mineral percentages in this limestone based on BSE images, EDS, and WDS results.

Table J.2. Estimated Mineral Composition of Limestone Part in RL.

Mineral	Area %
Calcite	91
Albite	8
Other (including iron oxides and apatite)	1